UNIVERSITY OF Southampton

University of Southampton Research Repository
ePrints Soton

Copyright © and Moral Rights for this thesis are retained by the author and/or other copyright owners. A copy can be downloaded for personal non-commercial research or study, without prior permission or charge. This thesis cannot be reproduced or quoted extensively from without first obtaining permission in writing from the copyright holder/s. The content must not be changed in any way or sold commercially in any format or medium without the formal permission of the copyright holders.

When referring to this work, full bibliographic details including the author, title, awarding institution and date of the thesis must be given e.g.

AUTHOR (year of submission) "Full thesis title", University of Southampton, name of the University School or Department, PhD Thesis, pagination

http://eprints.soton.ac.uk

UNIVERSITY OF SOUTHAMPTON

FACULTY OF ENGINEERING, SCIENCE AND MATHEMATICS

School of Electronics and Computer Science

A Comprehensive Scheme for Reconfigurable Energy-Aware Wireless Sensor Nodes

by

Alexander Stewart Weddell

Thesis for the degree of Doctor of Philosophy

May 2010

UNIVERSITY OF SOUTHAMPTON

ABSTRACT

FACULTY OF ENGINEERING, SCIENCE AND MATHEMATICS
SCHOOL OF ELECTRONICS AND COMPUTER SCIENCE

Doctor of Philosophy

A COMPREHENSIVE SCHEME FOR RECONFIGURABLE ENERGY-AWARE WIRELESS SENSOR NODES

by Alexander Stewart Weddell

Wireless sensor nodes are devices that perform measurements (of parameters such as temperature or vibration) and communicate over a wireless medium. A key benefit is that they can operate autonomously. Nodes are commonly battery-powered so that they can be deployed rapidly without the need to install a wired power supply; however, batteries must be changed when depleted and this can impose a costly maintenance requirement. Energy harvesting is an emerging field, which offers the possibility for nodes to be powered indefinitely from environmental energy (such as light, vibration, or temperature difference). The power generated from environmental energy is often limited and variable, and nodes must be able to adapt their operation to take account of the power available. There have been a number of demonstrations of wireless sensor nodes powered from harvested energy, but existing demonstrators are tailored for specific types of energy resource (constraining their use to applications with suitable energy availability). The existing interfaces between the energy hardware and the nodes' embedded software is bespoke and limited to specific devices, so it is impossible to exchange the energy hardware to adapt to differing energy availability.

The work described in this thesis delivers a comprehensive scheme for reconfigurable energy-aware sensor nodes, which overcomes the limitations of the existing systems and allows the energy hardware for sensor nodes to be connected together in a plug-and-play manner. The scheme has been evaluated by way of a prototype which accommodates a range of energy devices. The main contributions of this research are threefold: firstly, the system is enabled by a new hardware interface between the energy devices and sensor node; secondly, an embedded software structure is implemented to interface with the energy hardware; and thirdly, efficient energy-aware modules compliant with the scheme have been produced. The combined result is a novel energy subsystem for wireless sensor nodes that supports a range of energy devices and can deliver energy-aware operation for a range of microcontroller platforms, while imposing a minimal additional resource requirement to deliver this functionality.

Contents

Declaration of Authorship **xvii**

Acknowledgements **xix**

Nomenclature **xxiii**

Abbreviations **xxv**

1 Introduction **1**

1.1 Wireless autonomous sensing . . . 1
1.2 Outline of the AEASN project . . . 3
1.3 Justification for this research . . . 4
1.4 Contributions of this research . . . 6
1.5 What is 'reconfigurability'? . . . 8
1.6 Publications . . . 8
1.7 Document structure . . . 9

2 Background: Energy, Sensing, and Wireless Communication **11**

2.1 Introduction . . . 11
2.2 Energy storage . . . 11
2.2.1 Motivations and overview . . . 11
2.2.2 Non-rechargeable (primary) batteries . . . 12
2.2.3 Rechargeable (secondary) batteries . . . 14
2.2.4 Supercapacitors . . . 16
2.2.5 Other energy storage mechanisms . . . 16
2.2.6 Discussion . . . 17
2.3 Energy harvesting and wireless power transfer . . . 18
2.3.1 Motivations and overview . . . 18
2.3.2 Photovoltaics . . . 18
2.3.3 Vibration energy harvesting . . . 20
2.3.4 Thermoelectric energy generation . . . 25
2.3.5 Small-scale fluid flow . . . 27
2.3.6 Human power . . . 28
2.3.7 Inductive and RF energy transfer . . . 29
2.3.8 Hybrid energy harvesting technologies . . . 30
2.3.9 Summary and discussion . . . 30
2.4 Technologies for intelligent sensing . . . 32
2.4.1 The IEEE 1451 standards family . . . 32

2.4.2 Transducer electronic data sheets 33
2.4.3 Extensions to the electronic data sheet concept 34
2.4.4 System management schemes 34
2.4.5 Discussion 35
2.5 Wireless communication protocols 35
2.5.1 Overview 35
2.5.2 RF-based methods 35
2.5.3 Alternative communication methods 37
2.5.4 Networking and routing 38
2.5.5 Discussion 38
2.6 Energy-aware operation 39
2.6.1 Energy-aware routing 39
2.6.2 Energy-adaptive behaviour 39
2.6.3 Achieving energy awareness 41
2.6.4 Overall lifetime prediction and extension 42
2.6.5 Discussion 44
2.7 Wireless sensor node technologies 44
2.7.1 Microcontrollers, transceivers, and system-on-chip 44
2.7.2 Commercially-available sensor nodes 45
2.7.3 Discussion 46
2.8 Software and algorithm development 46
2.8.1 Software structures 46
2.8.2 Operating systems 47
2.8.3 Discussion 48
2.9 Existing systems 49
2.9.1 Wireless sensor system deployments 49
2.9.2 Systems featuring a single form of energy harvesting 50
2.9.3 Systems integrating multiple energy resources 52
2.9.4 Discussion 53
2.10 Summary 54

3 Development: Towards a Reconfigurable Energy Subsystem 55
3.1 Introduction 55
3.2 Design for reconfigurability 55
3.2.1 Plug-and-play energy subsystem 55
3.2.2 Modular design 58
3.2.3 Usage scenario 60
3.2.4 Major challenges and strategy 61
3.3 Energy Electronic Data Sheet (EEDS) 63
3.3.1 Overview and justification 63
3.3.2 Data sheet format 64
3.3.3 Hardware and interrogation method 65
3.4 Common Hardware Interface (CHI) 66
3.4.1 Overview and justification 66
3.4.2 EEDS interface 67
3.4.3 Interface format 67
3.4.4 Integration of multiple energy sources 69

3.5 Generalised system hardware specification 70
3.5.1 Energy multiplexer 70
3.5.2 Energy modules 71
3.5.3 Microcontroller requirements 72
3.5.4 Under- and over-voltage protection 73
3.6 Energy status determination and algorithms 73
3.6.1 Overview 73
3.6.2 Energy monitoring 74
3.6.3 Categorisation of load type 75
3.6.4 Supercapacitor state-of-charge and capacity 76
3.6.5 Battery state-of-charge and capacity 78
3.6.6 Power monitoring 80
3.7 Software structure 81
3.7.1 Overall software structure 81
3.7.2 The 'Energy Stack' 82
3.7.3 The 'Sensing Stack' 85
3.8 General system operation 86
3.8.1 Start-up 86
3.8.2 Default operation 86
3.8.3 Monitoring and active management 87
3.8.4 Network-level interactions 87
3.9 Towards a prototype to verify the approach 88
3.9.1 Overview 88
3.9.2 Evaluation criteria 88
3.10 Summary 89

4 Case Study: Deployment in a Prototype System – Hardware 91
4.1 Introduction 91
4.2 Overview of the case study 91
4.2.1 Scenario 91
4.2.2 Available energy sources 92
4.2.3 Utilised energy stores 94
4.3 Components and energy management circuits 94
4.3.1 Low-power system components 94
4.3.2 Connectors 96
4.3.3 EPROMs for energy electronic data sheets 96
4.3.4 State retention for device control 97
4.3.5 Over/Undervoltage protection and regulation 98
4.3.6 Power and energy estimation 99
4.4 Multiplexer module 102
4.4.1 Functional overview 102
4.4.2 Energy-awareness circuitry 104
4.4.3 Additional features 104
4.4.4 Start-up and voltage regulation 105
4.4.5 Data multiplexing 105
4.4.6 Overall efficiency 105
4.5 Energy modules 106

4.5.1 Photovoltaic module . . . 106
4.5.2 Vibration energy harvesting module . . . 110
4.5.3 Other energy-harvesting modules . . . 112
4.5.4 Mains module . . . 113
4.5.5 Primary battery module . . . 114
4.5.6 Secondary battery module . . . 115
4.5.7 Supercapacitor module . . . 117
4.6 System integration . . . 117
4.6.1 Complete system . . . 117
4.6.2 Default operation . . . 118
4.6.3 Overall evaluation . . . 119
4.7 Summary . . . 120

5 Case Study: Deployment in a Prototype System – Software 121
5.1 Introduction . . . 121
5.2 Microcontroller platform . . . 121
5.2.1 Platform capabilities . . . 121
5.2.2 Language, environment and debugger . . . 122
5.2.3 Low-power modes and energy characteristics . . . 123
5.2.4 Hardware abstraction layer functions . . . 124
5.3 Energy electronic data sheets . . . 126
5.3.1 Overview . . . 126
5.3.2 Functions for 1-Wire communications . . . 126
5.3.3 Performance costs of 1-Wire communications . . . 127
5.3.4 Data sheet format . . . 129
5.3.5 Example data sheet contents . . . 131
5.4 Embedded software structure . . . 133
5.4.1 Overall structure . . . 133
5.4.2 Communication stack . . . 133
5.4.3 Sensing stack . . . 135
5.4.4 Energy stack . . . 136
5.4.5 Application layer and control scheme . . . 136
5.5 Energy stack . . . 136
5.5.1 Physical Energy (PYE) layer . . . 136
5.5.2 Energy Analysis (EAN) layer . . . 139
5.5.3 Energy Control (ECO) layer . . . 143
5.6 Evaluation . . . 145
5.6.1 Implementing energy-adaptive behaviour . . . 145
5.6.2 Energy-related performance . . . 146
5.6.3 Embedded software features . . . 146
5.6.4 Comparison against state-of-the-art systems . . . 146
5.7 System testing and results . . . 147
5.8 Summary . . . 149

6 Conclusions and Future Work 151
6.1 Summary of work . . . 151
6.2 Interpretation of the results . . . 152

6.3 Recommendations for future work 154
6.3.1 Overview 154
6.3.2 Hardware development 154
6.3.3 Software development 155
6.3.4 Towards standardisation 155
6.4 A look to the future. 156

A Module schematics 157

B Energy Electronic Data Sheet Contents 163

C Selected Publications 165

Bibliography 191

List of Figures

1.1 Major parts of a sensor node 1
1.2 Two examples of environmental sensor network deployments 2
1.3 Telos wireless sensor 'mote' 3
1.4 S^{5}NAP node deployed on an air compressor 5
1.5 Trio wireless sensor node 5
1.6 Thesis chapter structure 10

2.1 End-of-life indication for lithium primary batteries 14
2.2 Comparison of rechargeable battery types 15
2.3 Efficiencies of PV cells relative to STC 19
2.4 Comparative efficiency of PV cells 19
2.5 Characteristics of Schott Solar ASI Indoor Photovoltaic Modules 20
2.6 Model of a linear, inertial generator 21
2.7 PMG Perpetuum's PMG17 vibration harvesting generator 22
2.8 A miniaturised electromagnetic microgenerator 23
2.9 Two-layer bender mounted as a cantilever 23
2.10 The AdaptivEnergy piezoelectric vibration energy harvester 24
2.11 Types of electrostatic energy harvester 25
2.12 The Micropelt Generic Power Bolt 26
2.13 Tellurex PG1 Power Generation Kit 27
2.14 Bosch Hydropower generator used with the MPWiNodeX 28
2.15 Wind-powered generators used by wireless sensor nodes 28
2.16 Intel WISP 30
2.17 Midé Volture hybrid energy harvester 30
2.18 Conventional and plug-and-play smart sensors 32
2.19 Star, tree, and mesh network topologies 36
2.20 Outline of the ZigBee Stack Architecture 37
2.21 The IDEALS/RMR system diagram 40
2.22 Priority balancing in IDEALS 41
2.23 The Texas Instruments CC2430EM and eZ430-RF2500 45
2.24 The OSI-BRM, IRM, Foundation Fieldbus H1 and ZigBee stacks 47
2.25 Energy management architecture 48
2.26 Hardware abstraction architecture implemented in TinyOS 2.0 48
2.27 The Glacsweb Mk II architecture 50
2.28 The Prometheus architecture and prototype 51
2.29 Photovoltaic cells 'harvest' energy from a ceiling-mounted light unit . . . 52
2.30 The Ambimax architecture and circuitry 53
2.31 The MPWiNodeX architecture and deployment 54

3.1 A modular energy subsystem connected to a sensor node 60
3.2 Conventional and multiplexed 1-wire bus configurations 66
3.3 Option 1 for multiple energy source combination 70
3.4 Option 2 for multiple energy source combination 70
3.5 Discharge of a supercapacitor through various loads 75
3.6 Current and power consumption of CC2430EM 77
3.7 Typical discharge profile of Duracell MN1500 alkaline cell 79
3.8 A combined stack 81
3.9 A basic template stack 82
3.10 An “Energy Stack” 83
3.11 A “Sensing Stack” 85

4.1 Bistable multivibrator 97
4.2 Undervoltage protection circuit 98
4.3 Overvoltage protection circuits 99
4.4 Combined undervoltage and overvoltage protection circuit 99
4.5 Test of combined undervoltage and overvoltage protection circuit 100
4.6 Example of voltage measurement circuit 101
4.7 Prototype multiplexer module 102
4.8 Simplified schematic of multiplexer module, showing data connections . . 103
4.9 Simplified schematic of multiplexer module, showing power connections . 103
4.10 Circuit board for the photovoltaic module 106
4.11 The developed PV energy harvesting circuit 108
4.12 SPICE model for small PV cells 108
4.13 Logarithmic fit of V_{oc} against illuminance 109
4.14 Comparison of switching converter against conventional diode 111
4.15 Circuit board for the vibration module 111
4.16 Circuit board for the mains module 113
4.17 Circuit board for the primary battery module 114
4.18 Circuit board for the supercapacitor module 117
4.19 Complete system connection 118

5.1 SmartRF04EB platform 123
5.2 MSP430F2274 power modes 124
5.3 Set-up for EEDS on energy module to be programmed 126
5.4 Oscilloscope trace of reading EEDS on supercapacitor module 129
5.5 A detailed combined stack 134
5.6 The SimpliciTI communication stack 135
5.7 MSP430 flash write voltage requirements 140
5.8 Calculation of e^8 using Taylor expansion 143
5.9 Annotated Hyperterminal output from second test 148

A.1 Multiplexer module schematic 158
A.2 Photovoltaic module schematic 159
A.3 Vibration module schematic 160
A.4 Mains module schematic 161
A.5 Supercapacitor module schematic 161
A.6 Battery module schematic 162

List of Tables

2.1 Non-rechargeable battery types and characteristics 13
2.2 Rechargeable battery types and characteristics 15
2.3 Typical indoor and outdoor brightness levels 19
2.4 List of vibration sources 21
2.5 Comparison of energy harvesting sources 31
2.6 Basic TEDS content, as defined in IEEE 1451.4-2004 33
2.7 Thermistor Template Summary 34

3.1 Outline format for the Energy Electronic Data Sheet 64
3.2 Module class codes 64
3.3 Examples of module type identifiers 65
3.4 Identifiers for modules in the energy subsystem 67
3.5 Common Hardware Interface: microcontroller to multiplexer module . . . 69
3.6 Common Hardware Interface: multiplexer to energy modules 69
3.7 Energy Priority Levels 75
3.8 Simplified discharge of alkaline AA cell 79

4.1 Interface pins from multiplexer module (address ‘0’) 104
4.2 Interface pins from multiplexer module (address ‘7’) 104
4.3 Interface pins from photovoltaic module 106
4.4 Parameters found for Indoor PV Module 109
4.5 Interface pins from vibration module 112
4.6 Interface pins from wind module 112
4.7 Interface pins from thermoelectric module 113
4.8 Interface pins from mains module 113
4.9 Interface pins from primary battery module 115
4.10 Interface pins from secondary battery module 116
4.11 Interface pins from supercapacitor module 117

5.1 Electronic Data Sheet for NiMH battery module 132
5.2 Electronic Data Sheet for photovoltaic module 133

B.1 Electronic Data Sheet for mains module 163
B.2 Electronic Data Sheet for vibration energy harvester module 163
B.3 Electronic Data Sheet for primary battery module 164
B.4 Electronic Data Sheet for supercapacitor module 164

Listings

5.1 Struct for energy module EEDS parameters 130
5.2 Measurement types for devices 130
5.3 Struct for multiplexer EEDS parameters 131
5.4 TParams union for storing module parameters 131
5.5 Parameters to enable energy-awareness for energy modules 132
5.6 Code to interface with Simple Packet Protocol communication stack . . . 134
5.7 Code to interface with SimpliciTI communication stack 135
5.8 Energy priority enumeration and threshold struct from ECO layer 144
5.9 Main task loop in shared application layer 145

Declaration of Authorship

I, Alexander Stewart Weddell, declare that the thesis entitled 'A Comprehensive Scheme for Reconfigurable Energy-Aware Wireless Sensor Nodes' and the work presented in the thesis are both my own, and have been generated by me as the result of my own original research. I confirm that:

- this work was done wholly or mainly while in candidature for a research degree at this University;
- where any part of this thesis has previously been submitted for a degree or any other qualification at this University or any other institution, this has been clearly stated;
- where I have consulted the published work of others, this is always clearly attributed;
- where I have quoted from the work of others, the source is always given. With the exception of such quotations, this thesis is entirely my own work;
- I have acknowledged all main sources of help;
- where the thesis is based on work done by myself jointly with others, I have made clear exactly what was done by others and what I have contributed myself;
- parts of this work have been published as listed in Section 1.6 of the thesis.

Signed:

Date:

Acknowledgements

I would like to sincerely thank Nick Harris and Neil White for their technical supervision and guidance throughout this PhD, and Geoff Merrett for his helpful and thorough contributions to collaborative work. I would also like to express my appreciation to Neil Grabham for his contributions in connection with the Adaptive Energy-Aware Sensor Network (AEASN) project, Bashir Al-Hashimi for his feedback on technical writing, and to Neil Ross for his analogue circuit design advice. Thanks also to Alex Rogers and Kirk Martinez for their helpful input as internal examiners over the course of this work.

I also wish to thank the Engineering and Physical Sciences Research Council (EPSRC) who provided funding to me through a doctoral training award and under Platform grant EP/D042917/1 ‘New Directions for Intelligent Sensors’, and the Data and Information Fusion Defence Technology Centre consortium for their financial assistance under the AEASN project. Thanks also to the School of Electronics and Computer Science for the provision of excellent research facilities and support.

My gratitude also goes to the other members of the Electronic Systems and Devices (ESD) group who have made me feel at home (including, but not limited to, Adam Lewis, Andrew Frood, Cheryl Metcalf, Dirk de Jager, Evangelos Mazomenos, Matthew Swabey, Mustafa Imran Ali and Russel Torah). Special thanks must go to my parents for their love, support and encouragement over many years. Finally, I would like to thank my wife, Jenny, for her love, understanding, and unwavering confidence in me.

To Jenny, with all my love.

Nomenclature

α	Ratio between resistors in voltage divider arrangement
α_ψ	Voltage factor
α_τ	Temperature factor
A	Cross-sectional area [m^2]
C	Capacitance [F]
c_T	Damping coefficient
d	Separation distance [m]
η	Carnot efficiency
ϵ_0	Permittivity of free space
E	Energy [J]
E_V	Illuminance [Lx]
I	Current [A]
I_0	Diode saturation current [A]
I_{mpp}	Maximum power point current [A]
I_{ph}	Photogenerated current [A]
I_{sc}	Short-circuit current [A]
k	Spring constant
k	Thermal conductivity of material [$WK^{-1}m^{-1}$]
k	Voltage ratio for photovoltaic cells
k_B	Boltzmann constant
l	Length [m]
λ	Wavelength of transmission [m]
m	Mass of oscillating object [kg]
m	Current ratio for photovoltaic cells
ν	Velocity of fluid [ms^{-1}]
P	Power [W]
P_0	Inital transmitted power [W]
φ_t	Remaining lifetime fraction
φ_E	Energy fraction
φ_L	Logarithmic discharge fraction
φ_V	Voltage fraction
q	Electronic charge [C]

q'	Heat flow through material $[W/m^2]$
ρ	Density of fluid [kg/m^3]
r	Radius of transmission [m]
R	Resistance [Ω]
t_ϵ	Expected lifetime
t_γ	Guaranteed lifetime
T	Temperature [K]
T_{high}	'Hot' side temperature [K]
T_{low}	'Cold' side temperature [K]
T_ϵ	Expected temperature [K]
T_ρ	Rated temperature [K]
V	Voltage [V]
V_0	Starting voltage [V]
V_{mpp}	Maximum power point voltage [V]
V_{oc}	Open-circuit voltage [V]
V_{start}	Initial voltage applied [V]
V_{max}	Maximum voltage reached [V]
w	Width [m]
y	Input displacement [m]
z	Spring displacement [m]

Abbreviations

μC	Microcontroller
ADC	Analogue-to-Digital Converter
AEASN	Adaptive Energy-Aware Sensor Networks
AM1.5	Air Mass 1.5
AMR	Automatic Meter Reading
ANSI	American National Standards Institute
ASI	Amorphous Silicon
CEDS	Component Electronic Data Sheet
CENS	Center for Embedded Networked Sensing
CHI	Common Hardware Interface
DIF	Data Information Fusion
DTC	Defence Technology Centre
EAN	Energy Analysis Layer
ECO	Energy Control Layer
EEDS	Energy Electronic Data Sheet
EMA	Energy Management Architecture
EP	Energy Priority
EPROM	Electrically Programmable ROM
EPSRC	Engineering and Physical Sciences Research Council
ESD	Electronic Systems and Devices
GPS	Global Positioning System

HAL	Hardware Adaptation/Abstraction Layer
HEDS	Health Electronic Data Sheet
HeH	Hybrid Energy Harvester
HIL	Hardware Interface Layer
HPL	Hardware Presentation Layer
HVAC	Heating, Ventilation and Air Conditioning
I/O	Input/Output
IDEALS	Information manageD Energy aware ALgorithm for Sensor networks
IEEE	Institute of Electrical and Electronics Engineers
IrDA	Infrared Data Association
ISA	International Society of Automation
ISM	Industrial, Scientific and Medical
KTN	Knowledge Transfer Network
LAN	Local Area Network
LPM	Low-Power Mode
MIT	Massachusetts Institute of Technology
NiCd	Nickel Cadmium
NiMH	Nickel Metal Hydride
PC	Personal Computer
PCB	Printed Circuit Board
PMBus	Power Management Bus
PP	Packet Priority
PRIMP	Priority-Based Multi-Path Routing Protocol
PV	Photovoltaic
PYE	Physical Energy Layer
PYS	Physical Sensing Layer
QoS	Quality of Service

RAM	Random Access Memory
RF	Radio Frequency
RF-ID	Radio Frequency Identification
RMR	Rule Managed Reporting
ROM	Read-Only Memory
SBD	Smart Battery Data
SEV	Sensor Evaluation Layer
SMBus	System Management Bus
SoC	System-on-Chip
SPR	Sensor Processing Layer
STC	Standard Test Conditions
TEDS	Transducer Electronic Data Sheet
TI	Texas Instruments
UHF	Ultra High-Frequency
WISP	Wireless Identification and Sensing Platform
WLAN	Wireless LAN
WPAN	Wireless Personal Area Network

Chapter 1

Introduction

1.1 Wireless autonomous sensing

"The powering of remote and wireless sensors is widely cited as a critical barrier limiting the uptake of this technology."

Energy Harvesting Technologies to Enable Remote and Wireless Sensing,
Sensors and Instrumentation KTN Technical Report [1].

Remote and wireless sensors, referred to hereafter as 'wireless autonomous sensors' or 'wireless sensor nodes', offer the facility to remotely monitor parameters such as temperature, pressure, and vibration, in machines, buildings, or the environment. These nodes will typically feature at least one type of sensor, a microcontroller (to manage and process data), a wireless communication interface (which is almost always radio frequency (RF) based), and a power supply (conventionally a battery, but potentially harnessing energy harvested from the environment). A typical architecture for a sensor node is shown in Figure 1.1.

The applications of this technology are extremely varied but key drivers for the popularity of wireless sensors are the high cost, or the impracticality, of installing wiring for

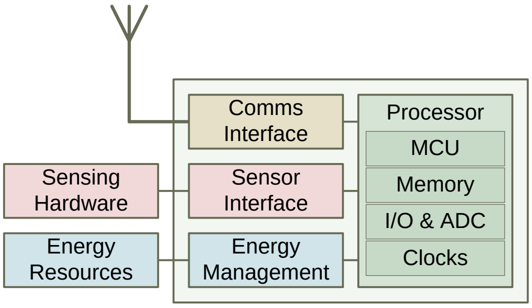

Figure 1.1: The major parts of a wireless sensor node.

conventional sensors. Wireless technology allows parameters to be monitored, or experiments to be carried out, which would previously have been prohibitively expensive or time-consuming. Furthermore, in contrast to conventional data-logging equipment, wireless sensors on remote long-term deployments permit parameters to be monitored with a high temporal resolution and provide a real-time, or near-real-time, representation of the situation.

Wireless sensing technology enables devices to be deployed quickly and easily by way of the fact that they are able to self-configure without the need for a fixed layout or infrastructure. State-of-the-art communication protocols allow sensor nodes to form mesh networks and work together to route information to a central point. Normally, nodes operate with a low duty cycle to conserve energy (consuming tiny levels of power while asleep), and utilise low-power communications which minimises their active energy consumption. This means that their average power requirement is very low and allows them to deliver operational lifetimes that are typically measured in months or years.

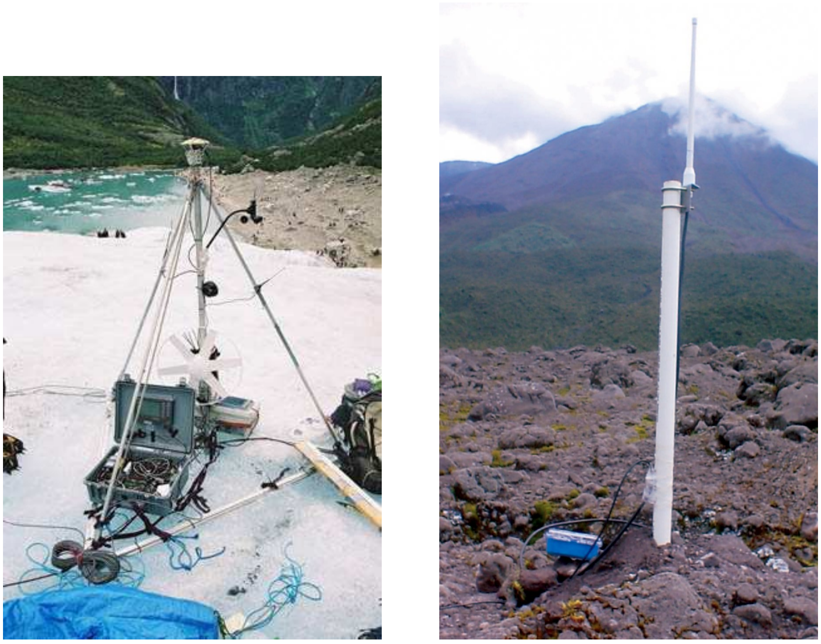

(A) Glacsweb base station

(B) Active volcano monitoring

Figure 1.2: Two examples of environmental sensor network deployments: (a) a Glacsweb base station is used to communicate with nodes buried deep in a Norwegian glacier (reproduced from [2]), and (b) a node performing seismic and infrasonic measurements on the side of an active volcano in Ecuador (reproduced from [3]).

Examples of real deployments of wireless sensor systems range from the relatively mundane to the extreme. Machinery condition monitoring is a popular application for this technology. For example, BP have utilised wireless sensor nodes to monitor the condition of machinery in one of their oil tankers [4]. More challenging applications include embedding wireless sensor nodes deep inside glaciers to monitor their dynamics [2], or on volcanoes to monitor seismic events [3] (as shown in Figure 1.2). Essentially, these are examples of applications where conventional sensing would be expensive or impractical, and where the lower complexity and deployment cost of wireless autonomous sensor systems enables parameters to be measured for a sustained period, and monitored remotely, with a higher spatial (and often temporal) resolution.

The Crossbow Telos 'mote', as shown in Figure 1.3, is a popular wireless sensor platform that integrates sensing hardware with a low-power microcontroller and a radio transceiver. This device is normally powered by a pair of AA non-rechargeable batteries, and the lifetime of the node is ultimately dependent on the the characteristics of the batteries and activity of the node (i.e. its duty cycle and the power consumption of its sensing hardware when performing measurements). Obviously the batteries must be replaced when depleted, which imposes a maintenance requirement that can prove costly over the course of long deployments.

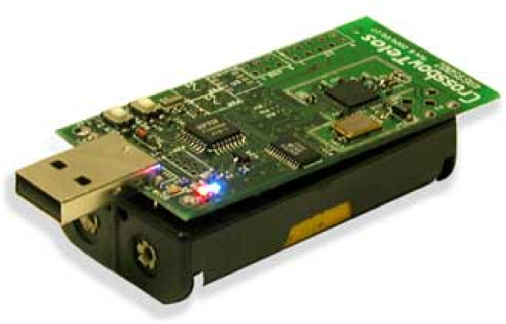

FIGURE 1.3: The Telos wireless sensor 'mote' (reproduced from [5]).

A common facet of wireless sensor nodes is that they are highly resource-constrained. They will typically have an 8-bit or limited 16-bit microcontroller with a relatively small amount of memory, and be restricted by their energy resources (operating from batteries or harvested environmental energy). They have low-power radios which often operate in relatively crowded radio frequencies and have a limited transmission range. The cost and physical size of devices are also common constraints, as are their weight and deployment location. For these reasons, the careful design, installation, and management of these systems is essential. This thesis will consider only low-power sensor devices which typically consume, on average, less than one milliwatt of power in general operation, which means that powering these devices from relatively low levels of harvested energy can be feasible.

1.2 Outline of the AEASN project

The research presented in this thesis has in part been undertaken under the Data Information Fusion Defence Technology Centre (DIF DTC) Phase II 'Adaptive Energy-Aware

Sensor Networks' (AEASN) project. The AEASN project was funded jointly by the UK Ministry of Defence and General Dynamics UK. The project had two main aims:

1. To allow wireless sensor nodes to efficiently manage their own energy resources, using energy harvested from their environment where appropriate. This should permit nodes to be energy-aware and facilitate sustained operation.
2. To permit groups of nodes to negotiate and co-ordinate their sensing activities, taking account of their energy status, to fulfil the requirements of the network.

The work presented in this thesis focuses on the first of these aims – delivering energy-aware nodes that are able to manage their energy resources efficiently and accept energy harvested from the environment. The research carried out by the author has fed into this project, and three of his conference publications have also been presented as deliverables of the AEASN project.

1.3 Justification for this research

Wireless sensor nodes must be capable of operating autonomously, and for many this means they must operate without the constraint of a wired power supply. Conventionally, such devices have been powered by non-rechargeable batteries which are replaced when depleted. However, energy harvesting (also known as energy scavenging) technology now offers the potential to sustain the operation of sensor nodes indefinitely. In this process, environmental energy is converted into electrical energy which is then used to directly power the sensor node, or is buffered (in rechargeable batteries or supercapacitors) for use later. Recent progress in the development of energy harvesting technologies (harvesting electrical energy from such sources as light, vibration, or temperature difference) now permits sensors to be free from the limitations of operation from non-rechargeable batteries. Indeed, the lifetime of the node will ultimately be limited by its other components, such as sensors or flash memory.

To deliver a long operational lifetime, nodes must ensure that they use energy carefully. Non-rechargeable batteries store a finite amount of energy which cannot be replaced, so nodes must operate efficiently in order to achieve their designed lifetime. Similarly, where nodes are powered from harvested energy they must, on average, use less power than is generated in order to deliver sustained operation. Energy is arguably the most critical resource for wireless sensors, and careful control of node activity to conserve energy is essential. Energy harvesting is often, by its nature, an inconsistent operation and the management of energy is a non-trivial task. Where nodes harvest energy from their environment, their energy status may change rapidly and adaptive behaviour is desirable. In addition, seemingly straightforward operations such as assessing the state-of-charge of certain energy storage devices can be difficult. The real-time assessment of the energy status of a sensor node can therefore be a highly complex task.

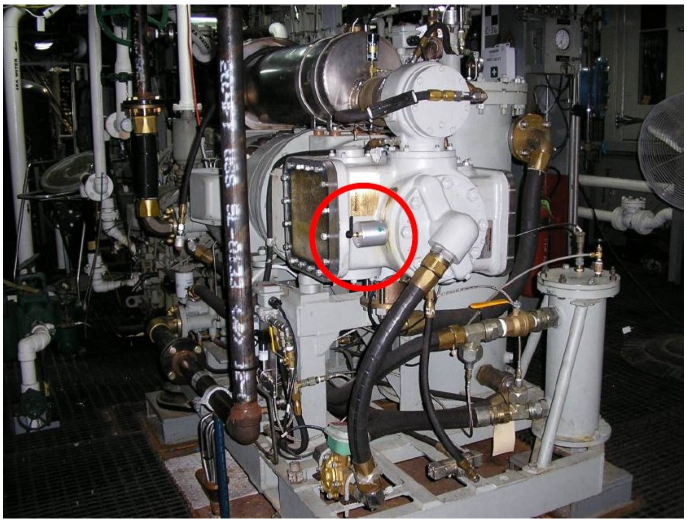

FIGURE 1.4: A S^{5}NAP vibration powered sensor node mounted on an air compressor during a trial (reproduced from [6]).

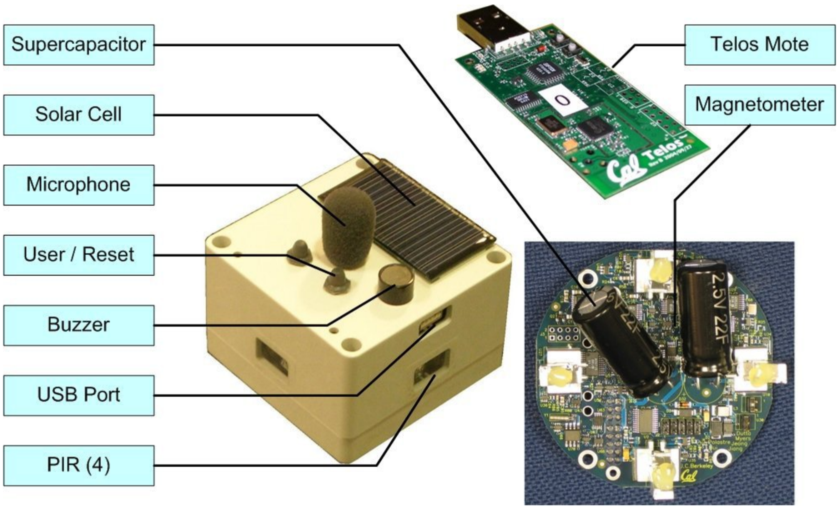

FIGURE 1.5: Trio wireless sensor node and its key components (reproduced from [7]).

At present, systems incorporating energy harvesting (such as the S^{5}NAP vibration-powered node shown in Figure 1.4, and the Trio outdoor solar-powered node shown in Figure 1.5) are designed for specific harvesting devices and are relatively inflexible. The re-configuration of the device to interface with an alternative energy harvesting device would require a re-design of the node's hardware and embedded software. Furthermore, there are very few nodes which allow the combination of multiple energy harvesting devices. To the best of the author's knowledge, there are no systems that allow the selection of appropriate energy hardware at the time of deployment (or, indeed, allow it to be changed *after* deployment). It may be argued that this is a major limiting factor for the applicability of wireless sensor nodes able to operate from environmental energy.

The justification for the work presented in this thesis is the development of reconfigurable, efficient, energy-aware wireless sensor nodes which are able to overcome these limitations. There is a need for devices to have a flexible energy subsystem that can accommodate a range of devices including energy harvesters, buffers, and non-rechargeable batteries. Information on the energy status of the system can be provided to the software application running on the node in order to control the node's activity level. As outlined in the following section, the scheme is verified on a sensor node in a challenging indoor environment, allowing energy components to be exchanged and for the node to recognise and handle these hardware changes, and remain aware of its energy status.

1.4 Contributions of this research

The scheme proposed in this thesis permits the energy resources of a sensor node to be configured in-situ by system installers at the time of deployment, and for the node to automatically recognise and manage its energy subsystem. For example, when the system is installed the appropriate types and sizes of energy harvesting and storage devices can be chosen and connected to the system. On first power-on, or indeed afterwards when a change is detected, the node interrogates a memory on each device to determine its operating parameters and other information. The introduced scheme permits multiple energy devices to be connected to a node, with the node able to address and manage each device individually. This represents a major step forward for the application of energy harvesting for sensor nodes, as nodes can now be efficient and energy-aware without being limited to a specific energy subsystem.

The scheme includes the implementation of a new embedded software structure, a novel common hardware interface to allow the sensor node to communicate with its reconfigurable energy subsystem, and a new 'energy electronic data sheet' format which allows data on parts of the energy subsystem to be stored on the modules themselves. Together, this represents a comprehensive scheme for reconfigurable energy-aware sensor nodes. This scheme is validated through the application of the methodology to a challenging application using a range of energy devices.

A prototype system has been deployed in an indoor environment, harvesting energy of the order of one milliwatt. It was developed under this scheme to sustain its operation, and has a plug-and-play energy subsystem which allows its energy components to be swapped at the time of deployment, or during its operation. In the deployment, the node is demonstrated with energy harvested from vibration, light, and thermal differences, with the energy being buffered in supercapacitors and rechargeable batteries. A non-rechargeable battery provides a last-ditch back-up for emergency use. The system is shown to operate from a range of devices, which are swappable during operation, and remains aware of its energy status throughout.

In line with the requirements detailed earlier, this thesis describes the development of processes to deliver reconfigurable, efficient, energy-aware sensor nodes. The main contributions of the research can thus be summarised:

1. **Electronic data sheets and hardware interfaces:** in order to deliver a reconfigurable 'plug-and-play' energy subsystem for wireless sensor nodes, it has been necessary to define an electronic data sheet format so that operating parameters can be stored on energy-related devices. This is a progression from the established 'transducer electronic data sheet' concept. A common hardware interface, which standardises the interface between the sensor node and its sensor hardware, has been developed to enable this data sheet to be read and allow the node's energy status to be monitored.

2. **Embedded software development:** an embedded software structure has been implemented which splits energy and sensor management tasks from the communications stack into their own separate software stacks. The energy stack interfaces with the energy hardware, including the electronic data sheets, through the hardware interface. It allows the application running on the sensor node to adapt its behaviour dependent on the amount of available energy.

3. **Energy harvesting and management:** circuits have been developed to manage energy from harvesting devices and batteries. Algorithms and circuits for the management of energy resources and determination of power status have also been developed. The dynamics of energy harvesting and storage devices have been characterised and implemented in the deployed system, with operating information being stored in the electronic data sheets and used by the embedded software.

Brought together, the work described in this thesis represents a comprehensive scheme for delivering reconfigurable wireless sensor nodes. The scheme defines the hardware and software interfaces between components, and provides a plug-and-play capability for the energy subsystems of nodes. The work has been verified through the deployment of the system in a demonstrator with a range of swappable energy components, and sensor node platforms, which are able to interface with the energy hardware.

The overall evaluation of the system is both quantitative and qualitative. Some parameters, such as the impact of adding circuitry to deliver energy-awareness, is relatively straightforward to evaluate; as is the additional processing overhead due to carry out these calculations. The net benefit to the system is in delivering energy-awareness through an integrated system. The process of developing and of deploying a system which is compliant with this scheme is explored and the benefits and drawbacks are expressed in terms of programming effort and ease of deployment.

1.5 What is 'reconfigurability'?

In the context of this thesis, 'reconfigurability' refers to the ability:

1. To select energy resources, as appropriate to the deployment environment, and connect them together at the time the system is installed.
2. To enable the energy resources to be exchanged while the system is operational, and for the system to recognise and adapt to these changes.
3. To realise these changes 'in the field' without access to specialist equipment: i.e. without needing to change the microcontroller's embedded software.

These capabilities mean that it is possible to set up the energy hardware on the device as appropriate to the environmental conditions, and to be able to reconfigure the energy hardware on the device without disrupting its operation. The reconfigurable system described in this thesis enables the system to remain energy-aware and manage its operation, regardless of the hardware used to power the device.

1.6 Publications

The following journal and conference papers have been produced as a result of the work carried out under this project:

1. Weddell, A. S., Harris, N. R. and White, N. M. (2008) "Alternative Energy Sources for Sensor Nodes: Rationalized Design for Long-Term Deployment". In: International Instrumentation and Measurement Technology Conference, May 12-15, 2008, Victoria, British Columbia, Canada.
2. Weddell, A. S., Harris, N. R. and White, N. M. (2008) "An Efficient Indoor Photovoltaic Power Harvesting System for Energy-Aware Wireless Sensor Nodes". In: Eurosensors 2008, 7-11 September 2008, Dresden, Germany.
3. Merrett, G. V., Weddell, A. S., Lewis, A. P., Harris, N. R., Al-Hashimi, B. M. and White, N. M. (2008) "An Empirical Energy Model for Supercapacitor Powered Wireless Sensor Nodes". In: 17th International IEEE Conference on Computer Communications and Networks, 3-7 August 2008, St Thomas, Virgin Islands (USA).
4. Weddell, A. S., Merrett, G. V., Harris, N. R. and Al-Hashimi, B. M. (2008) "Energy Harvesting and Management for Wireless Autonomous Sensors". Measurement + Control, 41 (4). pp. 104-108. ISSN 0020-2940

5. Weddell, A. S., Grabham, N. J., Harris, N. R. and White, N. M. (2008) “Flexible Integration of Alternative Energy Sources for Autonomous Sensing”. In: Electronics System-Integration Technology Conference, September 1-4, 2008, Greenwich, UK.

6. Merrett, G. V., Weddell, A. S., Harris, N. R., Al-Hashimi, B. M. and White, N. M. (2008) “A Structured Hardware/Software Architecture for Embedded Sensor Nodes.” In: 17th International Conference on Computer Communications and Networks, 3-7 August 2008, St Thomas, Virgin Islands (USA).

7. Merrett, G. V., Weddell, A. S., Berti, L., Harris, N. R., White, N. M. and Al-Hashimi, B. M. (2008) “A Wireless Sensor Network for Cleanroom Monitoring”. In: Eurosensors 2008, 7-11 September 2008, Dresden, Germany.

8. Weddell, A. S., Grabham, N. J., Harris, N. R. and White, N. M. (2009) Modular Plug-and-Play Power Resources for Energy-Aware Wireless Sensor Nodes. In: Sixth Annual IEEE Communications Society Conference on Sensor, Mesh and Ad Hoc Communications and Networks - SECON 2009, 22-26 June 2009, Rome, Italy.

A selection of these papers may be found in Appendix C. The author of this thesis has also co-authored a chapter entitled “Wireless Devices and Sensor Networks” for the book “Energy Harvesting for Autonomous Systems” (edited by Beeby, S. P., and White, N. M.) which is to be published by Artech House, London, in July 2010.

1.7 Document structure

The overall structure of this thesis is shown in Figure 1.6. Chapter 2 introduces the basis for the operation of sensor nodes: energy, sensing, and communications. It covers the available technologies for energy storage and generation, and how to monitor these resources. Intelligent sensing standards are also discussed, along with wireless transmission protocols relevant to sensing. It then looks at the current state-of-the-art in sensor nodes and existing systems operating from harvested energy. Later chapters present the fundamental work carried out in line with the aims of the project, along with description of practical developments including a demonstration system. Chapter 3 describes the design of a wireless sensor node as a reconfigurable system. The chapter covers the overall design of the system for reconfigurability, including the development of an energy electronic data sheet, common hardware interface, and algorithms for energy management. General structures for the system’s energy subsystem and its embedded software are also introduced. The development of prototype system hardware is described in detail in Chapter 4, with a discussion of the overall system design along with detailed consideration of each module developed. The embedded software implementation for the system is documented and evaluated in Chapter 5. This thesis concludes in Chapter 6 with a review of the work carried out and considers opportunities for standardisation and future development.

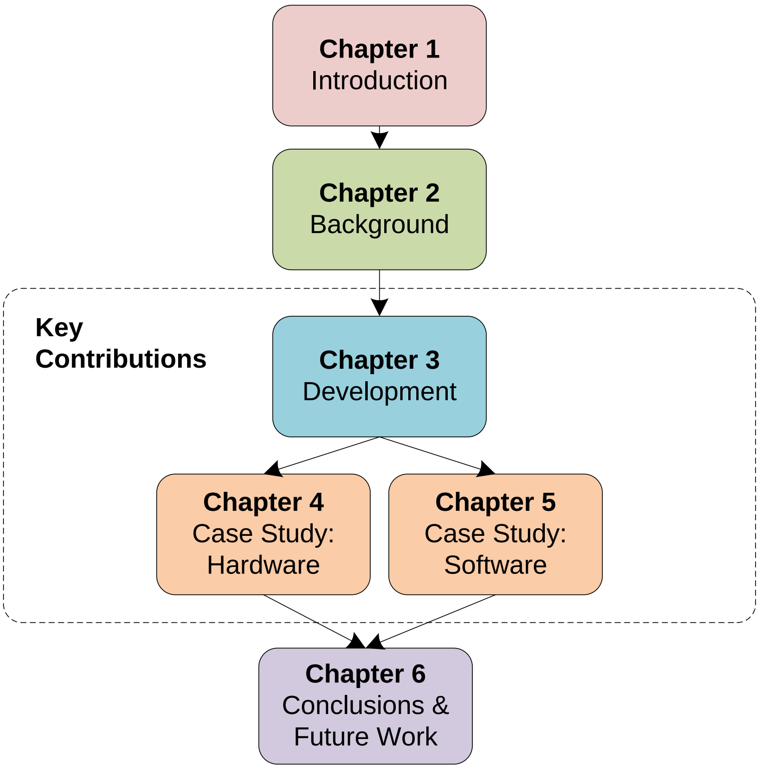

FIGURE 1.6: Thesis chapter structure.

Chapter 2

Background: Energy, Sensing, and Wireless Communication

2.1 Introduction

This chapter gives an overview of the technologies related to this project, and the current state-of-the-art in energy harvesting wireless sensor nodes. The energy devices covered are appropriate for milliwatt-scale sensor nodes, so large-scale energy generation and storage technologies (such as those used to augment or replace a mains electricity supply for high-power devices) are not covered. Technologies related to energy storage are introduced in Section 2.2, and energy harvesting and wireless power transfer technologies are discussed in Section 2.3. Standards and methods for intelligent sensing, including plug-and-play sensors and transducer electronic data sheets, are introduced in Section 2.4. Section 2.5 introduces wireless transmission protocols used by wireless sensor networks, and strategies for energy-aware operation are discussed in Section 2.6. Wireless sensor nodes and their underlying components are introduced in Section 2.7, and Section 2.8 discusses software and algorithm development. A range of sensor node deployments, including energy harvesting systems and a limited number of prototypes that support multiple energy devices, are introduced in Section 2.9.

2.2 Energy storage

2.2.1 Motivations and overview

As discussed in Chapter 1, wireless sensor nodes will normally operate from non-rechargeable batteries or (less commonly) energy harvested from their environment. The low rate of power generation from most energy harvesting devices means that they are generally unable to directly power nodes in their active mode, so it is normally necessary to 'buffer' energy to accommodate the periodic large bursts of current draw caused by duty-cycled operation (i.e. when the node becomes active after a period of 'sleep'). Electrical energy may also be stored for longer periods, for example overnight, to compensate for periods where energy cannot be generated. The buffering of energy is normally achieved by using rechargeable batteries, supercapacitors, or a combination of the two.

This section reviews a selection of popular battery and supercapacitor technologies, their characteristics, and considerations for their use with wireless sensors. Some alternative methods of energy storage are also considered, and the section concludes with a comparison between commercially-available energy storage devices considering factors such as energy density, leakage power, and cost.

2.2.2 Non-rechargeable (primary) batteries

Non-rechargeable (otherwise known as 'primary') batteries are by far the most prevalent technology for powering wireless sensor nodes, as they are relatively cheap and offer a high energy density compared to rechargeable batteries or supercapacitors. The batteries are either replaced when depleted, or the node is deployed with a battery which will last for the system's entire operational lifetime. In the field of low-power wireless sensor networks, two primary battery chemistries have achieved dominance:

1. In *short-term deployments*, or where sensor nodes are accessible and batteries can be changed without causing major disruption, *alkaline* (typically alkaline manganese dioxide, or similar) cells are most frequently used. This chemistry has a low self-discharge rate and hence a shelf-life of several years. This chemistry is very popular for use in consumer electronics devices, which means that its cost is relatively low.

2. For *long-term deployments*, where nodes may be inaccessible and battery replacement impractical or expensive, long-life *lithium* primary cells are generally used (typically lithium thionyl chloride $LiSOCl_2$). These have a very low self-discharge rate, and a higher specific energy and energy density than alkaline chemistries. These cells can have an operational life in excess of ten years, but are relatively expensive.

Detailed parameters for these battery types, along with information on other popular chemistries, are shown in Table 2.1. The nature of wireless sensor network deployments means that long lifetimes are desirable; otherwise the costs of regularly changing batteries could outweigh the savings made through not having to install cabling to sensors. The bursty characteristic of current draw by wireless sensor nodes when sensing and communicating must be supported by the battery without resulting in excessive voltage depression. These requirements rule out some common battery types, such as zinc carbon and smaller lithium coin cells, from use in this application.

	Zinc Carbon	**Alkaline**	**Lithium Manganese Dioxide**	**Lithium Thionyl Chloride**
Specific energy [Wh/kg][a,b]	85	145	380	230
Energy density [Wh/L][a,b]	165	400	715	535
Nominal voltage [V]	1.5	1.5	3.6	3.0
Open-circuit voltage [V][a]	1.6	1.5-1.6	3.65	3.3
Midpoint voltage [V][a,c]	1.25-1.1	1.25-1.15	3.6-3.3	3.0-2.7
End voltage [V]	0.9	0.9	3.0	2.0
Self-discharge [%/year][a,d]	7	4	1-2	1-2
Operating T [°C]	-10 to 50	-20 to 55	-60 to 85	-20 to 55
Discharge profile	Sloping	Mod. slope	Flat	Flat
Status	High production, decreasing popularity	Most popular primary battery	Mainly for special applications	Increasing consumer production
Advantages	Low cost	High capacity; good low-T low-rate performance	High E density, long shelf life	High E density, good low-T high-rate
Limitations	High gassing rate, poor performance	Moderate cost but best at high rates	Voltage delay after storage	Limited sizes and shipping

[a] At 20°C.

[b] For cylindrical cell.

[c] For favourable discharge conditions.

[d] Normally decreases with time of storage.

Table 2.1: Non-rechargeable battery types and characteristics (adapted from [8]).

One of the longest documented deployments of a wireless sensor – an Automatic Meter Reading (AMR) system for a water meter which has been operating for over 20 years – is powered by a Tadiran lithium primary cell [9]. The fact that lithium cells have been demonstrated operating for very long periods of time is a welcome verification of the application of this technology to long-term wireless sensing applications. An arguable drawback of these cells, however, can be their flat discharge profile. As shown in Figure 2.1, end-of-life for these lithium cells can only be detected passively up to 3% before cut-off (or actively, by applying a pulsed load to the cell, up to 15% before cut-off). In a deployment of ten years, this 3% warning corresponds to approximately three months, or a 15% indication is equivalent to 18 months. Providing that the sensor node draws the expected amount of current, this in itself is not problematic (three months is, in most applications, an acceptable amount of time to arrange battery replacement). In the case of a malfunctioning sensor that is drawing a substantial amount more current than expected, however, the warning period would clearly be much shorter. The difficulty of identifying the end-of-life or state-of-charge of primary batteries is a major drawback for their application in wireless sensor nodes. Primary batteries are resources that cannot be used after they have been expended (except for some negligible recovery effects); therefore, energy must be used conservatively at all times (to compensate for the poor resolution of energy-awareness) in order to ensure that desired system lifetimes can be achieved.

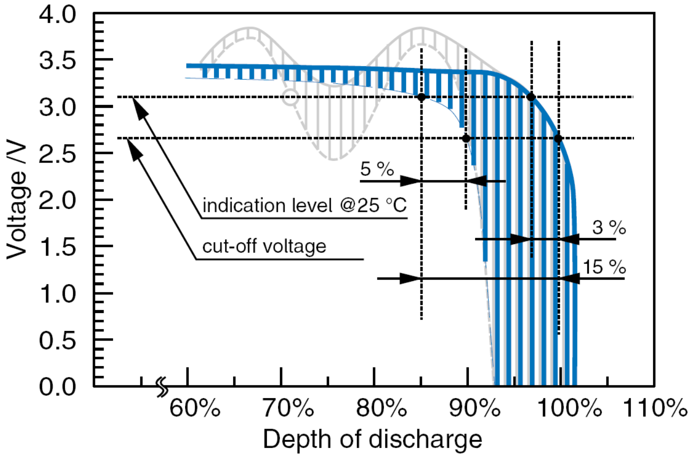

Figure 2.1: End-of-life indication for lithium primary batteries. The grey curve shows seasonal temperature cycles, the solid curve shows discharge on continuous load at +25°C, and the dashed curve shows the trend of test pulses (reproduced from Tadiran technical brochure [10]).

2.2.3 Rechargeable (secondary) batteries

Some of the most frequently-used rechargeable (also known as 'secondary') battery chemistries in wireless sensor network applications are lithium-ion, lithium-polymer, and nickel metal hydride. Figure 2.2 shows a comparison of the energy densities of rechargeable battery types; the battery capacity values quoted in data sheets, however, only give part of the story. The amount of energy that can be provided by a battery is highly dependent on the methods of charge and discharge, and the conditions in which it is kept [11]. For example, lithium-ion cells are highly sensitive to overcharge and undercharge, and thus protection circuitry must be built in. Different battery chemistries require other charging methods: lithium-ion batteries require a constant charging current until they have reached 90% capacity, followed by a constant voltage. NiMH and NiCd batteries prefer a constant current throughout the recharge process [12].

With modern cell constructions, memory effects are now negligible. NiCd cells have historically been most susceptible to this effect, but the Handbook of Batteries states that *"most users may never experience low performance due to memory effect ... the use of the term 'memory effect' persists, since it is often used to explain low battery capacity that is attributable to other problems"* [8]. The number of cycles that the battery can go through is dependent on its chemistry and other factors, but modern cells generally

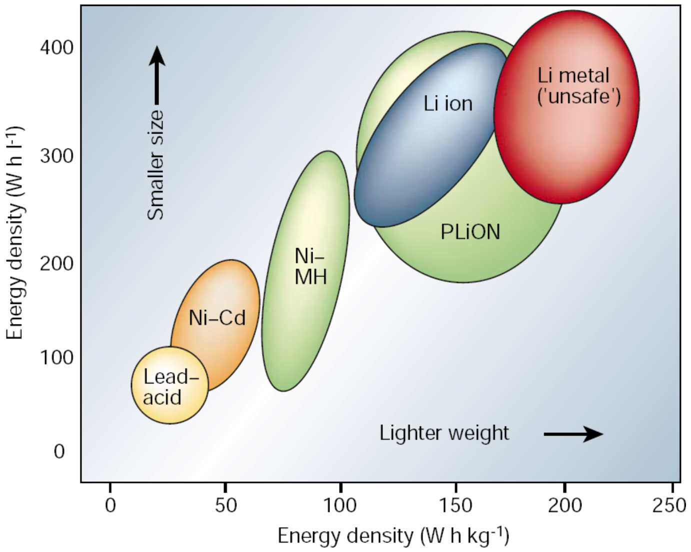

FIGURE 2.2: Comparison of rechargeable battery types in terms of volumetric and gravimetric energy densities (reproduced from Tarascon and Armand [13]).

have a lifetime of at least a few hundred cycles. Another parameter (rarely quoted, but important to energy-harvesting nodes) is the 'coulometric efficiency'. This indicates the proportion of energy stored against the energy expended in charging. A figure of 99.9% is typical for lithium-ion cells, but is somewhat lower for other battery chemistries (and highly dependent on charging conditions) [8]. Some typical parameters for the most commonly-used secondary battery types are shown in Table 2.2.

	Lead acid	**NiCd**	**NiMH**	**Lithium**
Specific energy [Wh/kg]	30	35	75	150
Energy density [Wh/L]	90	100	240	400
Nominal voltage [V]	2.0	1.2	1.2	4.0
Open-circuit voltage [V]	2.1	1.29	1.4	4.1
Operating voltage [V]	2.0-1.8	1.25-1.00	1.25-1.10	4.0-3.0
End voltage [V]	1.75	1.0	1.0	3.0
Self discharge [%/month]	4-8	15-20	15-25	2
Calendar life [years]	2-8	2-5	2-5	?
Cycle life [cycles]	250-500	300-700	300-600	1000+
Discharge profile	Flat	Very flat	Flat	Sloping
Advantages	Long life on float, T-independent	Good low-T high-rate	High E-density	High E-density
Limitations	Can't store discharged, low cycle life	Memory effect	Moderate cost	Low rate

[a] At room temperature 25°C.

TABLE 2.2: Rechargeable battery types and characteristics (adapted from [8])

2.2.4 Supercapacitors

Supercapacitors (also known as ultracapacitors, electrochemical capacitors, or electric double-layer capacitors) offer a much higher energy density than aluminium electrolytic capacitors, but retain many of their other characteristics. Unlike conventional capacitors (which have two 'plates' separated by a dielectric), supercapacitors have two layers of the same substrate (typically activated carbon) which store charge, separated by a very thin material. Their operation is more complex than conventional capacitors (but they loosely follow the standard capacitor equation), and due to their thin insulator they will typically have a lower operating voltage. They are relatively insensitive to charge/discharge cycling and require no special charging circuitry [14]. However, their energy density remains an order of magnitude below those of conventional secondary batteries and their leakage (or self-discharge) rates are also relatively high. Supercapacitors have been incorporated into self-powered sensing systems where they provide a cache between harvesting sources, a secondary battery, and a sensor node. Jiang *et al.* [15] carried out experiments to determine the self-discharge rates of a number of supercapacitors, and found that the worst-performing supercapacitor lost approximately 50% of its energy through leakage in 16 hours, and that the capacitor size does not give an indication of likely self-discharge rate. There is, however, some doubt over whether the observed effects were attributable to leakage, or the redistribution of charge within the supercapacitor.

A common range of supercapacitors is the Panasonic Gold series: their technical guide [16] has information on the modelling and behaviour of supercapacitors. Wireless sensor nodes, such as the those described in Section 2.7.1, draw around 30mA when fully active and communicating (excluding the current draw of any additional sensors or peripherals). The Panasonic HW series has a maximum operating voltage of 2.3V, maximum operating temperature of 70°C, and guaranteed lifetime of 1,000 hours [16]. Continued developments in supercapacitor technology are improving their characteristics. For example, the CAP-XX range of supercapacitors have thin prismatic packages, low self-discharge currents and are able to sustain high levels of peak current. For example, the HS208 model [17] has a typical leakage current of 1.0μA after being charged for 72 hours and can tolerate a comparatively high peak current of 20A.

2.2.5 Other energy storage mechanisms

Some alternative energy storage technologies exist. For example, fuel cells have been forecast to be a high-capacity replacement for batteries; however, current research indicates that, due to constraints on size and the requirement for precision machining, micro fuel cells are unlikely to offer substantially higher energy densities than primary batteries [18]. Even where electrodes can be microfabricated, the task of microfabricating the fuel reservoir and plumbing is substantial. Fuel cells, however, offer higher power densities and therefore may be of use in sensor nodes with a high current requirement. Some research micro-fuel cells have been demonstrated with success, including a fuel system providing 25mA from a thin-film cell with an area of 2cm^2 [19]. Alternatively, advances in micromachining have opened up the possibility of creating micro-heat engines to produce electrical power from hydrocarbon fuels. There are a number of possible approaches to design of the heat engine, including piston-based combustion engines, Wankel internal combustion engines, and micro gas turbine engines. The P_3 micro heat engine makes use of thermal expansion to generate electrical power by means of a piezoelectric material [20]. Conversely, radioactive sources could potentially offer massive energy densities – for example, the ^{63}Ni isotope has been used by Li and Lal [21] to actuate a conductive cantilever. Beta particles emitted from the isotope collect on the cantilever, which effects an electrostatic attraction, eventually causing the cantilever to contact the isotope and discharge, and the process restarts. Along similar lines, Fleurial [22] presents a survey of technologies, including the combination of Radioactive Heat Units (RHUs) with thermoelectric generators.

2.2.6 Discussion

This section has covered the available technologies for energy storage, focussing on primary and secondary batteries and supercapacitors (with some additional consideration of other energy storage mechanisms). In summary, primary batteries have the advantage that they have a high energy density, long shelf-life, and relatively low cost; however, they are a limited resource that must be replaced when expended. Some of the long-life technologies also have a stable discharge characteristic which limits the resolution of state-of-charge determination or end-of-life identification. Conversely, secondary batteries can be recharged, and offer broadly similar energy densities to those of primary batteries; however, they are sensitive to the number of charge/discharge cycles to which they are exposed, and must be charged in a controlled manner to maximise their lifetime. Finally, supercapacitors offer an energy density which is approximately an order of magnitude lower than those of batteries, exhibit capacitor-like behaviour, and are relatively insensitive to the method of charge or discharge. The choice of energy storage technology is highly dependent on the other considerations for the energy subsystem of the sensor node but, due to their favourable characteristics, supercapacitors are most commonly used in systems which feature energy harvesting technology.

2.3 Energy harvesting and wireless power transfer

2.3.1 Motivations and overview

In this thesis, 'energy harvesting' (also known as 'power harvesting', or perhaps most appropriately as 'energy scavenging') is defined as being the process in which electrical energy is produced through the exploitation of naturally-occurring environmental or human energy. Devices with a finite fuel supply (such as miniature fuel cells) fall outside the scope of this section and have already been considered in Section 2.2. The technologies behind the harvesting of power from light, vibration, and thermal differences are introduced here, along with detailed discussions about the realistic levels of power which can be derived and the methods of interfacing with the devices. Other, less common, energy harvesting methods are also considered in this section, along with wireless power transfer technologies.

A number of reviews of energy harvesting techniques have been published, with Roundy *et al.* [18] providing one of the most comprehensive surveys. Mateu and Moll [23] have also provided a rounded review, including some consideration of conversion circuitry design. Perhaps one of the most recent and comprehensive reviews of energy harvesting from the motion of humans or machines has been reported by Mitcheson *et al.* [24].

2.3.2 Photovoltaics

Photovoltaic (PV) cells produce electricity from photons by means of a semiconductor p-n junction. This technology is at a relatively advanced stage of development, and many deployment situations for autonomous sensors are lit by natural or artificial lighting (or a mix of both). Table 2.3 shows typical lighting levels in a range of situations. Reich *et al.* [25] have analysed the efficiencies of a range of photovoltaic cells at low illumination levels. The results of this investigation are of some interest, as they give an idea of the levels of power to be expected from solar cells located indoors in artificially-lit environments. Figure 2.3 shows the results of one such survey and indicates that the choice of cell technology is of great importance, particularly in low-light situations. Randall and Jacot have analysed whether the industry-standard test (known as AM1.5) to measure the performance of solar cells is of use to designers, where the intensity and spectral content of light sources is likely to differ greatly from ideal test conditions [26]. The difference between the performance of PV cells under filtered AM1.5 light and under fluorescent lighting has been analysed and some technologies exhibit significant performance changes, as shown in Figure 2.4.

Photovoltaic cells can be treated as voltage limited current sources, and are characterised by their open-circuit voltage (V_{oc}) and short-circuit current (I_{sc}), along with other parameters. As incident light levels drop, short-circuit current will typically decrease, while

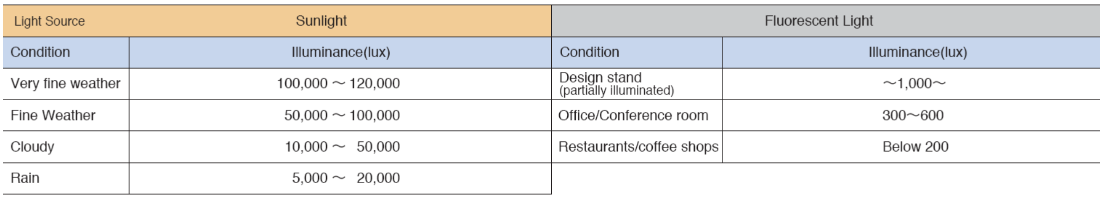

Light Source	Sunlight	Fluorescent Light	
Condition	Illuminance(lux)	Condition	Illuminance(lux)
Very fine weather	100,000 ～ 120,000	Design stand (partially illuminated)	～1,000～
Fine Weather	50,000 ～ 100,000	Office/Conference room	300～600
Cloudy	10,000 ～ 50,000	Restaurants/coffee shops	Below 200
Rain	5,000 ～ 20,000		

TABLE 2.3: Typical indoor and outdoor brightness levels (reproduced from [27]).

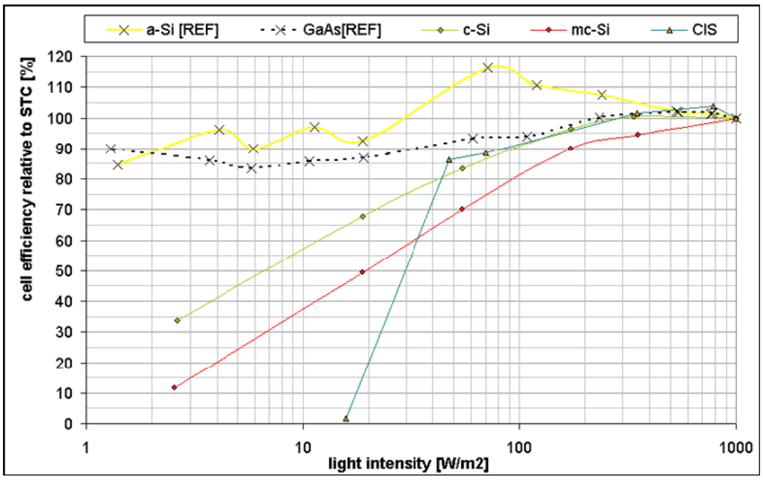

FIGURE 2.3: Efficiencies of a range of PV cell technologies at different light intensities relative to standard test conditions (STC) (reproduced from Reich *et al.* [25]).

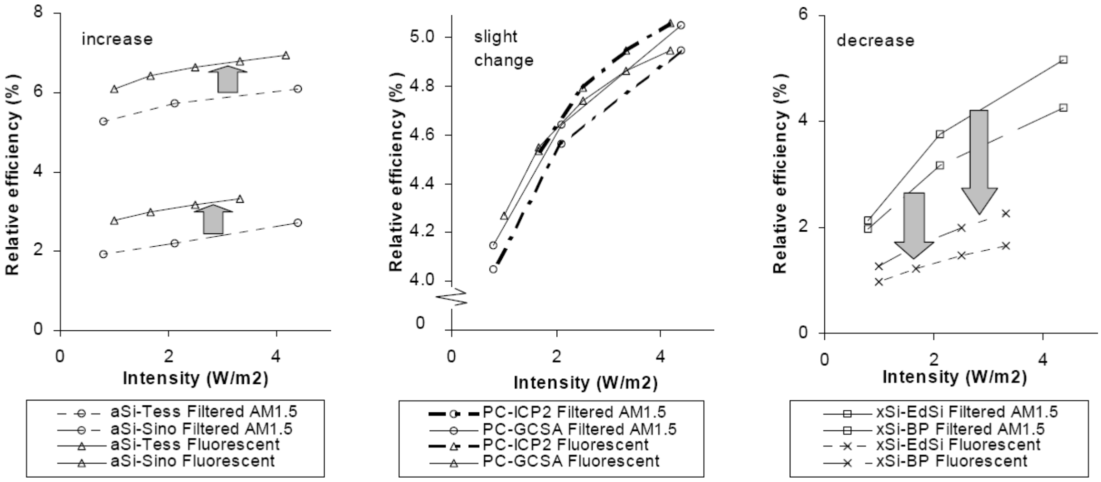

(A) Amorphous Si (B) Dye Cell (C) Crystalline Si

FIGURE 2.4: Comparative efficiency of PV cells under filtered AM1.5 and fluorescent spectrum light, for two samples of three PV cell technologies (reproduced from Randall *et al.* [26]).

open-circuit voltage will remain fairly constant. Figure 2.5 shows a photovoltaic module from Schott Solar, along with its performance curves at various light levels. This cell is optimised for indoor use and at lower light levels it has higher efficiency levels than alternative technologies. As an example, a module with dimensions 90mm x 72mm has a nominal power of 324μW at 200 Lux and 1.79mW at 1,000 Lux. A challenge is to run the cell at its optimal operating point in order to maximise the obtained power. Dynamic loads such as wireless sensor nodes cannot generally be run directly from the cell, as this will result in a varying load impedance; typically, a secondary battery or storage capacitor is used to buffer energy for the system.

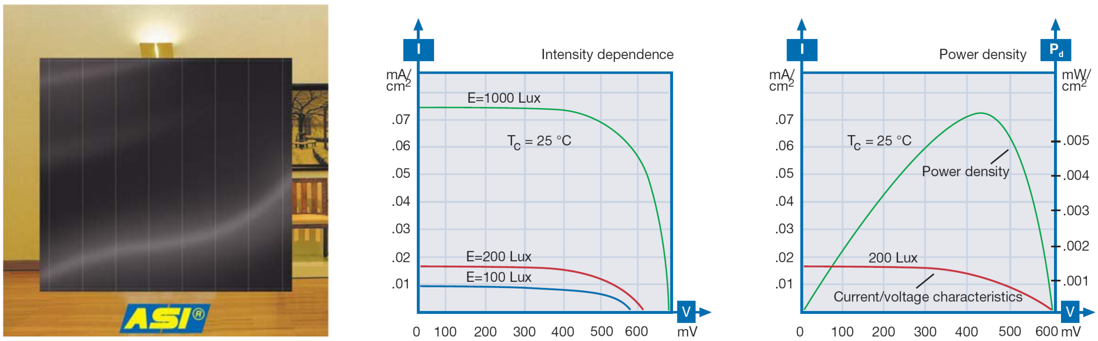

(A) Module (B) Intensity dependence (C) Power density

Figure 2.5: The appearance and operating characteristics of a Schott Solar ASI Indoor Photovoltaic Module (reproduced from [28]).

Cells are reliant on sufficient levels of light penetrating the glass to reach the p-n junction. Over a 10 year deployment, significant residue can be expected to build up on a sensor node package, especially in an industrial environment. This can significantly degrade the cell performance, reducing the harvesting efficiency. It must be ensured that the package can be cleaned easily, or that the effects of dust and residue are minimised.

2.3.3 Vibration energy harvesting

General principles

Vibration energy harvesting is a technology which allows electrical energy to be parasitically generated from (generally unwanted) vibrations, normally of machinery, to power electronic devices such as wireless sensors. Vibration energy harvesters have the advantage that, unlike photovoltaics, they are not subject to the effects of dust accumulation. Generators are typically one of three types which are discussed later in this subsection: electromagnetic, piezoelectric, and electrostatic. Table 2.4 shows the results of a survey carried out in the USA, which shows the peak acceleration and frequency of vibration of a range of objects; it may be noted that, as the mains frequency in the USA is 60Hz, a number of electrical devices in this table exhibit twice-mains-frequency vibrations.

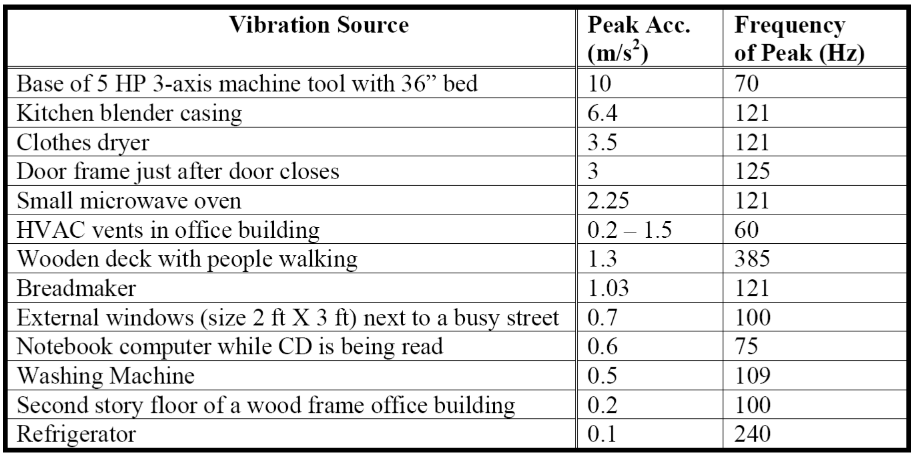

Vibration Source	Peak Acc. (m/s^2)	Frequency of Peak (Hz)
Base of 5 HP 3-axis machine tool with 36” bed	10	70
Kitchen blender casing	6.4	121
Clothes dryer	3.5	121
Door frame just after door closes	3	125
Small microwave oven	2.25	121
HVAC vents in office building	0.2 – 1.5	60
Wooden deck with people walking	1.3	385
Breadmaker	1.03	121
External windows (size 2 ft X 3 ft) next to a busy street	0.7	100
Notebook computer while CD is being read	0.6	75
Washing Machine	0.5	109
Second story floor of a wood frame office building	0.2	100
Refrigerator	0.1	240

Table 2.4: List of vibration sources with their maximum acceleration and peak frequency, carried out in the USA (reproduced from [29]).

Vibration energy harvesters can be coarsely modelled by the linear system shown in Figure 2.6. Here, m is the mass of the oscillating object, k is the spring constant, and c_T is the damping coefficient. Also, y is the input displacement and z is the resultant spring displacement. The term c_T is a combination of electrical and mechanical damping. In simple electromagnetic generators, the electrical damping is linear, but the damping effect becomes more complex for alternative generator types [30]. This simple model can be expressed by Equation 2.1.

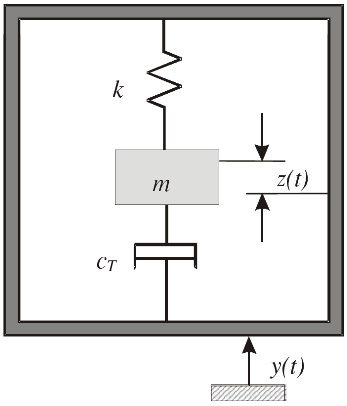

Figure 2.6: Model of a linear, inertial generator (reproduced from [31]).

$$m\ddot{z}(t) + c_T\dot{z}(t) + kz(t) = -m\ddot{y}(t) \qquad (2.1)$$

The detailed modelling of the behaviour of vibration energy harvesters is outside the scope of this thesis; however, it is important to note that the dynamics of the load attached to the generator can affect the electrical damping and hence the overall performance of the generator. Most generators are ‘tuned’ to specific frequencies (normally mains frequency or twice-mains-frequency, which are the most prevalent frequencies in electrical machinery). Some techniques have been developed to modify the resonant frequency of vibration energy harvesters, either by mechanical tuning or by adjusting the dynamics of the electrical damping of the system [32].

Electromagnetic

Electromagnetic generators normally use a resonant beam and coil arrangement, with movement of a magnet relative to a coil inducing an electrical current. A number of research groups have developed electromagnetic converters, with varying levels of success. This technology is particularly applicable to harvesting lower-frequency vibrations: for example, Amirtharajah and Chandrakasan's generator was designed to work with frequencies of approximately 2Hz (the frequency of footfalls for human walking), with a claimed power output from their generator of the order of 400μW [33]. Commercial generators are now able to harvest energy from vibrating machinery. PMG Perpetuum have developed two versions of their PMG17 generator [34] (shown in Figure 2.7) tuned to 100Hz and 120Hz, and FerroSolutions manufacture a similar device, the VEH-360, which is tuned to 60Hz [35].

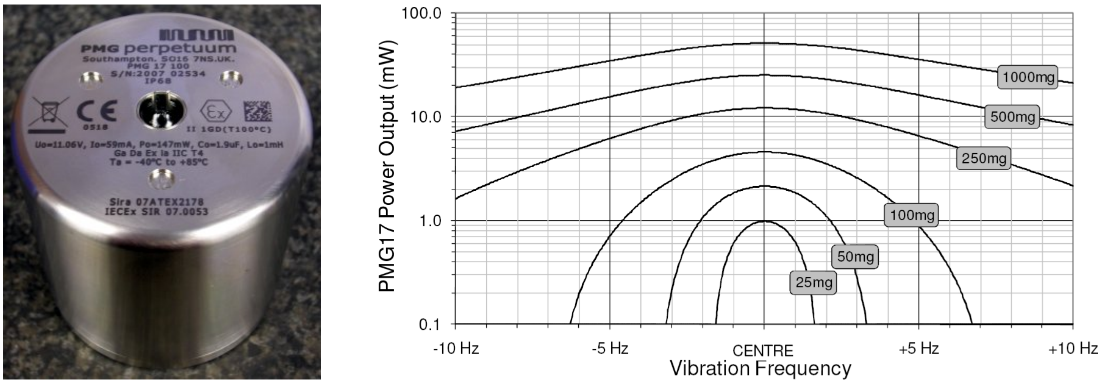

(A) Generator (B) Performance

Figure 2.7: PMG Perpetuum's PMG17 vibration harvesting generator, and its data sheet frequency response (reproduced from [34]).

Efforts are continuing to miniaturise the electromagnetic generator (the PMG Perpetuum model pictured has a height of 55mm and a diameter of 55mm). The device shown in Figure 2.8, developed by Torah *et al.* [36] has a total volume of approximately 1cm^3, and has been demonstrated powering a wireless sensing and transmission system. A drawback of this generator is its fragility and the intricate processes required in its manufacture: for example, the coil has 2,800 turns using 12μm diameter copper wire. While the manufacture of electromagnetic vibration energy harvesters is generally intricate and expensive, their major strength is that they are relatively low-impedance sources that produce moderate voltages that can be efficiently rectified and used to power electronic devices.

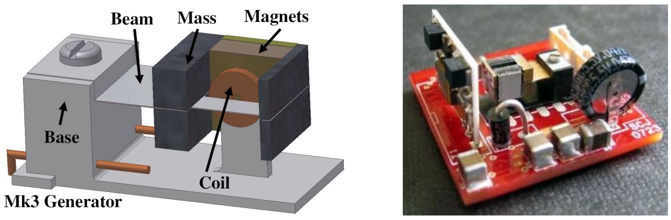

(A) Generator

(B) System

Figure 2.8: A miniaturised electromagnetic microgenerator: (a) the total volume of the generator is approximately 1cm^3, and (b) it has been incorporated into a wireless microsystem (reproduced from [36]).

Piezoelectric

Piezoelectric materials have two complementary properties: they deform when subjected to an electric field, or produce electrical charge when mechanically deformed. The second property is of greatest interest in this application, as it provides the basis for electrical power generation from vibration. Resonant structures can be fabricated, and the periodic deformation of the piezoelectric material causes electrical charge to be produced during each oscillation. Piezoelectric generators have the advantage that their design, analysis and fabrication is straightforward. It is relatively easy to produce a working prototype with satisfactory voltage and current characteristics, as shown by Roundy and Wright's prototype [37], which is based on the principle shown in Figure 2.9. In this example, the generator is simply formed of a piezoelectric beam and large mass. When the beam and mass arrangement are subjected to vibrations at their resonant frequency, deformation of the piezoelectric beam produces large voltages.

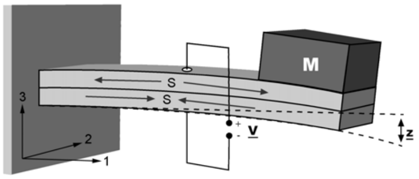

Figure 2.9: Two-layer bender mounted as a cantilever (reproduced from [37]).

An advantage of piezoelectric devices is that they do not need an additional voltage source to begin operation (differing from electrostatic generators in this respect), and are better suited to mass-production than electromagnetic generators. It may be summarised that piezoelectric generators share many of the advantages of electromagnetic and electrostatic generators. Piezoelectric generators, however, are not as suitable as electrostatic generators for production using standard MEMS processes. Another drawback is that they are high-impedance sources that produce high voltages but low current, which can be difficult to convert efficiently to DC. Piezoelectric-based vibration energy harvesting technology has been commercialised by AdaptivEnergy [38] (as shown in Figure 2.10) and Midé with their 'Volture' generator range [39].

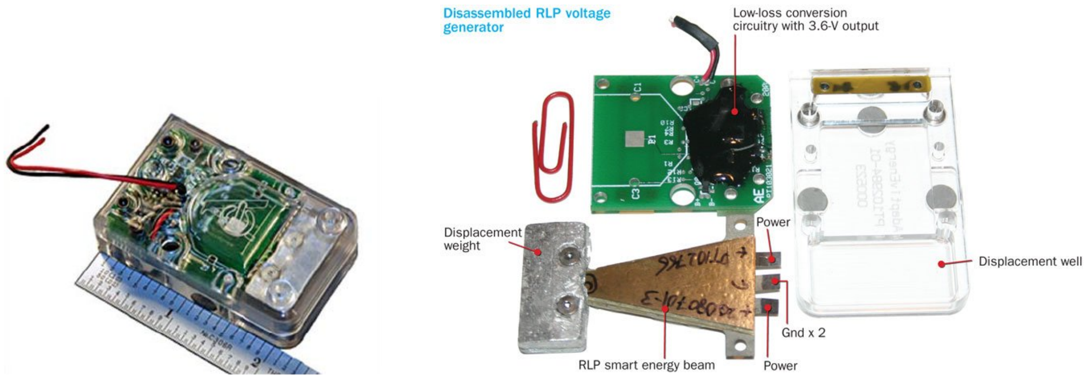
Disassembled RLP voltage generator
Low-loss conversion circuitry with 3.6-V output
Displacement weight
Power
Displacement well
Gnd x 2
RLP smart energy beam
Power

(A) Device

(B) Components

FIGURE 2.10: The AdaptivEnergy piezoelectric vibration energy harvester (a) in its packaging and (b) disassembled showing its components (reproduced from AdaptivEnergy promotional materials [38]).

Electrostatic

Electrostatic-based vibration energy harvesting requires two conductors moving relative to each other and separated by a dielectric (effectively acting as a capacitor). Movement in the conductors causes the amount of energy stored in the capacitor to change, which can be exploited to extract energy. There are two main modes of energy conversion: charge constrained and voltage constrained. The two methods are compared by Meninger *et al.* [40], with the conclusion that charge-constrained conversion delivers less energy by a factor of V_{start}/V_{max} (where V_{start} is the initial voltage applied and V_{max} is the maximum voltage reached), although there are hybrid alternatives which may deliver improved efficiency. Figure 2.11 shows the operating principles of the three main types of electrostatic generator. The in-plane gap closing type is believed to be the most efficient [29]. The performance of this device is expressed by Equation 2.2 which gives the voltage, V, stored across a rectangular parallel plate capacitor. Here, q represents the charge on the capacitor, d is the distance between the capacitor plates, ϵ_0 is the permittivity of free space, and l and w are the length and width of the capacitor plates.

$$V = \frac{qd}{\epsilon_0 lw} \tag{2.2}$$

Hence the capacitance, C, is given by Equation 2.3.

$$C = \frac{\epsilon_0 lw}{d} \tag{2.3}$$

Electrostatic generators are perhaps the best suited to fabrication using standard MEMS processes, but they have two main disadvantages. Firstly, they require an initial voltage to be applied across the capacitor plates in order to begin the conversion process (which means they are unsuitable for applications where a 'cold-starting' capability is required). Secondly, the requirement for the plates to remain separated (to avoid short circuit) necessitates the use of mechanical 'stops' to constrain the motion of the plates. This brings its own reliability issues. A number of attempts have been made to fabricate MEMS electrostatic generators but at the time of writing this report prototypes were experiencing reliability issues connected to the endurance of the devices. It appears likely that advances in processing techniques and design will yield positive results in the near future.

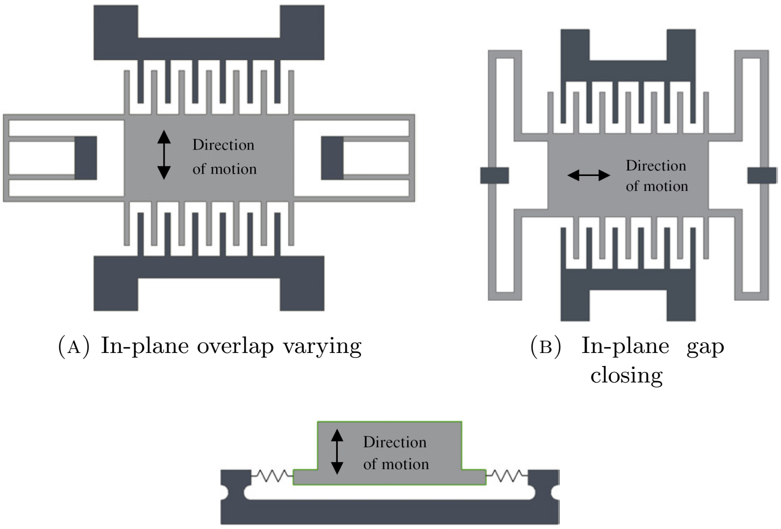

(A) In-plane overlap varying

(B) In-plane gap closing

(C) Out-of-plane gap closing

FIGURE 2.11: Variants of electrostatic energy harvesters (reproduced from [29]).

2.3.4 Thermoelectric energy generation

Thermoelectric generators exploit the Seebeck effect [29] to convert temperature differentials into an electro-motive force. The maximum efficiency of power conversion from a temperature difference is represented by the Carnot efficiency, η, shown in Equation 2.4, where T_{high} and T_{low} are the temperatures on the 'hot' and 'cold' sides of the thermocouple, and are measured in degrees Kelvin [29].

$$\eta = \frac{T_{high} - T_{low}}{T_{high}} \tag{2.4}$$

The maximum amount of power available may be estimated by quantifying the heat flow through a material. Roundy *et al.* [18] state that convection and radiation may be ignored at low temperature differentials. The amount of power (flow of heat) through a material is given by Equation 2.5. Here, q' is the heat flow through the material, k

is the thermal conductivity of the material, ΔT is the temperature difference across the thermocouple, and l is the length of the material.

$$q' = k\frac{\Delta T}{l} \tag{2.5}$$

Ongoing work in the field of thermoelectric energy generation appears to have the aim of exploiting thick-film techniques in combination with IC etching in order to create complex structures comprising thousands of leg thermocouples. Indeed, Fleurial *et al.* claim that *"for relatively small temperature differences, such as 10 to 20K, high specific power outputs in the 1 to 10 W/cm^3 range are potentially achievable provided that the legs be no thicker than 50 to 100 μm"* [41]. Böttner *et al.* [42] have produced a micro-thermogenerator using thin-film technology combined with micro-system technology. This has been commercialised by Micropelt, which has developed a prototype thermoelectric generator integrated into an M24 bolt, as shown in Figure 2.12. It may be observed that the power obtained from the device is highly dependent on the airflow it is exposed to. A separate development by Tellurex has produced a device which allows burning fuels to be converted into electrical energy by means of the their PG1 kit shown in Figure 2.13. This device has a heatsink with fan – the power provided by the thermoelectric generator is sufficient to run the fan, which forces airflow through the heatsink – thus improving the overall efficiency of the generator and increasing the level of generated electrical power.

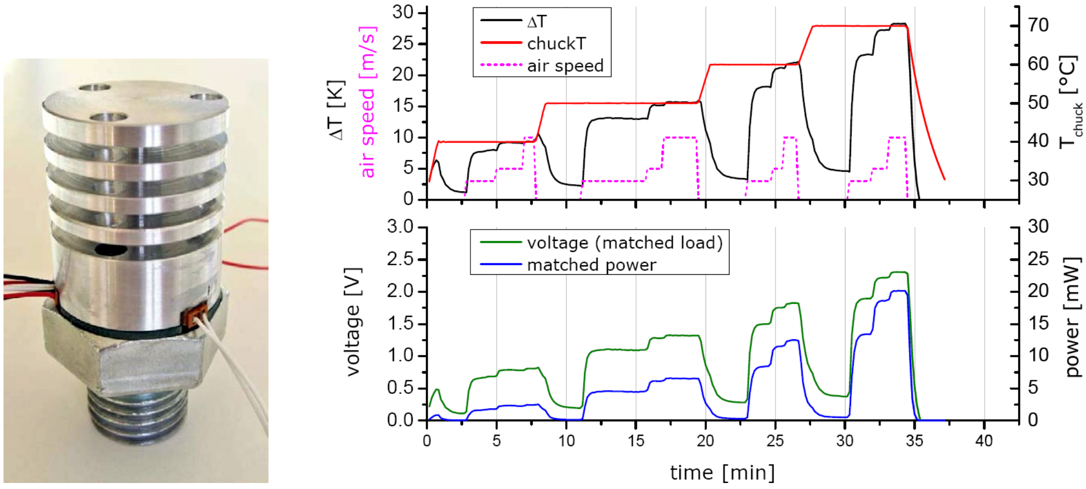

(A) Bolt

(B) Performance

FIGURE 2.12: The Micropelt 'Generic Power Bolt' based on an M24 machine bolt and its performance in natural and forced convection with air speeds of 3ms^{-1}, 5ms^{-1}, and 10ms^{-1}, demonstrating the effect of movement on efficiency of the harvester (reproduced from [43]).

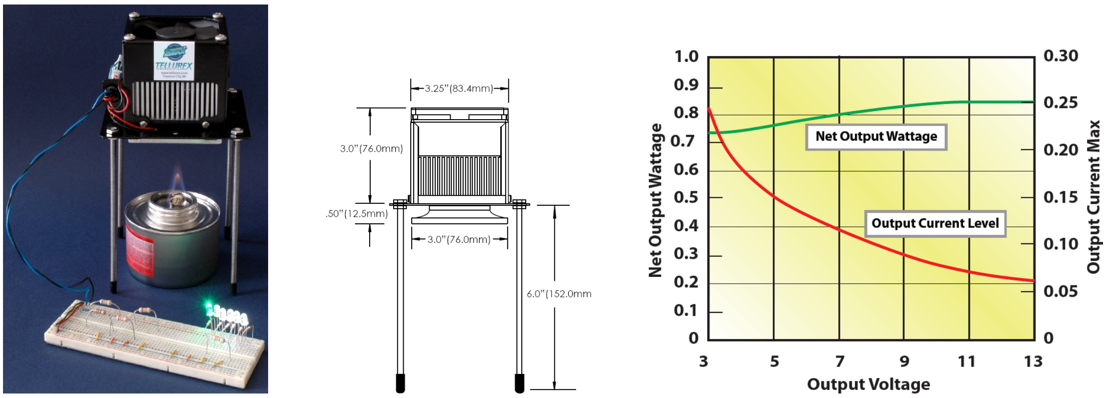

(A) System

(B) Dimensions

(C) Performance

Figure 2.13: The Tellurex PG1 Power Generation Kit, which generates electrical energy from an open flame, and its electrical performance (reproduced from [44]).

2.3.5 Small-scale fluid flow

The generation of power from wind or water flow is popular and successful on a large scale. This experience has been transferred to the generation of energy from small-scale fluid flow to provide energy to sensor nodes. Many sensors are located close to moving fluids: for example, liquids in pipes or air in ducts. The flow of fluid such as air or water past a sensor has the potential to provide a source of power, although it would be reasonable to assume that efficiency levels would be significantly lower for smaller devices. In their review of potential energy sources for wireless sensor nodes, Roundy *et al.* state that power densities from air flow are promising and warrant further research [18]. The potential power, P, from a moving fluid is given by Equation 2.6. Here, ρ is the density of the fluid, A is the cross-sectional area, and ν is the velocity of the fluid.

$$P = \frac{1}{2}\rho A \nu^3 \tag{2.6}$$

A device harvesting energy from the flow of water in a pipe, shown in Figure 2.14, has been used by Morais *et al.* [45]. The hydrogenerator was manufactured by Vulcano and is more commonly used in domestic water heating, providing electricity to ignite a gas boiler when water flows (with one of the main benefits being that the boiler does not need a mains electricity connection). The same project has also developed a vertical wind-powered generator shown in Figure 2.15a and 2.15b. Similarly, the AmbiMax project has used a small off-the-shelf wind turbine to power a wireless sensor node, as shown in Figure 2.15c.

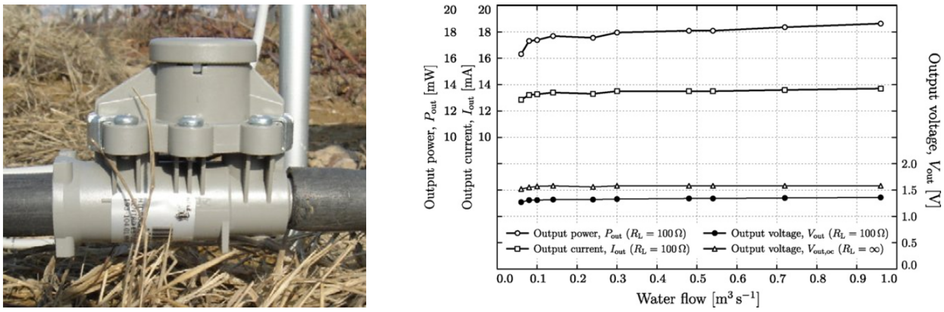

(A) Device (B) Performance

FIGURE 2.14: Bosch Hydropower generator used with the MPWiNodeX (reproduced from [45]).

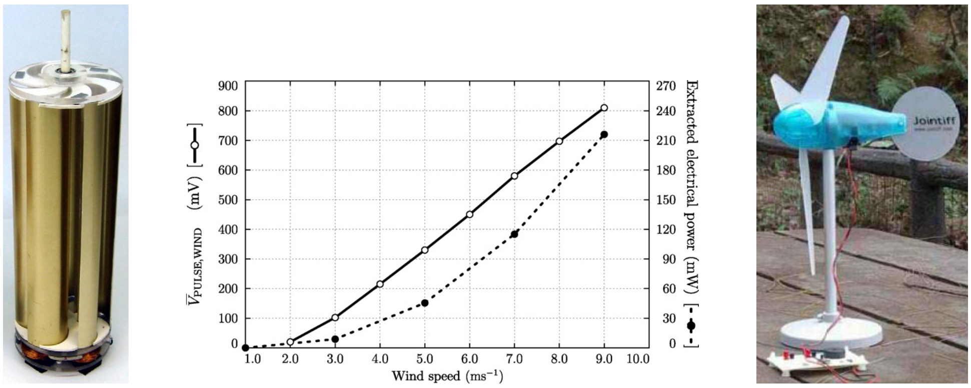

(A) (B) (C)

FIGURE 2.15: Wind-powered generators used by wireless sensor nodes: (a) is a prototype vertical unit used by Morais *et al.* and (b) is its performance at a range of wind speeds (reproduced from [45]) (c) is an off-the-shelf turbine used by Park *et al.* (reproduced from [46]).

2.3.6 Human power

Human power may be categorised as being either active or passive. An actively powered device requires the user to do a form of work that would not otherwise be done, specifically in order to power the device. Conversely, a passively powered device harvests energy from the user's normal bodily motion and properties, not requiring any additional work. Among the earliest human-powered wearable devices have been wristwatches; for example, the Seiko Kinetic range harvests power from arm movement, while Seiko's Thermic technology can power the wristwatch from the temperature difference between the skin and the surrounding air, by means of the thermoelectric technology discussed in Section 2.3.4. The ability to harness thermal energy at any point on the body adds an element of flexibility, in that a device need not be located at a point of maximum movement. There are drawbacks, however, in that the skin may naturally act to restrict blood flow to areas in contact with cold objects which obviously causes the skin temperature, and hence the magnitude of the heat gradient, to decrease and limit the amount of energy that can be harvested. It may be observed that the most promising and potentially unobtrusive source of energy is from footfalls. In the late 1990's, Massachusetts Institute of Technology developed the 'MIT Shoe' [47], aiming to generate power from heel strike energy or the flexing of the shoe. Starner and Paradiso present a thorough review of human generated power, including heat, respiration and blood pressure [48].

2.3.7 Inductive and RF energy transfer

Transmission of energy via RF (or induction) is already used by a number of devices including contactless smart cards and RF-ID tags [49]. The operating range of such devices is typically small (of the order of centimetres to metres) and the means of powering the device is normally directional. Equation 2.7 gives the power received by a wireless node, P, ignoring the effects of reflections or interference [30]. Here, P_0 is the initial transmitted power, λ is the wavelength of the transmission, and r is the radius of the transmission. RF is a common method of distributing power to embedded electronics. However, Paradiso and Starner [50] state that the potential of RF harvesting technology is limited, and that systems powered from an ambient RF source require a large collection area, or have to be located close to the radiation source. Nevertheless, Powercast has recently released products that are designed to harvest energy from transmitted radio waves [51].

$$P = \frac{P_0 \lambda^2}{4\pi r^2} \tag{2.7}$$

Intel Research have demonstrated two systems operating from RF-based wireless power transfer. The first system, known as WISP (Wireless Identification and Sensing Platform) has been shown to work with a UHF RF-ID reader which has a 4W effective radiated power. The WISP, complete with its 15cm antenna, is shown in Figure 2.16a and the voltage obtained from the harvesting subsystem is shown in Figure 2.16b. The same team have also demonstrated a system which is capable of harvesting energy from broadcast television signals. The device shown in Figure 2.16c was shown to harvest 60μW (sufficient to power a digital thermometer/hygrometer) when located 4km from a transmitter broadcasting at 960kW at 674-680MHz. The system features a 5dBi log periodic antenna which had to be manually oriented to face the transmitter with line-of-sight. While both developments are interesting, the limited power outputs and the requirement to be close to a dedicated transmitter (or have direct line-of-sight with a broadcast station using a manually-oriented antenna) limits their range of applications.

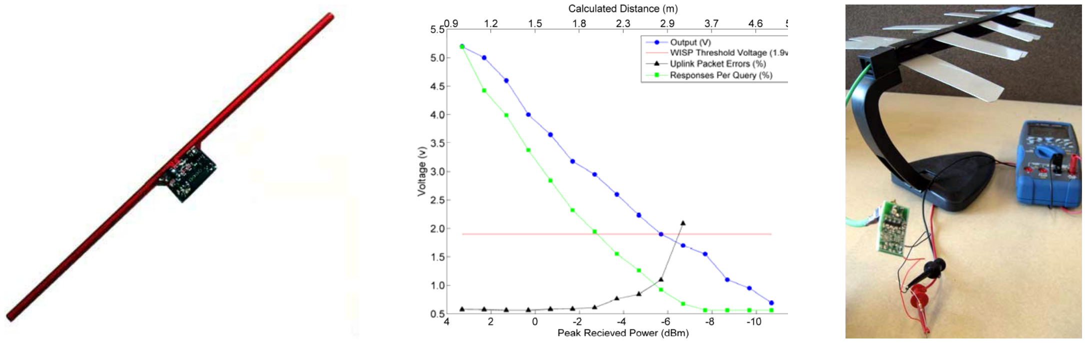

(A) (B) (C)

Figure 2.16: Devices from Intel Research (a) the WISP device which is a passive RF-ID tag with >1m range (b) its performance (c) a system harvesting energy from broadcast TV signals (reproduced from [52]).

2.3.8 Hybrid energy harvesting technologies

A limited number of systems have combined multiple energy harvesting sources, such as photovoltaic and wind (as in AmbiMax [46]), or photovoltaic, wind, and water flow (as in Morais *et al.* [45]). These existing systems are discussed in more detail in Section 2.9. There are also some modules that integrate two types of energy harvesting in a single device. The Midé Volture hybrid energy havester (HeH) combines a piezoelectric vibration energy harvester with an encapsulated photovoltaic module [53], as shown in Figure 2.17. Further, some hybrid photovoltaic-thermoelectric systems which aim to improve on the performance of conventional photovoltaic modules have been proposed and are currently under development at MIT [54].

Figure 2.17: Midé Volture hybrid energy harvester, with piezoelectric energy harvester and encapsulated photovoltaic module (reproduced from [53]).

2.3.9 Summary and discussion

A range of energy harvesting technologies have been developed, and some are available commercially. Table 2.5 summarises the power densities and readiness levels of a range of prominent energy harvesting technologies. Due to the maturity of the technology and the presence of significant levels of light in many environments, photovoltaic energy harvesting is the most established form of technology; however, the selection of the appropriate type of cell is important (especially in low-light or artificially lit environments). Developments have been made in recent years in the area of vibration energy harvesting: commercial devices which harvest vibration from the environment and convert it into electrical energy are now emerging in the marketplace. Present technologies are sensitive to specific vibration frequencies, so the technologies are typically applicable to deployment on machines working from a mains power supply or a at a fixed frequency. Thermoelectric devices are also being developed, but are perhaps the least mature major technology covered in this section of the thesis due to the difficulty of maintaining a suitable temperature difference across the thermocouple, and of using this to generate a sufficient voltage. Other technologies have also been discussed in this section, including the exploitation of fluid flow or wind power, and various forms of power from human heat and movement. Wireless energy transfer from induction or radio frequencies has also been considered, but the range of such technologies is limited and most rely on the use of a dedicated high-power transmitter to transfer power to the receiver.

Power Source	**Power** μ**W/cm**^{3}	**Buffering Required**	**Voltage Regulation**	**Commercially Available**
Solar (outside)	15,000[a]	Usually	Maybe	Yes
Solar (inside)	10[a]	Yes	Maybe	Yes
Temperature	40[a,b]	Usually	Maybe	Yes
Human Power	330	Yes	Yes	Soon
Air Flow	380[c]	Yes	Yes	Soon
Vibrations	200	Yes	Yes	Yes

[a] Denotes sources whose fundamental metric is power per **square** centimetre.

[b] Demonstrated from a 5°C temperature differential.

[c] Theoretical value; assumes air velocity of 5m/s and 5% conversion efficiency.

Table 2.5: Comparison of energy harvesting sources for wireless sensor networks; adapted from [18]. Table shows realised power density for each harvester type.

In summary, the maturity of photovoltaic cell technologies means that they are the natural choice in environments with significant levels of light; where fixed-frequency vibration is present, vibration energy harvesting is a feasible solution; and where significant temperature differences are present, these can be exploited by emergent thermoelectric energy generation. There are also technologies available which can exploit wind energy or the fluid movement. The harnessing of human heat and movement is not a well-developed area, but wireless energy transfer is an interesting area with significant limitations with regard to its effective range and delivered power.

2.4 Technologies for intelligent sensing

2.4.1 The IEEE 1451 standards family

The IEEE 1451 family of standards define a common communication interface for transducers and processors. The standards deliver plug-and-play capabilities to industrial sensors by defining common interfaces and electronic data sheet templates for transducers. This allows data acquisition systems to obtain, scale, and interpret transducer data without the need for manual configuration when installed. A 1451.4-compliant system will normally consist of a smart sensor that is connected to a data acquisition system, which interfaces (through a network-capable application processor) over a network to a display device such as a PC.

An example of a typical smart sensor is from the Watlow INFOSENSE-P transducer family, which implements the IEEE 1451.4 standard. As shown in Figure 2.18, the smart sensor has its 'Transducer Electronic Data Sheet' (TEDS) data stored in a memory on the device's connector, rather than the conventional approach of printing the information on a tag attached to the cable. The process of installing, identifying, and calibrating the transducer is therefore automated and takes place as soon as the device is attached to the system. In practice, TEDS is a very useful feature for autonomous sensors as it adds a plug-and-play capability to conventional 'dumb' sensors. By allowing devices to store detailed operational, interfacing, and identification data about themselves, it frees system installers from having to individually configure the interfaces between digital systems and analogue sensors. This can reduce the deployment cost of sensors and increase reliability.

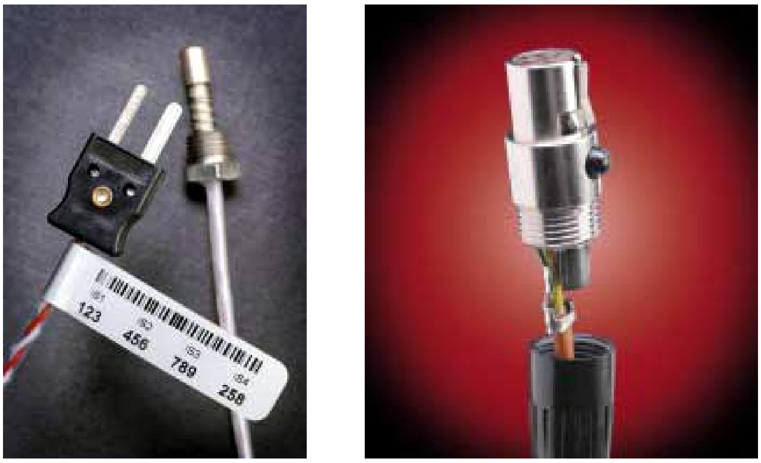

(a) INFOSENSE (b) INFOSENSE-P

Figure 2.18: Conventional and plug-and-play smart sensors. Device (a) has configuration data on an attached label that must be manually entered into the interface system, while (b) stores this data on an EPROM memory, integrated into the plug, which can be automatically read. Images reproduced from Watlow data sheets [55].

Description	Bit Length	Allowable Range
Manufacturer ID	14	17-16381
Model Number	15	0-32767
Version Letter	5	A-Z (data type Chr5)
Version Number	6	0-63
Serial Number	24	0-16777215

Table 2.6: Basic TEDS content, as defined in IEEE 1451.4-2004 (reproduced from [56]).

2.4.2 Transducer electronic data sheets

Transducer electronic data sheet format

TEDS information is stored in electronic memories on transducers. A range of data about the transducer can be stored, and depends on the type of transducer, the template it corresponds to, and the decision of the manufacturer to provide any further information. Basic TEDS information must be stored, which identifies the manufacturer (by means of a number that is allocated by the IEEE Registration Authority) and stores the model and version numbers of the device, along with its serial number. This information is sufficient to uniquely identify the transducer. The basic TEDS format is shown in Table 2.6.

Further to this basic information, the TEDS contains a wider variety of detailed data about the operation and calibration of the transducer. For example (with the systems shown in Figure 2.18) only four calibration points are given on the tag, while the TEDS can store the parameters of the complete calibration curve. This results in more accurate interpretation of transducer data. The template shown in Table 2.7 is for a thermistor. In this example, the information is useful to the processor as it provides the information for the raw output from the transducer to be converted into an accurate temperature value. It also gives information about the physical interface with the analogue transducer.

Supporting hardware

TEDS data is typically stored in an ‘electrically programmable read-only memory’ (EPROM), and the digital interface with smart transducers is based on the Maxim/ Dallas 1-Wire protocol [58]. In this master/slave interface, the master (i.e. the data acquisition unit) supplies power and communicates over a single wire, using a defined sequence of time-based commands [59]. A number of 1-Wire devices can be attached to the same 1-Wire bus and controlled individually by a single master. At the time of writing, 1-Wire EPROM devices were available from Maxim/Dallas in sizes between 1kbit and 64kbit, and are the only EPROM device mentioned in the IEEE 1451.4-2004 [56] specifications.

Property	Description	Access	Bits	Units
TEMPLATE	Template ID	–	8	–
%ElecSigType	Transducer electrical signal type	ID	–	–
%MinPhysVal	Minimum temperature	CAL	11	°C
%MaxPhysVal	Maximum temperature	CAL	11	°C
%MinElecVal	Minimum resistance output	CAL	18	Ohms
%MaxElecVal	Maximum resistance output	CAL	18	Ohms
%MapMeth	Mapping method	ID	–	–
%RTDCoef_R0	Resistance of thermistor at 0°C	ID	20	Ohms
%SteinhartA	Steinhart-Hart Coefficient A	ID	32	1/C
%SteinhartB	Steinhart-Hart Coefficient B	ID	32	1/C
%SteinhartC	Steinhart-Hart Coefficient C	ID	32	1/C
%RespTime	Sensor response time	ID	6	seconds
%ExciteAmplNom	Nominal current excitation	CAL	8	Amps
%ExciteAmplMax	Maximum current excitation	ID	8	Amps
%SelfHeating	Self heating constant	ID	5	W/°C
%CalDate	Calibration date	CAL	16	–
%CalIntitials	Calibration initials	CAL	15	–
%CalPeriod	Calibration period	CAL	12	days
%MeasID	Measurement location ID	USR	11	–

Table 2.7: Thermistor Template (ID=38) Summary (reproduced from [57]).

2.4.3 Extensions to the electronic data sheet concept

The concept of electronic data sheets has been taken forward by Bandari *et al.* [60], who have developed the ‘component electronic data sheet’ (CEDS), which stores information about electrical and mechanical components in a system. This forms part of a process for ‘integrated systems health management’ (ISHM) in which the overall reliability of systems is optimised by increasing the level of information stored about each individual component’s operating parameters (in the case of their example, for a rocket testing facility). Schmalzel *et al.* [61] extend the concept to the ‘health electronic data sheet’ (HEDS) and further to xEDS, meaning that the electronic data sheet concept may be applied to other devices and applications.

2.4.4 System management schemes

Two major standards enabling intelligent system management have been developed. The first, entitled ‘System Management Bus’ (or SMBus) [62] was initially defined by Intel in 1995 with the purpose of enabling system management in PCs and servers. Devices such as temperature sensors, fans, and voltage sensors could be monitored and managed over a standard interface (which was based on the I^2C protocol). The actual commands used over the interface were to be defined by hardware manufacturers and are not specified in the standards. The standard proved particularly popular for batteries, especially laptop batteries, for which an add-on standard was developed by Duracell and Intel – defining ‘Smart Battery Data’ (SBD) [63]. The second major standard to be developed is entitled ‘Power Management Bus’ (PMBus) [64]. This standard defines the format of data exchanges between power-related devices; for example, the READ_VCAP command returns the voltage on the energy storage capacitor. These standards are best suited to higher-power complex computing systems and are perhaps less suited to resource-constrained wireless sensor nodes due to the overheads of the management scheme.

2.4.5 Discussion

The IEEE 1451 standard for plug-and-play industrial sensors offers real benefits to system installers, simplifying the deployment and configuration of wired sensors. This is enabled, in part, by the transducer electronic data sheet format (which standardises the format of the configuration and interface parameters for devices); the concept has been extended to CEDS and HEDS , and further to xEDS, meaning that electronic data sheets can be used for a range of applications. The SMBus and PMBus standards facilitate a common interface for system management in desktop computers and servers. No comparable interface standards or systems exist for power or system management in wireless sensor nodes, particularly for sensor nodes operating from harvested energy. The author of this thesis believes that there is a compelling case for the energy devices on sensor nodes to feature electronic data sheets with their operating parameters, in order that the system can effectively monitor and manage its energy subsystem, and so that the energy hardware of the sensor node could be connected at the time of system deployment. This concept is discussed in greater detail in Chapter 3.

2.5 Wireless communication protocols

2.5.1 Overview

Wireless sensor network communications generally have a low data rate, with a short transmission range (typically between 10-100 metres) and a low duty cycle. Short-range wireless communications can be delivered via a range of media, including infra-red, radio frequency, magnetism, and acoustics. RF communications have achieved dominance for wireless sensor networking, mainly due to their low component cost, early standardisation, and applicability to a wide range of deployment environments. Other technologies, however, have niche applications where radio communications are impractical. Dependent on the complexity of the protocol, schemes can permit star, tree, and mesh network topologies (as shown in Figure 2.19).

2.5.2 RF-based methods

The dominant basic standard for short-range RF wireless sensor communications is IEEE 802.15.4 [65]. The standard defines the radio channels and transmission schemes to be

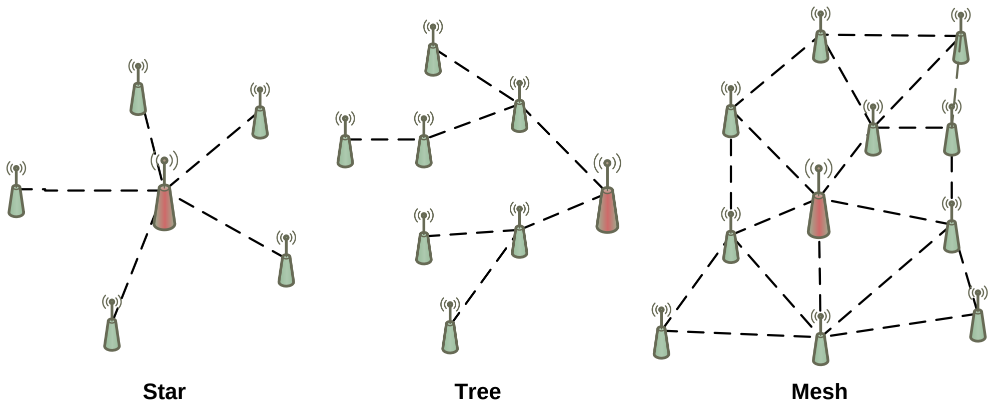

FIGURE 2.19: Star, tree, and mesh network topologies.

used in wireless personal area networks (WPANs) and facilitates (but does not directly implement) schemes which allow data to be routed through a number of sensor nodes. The initial release of the standard (IEEE 802.15.4-2003, which is widely used) defines physical channels in the Industrial, Scientific and Medical (ISM) bands at 868MHz in Europe, 915MHz in North America, and 2.45GHz worldwide. The 2.45GHz band has been widely adopted, and offers data rates up to 250kbit/s and a transmission range of up to 100 metres. Since the release of IEEE 802.15.4-2003, there have been two revisions to the standard.

Additional functionality has to be added to 802.15.4 to deliver routing, network management, and application support. To this end, the ZigBee Alliance has defined standards for embedding wireless communications capabilities [66]. ZigBee-compliant devices are capable of star, tree, or mesh network topologies, potentially taking several hops to route data from one sensor (through other nodes capable of routing) to a central data collector. The ZigBee stack is shown in Figure 2.20 and is intended to be based on cheaper hardware than Bluetooth, with a simpler software stack and much lower energy requirement. Many of the energy savings are derived from faster handshaking, with ZigBee devices able to join a network and make a transmission in a very short time period. Other 802.15.4-based protocols, such as MiWi [67] and WirelessHART [68], have been developed but do not have the capabilities, support, or level of acceptance of ZigBee.

Wireless local area networks (wireless LANs or WLANs) are defined by the IEEE 802.11 ‘WiFi’ standard (first released in 1997) and its amendments [69]. 802.11g [70], a recent international amendment to the original standard, operates at 2.45GHz and permits data rates of up to 54Mbit/s with a range of up to 140 metres. Wireless LAN has a much higher power requirement, and higher data rate, than wireless personal area network (WPAN) radio protocols, meaning it can place costly demands on battery-powered devices. Effectively, WLAN protocols are capable of implementing star or tree topologies. The current version of the Bluetooth protocol, version 2.1, supports data rates up to 3Mbit/s at a range of up to 10 metres. ‘Bluetooth Low Energy’ technology

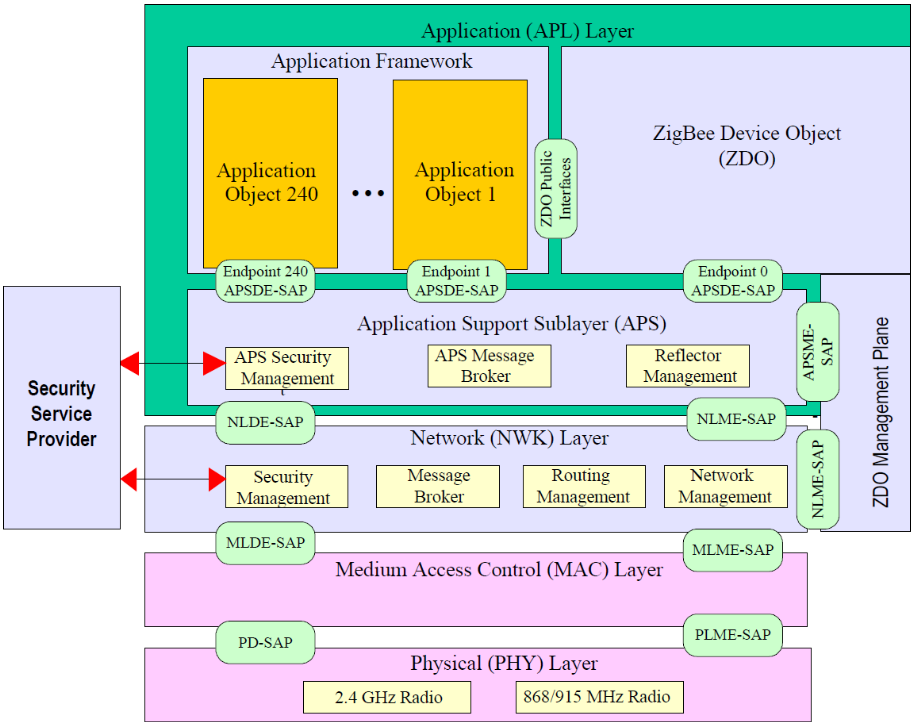

Figure 2.20: Outline of the ZigBee Stack Architecture (reproduced from [66]).

is set to be included in future Bluetooth standards, and has the aim of allowing ultra low-power end devices to operate for over a year from a single coin cell. None of the Bluetooth technologies are able to route data packets, with all being capable only of star network operation (i.e. all end devices must communicate directly with their host).

Texas Instruments have developed two proprietary protocols. Their Simple Packet Protocol (SPP) is included in their demonstration applications, and features address recognition, acknowledgement, retransmission and error checking [71]. It interfaces with their IEEE 802.15.4-compliant transceivers, but is not a compliant protocol as such. A newer development is their SimpliciTI Network Protocol, which supports a similar set of devices and is in active development, first released as a stand-alone product in 2007 [72].

2.5.3 Alternative communication methods

In very short range (less than a metre) line-of-sight applications, infra-red may be a viable solution. IrDA offers data rates of between 115.2kbit/s and 16Mbit/s [73]. Devices must be aligned accurately as transmission cones can be as little as 15° which means that, in practice, devices would have to be permanently fixed in position to guarantee a reliable data link. This property does have some advantages for security of transmissions, but this is rarely of interest in wireless sensor networks. Alternatively, acoustic-based communications are occasionally used in sensor networks. Some wireless sensor nodes use sound and radio transmissions in combination, so that the difference between the time of arrival of the two transmissions can be measured to determine the distance between transmitter and receiver [74]. In underwater environments, communications are most frequently acoustic, such as the CORAL miniature communication subsystem [75]. There have been some radio technologies developed for underwater communications, for example the S1510 Underwater Radio Modem from Tritech [76], but these systems generally use low frequencies, high transmission powers, and large antennae. A new technology, known as RuBee, is being developed under IEEE standard P1902.1 [77]. RuBee devices have a low frequency radio (around 131kHz) with a very small antenna compared to their wavelength (which is approximately 2.3km) and operate in the 'near field', hence exploiting the effect of magnetic induction. RuBee signals can travel through metal, water and solid objects far more effectively than ultra high frequency RF transmissions. The maximum range achievable by RuBee is approximately 30 metres, and its data rate is a comparatively slow 1.2kbit/s.

2.5.4 Networking and routing

The aim of routing protocols is to get data from one point in the network to another point in an efficient manner. The efficiency of a routing protocol may be judged on overall energy consumption, the number of hops, and sometimes the evenness of the distribution of energy consumption across all nodes on the network. Many protocols aim to extend the useful life of the network without compromising on the delivery of data. Often there is a trade-off between latency and power consumption. Al-Karaki and Kamal [78] have produced an excellent survey of routing techniques for wireless sensor networks. The authors of the survey categorise the routing techniques as either flat, hierarchical, or location-based. The protocols are also classified as multipath-based, query-based, negotiation-based and QoS-based. They discuss the main challenges and design issues, including node deployment schemes, data reporting methods (time-driven, event-driven, query-driven or a hybrid), and quality of service and scalability issues. Routing is a notoriously complex area of research, and favourable results obtained through simulation are rarely realised in the field. It is not possible to go into detail here about the different schemes, but they form the basis of energy-adaptive algorithms described in Section 2.6.

2.5.5 Discussion

The field of wireless communications for sensor networks is wide and growing, with an overwhelming number of publications in the field (many of which are of dubious real value). Wireless communication technology is not a major focus of this thesis, but is instead an enabler to demonstrate the concept of reconfigurable energy-aware wireless sensor nodes. A small number of technologies (IEEE 802.15.4, ZigBee, Bluetooth Low Energy) are established, or likely to become established, in the field of low-power wireless sensor nodes. Other schemes are of peripheral interest, but have not yet achieved a critical level of acceptance or have much higher power requirements. The work carried out in this thesis is implemented on hardware which is capable of 2.45GHz IEEE 802.15.4, or similar, radio transmission schemes.

2.6 Energy-aware operation

2.6.1 Energy-aware routing

Leading on from Section 2.5.4, a limited number of schemes exist to achieve energy-aware routing. In conventional (non energy-aware) protocols, continuously using the most 'energy efficient' paths to route data to a sink can lead to a disproportionate amount of energy being used by nodes along the preferred path. A number of routing schemes are energy-aware, and aim to extend the life of the network through managing the decline of the network by sharing routing tasks evenly between nodes [79].

Few schemes are able to cope with the rapidly-changing energy status of an energy-harvesting node. Notable examples, however, include the scheme developed by Shah and Rabaey [80], which associates probabilities with route paths (dependent on residual energy and amount of energy required to route data through that path). By associating probabilities with each path, the energy expenditure can be equalised across the network (as packets are routed in line with the probabilities, sharing the workload between a number of paths). A similar scheme is the priority-based multi-path routing protocol (PRIMP) developed by Liu *et al.* [81], which marks nodes as high priority or low priority dependent on their energy status (or on the accumulated number of hops required to route data to the sink). This is done at the time of 'interest propagation', where requests for data are sent out and the route for returned data is set up. Voigt *et al.* [82] propose a varitation of diffusion which takes the stored energy, along with the energy harvested from a photovoltaic module, into account when routing packets. Perhaps the most intricate energy-aware scheme is described by Kansal and Srivastava [83], who look at using information on energy harvesting patterns to predict future energy input and hence make intelligent decisions for routing packets.

2.6.2 Energy-adaptive behaviour

Energy-adaptive behaviour, or energy-aware algorithms, are useful as they permit the sensor node to use information on its energy status to adjust its participation in the network (generally increasing its activity when energy is plentiful, or decreasing it when energy is restricted). Communications tasks are normally taken to be the most energy-intensive operation for sensor nodes, but energy-aware algorithms may also control sensing or processing tasks which also consume large amounts of power. Perhaps the simplest form of energy-aware algorithm is one proposed by Delin *et al.* [84] in which nodes enter a sleep state when their stored energy drops below a threshold value, and wake up again when they have been recharged sufficiently by the solar cell. Cianci *et al.* [85] have used threshold rules to balance the workload between a group of nodes in a network. Other algorithms use distributed processes to permit redundant nodes (i.e. those nodes whose communications or sensing coverage is duplicated by other nodes) to sleep to conserve energy [86].

Merrett *et al.* [87] have developed schemes to discard messages of low importance in the interests of ensuring that high-importance messages can traverse the network. Their schemes are collectively known as IDEALS/RMR (Information manageD Energy aware ALgorithm for Sensor networks with Rule Managed Reporting). Central to the concept is the classification of the energy status of the node by its Energy Priority (EP), and the importance of the message by its Packet Priority (PP). The complete system diagram for IDEALS/RMR is shown in Figure 2.21 [87].

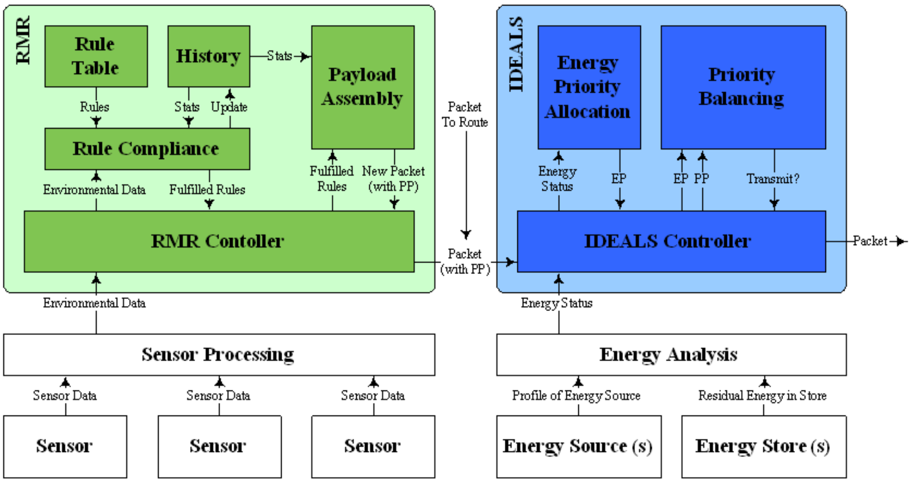

Figure 2.21: The IDEALS/RMR system diagram introduced by Merrett *et al.* (reproduced from [87]), showing how packet priorities and energy priorities are generated.

In this scheme, messages containing more information are given a lower ‘Packet Priority’ (PP) number – i.e. the most important messages are allocated PP = 1 and for the lowest priority messages PP = 5. The energy status of the nodes is classified with a high ‘Energy Priority’ (EP) number for higher energy availability. For the case where the energy store is empty (i.e. the node cannot sustain even a single transmission), the node is allocated EP = 0.

Merrett *et al.* also introduce the concept of ‘priority balancing’, in which message priorities and power priorities are balanced. For example, a node with plenty of energy will transmit messages of all information levels. Conversely, a node with constrained energy reserves will only transmit messages of very high importance (i.e. low PP values). Thus, in order to maintain the operation of the node, and in turn the network, sensor nodes only transmit messages when this is sustainable. For example, when a node has EP = 4, it will only transmit messages with PP $\leq$ 4. The process of priority balancing is

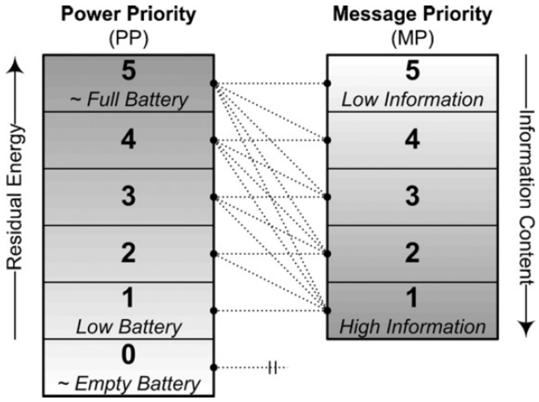

FIGURE 2.22: Priority balancing in IDEALS (reproduced from [87]), which shows how the energy priority is balanced against the packet priority.

shown in Figure 2.22. It should be noted that the range of priority values (in this case EP $= 0 \ldots 5$ and PP $= 1 \ldots 5$) is largely an arbitrary choice, but the EP must start at 0 and PP at 1, with both the EP and PP having the same maximum value.

While the figure refers only to battery-powered nodes, the scheme can also be applied to any form of energy store and is highly suited to wireless sensor nodes that harvest energy from their environment and can therefore have a rapidly-changing energy status. In this way, the system will always operate to ensure that important messages can traverse the network, dropping fewer important messages where necessary to conserve energy and hence sustain the operation of the network. Merrett also makes the distinction between 'relative thresholds' and 'absolute thresholds'. This allows networks comprised of nodes with differently configured energy subsystems to cooperate (nodes either set their EP by the absolute amount of energy stored, or by proportionally how 'full' their energy stores are).

2.6.3 Achieving energy awareness

The energy-adaptive algorithms described in Section 2.6.2 must be able to monitor the energy status of the node. At its very simplest, the system should monitor the amount of energy stored by the system at a given time; this may be as straightforward as determining the energy stored on a capacitor by measuring its voltage and using the standard capacitor equation. In systems with multiple energy sources and stores, the situation can be complex and the monitoring of the energy subsystem should report with sufficient detail to enable appropriate decisions to be made. For example, the new system architecture described later in this thesis supports up to six different energy devices. These may include energy stores (such as supercapacitors and primary or secondary batteries) and energy sources (including mains adapters and energy harvesting devices).

Ultimately, the application running on the sensor node will need to assess the energy stored on the node by individually monitoring each energy device. It must determine the level of stored energy (in supercapacitors and batteries) and as a basic requirement must classify this as rechargeable or non-rechargeable (i.e. the system must know whether the resource it is using is capable of being recharged, or if it is a single-use resource). More complex systems may take the degradation of the energy store into account (for example, by attaching a higher 'cost' to the use of a rechargeable battery over that of a supercapacitor due to the lower cycle life of the former) and thus ensure that the application is aware of the true impact of energy usage. Clearly, the discharge characteristics of different battery chemistries are also variable and must be taken into account when measuring energy (for batteries, subjecting cells to a large known load and comparing this to the discharge curve is a common way to assess their state-of-charge [88]).

In a similar way to estimating the stored energy, the rate of power generation from energy sources must also be determined. For a mains adapter the rate of generation is typically rapid and hence need not be computed (the system may merely look at whether such resources are 'on' or 'off'); however, for devices such as vibration energy harvesters and photovoltaic modules, the rate of power generation is variable and must be more carefully computed. In general, the nominal power of energy harvesting devices may be estimated by analysing the open-circuit voltage of the harvesting device or by putting its output through a fixed load and monitoring the operating voltage. The measured data are then combined with device models to determine the rate of energy generation.

Delivering energy-awareness for resource-constrained embedded systems is a non-trivial task and is highly dependent on the use of device models. Clearly such models must be highly simplified to reduce their memory requirement and computational complexity, but must be of a sufficient quality to ensure their accuracy. Other effects such as the tolerance of components and their degradation over time may also act to reduce the accuracy of estimates. To be used by algorithms such as IDEALS/RMR, the energy status of the node must be classified into discrete levels as shown in Figure 2.22. Clearly, the act of energy monitoring on sensor nodes is potentially a complex task, but the aim is to deliver a 'good' estimate of the energy status (sufficient for use by energy-aware algorithms) without using too much energy in performing the associated measurements and calculations.

2.6.4 Overall lifetime prediction and extension

A major motivating factor behind the development of wireless sensor node technology is that nodes can be deployed for long periods without the need for regular maintenance. Clearly, the overall lifetime of a sensor node is dictated by the lifetime of its individual components, including the power supply. Sections 2.2 and 2.3 have already covered the capacities and other properties of energy stores, and the potential power output from energy harvesting devices (along with the expected lifetime of primary batteries). Many components have a 'guaranteed lifetime', which may be relatively short (for example, capacitors often have a 1,000 hour lifetime at the extremes of their rated conditions). The actual expected lifetime is dependent on a number of factors including temperature and voltage, but the expected lifetime may be many times the guaranteed lifetime. Ideally, for an energy-aware sensor node, the gradual degradation of the energy hardware would be compensated for and the node should adapt its operation accordingly.

Taking an example, a Panasonic Gold 1F HW series supercapacitor [16], which has a 1,000 hour guaranteed lifetime at its maximum voltage and temperature (being 2.3V and 70°C): at the end of the guaranteed lifetime, their capacitance can be expected to have dropped by no more than 30% and their internal resistance to have increased by no more than four times. The expected lifetime is not a guaranteed value, but can be estimated by Equation 2.8 (provided by Panasonic [16], where t_ϵ is the expected lifetime, t_γ is the guaranteed lifetime, α_τ is the temperature factor and α_ψ is the voltage factor. Considering the use of the device for a sensor node operating at between 2.0 and 3.6 volts (3.6 volt maximum), at a temperature of 30°C and with a maximum current draw of 25mA the expected lifetime of the supercapacitor can be calculated. Given that the node is operating at up to 3.6 volts, and each device has a rated maximum voltage of 2.3V, it will be necessary to connect two supercapacitors in series. This results in an effective capacitance of 0.5F, and a maximum voltage across each device of 1.8 volts.

$$t_\epsilon = t_\gamma \times \alpha_\tau \times \alpha_\psi \tag{2.8}$$

Panasonic state that the temperature factor, α_τ is expressed by Equation 2.9, which expresses the fact that the life doubles for each 10°C temperature decrease (which is apparently found from the Arrhenius equation). Here, T_ρ is the rated temperature and T_ϵ is the expected temperature. Thus, at 30°C for a device rated at 70°C, the temperature factor is found to be 16. Investigations into large supercapacitor behaviour indicate that the expected lifetime will also double for every 0.1V operating voltage reduction [89]. Therefore at a voltage of 1.8V the voltage factor, α_ψ is 5. Hence, for this device, the expected lifetime (in hours) is found to be 80,000. This corresponds to an expected lifetime of approximately nine years. Note that an increase in operating temperature of 10°C will effectively halve the expected lifetime.

$$\alpha_\tau = 2^{\frac{T_\rho - T_\epsilon}{10}} \tag{2.9}$$

Flash data retention is specified at a minimum of 100 years at 25°C for TI microcontrollers such as the MSP430. Flash lifetimes at higher temperatures can also be predicted by using the Arrhenius equation. At 50°C, memory retention can be expected to fall to 17 years [90]. Other limitations include the number of write cycles to flash memory. There are also some concerns that the progression towards reduced feature sizes in integrated circuits may reduce their endurance due to the propagation of materials within the device (there are, however, some power-related reasons why feature sizes for low-power microcontrollers remain relatively large). Increased temperatures affect other parts of the system such as the energy store and harvesting device. Designers must consider the effects of the operating environment on all aspects of the system in order to ensure that the required operating lifetime is achievable.

2.6.5 Discussion

Energy-aware operation can extend the effective lifetime of sensor nodes and allow them to optimise their operation to adapt to their energy status. This section has introduced the existing schemes for energy-aware routing, energy-adaptive behaviour, and achieving energy-awareness along with a consideration of the designed lifetime of components of a sensor system. The means of delivering energy-awareness, and energy-adaptive behaviour, is non-trivial and at present is not a well-defined process. Existing systems must be highly tailored to the energy hardware deployed, and there is no mechanism for the automatic configuration of energy-aware systems, or of representing the method of monitoring the energy status of the device. It is the view of the author of this thesis that, due to the increasing complexity of the energy hardware of wireless sensor nodes (incorporating a range of energy devices), such a scheme is required.

2.7 Wireless sensor node technologies

2.7.1 Microcontrollers, transceivers, and system-on-chip

A number of low-power microcontrollers have been developed for use in resource constrained wireless sensing applications. Examples include the TI MSP430 [91], a 16-bit RISC mixed-signal processor, which is used in Crossbow motes (described later in this chapter) and has achieved dominance for use in wireless sensor network applications. Generally, microcontrollers used in wireless sensor networks will feature very low sleep currents of around 1μA, fast wake-up times, and the ability to interface with a range of peripherals including radio transceivers and analogue sensors. Other options for low-power microcontrollers include the 8-bit RISC Microchip XLP PIC range [92], and Atmel AVR microcontrollers [93]. Some higher-power node platforms are based on ‘larger’ processors (for example, the Imote2 platform [94] is based on the Marvell PXA271 XScale processor). The sleep current for these devices is typically around 100 times that of the low-power microcontrollers (although their active-mode power consumption is comparable) which makes these devices more suited to less energy-constrained applications and where higher processing power is required.

In wireless sensor nodes, an RF transceiver generally provides the interface between the microcontroller and the physical communications channel. The most widely-adopted protocol for wireless sensor networks is IEEE 802.15.4-2003, and a typical transceiver is the TI CC2420, as evidenced by its use in Telos motes [5]. Many of the requirements of the protocol are implemented in hardware (such as data handling and buffering, burst transmissions, encryption and authentication, clear channel assessment, quality indication, and timing information). It is a requirement of 802.15.4 transceivers that they must have an adjustable output power. Settings for the transmit power, along with various other parameters, are accessed via memory registers on the transceiver. Further developments have led to single-chip solutions being developed, for example the Texas Instruments (TI) CC2430 integrates an enhanced 8051 microcontroller and 802.15.4-compliant transceiver onto a single chip. A CC2430 evaluation module is shown in Figure 2.23 alongside an eZ430-RF2500 module: the eZ430 has a separate MSP430 microcontroller and transceiver whereas the CC2430 has a single chip. TI have recently developed the CC430, which integrates an MSP430 and sub-GHz radio transceiver in a 9.1mm x 9.11 system-on-chip package [95].

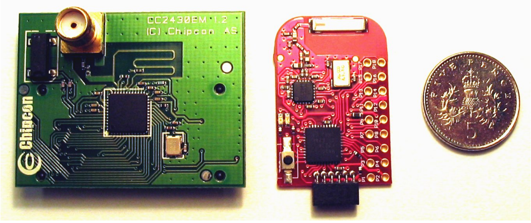

FIGURE 2.23: The Texas Instruments CC2430 evaluation module and eZ430-RF2500 next to a five pence coin.

2.7.2 Commercially-available sensor nodes

A number of wireless sensor platforms have been developed, each having different capabilities and features such as on-board sensors or processors. Motes developed at the University of California, Berkeley, have been commercialised through Crossbow Technology Inc., and have achieved dominance through their flexible interfacing, small size and reasonable cost. A good background to the family of motes is given by Polastre *et al.* [5]. Used by over 100 research organisations, the motes are normally loaded with TinyOS (an embedded operating system for wireless sensors) and are available in a number of incarnations with a range of sensor boards available.

The latest sensor platforms produced by Crossbow are the TelosB and Imote2. TelosB is the low-power MSP430-based platform, and the Imote2 is a high-bandwidth sensing platform featuring an enhanced processor and larger memory, along with the flexibility to communicate via a range of protocols including IEEE 802.11 and Bluetooth [96]. A major competitor to the Imote2 is the Sun SPOT from Sun Microsystems [97], which has 32-bit ARM CPU and is Java-based, which may appeal to many software developers.

A number of bespoke platforms have also been developed – including those nodes produced as part of the Glacsweb [98] and ScatterWeb [99] projects. Some users find the commercially-available motes too restrictive, expensive, or large for the intended application, and some require specialist capabilities that cannot be accommodated by the mote platform. Benefits may be gained from custom-designing sensor nodes, but this is no simple task and is beyond the capabilities of most end-users of the sensor node hardware, which has in part led to the dominance of Crossbow motes.

2.7.3 Discussion

A range of sensor nodes are commercially available, with systems based on the Texas Instruments MSP430 now becoming dominant. Most systems incorporate 2.45GHz radio transceivers, with many being IEEE 802.15.4-2003 compliant. Typical wireless sensor nodes draw a sleep current of $<1\mu$A and an active current of approximately 25mA. A number of system-on-chip microcontrollers and radio transceivers are now available, meaning that systems can potentially be made very small. Capable of operating at very low duty cycles (typically below 1%), these devices are able to operate comfortably from average power levels of <1mW. These devices normally have a large number of input and output ports, being capable of performing analogue-to-digital conversion on selected pins. The increasing capabilities of microcontrollers in this area, and their low power consumption, means they are now capable of operating from harvested energy and of monitoring their energy hardware using their input/output pins.

2.8 Software and algorithm development

2.8.1 Software structures

Sensor node embedded software is almost always built around the communication stack: Figure 2.24 shows the stack structures for a range of wired and wireless communication protocols. The reasons behind the dominance of communication stacks in sensor nodes are largely historical; the most complex hardware module in sensor nodes was normally the communications subsystem. Moves towards integration and SoC have added further features (such as sensor processing and energy management) to what was previously just the communications module. This has added pressure to integrate the embedded software for interfacing with further external devices into the communication stack. The result of this is a relatively complex and unstructured stack, with the ‘application’ layer hosting a number of disparate functions. The reader can refer back to Figure 2.20 which shows the ZigBee stack with the application layer being subdivided into the application framework, application support sublayer, and ZigBee device object.

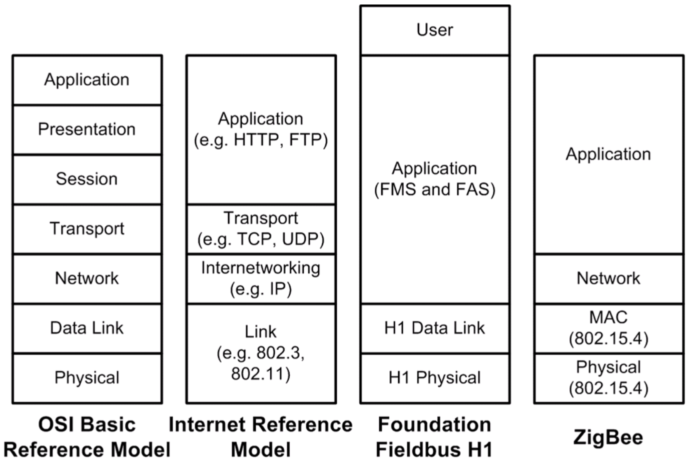

Figure 2.24: The OSI-BRM, IRM, Foundation Fieldbus H1 and ZigBee communication stacks (reproduced from Merrett *et al.* [100]).

The increasing complexity of the communication stack is a result of evolution rather than forward-planning. It may be argued that communications software stacks are becoming less important (with moves towards implementing many communication tasks in hardware), with operations such as sensor signal processing gaining emphasis. Indeed, one could say that sensing, and power management for self-powered sensors, justify having their own individual stacks rather than being forced into the top layer of the communication stack. A notable system which breaks with this conventional structure is TinyOS 2.0, which has separate interfaces based on the type of peripherals it interfaces with (and is discussed in detail in Section 2.8.2).

Alternative systems for structuring the energy management capabilities of the sensor nodes are outlined by Jiang *et al.* with their Energy Management Architecture (EMA) [101], which is shown in Figure 2.25. The scheme permits users to set 'policies' about the operation of the sensor node, meaning that the sensor node can manage its resources to achieve these aims. Examples are given for a range of deployment types; for example, an Arctic monitoring scenario prioritises tasks in the following order: (1) a one-year network lifetime, (2) a 1Hz sensor sampling frequency, (3) mesh networking/data storage, and (4) maximised sampling rate.

2.8.2 Operating systems

The TinyOS operating system is open-source, and designed for wireless embedded sensor networks. It is geared towards Crossbow motes and written in nesC [102]. It has a component-based architecture, and is claimed to make the design of wireless sensor network solutions straightforward. It is not, however, well-respected in the wider community, with it being seen as over-restrictive and complex [103]. Despite its limitations, no other operating systems have achieved the prominence of TinyOS.

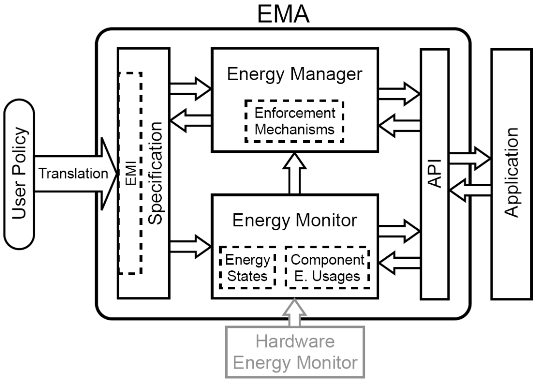

FIGURE 2.25: Energy management architecture (reproduced from Jiang *et al.* [101]).

TinyOS 2.0, based on a new hardware abstraction architecture outlined by Hanziski *et al.* [104] and shown in Figure 2.26, is now being used by the community. The architecture effectively divorces the application running on the sensor node from the detail of interfacing with its hardware, thus permitting applications to be used on a range of platforms with the appropriate interfaces being provided by Hardware Interface Layer (HIL), Hardware Adaptation Layer (HAL), and Hardware Presentation Layer (HPL) for each piece of hardware, implemented in this scheme.

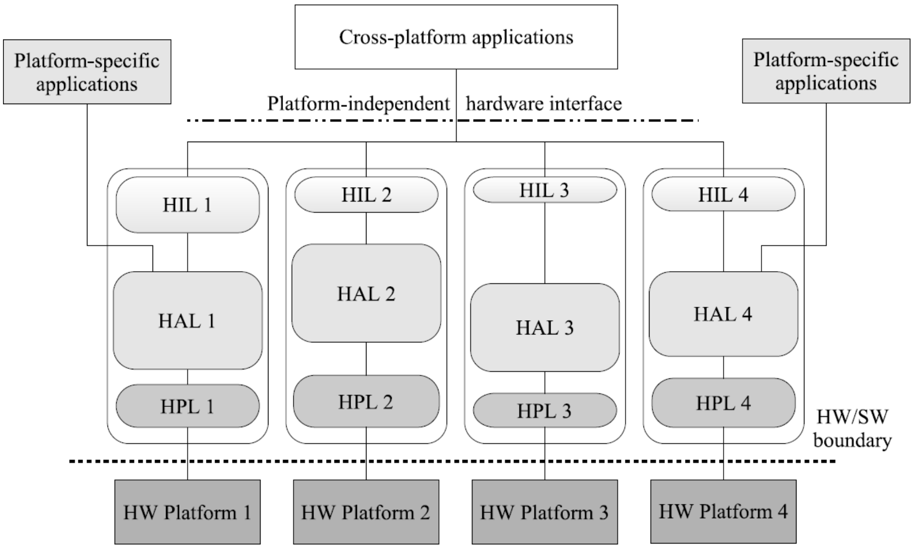
Cross-platform applications
Platform-specific applications
Platform-specific applications
Platform-independent hardware interface
HIL 1
HIL 2
HIL 3
HIL 4
HAL 1
HAL 2
HAL 3
HAL 4
HPL 1
HPL 2
HPL 3
HPL 4
HW/SW boundary
HW Platform 1
HW Platform 2
HW Platform 3
HW Platform 4

FIGURE 2.26: Hardware abstraction architecture implemented in TinyOS 2.0 (reproduced from [104]).

2.8.3 Discussion

The original TinyOS was not well-respected in the wider community, but the new software structure implemented in TinyOS 2.0 is promising as it will deliver platform-independence to applications running on sensor nodes. The programming languages and compilers used for embedded software development are highly dependent on the support given by the microcontroller manufacturers, although ANSI C is the dominant language for most low-power platforms. The historical dominance of the communication stack has resulted in a number of schemes (including ZigBee) being heavily structured around this stack; however, some modern structures have given greater importance to energy management and sensor interfacing. Chapter 3 of this thesis introduces a new hardware and embedded software structure to formalise this relationship, allowing the sensor node to manage its energy and sensing resources alongside its communication activities.

2.9 Existing systems

2.9.1 Wireless sensor system deployments

A limited amount of useful information can be gained from simulation, and a growing number of sensor network deployments are being documented. Deployments are important for the successful development of wireless sensor network technologies, as they allow algorithm simulations to be verified and the design of sensor networks to be driven by real applications and experiences. The highest-profile network deployments have mainly been for environmental monitoring, although there have been a range of other deployments aiming to demonstrate large-scale networks or to test the effectiveness of energy harvesting technology.

The University of Southampton has been involved in a number of sensor network deployments for environmental monitoring. The Glacsweb [98] project, pictured in Figure 2.27, monitored the behaviour of the Briksdalbre arm of the Jostedal Glacier National Park in Norway until the melting in 2006 resulted in the glacier becoming too steep and dangerous to work on. Nodes were deployed deep into the ice, and measured pressure, temperature, and tilt. It should be noted that many of the nodes (designed for a lifetime of up to 10 years) outlasted the glacier they were embedded in. A glacier represents an extremely harsh environment for wireless sensors, with nodes being exposed to low temperatures, high pressures, and having to operate in a very difficult radio propagation environment.

Elsewhere, wireless sensors have been deployed in a range of environmental monitoring projects. Nodes have been used to monitor seismic events on the Volcán Reventador volcano in northern Ecuador [3], with a network comprising 16 nodes spread over a 3km-wide area. Sensors have also been used to monitor the habitat of petrel on Great Duck Island, with up to 150 Crossbow-based motes deployed (*weather motes* monitored surface conditions and *burrow motes* monitored the condition and occupancy of nesting burrows) [105]. ZebraNet used nodes equipped with GPS to monitor the movement of zebra in the Sweetwaters game reserve in central Kenya with mixed results: a detailed analysis of the hardware issues is presented in a paper by Zhang *et al.* [106].

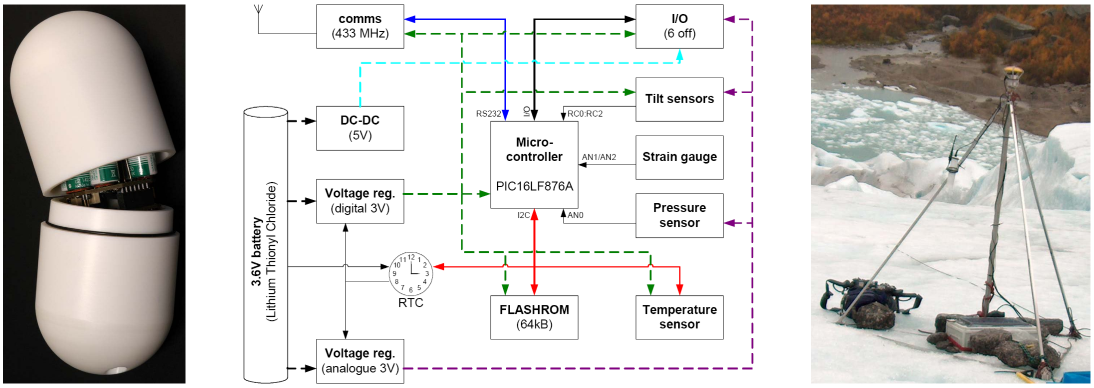

(A) Probe

(B) Architecture

(C) Base station

FIGURE 2.27: The Glacsweb Mk II architecture (reproduced from [98]).

Some large-scale sensor network deployments have been reported. The largest of which, ExScal [107] has deployed around 1,200 nodes over a 1.3km by 300m open space. Precision agriculture appears to be a large and growing application area for wireless sensing technology. A number of reported deployments have used nodes to monitor soil parameters such as moisture content over a wide area [108, 109]. A range of other test beds and deployments have been described in the literature, including some by the Centre for Embedded Networked Sensing (CENS) [110]. Details of systems incorporating energy harvesting are discussed in the following subsections.

2.9.2 Systems featuring a single form of energy harvesting

A number of projects have used energy harvesting technologies to deliver sustainable power for wireless sensor nodes. Photovoltaic modules are by far the most prevalent form of energy harvesting technology – in part due to the plentiful supply of light in many deployment settings, their simplicity and low cost. Nodes conventionally store electrical energy in supercapacitors or batteries to achieve operation in darkness and during bursts of high current draw. A notably sophisticated solar energy harvesting platform, Prometheus, buffers energy both in supercapacitors and a lithium polymer rechargeable battery [15]. The system architecture is shown in Figure 2.28 along with a photograph of a prototype. The supercapacitors are used for short-term energy storage, while the battery stores excess energy during the day and is used to top up the supercapacitor when it becomes depleted (for example, overnight during darker winter months). In this way, stress on the battery is minimised (supercapacitors are far less sensitive to repeated charge/discharge cycling than batteries), and the system could be expected to last longer than simpler systems such as Heliomote [111], which buffer energy only in batteries.

Several larger networks incorporating solar energy harvesting have been deployed. Under

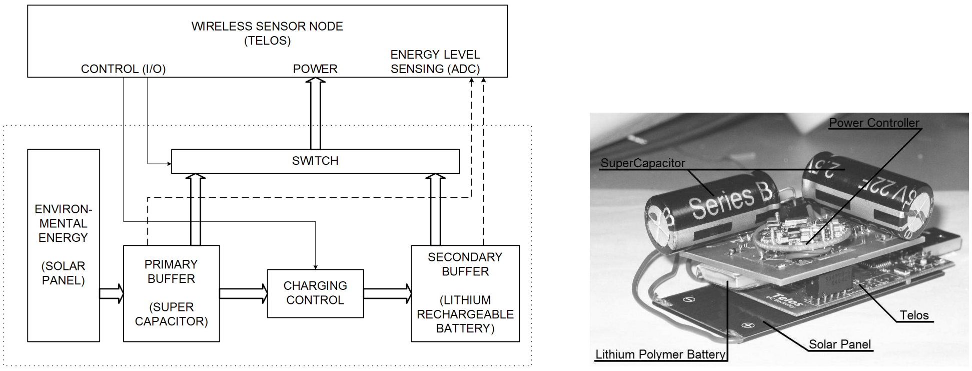

(A) Architecture

(B) Node

Figure 2.28: The Prometheus architecture and prototype (reproduced from [15]), which incorporates a solar cell and stores energy in a battery and supercapacitors.

the Trio project, a test bed of 557 solar-powered motes were deployed in 2005 over an area of 50,000m^2 [7]. The Trio motes are based on the Prometheus energy harvesting system. The actual deployment exposed a range of problems, including oversights in the energy harvesting device (solar cells were obscured by dirt and bird droppings), issues with transfer of energy between the primary and secondary stores, and the high power requirement of the TinyOS operating system. Over-the-air programming was severely disrupted by nodes power cycling and losing the contents of their memories, and frequent resets led to excessive amounts of network traffic in some areas.

Another sensor network deployment powered from light is reported by Voigt *et al.* [82], which also has a focus on energy-aware routing and network management. Separately, Corke *et al.* [112] describe a long-term deployment of solar energy harvesting nodes based on batteries, and conclude that supercapacitors are essential for delivering extended system lifetimes. Eliasson *et al.* [113] present a system which harvests energy by means of a photovoltaic cell with energy being buffered in a supercapacitor, and occasionally switches in a non-rechargeable battery to provide power for high current-drain, high-priority tasks. Further developments on photovoltaic energy harvesting motes include the HydroWatch system at University of California, Berkeley, which attempts to consider the impact of various circuit elements during the development of the system [114].

Several prototype systems incorporating vibration energy harvesting have been developed. For example the S^{5}NAP [6], pictured earlier in Figure 1.4, uses a commercially-available electromagnetic vibration energy harvester to power an accelerometer-based condition monitoring system. In a separate development, shown in Figure 2.8, a micro-generator with a volume of less than 1cm^3 has been developed in conjunction with a custom sensor node [36]. In both systems, energy harvested from vibrations is buffered in supercapacitors to permit nodes to draw large bursts of power during radio transmissions and sensing operations. Recently, GE Energy have incorporated vibration energy harvesters in their Insight.mesh system which monitors oil refinery machinery [115].

Very few sensor node deployments based on thermoelectric energy harvesting have been reported in the literature. Typically, systems have depended on a very large temperature gradient being present in order to deliver sufficient levels of energy; for example, an investigation successfully deployed a wireless sensor network on aluminium smelters in a factory [116]. Further developments in thermoelectric energy harvesting devices have substantially increased their efficiencies. EnOcean have demonstrated the ECT100 thermal energy harvester kit, which incorporates a thermoelectric energy harvester and radio transmitter module [117].

Most of the literature on solar energy harvesting focusses on outdoor deployments where light is plentiful and energy need not be carefully managed. A small number of papers have been published, describing the development of systems to harvest energy from indoor (low-intensity) lighting. Perhaps the most tenuous use of indoor solar energy harvesting is presented by Hande *et al.*, in which energy is 'harvested' from a ceiling-mounted fluorescent lighting unit in order to power a wireless routing node. As shown in Figure 2.29, around 25% of the light unit is obscured by photovoltaic cells [118]. This type of parasitic energy harvesting is undesirable as it directly impacts on the performance of the device it is attached to (in this case, substantially reducing the amount of light radiating from the light fitting). A rather more useful report on the subject of low-power photovoltaic energy harvesting is by Leder *et al.*, with a basic circuit for storing energy in a supercapacitor and quick start-up for the circuit provided by charging a smaller capacitor directly through a linear regulator [119]. Dondi *et al.* present a model for a photovoltaic cell and a method of tracking the maximum power point of a large cell by using a smaller secondary cell to provide a voltage reference [120]. Texas Instruments have recently released a version of their eZ430-RF2500 which is powered from a photovoltaic module, and is capable of operating indoors [121].

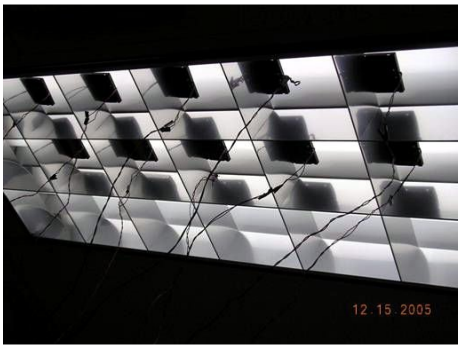

Figure 2.29: Photovoltaic cells 'harvest' energy from a ceiling-mounted fluorescent unit, but obscure much of the light (reproduced from Hande *et al.* [118]).

2.9.3 Systems integrating multiple energy resources

Few projects have incorporated multiple energy resources onto a single node. An early example is PUMA [122], developed at the University of California, Irvine, which uses power routing switches to connect parts of a sensor node to energy harvesting devices, depending on the amount of energy being harvested, in order to reduce battery usage. AmbiMax [46], a further development by the same team, is a notable example which combines energy harvesting from wind and light and stores it in supercapacitors and lithium rechargeable batteries. An advantage of the AmbiMax power module is that it is entirely analogue and autonomous; however, the system design must be adapted to accommodate changes of energy resource. Furthermore, the sensor node powered by the module has no means of finding out the levels of production or availability of energy, as the output voltage of the module is fixed at 4.1V. The AmbiMax system is shown in Figure 2.30.

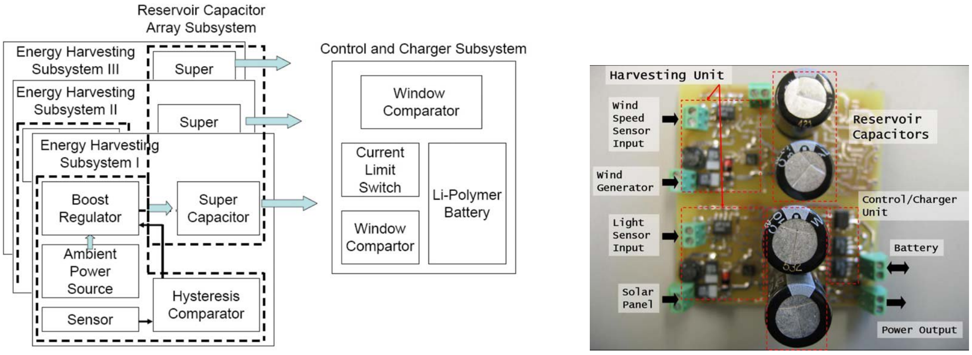

(A) Architecture (B) Circuit

Figure 2.30: The Ambimax architecture and circuitry (reproduced from [46]).

An alternative system is MPWiNodeX [45], which is capable of using energy from wind, water flow, and sunlight to power a sensor node for precision agriculture applications. However, the type of energy store cannot be changed, and the energy sources only give a coarse indication of their status (they cannot be actively managed). This system has been developed for a precision agriculture application, and its architecture is shown in Figure 2.31 along with a photograph of the deployment of a prototype system. The three energy sources were capable of providing an average current of 58mA, which exceeds the current requirement of the wireless sensor node in its active mode.

2.9.4 Discussion

A large number of sensor network deployments have been reported in the literature. Some of the most common applications of the technology are for environmental investigations and machinery condition monitoring. The largest reported sensor network comprised 1,200 nodes, and the largest deployment of energy-harvesting nodes comprised 557 solar-powered nodes. The majority of nodes powered by environmental energy simply harvest energy from solar cells; deployments of nodes using other harvested power sources are much less common. A small number of projects have utilised power harvested from a range of sources; however, these systems have been configured for specific power sources and are relatively inflexible. The state-of-the art in self-powered wireless

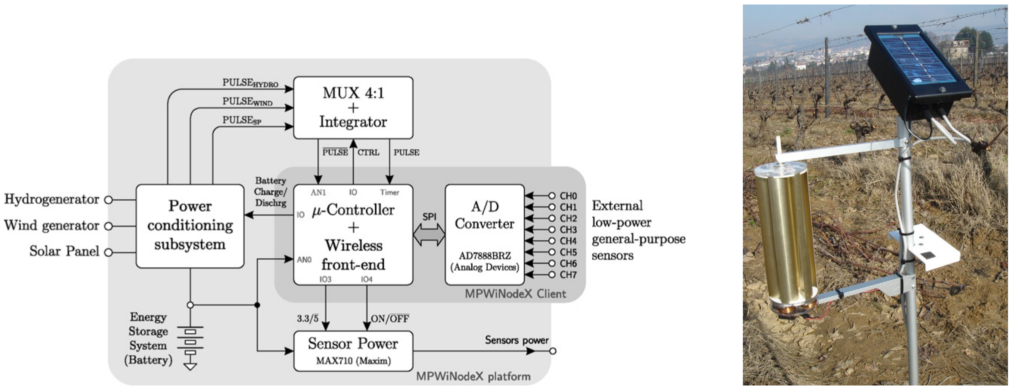

(A) System Architecture

(B) Deployment

FIGURE 2.31: The MPWiNodeX architecture and deployment (reproduced from [45]).

sensor nodes does not allow the energy subsystem to be reconfigured and has limited energy-awareness or energy-management functionality. The scheme proposed in Chapter 3 introduces methods to overcome these limitations.

2.10 Summary

This chapter provided an overview of energy technologies and other background related to sensing and wireless communications. Energy harvesting technologies such as photovoltaics, thermoelectrics, and small-scale fluid flow, have been used in this project and are discussed in later chapters. Energy storage devices including supercapacitors and primary and rechargeable batteries, are also used. The plug-and-play architecture for the energy hardware of sensor nodes, developed under this project, draws inspiration from the TEDS standard. The prototype system delivers energy-awareness to enable adaptive operation, while remaining hardware-agnostic. The prototype system transmits data wirelessly and has been developed for the CC2430 and MSP430 platforms, but is written in C so could be used in a range of microcontrollers. The limitations of existing sensor nodes which incorporate energy harvesting, or even a range of energy devices, have also been discussed and these shortcomings are addressed by the plug-and-play system, the architecture of which is discussed in detail in Chapter 3.

Chapter 3

Development: Towards a Reconfigurable Energy Subsystem

3.1 Introduction

This chapter defines the interfaces and design for the reconfigurable system architecture, outlining many of the key contributions of this work. The overall structure of the system is described in Section 3.2 with a discussion of how the individual aspects fit together to deliver a complete system architecture. The new aspects proposed include 'energy electronic data sheets' (EEDS), which are discussed in Section 3.3, and a 'common hardware interface' (CHI) between the energy modules, which is defined in Section 3.4. A generalised specification for the hardware of each energy module can be found in Section 3.5, and methods and algorithms for determination of the energy status of the node may be found in Section 3.6. The novel software structure which has been utilised in this project is defined in Section 3.7. The general operation of the system is covered in Section 3.8, and the requirements of a prototype to verify this approach are discussed in Section 3.9. The prototype system, or case study, is described in chapters 4 and 5.

3.2 Design for reconfigurability

3.2.1 Plug-and-play energy subsystem

As outlined in Chapter 2, wireless sensor nodes may be powered by a range of energy hardware including energy harvesters and energy storage devices, as well as conventionally by primary batteries. At present, systems are designed for specific energy hardware and are difficult to adapt for different environmental conditions; there is also a tendency to over-engineer systems to 'guarantee' a certain operational lifetime (although this may not actually be realised in practice). It is clearly desirable to be able to mix and match the energy hardware on the sensor node dependent on the expected activity of the node and its available environmental energy (for example, a node may have photovoltaic and thermoelectric energy harvesters, a supercapacitor energy store and a primary battery). It is also advantageous for the sensor node to be able to adapt its activity to the available energy, to best exploit resources and achieve continuous operation (at the simplest level, it may adjust its duty cycle based on the amount of stored energy; more complex systems may learn the dynamics of the energy source and adapt to this), and in order to do this there must be a good interface between the embedded software and the energy hardware.

While a limited number of deployments have already employed multiple energy harvesting devices, or hybrid energy storage and management systems, these were not truly flexible as they were tailored for specific energy hardware and could not be configured in-situ. Additionally, the energy-awareness capability of these existing systems was highly restricted, in many cases with the system only being able to monitor the voltage across its energy storage device(s) in order to assess the power status of the node. Because of this restriction, systems of this type are unable to detect the poor performance (or possible malfunction) of energy harvesting devices, or observe the dynamics of energy generation. Indeed, the only energy metric they typically use for deciding on their activity level is the amount of stored energy. These limitations are potentially serious for the end-users who would be deploying and using these devices, for the following reasons:

1. The ability of present systems to accommodate only a **limited set of energy harvesters or storage devices** limits their deployments to only those areas that feature suitable environmental conditions for that set of devices. To achieve energy-awareness with changeable hardware, and even support the use of primary batteries in certain conditions, the hardware must be much more flexibly designed than is the case at present. Ultimately, the end-user will want to select the appropriate energy hardware for the deployment location, rather than the other way around, and choose an appropriate node platform first before considering its energy resources.

2. If designed for a specific configuration, **the embedded software on the microcontroller has to be extensively modified** to interface with a modified energy subsystem. Energy-aware systems are, at present, highly tailored towards the energy hardware they are designed for and are difficult to adapt; this means that the software of the sensor node, along with the hardware, limits the range of energy devices that can be accommodated while remaining aware of its energy status. This limitation means that applications for energy harvesting-capable devices are limited to specific, niche scenarios where the deployment fits with the energy device that the energy subsystem design has been developed for.

3. As mentioned earlier, **the energy-awareness of many existing systems ex-**

tends only to the energy stores, and no active monitoring or management of the energy sources (such as energy harvesting devices) is carried out. In systems with multiple energy harvesters, this means that the relative performance of each device cannot be monitored for efficacy, that any patterns in the generation of energy cannot be reliably detected, and that the diagnosis of any energy-related faults on the node is non-trivial. The ability to monitor the performance of each harvesting device would allow the identification of otherwise undetectable problems (such as the poor performance of a photovoltaic module, for example due to dust accumulation) or periodicities (for example, a node being powered by vibration from a piece of machinery that runs at set times during the day).

I make the case here that a 'plug-and-play' capability, which would facilitate the configuration of energy hardware at any time leading up to the deployment and first switch-on of the system, is highly desirable. This hardware would by default act to provide power to the microcontroller, and the software running on the microcontroller would be able to recognise and manage its energy hardware (being able to measure both the amount of energy stored and the level of power being generated). Furthermore, a system capable of plug-and-play operation would recognise changes to the hardware of the system and allow these to be taken into account, thereby achieving the 'reconfigurability' described in Section 1.5. Thus, the system requires:

1. A modular design, with each energy 'module' incorporating its own power conditioning and management interface circuitry.
2. The ability to be plugged together at the time of deployment, and modified afterwards, with energy devices being attached, exchanged, or removed as required.
3. Embedded software which can recognise, adapt to, and manage the reconfigurable energy subsystem and use knowledge of its energy status to control the node's overall operation.

These three broad requirements form the basis of the work described in this thesis: the development of a reconfigurable energy subsystem for wireless sensor nodes. The aim of the reported work is to provide a generalised scheme that permits this energy-adaptive behaviour, but in a hardware-agnostic way (i.e. without being constrained to specific types of energy device). The following subsections outline the requirements of the modular design, the usage scenarios for the described system, the major challenges, and the general strategy that has been adopted. Clearly, the provision of these capabilities should not adversely impact on the overall performance of the system: it would be useless if the additional management hardware rendered the system significantly less efficient or unable to perform its sensing tasks. The overall aim is that the tangible benefits of the system (in achieving energy-awareness for a plug-and-play reconfigurable system) outweigh any drawbacks (in the potential loss of quantifiable efficiency of power conversion circuitry, and additional processor cycles taken in managing the system). Obviously this is weighing a subjective measure against one that can easily be determined; however, this will be set in context and evaluated in line with the criteria outlined in Section 3.9.2.

3.2.2 Modular design

With a potentially complex energy subsystem that is able to support multiple energy sources and stores, it is important that a standardised modular approach is used for the design of the hardware in the energy subsystem. As already expressed in Section 3.2.1, there is a need for a system that can be plugged together at the time of system deployment, with the appropriate energy and sensing hardware being attached, and for the individual modules in the system to interface to deliver a reliable and robust power supply that can both be monitored and managed by the microcontroller on the wireless sensor node. It has been stated that each energy module should have its own power conditioning and management interface circuitry, but as yet a scheme has not been introduced that permits multiple energy devices to be attached to a sensing system in such a way. The system described here enables a plug-and-play energy subsystem by means of a modular architecture. The modular scheme outlined in this thesis includes the following elements:

1. A **multiplexer module** that accommodates a number of energy modules, being connected through sockets on the multiplexer module circuit board. The multiplexer module has no real 'intelligence' and is simply a common path for power lines, provides voltage regulation circuitry, and appropriate multiplexer facilities to allow measurement and control of the energy subsystem to take place. This board interfaces directly with the microcontroller, providing its regulated power supply and having a number of additional interface pins to facilitate communication with the microcontroller. The multiplexer module also has an EPROM memory which can be interrogated by the microcontroller, storing basic information such as how many sockets the multiplexer module has, and what voltages it supports.

2. Multiple **energy modules** which may be used for either the generation or storage of energy. An energy module includes the actual energy device and its power conditioning and management circuitry. It also has an EPROM memory which stores its operating parameters, which is readable by the microcontroller. These parameters permit the microcontroller to interpret measurements from the module in order to estimate the amount of power being generated or energy stored, and also to learn how the device may be controlled (if applicable). The energy modules are connected to the multiplexer module through sockets; the power outputs from

the energy modules are effectively connected together through the multiplexer module, thus forming a common 'raw' (or unregulated) voltage rail.

3. A **microcontroller** that interfaces with, and obtains its power supply from, the energy subsystem. There is a certain resource commitment from the microcontroller in order that it may effectively manage its energy subsystem: for the purposes of the system developed in this project, the requirement is the equivalent of eight I/O pins (with at least one being connected to the internal ADC). There is also an impact on the embedded software of the node: unlike conventional systems, a dedicated software 'stack' interfaces with the energy hardware. While these are extra resource requirements for an already resource-constrained system, they enable a number of benefits including the ability to react to changes in the energy hardware and allow the system to be reconfigured in a plug-and-play manner.

The requirements of the proposed scheme can realistically be achieved with common microcontrollers used in wireless sensor nodes. Modern communication stacks such as ZigBee already impose a substantial overhead in terms of memory, code size and processor time, and the proposed energy scheme has a low level of complexity in comparison. While this scheme requires an additional circuit board (the 'multiplexer' module) and a standardised way of interfacing with the energy devices, it is anticipated that in the future, should the scheme become widely adopted, it will be trivial to integrate the multiplexer functionality onto the same PCB as the microcontroller. While there is a requirement for a 'standard' voltage and communication scheme between the energy modules and the microcontroller, there is little additional circuitry required above that already used on sensor nodes – it is just distributed to the energy devices, rather than being integrated onto the main circuit board of the sensor node.

An example of a typical configuration for the developed system is shown in Figure 3.1. Here, the energy subsystem is comprised of three separate energy harvesters (vibration, photovoltaic, and thermoelectric), with energy being buffered in a supercapacitor and optionally in a NiMH secondary battery. A lithium primary battery provides an emergency backup facility. The lines between modules denote physical wires and, in the prototype developed in the case study in Chapter 4 and Chapter 5, form cables that physically plug into sockets on the multiplexer module. The actual socket that each energy module is connected to is unimportant, as this is a flexible plug-and-play system (the power conditioning and switching circuitry is on the modules themselves, therefore little additional hardware is needed on the multiplexer module). The microcontroller interfaces with the energy subsystem as shown, and has a separate interface with its sensing hardware and the antenna (as is conventional for wireless sensor nodes).

It should be noted that the 'default' behaviour of modules in the energy subsystem is to harvest energy to charge up the rechargeable energy stores and to provide power to the microcontroller. The system supports non-renewable energy resources such as primary

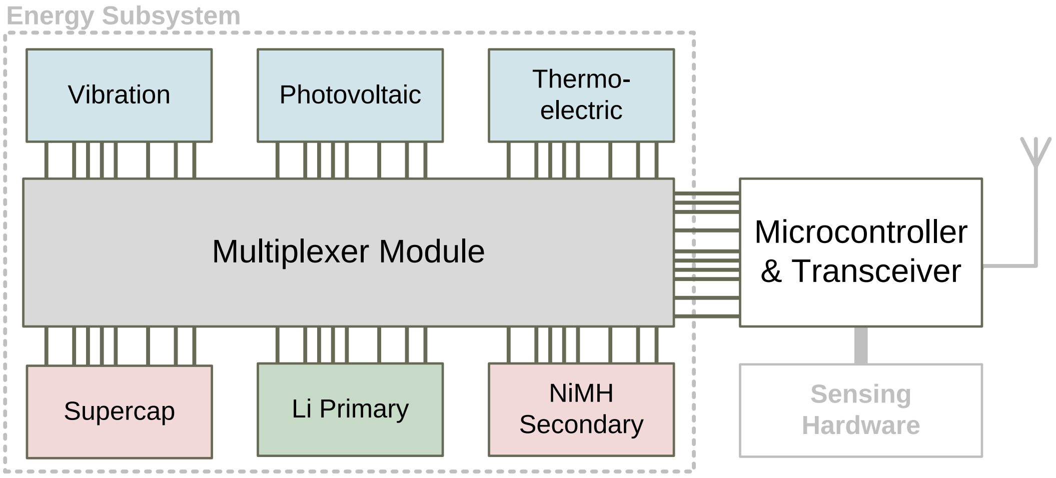

FIGURE 3.1: A modular energy subsystem connected to a sensor node. Energy modules are connected through the multiplexer module to provide the node's power supply.

batteries: the default behaviour for these types of resource is to not use them (unless this is requested by the microcontroller); these types of energy module may also be fitted with 'push-button' switches to allow the system installer to override this temporarily, until the system starts up and the microcontroller takes over management operations. For example, this may be useful to allow a primary battery to provide initial start-up power for a system after it is first installed.

3.2.3 Usage scenario

Ultimately, the usage scenario for this system is for the energy hardware to be connected together at the time of system deployment, and for it to be reconfigurable afterwards (through the addition, removal, or exchange of energy modules). The process of system design and installation, however, will take into account the sensing tasks for the device as well as the available environmental energy. It is expected to follow these steps:

1. The **deployment location and sensing methodology** should be decided on. An appropriate location should be chosen for deploying the sensor node, and a site survey carried out to determine the available environmental energy (including light, vibration, and potential temperature difference).

2. The **transducer, communication, and sensor node** requirements should be identified. The overall energy demand of the sensor node should be estimated, appropriate energy modules selected, and the complete design's feasibility should be verified in combination with the results of the site survey.

3. The **microcontroller on the sensor node can be programmed**, with its ports being configured as appropriate to interface with its sensors and energy subsystem

to deliver an appropriate sensing scheme. The system has a software ‘energy stack’, which means that there is no need to mandate particular energy modules.

4. The **system can now be deployed**. The appropriate energy modules should be connected at the time of installation. The microcontroller will now start up automatically and auto-detect the energy hardware connected.

5. The **system will monitor and manage its energy resources**, with information about the energy status being made available to the application running on the microcontroller. If desired, the system will also be able to monitor the efficacy of energy devices, reporting as appropriate in order to detect faults and monitor the energy status.

6. If necessary, **modules on the energy subsystem can be added, removed, or exchanged** at any time. No reconfiguration of the embedded software is required, as the system can auto-detect any changes made and continue to manage the energy subsystem.

It is anticipated that system designers will call upon a ‘library’ of energy modules in a similar way to how batteries are selected today. There will obviously be cost considerations regarding the selection of modules, and the dynamics of the environmental energy resource must also be taken into account. For example, if considering the use of a photovoltaic module, one will typically need to model the dynamics of the system over a 24-hour period (to cover both day and night) and ensure that the energy subsystem is capable of supplying energy to maintain the sensing schedule. Similarly, if the system is powered from ‘waste energy’ from the machinery it is mounted on (for example, on a pump powered from mains electricity), one must consider the effects to the energy subsystem of a malfunction or failure of that machine, and whether this should affect its sensing abilities.

3.2.4 Major challenges and strategy

As discussed in Chapter 2, wireless sensor nodes are highly resource-constrained. They are based on microcontrollers with relatively small amounts of memory, low clock speeds, and a restricted number of inputs and outputs. The energy resources for these devices are also very limited: conventionally, primary batteries have been used (which are normally expected to last for months or years, meaning that average power consumption must be very low), and energy harvesting devices are also becoming established (most of which produce less than 1mW of power). This project is concerned with the development of a flexible energy subsystem that can accommodate a range of energy resources. Energy harvesting sources which deliver between 100μW and 10mW during normal operation are considered. This power level alone is insufficient to power typical sensor nodes in their active mode (when transmitting or receiving data), therefore system operation must be duty-cycled and harvested energy must be accumulated during periods when the node is ‘sleeping’.

In order to make best use of its energy resources, especially where energy harvesting provides power to the system, energy-awareness is essential. Energy-aware operation permits the node to adapt its activities to exploit plentiful or scarce energy resources, and potentially to learn and predict any patterns in energy availability. When only a small amount of energy is buffered (such as where only a supercapacitor used for this purpose), sufficient energy for less than a minute of active power consumption may be stored. If the node fails to adapt its activity to its energy status, the stored energy may quickly become absolutely depleted. This is undesirable for two reasons: firstly, the node will be forced to turn off and therefore may miss important events; and secondly, the node will have to go through a full start-up process when it has accumulated sufficient energy to turn on, wasting further energy and potentially losing some important data that may have been stored in volatile memory.

Achieving energy-awareness in this application is challenging, but strategies have been adopted in this project to reduce the computational load and storage requirements, and the overall impact on the energy efficiency of the system. This reaches from the algorithms used to calculate power and energy, down to the circuitry added to each device to facilitate the functionality. There is also a trade-off between precision and energy consumption: some mathematical processes such as Taylor expansions gain precision when taken to more terms; also, many ultra low-power components (such as operational amplifiers) have notably poorer performance than their high-power counterparts. Ultimately, a precise calculation for energy stored or power generated is neither needed nor possible: in general, a tolerance of at least ±10% on estimates of energy status is acceptable as this is within the tolerance of many components, and all that is required is an indicative figure on which to base decisions about the node’s activity level.

Delivering a flexible reconfigurable system architecture is also non-trivial. The approach adopted in this project is to effectively use a ‘go-between’ circuit board between the energy harvesting/storage device and the multiplexer module, to deal with power conditioning, enable the management and monitoring functionality and host an electronic memory that can be interrogated by the microcontroller. The energy harvesting/storage device and this circuit board are together known as an energy module. The circuitry on each energy module typically includes low-resistance transistor-based switches to implement the additional functions. For example, when the microcontroller wishes to measure the nominal power from the photovoltaic module, it will send the measurement control line high, which will cause the photovoltaic cell’s positive terminal to be disconnected from the load; the control line will also power an op-amp, which will buffer the resultant open-circuit voltage and allow the nominal power to be estimated (through parameters stored in the electronic data sheet on the module).

Ultimately, the energy-aware system developed in this project is reliant on three novel elements (which are described, in turn, in the following sections of this chapter):

1. **Energy Electronic Data Sheets:** these store relevant operational information for energy devices in EPROM memory on the energy modules themselves, allowing the microcontroller to execute and interpret measurements, and manage the module. The electronic data sheets have a set format, which is defined in Section 3.3.

2. **Common Hardware Interface:** this is the interface between the energy modules, the multiplexer module, and the microcontroller. It allows the microcontroller to obtain information about its energy hardware and act to monitor and manage these resources. The format of the common hardware interface is defined in Section 3.4.

3. **Embedded Software Structure:** provides a 'stack' structure, which is similar to the communications stack, that enables the application on the microcontroller to interface with the energy hardware. The format of the software structure is described in Section 3.7.

3.3 Energy Electronic Data Sheet (EEDS)

3.3.1 Overview and justification

The concept of using electronic data sheets for a range of components was introduced in Section 2.4.3. It is extended here by the proposed use of electronic data sheets, to be known as the 'Energy Electronic Data Sheet' (EEDS), to store parameters of energy modules. The aim of the EEDS is to promote the reconfigurability of the energy resources of sensor nodes by storing parameters related to the operation of each energy module on the modules themselves, rather than hard-coding this information into the embedded software of the sensor node (as is the case with present systems). The data sheet identifies the type of module, for example vibration energy harvester, and its operating parameters including how the power generated corresponds to its measured voltage, and how to interpret measurements from the device. This enables autonomous sensors to monitor and manage the status of the individual modules in their energy subsystem, thus delivering an architecture which achieves energy-aware operation. The design of the enabling hardware is described in Section 3.4, and supports a number of energy devices while permitting each EEDS to be individually read by the microcontroller.

3.3.2 Data sheet format

The basic EEDS structure is shown in Table 3.1. This permits the microcontroller to obtain sufficient information to identify, interpret and manage each energy module. It is anticipated that, for later revisions of the data sheet format (should the work be taken forward to standardisation), descriptors such as manufacturer ID and model number would also be included, as is presently the case with TEDS, to provide traceability for modules. This could be managed by an organisation such as the IEEE.

Field	**Size**	**Description**
Device ID	64 bits	Serial number of EPROM memory
Module Type	8 bits	Identifies class of module and its capabilities
Parameter 1 Parameter 2 ...	8 bits 8 bits 8 bits	Dependent on module class; parameters enable energy calculations

Table 3.1: Outline format for the Energy Electronic Data Sheet.

The parameters stored in the EEDS are sufficient for the microcontroller to infer how to interface with the energy hardware and interpret the measurements obtained (i.e. translate voltage measurements into estimates of instantaneous power or stored energy). For example, for a rechargeable battery, the EEDS will indicate that the charging and discharging of the device can be switched on or off via the digital interface, and that the measurement control line connects the battery across a known load (defined in the data sheet) so that its state-of-charge can be estimated. The state-of-charge of the battery can be inferred from a piecewise-linear representation of the discharge curve, by using the measured voltage across a known load. From this, along with information on the capacity of the battery, the usable stored energy can be estimated by the microcontroller.

The class codes for energy devices are shown in Table 3.2. It may be observed that energy modules are classified as energy stores or sources. Stores include batteries (primary and secondary), capacitive storage devices, and any other device whose primary function is to *store*, rather than *generate*, energy. Conversely, energy sources include energy harvesting devices (such as devices generating energy from light, vibration, or temperature difference) along with other energy sources such as mains electricity or wireless power transmission technologies. The ‘00’ classifier is intended for use only by multiplexer modules, and class ‘11’ is reserved for future use (it may be used to identify energy consumers, should the scheme be extended).

Code	**Description**
00	Multiplexer
01	Energy Store
10	Energy Source
11	Undefined (reserved for future use)

Table 3.2: Module class codes.

Initial EEDS identifiers for devices are shown in Table 3.3. The first two bits of the type identifier correspond to the codes expressed in Table 3.2. The middle four bits define the type of device: for the multiplexer (which is a special case), this describes how many ports it has, while for other devices it simply expresses what type of module it is (e.g. for an energy storage device, 0010 is a rechargeable battery). The last two bits of the code indicate the function of the control lines from the microcontroller (i.e. for the rechargeable battery, the first bit indicates that the module's discharge can be turned on or off by the first control line, and the second bit indicates that its charging function can be controlled by the second control line). As a complete example, 01**0001**10 represents an energy storage device – a primary battery – whose discharge can be controlled through the first control line (but which cannot be recharged). This scheme is used by the prototype system developed as part of the case study reported later in this thesis.

Class	**Description**
00**0110**00	Multiplexer module - 6 inputs
01**0001**10	Primary battery
01**0010**11	Rechargeable battery
01**0011**00	Supercapacitor
10**0001**00	Mains module
10**0010**00	PV module
10**0011**00	Vibration (electromagnetic) harvester
10**0100**00	Vibration (piezoelectric) harvester
10**0101**00	Vibration (electrostatic) harvester
10**0110**00	Thermoelectric harvester
10**0111**00	Wind harvester

Table 3.3: Examples of module type identifiers.

3.3.3 Hardware and interrogation method

As discussed in Section 2.4.2, TEDS is most commonly implemented with Maxim-Dallas 1-wire EPROMs. 1-wire devices communicate using a timing-specific protocol and require only two connections: ground, and a combined data and power pin. The capabilities of the 1-wire protocol mean that it is possible for a large number of devices to share the same single-wire bus. The addressing of devices in this configuration is not straightforward as the master has to go through an initial search process to identify all devices on the line in order to determine their serial numbers; when it has done this, it will still be uncertain about the actual physical location of each device. In most applications, this does not matter; however, in this situation, it is essential to know which device is connected to which specific port on the multiplexer module in order that it may be monitored and managed individually (using the port number as the address). In this system, this problem is mitigated by the connection of 1-wire devices through a multiplexer, meaning that EEDS can be addressed on a module-by-module basis rather than using the ID of the 1-wire device on a shared bus. The two interface schemes are shown in Figure 3.2. Further detail on the hardware interface implemented in this system is given in Section 3.4.

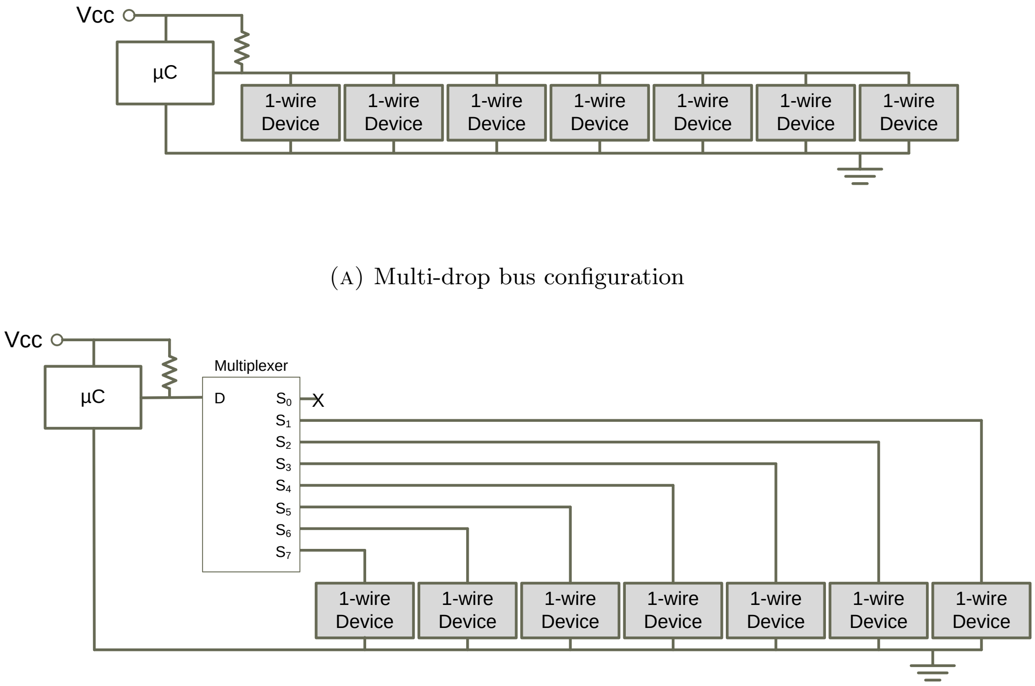

(A) Multi-drop bus configuration

(B) Multiplexed bus configuration

FIGURE 3.2: Conventional and multiplexed 1-wire bus configurations.

3.4 Common Hardware Interface (CHI)

3.4.1 Overview and justification

Microcontrollers have a limited number of I/O pins available, especially those that are connected to internal ADCs, and it is necessary to conserve these as far as possible. Furthermore, within the scheme of EEDS-equipped modules, it is important that the microcontroller is able to access each module independently – firstly in order to determine its data sheet parameters, and secondly to perform measurement and control operations. In the scenario outlined earlier, it would be unrealistic to expect that each module would have multiple direct connections to I/O pins of the microcontroller. For this reason, it is necessary to multiplex parts of the system to make best use of resources and allow queries to be effectively executed. A multiplexer module is employed in this scheme, that enables five signals (one 1-wire EEDS line, and four other general I/O including one analogue signal line) to be routed to each module from the microcontroller. Up to six individual energy modules are supported.

3.4.2 EEDS interface

A drawback of 1-wire devices is that they draw current when connected to the supply – even when not actively communicating with the host. In order to isolate all 1-wire devices, the first multiplexed channel (address ‘0’) is used for ancillary communication between the microcontroller and the multiplexer module, without a 1-wire device installed on this channel. The microcontroller leaves the address lines in this state when not actively communicating with the energy modules, thus minimising the power consumed by the 1-wire bus, and this permits the multiplexer module to use the measurement line to trigger an interrupt on the microcontroller (e.g. it can be used to indicate that a voltage threshold has been passed). The maximum number of energy modules supported by this scheme is six (three address lines enable eight channels, two of which are used for communication with the multiplexer module). The allocation of two addresses to the multiplexer module allows the EEDS for the multiplexer module to be read through address ‘7’, and leaves the remaining addresses (channels ‘1’ through to ‘6’) for other energy modules. The presence of a multiplexer module EEDS on a channel other than ‘7’ would indicate a configuration or hardware error.

3.4.3 Interface format

With the conventional method of searching a 1-wire bus outlined earlier, in this application it would still be unclear which module is connected to each multiplexer module socket (hence making monitoring or control of energy modules through their correct sockets impossible). In this system, the 1-wire EEDS devices are connected through the multiplexer module in the same way as the control and measurement signals, so that they can be accessed one module at a time (by channel rather than serial number), corresponding to the actual socket the modules are connected to on the multiplexer module. The scheme shown in Table 3.4 is used to define the multiplexed address of each module.

Address	**Binary**	**Channel**	**Module Type**	**Functionality**
0	000	-	Multiplexer	Low-Power Monitoring
1	001	1	Energy module	Module-dependent
2	010	2	Energy module	Module-dependent
3	011	3	Energy module	Module-dependent
4	100	4	Energy module	Module-dependent
5	101	5	Energy module	Module-dependent
6	110	6	Energy module	Module-dependent
7	111	-	Multiplexer	Active interrogation

Table 3.4: Identifiers for modules in the energy subsystem. The multiplexer module has addresses ‘0’ and ‘7’, energy modules are accessed through addresses ‘1’ to ‘6’.

By first querying address ‘7’ (the multiplexer module) the EEDS of this module can be read in order to determine its operating parameters. These parameters include, most importantly, the number of sockets it has (up to six), its minimum cut-off voltage, maximum supply rail voltage, and regulated voltage. In this way, through this common interface, the microcontroller can self-determine the energy subsystem's parameters by sequentially querying the EEDS on all devices attached through the multiplexer module. It will also understand the function of each control and measurement line for the individual modules.

It is the task of the multiplexer module to ensure that the supply voltage and ADC inputs that the microcontroller receives are not damaging to the device, nominally by means of diode-clamping to the supply output rails. The modules are also required to ensure that the measurement outputs they give are within the valid range of 0V to 1V, which is compatible with the ADCs on low-voltage microcontrollers used in wireless sensor nodes, as introduced in Section 2.7.1.

It is not necessary to mandate specific sockets on the multiplexer module for specific energy module types as all switching hardware is located on the modules themselves, rather than on the multiplexer module. However, it should be noted that each module is responsible for self-regulating its output voltage to the maximum supported by the multiplexer module (in the case of the prototype modules produced under this project, it was 4.5V). In the case of harvesting modules, this means that a voltage regulator, or voltage detector and isolation transistor arrangement, may be necessary for the purposes of overvoltage protection. It is also essential that digital communication lines are able to interpret voltages in the regulated supply range so that they can be managed by the microcontroller.

In summary, the multiplexer module simply acts as a go-between, allowing the node's microcontroller to interface with the energy modules. There are two types of connection: microcontroller to multiplexer, and multiplexer to energy module. These are described in the following subsections.

Microcontroller to Multiplexer

For the interface between the microcontroller and the energy subsystem, the aim is to provide a good level of functionality, while minimising the number of microcontroller I/O pins required. The lines listed in Table 3.5 are provided between the microcontroller and the multiplexer module. Two lines are for the power supply, the other eight connect to the equivalent of one 8-bit port on the microcontroller (the required interface is comprised of one ADC input, four digital outputs, and two bidirectional digital I/O pins). These resource requirements are conservative: the CC2430 and MSP430F2274 microcontrollers, introduced in Section 2.7.1, have 21 and 32 general purpose I/O pins (with 8 and 12 of these being ADC-enabled pins) respectively.

Pin	Connector	Description
1 2 3	Mux Address 0 Mux Address 1 Mux Address 2	Digital lines to control all multiplexers
4	1-wire EEDS line	Digital 1-wire interface
5 6	Measurement Control Measurement	Initiates measurement Analogue measurement output
7 8	Device Control Device Control	Control outputs to module, these are bi-directional (control state can be determined)
9 10	Vreg GND	Supply voltage output (direct to microcontroller)

Table 3.5: Common Hardware Interface: connections between microcontroller and multiplexer module.

Multiplexer to Energy Modules

The interface between the multiplexer module and each energy module is comprised of eight lines, as shown in Table 3.6. The 1-wire EEDS line, one measurement control line, one measurement line, and two digital bidirectional I/O lines are passed through to each energy module after multiplexing. The ground and supply terminals from each module directly connect to the ground and raw voltage rails on the multiplexer module. Furthermore, the regulated voltage from the multiplexer module is fed back to each energy module to facilitate digital communications with the microcontroller without the need for level-shifting (otherwise the microcontroller would likely be exposed to out-of-range and damaging digital voltages).

Pin	Connector	Description
1	1-wire EEDS line	Digital 1-wire interface
2 3	Measurement Control Measurement	Initiates measurement Analogue measurement output
4 5	Device Control Device Control	Control outputs to module, these are bi-directional (control state can be determined)
6	Vreg	Regulated voltage used as supply to μC
7 8	Vout GND	Raw voltage interface

Table 3.6: Common Hardware Interface: connections between multiplexer module and energy modules.

3.4.4 Integration of multiple energy sources

There are two main options for combining separate energy harvesting devices on a single node. Figure 3.3 shows a system where two energy sources act through diodes to charge a single supercapacitor adjacent to the microcontroller, and Figure 3.4 shows a scheme where each energy source has a separate supercapacitor which feeds energy to the microcontroller via a diode. Option 1 can potentially offer better long-term performance where both sources act to maintain a high voltage on the supercapacitor. Option

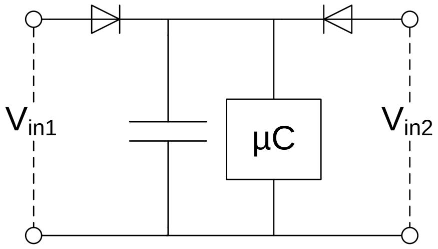

Figure 3.3: Option 1 for multiple energy source combination. Features a single supercapacitor adjacent to the microcontroller.

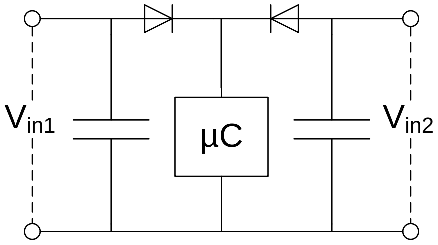

Figure 3.4: Option 2 for multiple energy source combination. Features separate supercapacitor for each energy source.

2, while featuring a higher component count, may offer faster start-up times as energy sources could charge up smaller capacitors – only one of which is required to reach the microcontroller's turn-on voltage for the system to function. The system developed under this project uses a variant of the Option 1 scheme: all power conditioning electronics are located on the energy modules.

3.5 Generalised system hardware specification

3.5.1 Energy multiplexer

The purpose of the multiplexer module is to permit the interconnection of energy modules, to supply a stable power supply to the microcontroller, and to allow it to monitor and manage the energy modules through their data lines. The multiplexer module, as a minimum, features the following hardware:

1. Five 8-to-1 multiplexers (one 1-wire line, one analogue measurement line, one digital control, and two bidirectional digital I/O) to facilitate the connection of up to six energy modules; smaller multiplexers can be used to facilitate connection of fewer modules.

2. Undervoltage protection circuit to inhibit supply to microcontroller.
3. Voltage regulation (nominally to 3.0V) for microcontroller and 1-wire devices.
4. Diode clamping on bi-directional lines.
5. Pull-up resistor on microcontroller side of 1-wire multiplexer.
6. Pull-down resistors on address lines of multiplexers.
7. Query facility to measure raw voltage – scaled to 0-1V range.
8. Small low-ESR capacitor to act as operating buffer.
9. 1-wire device programmed with multiplexer EEDS.
10. Up to six sockets for connection of energy modules.

The components selected for this module should draw as little current as possible and should not adversely impact on the overall efficiency of the system. The 8-to-1 multiplexers must be capable of operating at voltages down to the minimum supply voltage from the multiplexer module (nominally 2.0V). The undervoltage protection circuit acts to disconnect the microcontroller if the unregulated voltage of the system drops below this minimum value. Diode clamping on the bi-directional lines ensures that signals from the energy modules do not exceed the supply voltage of the microcontroller.

The 1-wire pull-up resistor facilitates 1-wire communications by pulling up the 1-wire bus line. Pull-down resistors on the address lines ensure that the multiplexers revert to address 0 (for low-power monitoring) when the microcontroller is not actively communicating. This also has the effect that the 1-wire pull-up resistor is isolated when the device is not active, thus the power consumption of the module is minimised.

Given that MSP430 microcontrollers have a typical supply voltage range of 1.8-3.6V, and the CC2430 requires 2.0-3.6V, in order to support a wide range of microcontrollers the multiplexer module in the prototype will regulate the supply voltage to between 2.0V and 3.0V. The multiplexer module supports an unregulated ‘raw’ voltage that is higher than the maximum supply voltage of the microcontroller. It is believed that this will normally be 4.5V as this is the maximum voltage supported by many commercially-available supercapacitors.

3.5.2 Energy modules

Each energy module will feature the following hardware:

1. Switches and diodes to prevent the unwanted backflow of energy to harvesting devices from the multiplexer module.

2. Optional switching hardware to allow the querying of the module's energy status.
3. Optional resistor divider to bring analogue measurements into the range of the microcontroller's ADC, buffered by an operational amplifier.
4. Optional 'persistent' management channels, for example to maintain the 'charge' or 'discharge' enable control status for battery modules.
5. 1-wire device programmed with module EEDS.
6. Overvoltage protection limiting the module's output voltage, if necessary.
7. A socket to enable connection with the multiplexer module.

Essentially, the purpose of the energy modules is to ensure that they generate, buffer, or otherwise supply energy to the multiplexer module in order that it can reliably and efficiently supply power to the microcontroller. Given that the multiplexer module will generally operate with an unregulated voltage of up to 4.5V, it is expected that energy modules will also self-regulate their outputs to this maximum. Each module is effectively able to operate autonomously, and must function in a stable manner without external control.

Care must be taken when designing energy modules to ensure that they will allow the system to start from 'cold'. A further detail is that the energy module should not be damaged by not being connected to the multiplexer module (i.e. they should not rely on their outputs being connected in order to maintain safe operation). Therefore, as a general rule:

- Energy harvesters and mains electricity modules should be designed to initialise supplying energy to the system by default.
- Fast-response buffers, such as supercapacitors, should (on system start-up) default to permitting both charge and discharge.
- Slow-response buffers, such as rechargeable batteries, should by default be permitted to discharge (but may support a manual override facility, e.g. using push buttons).
- Primary energy sources (such as non-rechargeable batteries) will normally have a push-button control to allow the system to cold-start on initial installation, then be managed by the microcontroller. Their default status will, however, be 'off'.

3.5.3 Microcontroller requirements

To provide the interface with the energy subsystem, the microcontroller needs to have eight I/O pins available. One of these must be configurable as an ADC input, four as digital outputs, and a further three as bidirectional reconfigurable digital inputs or outputs. The microcontroller should be capable of entering a 'sleep' mode with a current draw of around 1μA and be woken by interrupts (either external or timer-driven). Ideally the microcontroller will incorporate a 'sleep timer' which will permit it to wake up after a defined time period. The microcontroller should incorporate at least a basic 8-bit processor with sufficient memory to include both the interface with the energy subsystem and the other processing and communication functions.

3.5.4 Under- and over-voltage protection

Wireless sensor systems based on microcontrollers are sensitive to their supply voltage. For systems which include energy harvesting, this can be problematic as a characteristic of these is that their output voltage will typically vary over time, dependent on the charge state of the energy store, the amount of energy being harvested, and the dynamics of energy usage by the sensor node. It is, therefore, important that the power management electronics act to prevent the microcontroller from being supplied with an excessive voltage, as driving the device outside its 'absolute maximum ratings' is likely to cause permanent damage. It is also essential to ensure that the microcontroller does not attempt to switch on before the output voltage from the circuit has passed the minimum operating voltage for the microcontroller. Attempting to start a microcontroller when the voltage is too low will cause the microcontroller to behave unpredictably, and experiments carried out under this project indicate it is likely to cause excessive power to be drawn, thus meaning that the sensor node is unlikely to start up reliably, and will draw excessive amounts of current (meaning that the node's energy stores are likely to deplete rapidly).

3.6 Energy status determination and algorithms

3.6.1 Overview

In order for sensor nodes to react to changes in their stored energy, the node must be able to effectively compute its energy status. In the scheme proposed in this thesis, the node must support a range of energy hardware and use appropriate methods to calculate the level of stored energy. It must also present information on the energy status in a standardised way, so that the application running on the sensor node can effectively interpret this information. This section explores methods for calculating and presenting the energy status of the sensor node, including methods for calculating the stored energy in batteries and supercapacitors, and uses a discretised 'energy priority' scheme for representing the levels of stored energy.

3.6.2 Energy monitoring

It is important for energy-aware systems to have an indication of the state of charge of energy stores, in order that systems can adjust their behaviour dependent on their energy status. There are a number of different ways of calculating the energy status value, and up to now most methods have represented the stored energy, or voltage, as a percentage. Rather than simply an indication of how 'full' the energy store is, though, it may be more helpful to get an idea of *how long a node can operate for compared to its neighbours*. To represent this, the author proposes the introduction of φ_t, the remaining lifetime fraction compared to when the energy store is full. A value of 0% means that the node has insufficient energy to remain operational, and a value of 100% means that the energy store is full. Values between 0% and 100% represent normal operation of the node, with 50% meaning that the node's energy store is half way through (from a time perspective) being discharged.

Figure 3.5 shows an example of the discharge profile of an ideal 1F supercapacitor through a 450Ω resistor, 70mA current load, or 200mW power load. These values were chosen as they draw similar levels of current at 3V. The simulation was started at 3.0V as this is a typical 'maximum' voltage used to power microcontrollers on sensor nodes. The graph shows that the load type has a major effect on the discharge characteristics, with the curves diverging substantially as the capacitor discharges. In this example, the constant-power discharge curve reaches 2.0V approximately 32% faster than the constant-resistance curve; 2.0V is a typical minimum voltage at which microcontrollers will function. This investigation was carried out in simulation as it would not be possible to ensure that real supercapacitors had exactly the same level of charge at the start of each test, due to their complex characteristics and long time-constants.

Clearly the dynamics of discharge have a major impact on the endurance of the power supply. Assuming a resistive discharge profile when the load is actually power-dominated can result in overly optimistic remaining lifetime calculation results, and for these estimates to decrease much more rapidly than expected towards the end of its lifetime (an undesirable situation as it would lead to an accelerated decline in resources).

The value of φ_t represents the node's proportion along the theoretical *time* axis from being fully charged to 'empty' (in the case of the CC2430EM, this is from 3.6V to 2.0V). The reader may question the value of using the 'time' axis when nodes are energy-harvesting and their stored energy may increase as well as decrease. This method is simply a snapshot of the present energy status of the node, and the value calculated is just a representation of how 'charged' a node is while being adjusted for the method of discharge of the energy store (be it resistive, power, or current). A more thorough explanation of the categorisation of discharge methods is given in Section 3.6.3, and methods for calculating the state-of-charge and remaining lifetime fraction for supercapacitors and batteries are given in sections 3.6.4 and 3.6.5.

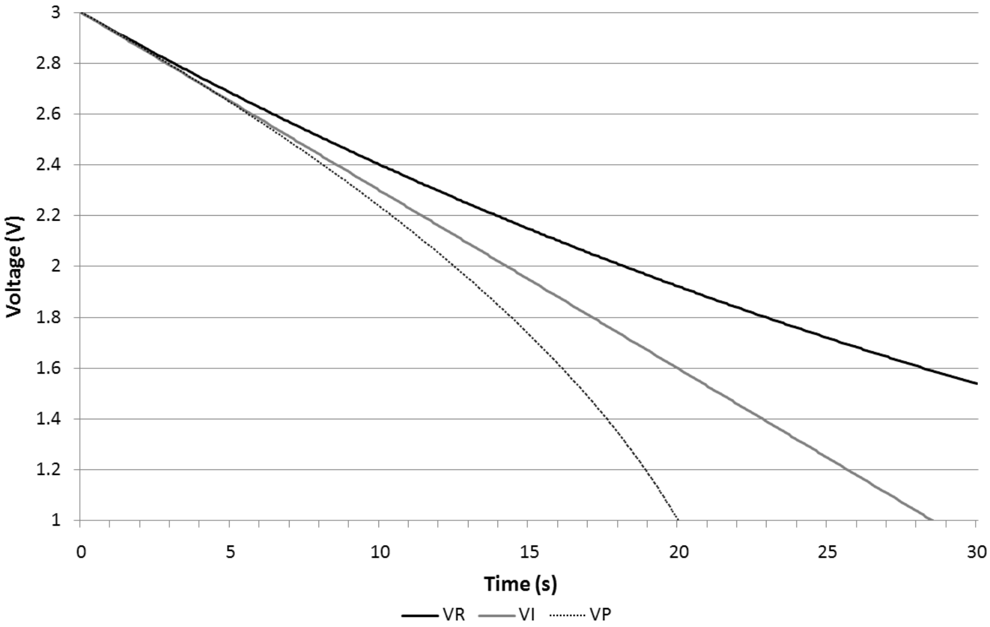

Figure 3.5: Simulated discharge of a 1F supercapacitor through a 450Ω resistor, 70mA current load, and 200mW power load. Shows divergent behaviour with time.

The concept of energy priorities was introduced in Section 2.6.2. The system of energy priority levels used in this project is shown in Table 3.7. Through this method, the activity of the system is controlled by its energy status. The energy status information is updated periodically and is classified as one of the energy priority values. The provision of eight different classifications is largely arbitrary. The relative threshold values are adjustable in software. This is a flexible system that allows the operation of the system to be adjusted based on its energy status.

Priority	**Max %**	**Description**
EP_Mains	–	Operating from mains power
EP_5	–	Intermediate energy levels
EP_4	80	
EP_3	60	
EP_2	40	
EP_1	20	Very limited energy
EP_Empty	2	Cannot sustain activity
EP_Unknown	–	Error calculating status/unknown

Table 3.7: Energy Priority Levels.

3.6.3 Categorisation of load type

In the context of state-of-charge determination or calculation of the remaining lifetime fraction, it is helpful to know what the dynamics of the load are. Here, the discharge types are given three categories. These categories do not imply that a constant load exists – rather, that the dynamics of the load in response to a changing supply voltage are closest to that of the analogous component (be it resistance, current or power).

Resistive-dominated discharge

In this type of discharge, the load's response to changing supply voltage is similar to that of a resistor. It is not implied that the load imposes a constant resistance on the energy store. For example, for a given activity level, the node will draw around 50% more current at 3V than it would at 2V, which can be modelled by $V = IR$.

Current-dominated discharge

Here, the load responds to changing voltages in a similar way to a current source. For a given activity level, the current drawn from the store is constant, but the power used changes, dependent on the relationship $P = VI$. Therefore, at 3V, the node will consume around 50% more power than at 2V.

Power-dominated discharge

This type of discharge implies that the load responds to changing voltages in a similar way to a power source. For a node with a given activity level, the power drawn is constant but the current drawn depends on the relationship $I = P/V$. Therefore, at 3V, the node draws 33% *less* current than at 2V.

3.6.4 Supercapacitor state-of-charge and capacity

There will typically be a range of voltages over which a microcontroller can operate: for the CC2430, this is between 2.0 and 3.6V. Obviously, if such a microcontroller is driven directly from an energy store, the energy stored when the voltage is below 2.0V is effectively unusable. For a capacitor, the following methods for determining the energy status (φ_t, the fraction of operating time remaining compared to when the store is full) are applicable, and largely rely on the relationship $E = \frac{1}{2}CV^2$:

1. **Energy fraction φ_E:** this is simply a measure of how 'full' the energy store is, and is most useful when the load imposes a *power-dominant* requirement on the store. It is calculated by determining the usable energy stored, and dividing by the maximum usable energy if the store was full.

2. **Voltage fraction φ_V:** this value assumes that the load imposes a *current-dominant* requirement on the store. It is calculated by dividing the usable voltage range by the maximum usable voltage range.

3. **Logarithmic discharge fraction φ_L:** this value assumes a *resistive-dominant* load is present across the store. It gives an indication of the proportion of time

remaining, expressed as a percentage (where 100% is fully charged, 0% is when the store is at the minimum voltage, and 50% is half way along the *time* axis between the two values) with the simplifying assumption that the capacitor is discharged through a resistive load.

Clearly, a value for the energy proportion is not particularly helpful if the load across the store behaves as a current- or resistance-dominant consumer, as in these cases the power requirements of the node vary with the amount of energy stored (and hence the store voltage). The energy fraction may be calculated by means of Equation 3.1.

$$\varphi_t = \varphi_E = \frac{E - \min(E)}{\max(E) - \min(E)} \tag{3.1}$$

Where E is the amount of energy stored by the system at a given time. $\min(E)$ is the energy at the store's minimum voltage, and $\max(E)$ is the energy at its maximum voltage. This gives a rough idea of the energy status of the node, but is reliant on the assumption that the load is a power-dominated consumer.

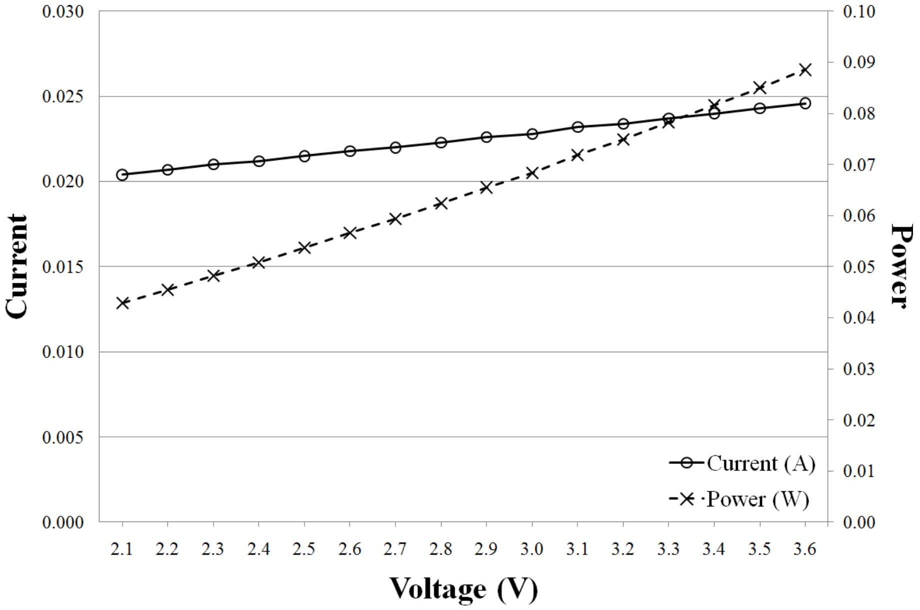

FIGURE 3.6: Current and power consumption of CC2430EM at various supply voltages.

Investigations carried out under this project show that, when exposed to varying voltages, a CC2430EM module under a continuous sense/transmit cycle behaves more closely as a current-dominant load than resistive or power-dominant. A graph of the current and power consumption of the device is shown in Figure 3.6. The voltage fraction gives an indication of the state-of-charge of the capacitor assuming it is discharged by a current which is independent of the store voltage or energy, and hence $I = CdV/dT$, used in Equation 3.2.

$$\varphi_t = \varphi_V = \frac{V - \min(V)}{\max(V) - \min(V)} \tag{3.2}$$

Where V is the store voltage at a given time. $\min(V)$ and $\max(V)$ are the minimum and maximum store voltages.

Finally, the logarithmic discharge fraction exploits the fact that the voltage across a capacitor obeys the relationship $V = V_0 e^{-t/CR}$ for a constant resistance and capacitance (where V_0 is the initial voltage, t is time elapsed, and C and R are capacitance and resistance respectively). This can be rearranged to find t, as shown in Equation 3.3.

$$t = CR \ln \frac{V}{V_0} \tag{3.3}$$

Thus to find the logarithmic discharge fraction the result, Equation 3.4, is independent of t, C, and R.

$$\varphi_t = \varphi_L = 1 - \frac{\ln \frac{V}{\max(V)}}{\ln \frac{\min(V)}{\max(V)}} \tag{3.4}$$

This quantity is the most computationally expensive to calculate, with results for the actual time taken to carry out a complete calculation given in Section 5.5.2. It is likely to give a useful indication of charge status, as it assumes a resistive discharge of the energy store (i.e. the amount of energy consumed by the system is dependent on the store voltage, which is in turn dependent on the energy stored). This calculation can be implemented on microcontrollers using a Taylor expansion. The expansion of the natural logarithm is shown in Equation 3.5. Taking the expansion to its fourth term results in a typical error of approximately 3%, and to its fourth term the error is around 1%. This will normally be sufficiently accurate to give a good idea of the state-of-charge of the system.

$$\ln x = (x-1) - \frac{(x-1)^2}{2} + \frac{(x-1)^3}{3} - \frac{(x-1)^4}{4} + \dots \tag{3.5}$$

3.6.5 Battery state-of-charge and capacity

For conventional primary cells, such as alkaline manganese dioxide batteries, the closed circuit voltage (CCV) of the cell must be measured to give an accurate idea of their state of charge. Measuring the open circuit voltage (OCV) of the cell will not give an accurate indication of the service life remaining as it is subject to recovery effects and other phenomena. The CCV can be determined by placing the battery under load and measuring its voltage. The load is dependent on battery size, but Energizer recommends a 10Ω load is used for a single 1.5V AA-size cell [88]. The resultant CCV can then be traced across to the voltage profile of the cell, such as that given by the manufacturer as in Figure 3.7 [123], and mapped to straight lines through a piecewise-linear approximation (to simplify implementation in microcontrollers) as shown in Table 3.8.

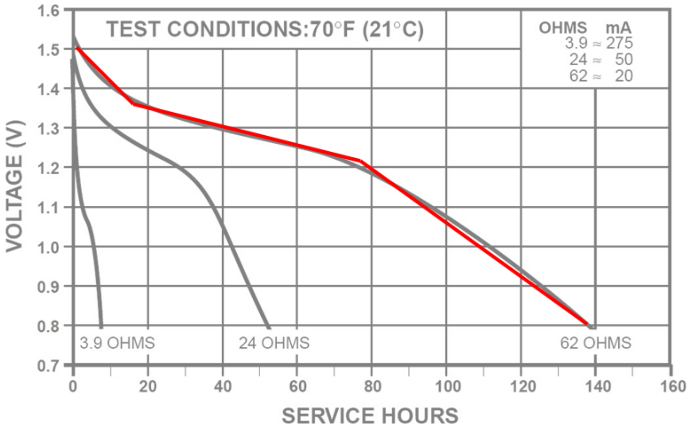

Figure 3.7: Typical discharge profile of Duracell MN1500 alkaline cell under various impedances [123]

Point	Voltage V	Service Hrs	Rem. Lifetime
1	1.52	0	100%
2	1.37	15	86%
3	1.22	79	27%
L	1.00	108	0%
4	0.80	140	-29%

Table 3.8: Simplified discharge profile: Duracell alkaline ‘AA’ cell through resistive load, corresponds to 62Ω discharge curve.

Any discharge curve can be approximated to a series of straight lines and stored in memory. The choice of curve will depend on the type of load normally attached to the battery. It must be noted that use of a resistive discharge curve does not imply that the microcontroller behaves as a constant resistance at all times: purely that its dynamic power consumption due to different voltages varies in line with that of a resistor.

The interrogation process is straightforward, but imposes a further energy requirement on the battery. For example, if an alkaline AA battery is tested once per hour for one year (and each test takes one second), with a 10Ω load, this will consume around 2.2% of the battery’s total capacity. The system designer must trade off higher resolution on the battery state-of-charge against excessive energy wastage in testing.

Lithium-thionyl chloride cells, in common with many other lithium primary battery chemistries, feature a stable operating voltage of around 3.6V until they become depleted [10]. Hence, state-of-charge determination is non-trivial, and systems must estimate the amount of energy used to identify their energy status. End-of-life identification for $LiSOCl_2$ batteries, however, is possible. With a pulsed discharge, similar to that used to identify state-of-charge in alkaline batteries, end-of-life can be identified up to 15%

before the cut-off voltage. Otherwise, continuous loading of the cell will only permit passive identification of end-of-life up to 3% before cut-off. The response of the cell can be sensitive to temperature variation, so care must be taken to ensure that any larger voltage drops with pulsed discharges are not due to seasonal variations.

3.6.6 Power monitoring

While most decisions about the activity level of the node will use information about the energy stored in batteries or supercapacitors, it is also useful to have a knowledge of the power profile of the system. For example, it may be useful to be able to predict when energy is likely to be harvested as well as the instantaneous amount of power being supplied. Indeed, it may also be useful to monitor individual energy devices to ensure that they are operating correctly (and as designed). In the scheme outlined in this thesis, the EEDS stores the operating parameters of the energy modules in order that the amount of stored energy, or generated power, can be measured. Typically, the method for determining the amount of power being generated will use one of the following methods:

1. **Closed-circuit Current Measurement:** with the harvester (or normally the rectified/regulated output from the harvester) connected across a known (typically resistive) load, the power delivered across that load can be calculated. Clearly this is dependent on the assumption that the power being delivered by the harvester across the 'test' load is similar to that being delivered to the actual load.

2. **Open-circuit Voltage Measurement:** with the harvester (not its regulated/rectified output) disconnected from any load, its open-circuit voltage can be measured. From this, the nominal output power may be calculated. This is most suitable for harvesting devices with a DC output, such as photovoltaic cells or thermoelectric generators, but the absence of any load means that the actual output power must be estimated in software.

3. **In-line Current Measurement:** this method uses a small in-line resistor to measure the actual amount of current being delivered by the harvester to the load. While this is theoretically the most accurate type of measurement as it reflects the actual amount of power being delivered, it has a number of drawbacks. Firstly, the efficiency of the system will be affected if the sense resistor is left in line at all times, or complex switching hardware must be used to enable the connection of the sense resistor during measurements. Secondly, the resistor must be small in order to minimise the effects of the resistance; this means that the resulting voltage measurement will be small. Thirdly, the resistor must be connected on the positive supply line, meaning that the measured voltage will be differential, again requiring additional processing and introducing additional error.

3.7 Software structure

3.7.1 Overall software structure

Given the aim of developing a consistent scheme for resource management for wireless sensor nodes, it follows that the embedded software should have a defined structure. Section 2.8 gave a justification for the development of a software structure in which energy and sensor management are devolved into their own individual stacks rather than being integrated into the application layer of the communication stack. A software structure[1] [124] has been developed, comprising separate communications, energy, and sensor stacks linked through a shared application layer and is shown in Figure 3.8. A consistent solution has been presented, in which each stack features 'interface', 'medium', and 'management' layers (in line with the basic template stack in Figure 3.9). For completeness, the communications stack shown here has three levels, but for simplicity it is not anticipated that pre-existing communication stacks would be shoehorned into this scheme. There is no reason why the number of stacks could not be extended beyond the three implemented in the prototype to include other functions such as locationing, but this is beyond the scope of this project.

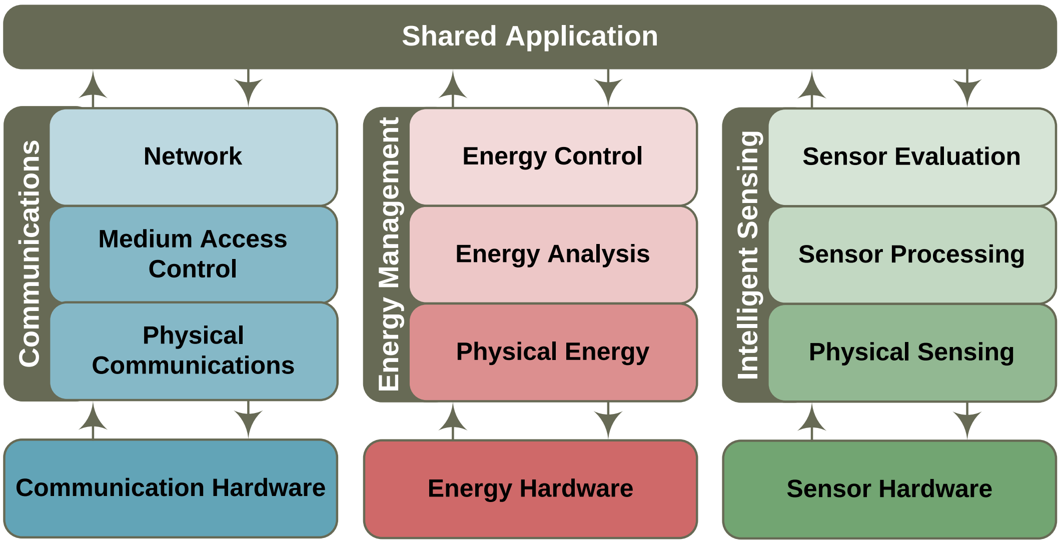

FIGURE 3.8: A combined stack, comprising stacks for communications, energy management, and sensing. Reproduced from [124].

A three-layer stack structure was chosen, after much deliberation, as it offered the most logical method to separate the device interface into discrete levels, while offering the facility for distinct interfaces to be offered between each layer. From a high-level point of view, the interface layer deals with the physical interface with the device, the medium

[1] The "Unified Framework" was initially conceived by Merrett, and early definition work was carried out jointly by Merrett and Weddell, being documented in a technical report [100], and later published [124]. Further work, particularly in the definition, development, and deployment of the Energy Stack, has been carried out by Weddell.

layer deals with processing of this information, and the management layer deals with high-level processing. For the example of the energy management stack, the physical layer carries out switching to take measurements and control the energy modules, the analysis layer translates those measurements using the device models, and the management layer takes this information to provide high-level data to the application. The chosen architecture permits modules in each layer to be swapped, without affecting the rest of the stack layers. For example, a highly-developed management layer may be implemented on more capable microcontrollers which may enable prediction to be used to dictate the behaviour of the node.

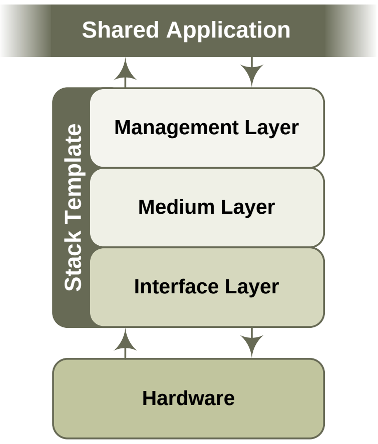

FIGURE 3.9: A basic template stack, reproduced from [124].

3.7.2 The 'Energy Stack'

Overview

The energy management software tasks are modularised and arranged into the 'energy stack', shown in Figure 3.10, which resides on the microcontroller. Here, the energy management process is divided into three layers, with an emphasis on modularisation and re-usability:

- **Energy Control Layer (ECO)**: takes a high-level view of the energy subsystem – presenting information about the overall energy status of the node and responding to queries. It can make decisions to maintain the operation of the node, and may also indicate trends in the energy subsystem.
- **Energy Analysis Layer (EAN)**: is concerned with device models, processing requests from the ECO layer and interpreting data from the PYE. It also carries out operations and measurements at the request of the ECO.
- **Physical Energy Layer (PYE)**: executes the lowest-level operations, such as configuring ports, obtaining ADC readings, and controlling inputs and outputs.

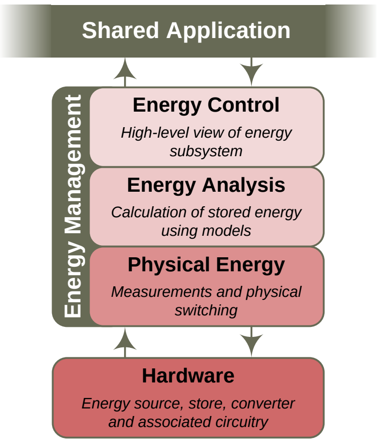
Shared Application
Energy Management
Energy Control
High-level view of energy subsystem
Energy Analysis
Calculation of stored energy using models
Physical Energy
Measurements and physical switching
Hardware
Energy source, store, converter and associated circuitry

FIGURE 3.10: An "Energy Stack", reproduced from [124].

Energy Control (ECO) Layer

The energy control layer presents an interface to the shared application layer. The basic interface includes the energy priority value of the system, along with functions to permit the energy priority thresholds to be changed. It may also be useful for the application layer to ascertain the supply voltage of the node, and possibly the raw values of energy stored and other system-level energy parameters. The tasks of the ECO layer are broadly as follows:

1. **Query processing:** To process general queries from the shared application layer, such as to determine the present supply voltage, energy priority of the node, and parameters related to energy generation.
2. **Reporting:** To report the results of queries, by setting the energy priority level and other variables accessible from the ECO to the application layer. It may also detect trends and report these.
3. **Decision-making:** In more developed systems, to make decisions to maintain the energy integrity of the node by, for example, transferring charge between energy stores or activating energy converters.

Effectively, the ECO layer takes the highest-level view of the energy subsystem and manages the resources below it. The ECO layer presents a generic interface, so that the method of interfacing between the application layer and the energy stack are standardised regardless of the exact nature of the energy subsystem.

Energy Analysis (EAN) Layer

The energy analysis layer provides the interface between the ECO and the PYE layers. While not being concerned with the detailed operation of switching and measurement hardware, it uses energy device models in order to compute energy and power levels from sensed parameters. It initiates voltage measurements, physical switching, and reconfiguration of the energy subsystem, all through the PYE layer. The aim is to provide a consistent interface to the ECO layer, independent of the connected hardware.

1. **Interpretation:** Through using energy source and store models, this layer has the task of converting raw sensed values from the PYE and interpreting this as adjusted energy or power levels. For example, for a supercapacitor energy store the PYE will measure a voltage of 2.0V, and the EAN uses the $E = CV^2/2$ equation to convert this to an energy value.

2. **Measurement requests:** The layer will process measurement requests from the EAN and obtain values through the PYE. Values may be interpreted with the help of models, as above, where necessary.

3. **Command execution:** Executes commands related to the energy subsystem on behalf of the EAN. Directs the flow of energy by initiating switching of transistors etc., by means of the PYE layer.

In summary, the EAN layer mainly deals with the coordination of measurement operations and the interpretation of values from the PYE by means of device models. The aim is to provide a common interface for the ECO, so that the stack structure remains consistent, independent of the detail of the energy subsystem.

Physical Energy (PYE) Layer

The main task of the physical energy layer is to provide an interface with the node's physical energy hardware. This includes the following tasks:

1. **Configuring inputs and outputs:** To set up the interface between the node hardware and its energy subsystem. Examples are configuring ADC parameters, or setting up microcontroller pins as inputs/outputs.

2. **Obtaining values from inputs:** Obtaining raw values for parameters on input pins. Through interfacing with ADC hardware and obtaining raw readings, values can be made available to the EAN layer.

3. **Controlling outputs:** For controlling the performance of the energy subsystem. For example, setting pins high or low to control switching of transistors to isolate energy sources for performance measurement.

The layer acts to hide the complexities of interfacing with the hardware of the energy subsystem from the EAN layer. This layer isolates the rest of the system from the intricacies of interfacing with the actual energy hardware it is deployed on. Again, the aim is to present a common interface to the EAN layer, regardless of the deployed hardware.

3.7.3 The 'Sensing Stack'

The design of the intelligent sensing stack, shown in Section 3.11, is similar to that of the energy management stack. The software tasks for sensor interfacing are modularised and arranged into the 'sensing stack', comprised of the layers as described here:

- **Sensor Evaluation (SEV):** takes a high-level view of the sensing devices on the system – responding to queries for sensor readings and presenting important information about sensors or the sensed data. This layer may also perform trend detection and implement the packet priority features of IDEALS/RMR.
- **Sensor Processing (SPR):** uses device models to provide an adjusted sensor reading, taking account of linearisation and offset adjustments, and providing error bars if appropriate.
- **Physical Sensing (PYS):** interfaces with the physical sensor hardware through ADCs or digital communication ports, obtaining raw measurements.

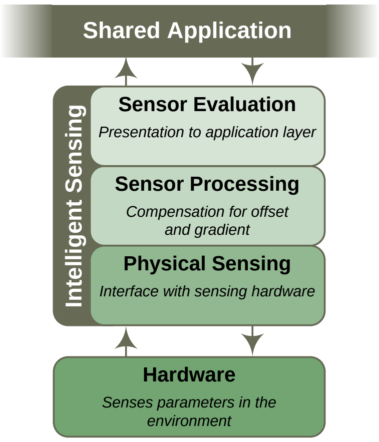
Shared Application
Intelligent Sensing
Sensor Evaluation
Presentation to application layer
Sensor Processing
Compensation for offset and gradient
Physical Sensing
Interface with sensing hardware
Hardware
Senses parameters in the environment

FIGURE 3.11: A "Sensing Stack", reproduced from [124].

The focus of this project is on energy management and the development of the system to contain stacks for interfacing with sensing, energy, and communications hardware. The main task of the sensing stack in this instance is to provide data to be transmitted by the system. A basic sensing stack has been implemented in the prototype and is described in Section 5.4.

3.8 General system operation

3.8.1 Start-up

On initial system start-up, the EEDS on the multiplexer module is queried by the microcontroller on the sensor node. This provides information including how many energy modules are supported by the multiplexer module. The microcontroller then queries the other modules in the energy subsystem. The important parameters are stored in the microcontroller's memory, and hence it is not necessary for the microcontroller to regularly query the EEDS on the modules as a matter of course.

The default behaviour of systems on first installation is to allow the energy harvesting device(s) to charge up the short-term energy stores (such as the supercapacitor modules). Once the store voltage passes a threshold (nominally 2.1V, but ultimately dependent on the minimum operating voltage of the microcontroller), the system connects the power supply to the microcontroller, which then starts up and tests its voltage. When this has reached a suitable level (nominally 2.7V) the microcontroller will perform the first energy-intensive tasks such as scanning its energy subsystem.

The first scan of the energy subsystem is used to ascertain which sockets are occupied, what types of device are present, and their operating parameters. From this initial scan the microcontroller can reach an estimate of the amount of energy stored by the system. This data is stored in the microcontroller memory, so the EEDS of each module need only be scanned once (1-Wire activities are energy-intensive so it is undesirable to carry out unnecessary communications).

3.8.2 Default operation

In normal operation (after the configuration phase), the microcontroller periodically monitors the energy modules in order to gauge the energy status of the sensor node. To do this, the multiplexer address lines are set to the device of interest, and the control and measurement lines are used to control the modules and obtain measurements. For example, with the photovoltaic module, the measurement control line is used as an output to cause a transistor to disconnect the cell from its load, and the open circuit voltage of the cell can be measured through the analogue measurement line. In other situations, the lines are used to connect the harvesting source to a known load to estimate the power being generated.

Furthermore, some modules will be managed by the microcontroller. For example, it may be desirable to only switch a primary battery into the system if there is a high-priority message to be transmitted by the device and its energy status is low. In this situation, one of the bi-directional digital lines can be used to enable the discharge of the battery to the load (in normal operation, other lines can be used to gauge the state-of-charge of the battery or its connection status). In general, the control line must have persistence. This is because the bi-directional lines are multiplexed and it is desirable for the microcontroller to be able to alter settings on a module and ensure that they will be maintained in their requested state after the multiplexer is switched away from their address.

Some modules, such as rechargeable batteries, require different types of control which is why two bidirectional digital control lines have been allocated for these operations. This provides a high level of flexibility when used in combination with the additional digital measurement control and analogue measurement lines.

3.8.3 Monitoring and active management

The microcontroller keeps a table of which sockets on the multiplexer module are occupied. The microcontroller will periodically re-scan the sockets on the multiplexer module, by issuing a reset pulse on the 1-Wire bus for each socket, then listening for a presence pulse from the 1-Wire EPROM in response. By comparing the presence pulses received against its table of known connections, newly connected or disconnected modules can be detected. Newly-connected modules can be interrogated for their full data sheet, while disconnected modules can be deleted from memory and removed from future calculations.

An important note, however, is that hardware changes could be missed if devices are quickly swapped on the same socket. For example, if a battery module on socket 2 is swapped for another device, and this happens within the period between scans, the microcontroller will detect a device still present in that socket and not realise that the module has been exchanged. This drawback can be countered by scanning the serial number of each module after the presence pulse is detected: clearly this is process will consume more energy, but will result in increased confidence in the energy estimates.

3.8.4 Network-level interactions

As discussed in Section 2.6, a number of schemes exist to facilitate energy-aware interaction between sensor nodes in a wireless sensor network. This proposed scheme, and in particular the embedded software architecture, acts to structure the node-level processing in order to simplify these interactions. The energy stack acts to present the application layer with a simple 'energy priority' value. In future iterations of the system, the sensing stack will provide data with a 'packet priority' value, and messages needing to be routed will be received through the communications stack (with their own packet priority values). This will implement the proposed IDEALS/RMR scheme which was proposed by Merrett *et al.* [87] and was discussed earlier. The scheme facilitates 'priority balancing' in which unimportant messages are discarded when energy is scarce, thus ensuring that important messages are still able to traverse the network. Similarly, when energy is plentiful, node activity is increased to make best use of the available energy (which would otherwise be wasted). It may be envisaged that nodes will be able to share their energy status and negotiate to share sensing tasks; this is particularly of interest in applications where sensing is the dominant consumer of energy (as opposed to communications), such as in gas sensing or image processing.

3.9 Towards a prototype to verify the approach

3.9.1 Overview

The scheme described in this chapter has been devised to deliver a plug-and-play capability for reconfigurable energy-aware wireless sensor nodes. It comprises a common hardware interface, electronic data sheet format, and a hardware interconnect scheme that is intended to maximise the flexibility of the system while maintaining efficiency and a relatively low component count. The system has a modular design, with each energy module having its own power conditioning and management interface circuitry, along with an electronic data sheet. It is intended to allow the energy hardware of sensor nodes to be connected together at the time of deployment, and an embedded software architecture has been devised which interfaces with the energy hardware. As the major parts of the system have now been defined, it is important that the validity of the scheme is verified by way of a prototype. The proposed scheme is implemented and validated through the use of a case study (prototype system). The hardware for this is described in Chapter 4 and the embedded software is documented in Chapter 5. The case study represents a realistic and demanding application of the proposed scheme. It incorporates a range of energy resources including energy harvesters and other energy-related devices such as batteries and even a 'mains' electricity supply.

3.9.2 Evaluation criteria

The main contributions of this work were stated in Section 1.4. The proposed architecture will be evaluated by way of a case study reported in the following chapters, which will assess the effectiveness of those contributions. In short, the evaluation of the work will follow this strategy:

1. **Energy harvesting and management:** The performance of each energy module will be explored. This will include analysis of overall efficiency, the impact of

the added energy management or control circuitry, and (where relevant) the quiescent power draw will also be assessed. The associated overheads of the prototype multiplexer module will also be evaluated.

2. **Embedded software development:** The energy-related functionality of the node will be evaluated in terms of the programming effort in delivering energy-aware operation, and the applicability of the embedded software to cross-platform operation. The energy impact of processing operations will be explored, as will its applicability to different hardware (e.g. the impact of mathematical operations on microcontrollers equipped with hardware multipliers or low-power modes). The overall effectiveness of thee energy-aware functionality will be assessed through the case study.

3. **Electronic data sheets and hardware interfaces:** The overall operation of the prototype will be reported, with particular reference to the start-up and plug-and-play features of the system. In particular, the energy demands of the EEDS and CHI will be explored. The applicability of these features to a range of energy hardware will be assessed and any limitations of the prototype system will be stated.

Each aspect of the system will be individually evaluated and the overall performance of the system is summarised in Chapter 6.

3.10 Summary

This chapter defined the interfaces and design for the reconfigurable system architecture, defining many of the key contributions of this work. The overall structure of the system was described, along with a discussion of how the individual aspects fit together to deliver a complete system architecture. The new aspects of the system architecture comprise ‘energy electronic data sheets’ and a ‘common hardware interface’ between the energy modules, which were both defined. A generalised specification for the hardware of each energy module (including the multiplexer module and energy modules) was provided, and methods and algorithms for determination of the energy status of the node were also presented. The novel software structure which has been utilised in this project was also discussed. The general operation of the system was covered, and the requirements of a prototype to verify this approach were also discussed. The prototype system, or case study, which has been used to verify this approach and delivers a reconfigurable system is now described in chapters 4 and 5.

Chapter 4

Case Study: Deployment in a Prototype System – Hardware

4.1 Introduction

The architecture proposed in Chapter 3 is evaluated by way of a case study which is outlined in this chapter, along with the hardware design of the reconfigurable system. Section 4.2 outlines the situation of the case study deployment, and the energy devices that have been chosen for the evaluation. The basic circuitry which has been designed to enable energy-awareness, voltage regulation, and other functionality for the system, is described in Section 4.3. The hardware design of the multiplexer module is detailed in Section 4.4, and the designs of the energy modules are discussed in Section 4.5. The integrated system is discussed in Section 4.6. The design of the embedded software to interface with this hardware is documented in Chapter 5.

4.2 Overview of the case study

4.2.1 Scenario

The aim of the case study is to provide a realistic representation of the types of energy resource that a sensor node may have access to on a typical industrial monitoring deployment. These include harvestable environmental energy such as indoor artificial lighting, machinery vibration, temperature difference, or air flow. As the architecture proposed in this thesis is intended to be a comprehensive scheme for the energy subsystems of sensor nodes, the case study also incorporates more 'conventional' methods of powering the node, such as primary batteries (which may also be used in systems primarily using energy harvesting, but as an 'emergency' supply of energy), and even a wired power supply. Energy is capable of being buffered in devices including supercapacitors and secondary batteries. The specific devices selected for this case study represent what is commercially available and realistically able to provide power for a sub-milliwatt wireless sensor node.

The sensor node uses the electrical energy provided by these resources to carry out sensing, processing, and transmission of sensed data. The actual sensing application is not a focus of this thesis, so a simple temperature sensing application is used to demonstrate the capabilities of the system. Consideration is given to the power requirements of sensing operations, and the system is designed in such a way as to accommodate more energy or processor-intensive tasks such as vibration analysis. The system developed for this case study demonstrates, and enables the evaluation of, the energy-adaptive features of the architecture, implementing the hardware specification defined in Chapter 3.

4.2.2 Available energy sources

Light: photovoltaics (PV)

Initial measurements indicated that lighting on the author's desk in the ESD lab varied between 700 and 1,200 lux (depending on time of day). Amorphous silicon (a-Si) photovoltaic cells have a relatively high efficiency at low light levels, compared to other types of cell, which makes them particularly suited to use indoors. Therefore, a number of photovoltaic cells were procured from Schott Solar GmbH. The cells (part number 1116929) have dimensions 90x72mm and at 1,000 lux will generate approximately 1.8mW at 3.33V and 0.537mA. Low indoor light levels mean that power tracking circuitry designed for outdoor use is often too power-hungry to operate indoors. Conventionally, indoor PV energy harvesting circuits will simply consist of a diode between the PV module and a battery or capacitor, which inhibits the reverse flow of energy from the store when the cell is not exposed to sufficient light. This arrangement is particularly inefficient when charging a supercapacitor from empty, as in this situation the PV module is forced to operate far from its maximum power point (MPP) voltage. For the purposes of this investigation, a maximum power point circuit suitable for indoor use has been developed and is described in detail in Section 4.5.1. It has been designed to interface with photovoltaic modules that operate with a nominal voltage of around 3-5V and with a nominal power output of around 1mW under typical lighting conditions.

Vibration: electromagnetic vibration energy harvester

As part of the AEASN project described in Section 1.2, a colleague (Neil Grabham) developed a circuit to interface with a vibration energy harvester. This circuit was then adapted by the author of this thesis to interface with the plug-and-play architecture developed under this project. The vibration energy harvester is a prototype Perpetuum device, and generates energy from twice-line-frequency vibrations (in this case, 100Hz). Its performance can be assumed to be similar to that of the Perpetuum device shown in Section 2.3.3. The harvesting device gives an AC output, which must be rectified for use by the sensor node. For the purposes of this case study it will be assumed that the device is deployable on a machine with those frequencies, at a suitable amplitude, in order to provide power to the system. The vibration energy harvesting module is described in Section 4.5.2.

Other energy harvesting sources: air flow, temperature difference

A number of other modules were developed under the AEASN project to interface with the plug-and-play system. These are of peripheral interest to this project and therefore are only covered briefly here. The modules included:

1. A **thermoelectric energy harvester** (which was based on an off-the-shelf thermoelectric generator from Tellurex) which permitted milliwatts of power to be generated from substantial temperature differences. The module incorporated a heat sink and small fan which worked to increase the temperature gradient; the fan could optionally be self-powered by the thermoelectric module or driven from an external power supply to simulate a flow of air past the device. The device provided a DC output which had to be regulated for use by the sensor node.

2. A **miniature wind turbine**, which used an adapted Mathmos Wind Light as its power source. Again, the device could generate milliwatts of power from substantial air flows of several metres per second. The device provided an AC output which had to be rectified to DC for use by the sensor node.

These modules were then adapted to interface with the plug-and-play system developed in the course of this work. The functionality and connections for these modules are described in Section 4.5.3.

Mains electricity

In situations where mains (or any inexhaustible supply of) electricity is available, this can be exploited by the mains electricity module. Mains power must first be regulated to 5-11.5V DC by a mains power adapter before being fed into the module, which will then regulate the power supply for the sensor node. The use of an off-the-shelf power adapter was considered essential for safety reasons. The mains electricity module is described in Section 4.5.4.

4.2.3 Utilised energy stores

Primary batteries

Typically, conventional nodes are run from primary batteries, which are generally either alkaline or lithium chemistries. For the purposes of this investigation, a module was developed to accommodate alkaline (with two cells connected in series) or lithium thionyl chloride (standalone) cells. The AAA alkaline cells had a nominal 1.5V operating voltage and 1200mAh capacity, and 1/2AA lithium cells had a nominal 3V operating voltage and 950mAh capacity. The module will also accommodate non-rechargeable lithium manganese coin cells such as the CR2430.

Secondary batteries

Recent developments in low self-discharge NiMH cells prompted the choice of Sanyo Eneloop cells for this project. The AAA-size cells have a nominal 1.2V operating voltage and 800mAh capacity. They are accommodated by the module developed for primary batteries, with the addition of a number of components to allow recharging of the cells. Their low self-discharge rate and ease of recharging makes them especially suitable for this application. Due to the small amounts of power available, and the complexities of charging, it was decided not to use lithium-based rechargeable chemistries.

Supercapacitors

Two types of supercapacitor were used in this project, accommodated by the supercapacitor module. Two radial Panasonic Gold supercapacitors (with nominal 1F 2.3V capacity) can be connected in series, or one CAP-XX supercapacitor (nominal 0.22F or 0.55F, 4.5V capacity) can be used. Provision is also made for balancing resistors to be fitted. These capacitor types were chosen as they are commonly used in energy harvesting systems, and are of low cost and moderate capacity.

4.3 Components and energy management circuits

4.3.1 Low-power system components

In this case study, a number of components are required to provide the energy management and measurement functionality for the system. Clearly, as the node is running from sub-milliwatt power sources, the quiescent current consumption of these components must be minimised and the 'on'-resistance of components in the power path must also be kept to a minimum. For this reason the following components are used extensively in this case study, as they offer good levels of performance against these metrics. The selected data are given to allow the reader to appreciate the dynamics and importance of these carefully-selected system components.

Measurement and control

The operational amplifiers, comparators and multiplexers used in the prototype modules are used to control module states and take measurements of system parameters.

- **Comparator:** National Semiconductor LMC7215. This is a push-pull output comparator which operates from a 2-8V supply and draws 0.7μA quiescent current.
- **Operational Amplifier:** ST Microelectronics TS941. This is a rail-rail output op-amp which operates from a 2.5-10V supply (but has been tested by the author down to 2V with minimal loss of resolution) and draws a 1.2μA quiescent current.
- **Data multiplexer:** Analog Devices ADG708. This low-voltage 8-channel analogue switch operates between 1.8-5.5V. It has a maximum quiescent current consumption of 1μA and on-resistance of 3Ω.

Power switching and rectification

These switching and rectification components are used at many points in the system, acting to inhibit the reverse flow of energy or isolate parts of the system that are not in use, and therefore reduce the power wasted by the system. They also enable parts of the system to be switched on to take measurements or permit charging/discharging of energy stores.

- **PMOS transistor:** International Rectifier IRLML6401. This is a power MOSFET with a minimum 0.4V gate threshold, and an on-resistance of 0.05Ω with a V_{GS} of 2.5V and a low drain current.
- **NMOS transistor:** International Rectifier IRLML2502. Another power MOSFET, with a minimum gate threshold voltage of 0.6V, and an on-resistance of 0.04Ω with a V_{GS} of 2.5V and a low drain current.
- **JFET-N transistor:** NXP PMBFJ309. This has a minimum cut-off voltage of 1V and typical drain-source on-state resistance of 50Ω. With a 50Ω resistance, a 1mA current will lead to an approximate voltage drop of 150mV.
- **Schottky diode:** NXP BAT754. This is a small-signal Shottky barrier diode that is available in a number of configurations. With a 1mA forward current, it has a voltage drop of 260mV.

Voltage regulation

These components act to provide a regulated voltage to the microcontroller (in the case of the multiplexer module), or to the raw voltage on the multiplexer module (in the case of the other modules). They deliver the facility for under- and over-voltage protection.

- **Voltage detector:** Torex XC61CC. This series of CMOS voltage detectors are widely available in 2.0V, 2.7V, 3.0V and 4.5V versions. They consume around 0.7μA quiescent current and have CMOS active-high outputs.
- **Linear regulator:** Torex XC6215. This series of linear voltage regulators has an enable input, which makes it suitable for being controlled by an XC61CC voltage detector. It has a quiescent current draw of 0.8μA, and 100nA in standby.
- **Switching step-down regulator:** Maxim Integrated Products MAX639. This step-down DC-DC converter has a 10μA quiescent current draw.

4.3.2 Connectors

As defined in tables 3.5 and 3.6, the interface between the multiplexer module and the energy modules require 8 lines, and the interface between the microcontroller and the multiplexer module has 10 lines. The cost of connectors is important, as is their robustness. It is expected that the energy modules will be connected and disconnected more frequently than connectors between the microcontroller and the multiplexer module. It is for these reasons that RJ45 connectors have been selected for the interface between multiplexer and energy modules in this project. The connection between the microcontroller and the multiplexer module is via a 2 x 5-way 0.1” pin header. In future systems, however, it is anticipated that a stacking system would be used (facilitated by the reduced size of circuit boards on energy modules) to reduce the overall footprint of the system. A stacking 36-way connector would be suitable for both the interconnection of energy modules, and their connection to the multiplexer module.

4.3.3 EPROMs for energy electronic data sheets

The memory device selected to store the EEDS for this system is the DS2502+ 1kB add-only EPROM. Each device has a unique serial number and 1024 bits of programmable memory, partitioned into four pages. Its maximum communication speed is 16.3kbps, and communications are enabled by a $\approx$5kΩ pull-up resistor on the 1-wire bus. The device is rated for operation between 2.8V and 6.0V from -40°C to +85°C, but its operation in this system has been successfully tested down to 2.0V at room temperature. The device must be programmed before deployment in the system, as it requires programming voltages of around +12.0V, which are not common on sensor nodes (a large amount of additional hardware would be required to achieve this voltage through level-shifting and voltage boost circuitry).

4.3.4 State retention for device control

Normally, power generated by energy harvesters will be exploited whenever it is available – being used to power the sensor node, or to recharge energy stores such as supercapacitors or rechargeable batteries. Conversely, in the case of energy stores or non-rechargeable sources such as primary batteries, it is commonly desirable to be able to turn these devices 'on' or 'off' to enable or disable discharging (to conserve energy for another time). In the case of rechargeable batteries, it may also be desirable to be able to disable recharging to ensure that any available power is used directly to power the microcontroller instead of to recharge batteries. As these energy modules are normally controlled by the microcontroller via the multiplexer module, it is essential that modules are able to 'remember' their state. The microcontroller may only connect to the energy module for management purposes once every few seconds or minutes (or potentially hours), so a capability must be implemented to allow devices to remember their status for extended periods. For this application, a bistable multivibrator, shown in Figure 4.1 is a useful circuit.

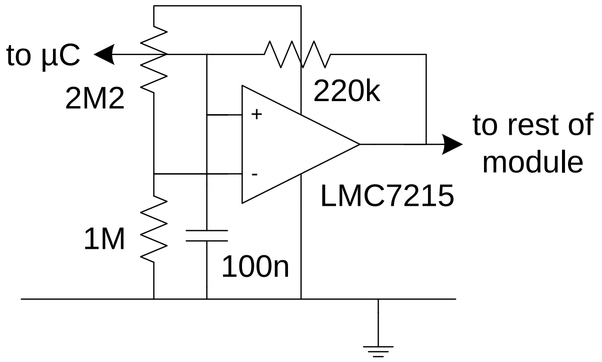

Figure 4.1: Bistable multivibrator circuit. Used for charge/discharge control state retention on energy modules.

The bistable multivibrator allows the state of the circuit to be retained. The circuit utilises a comparator, and the state of the output is stored on a capacitor. This has the effect that the current 'state' of the energy module can be both set and read by the microcontroller (hence it must be connected to a bidirectional digital pin). As will be discussed later, it is possible for some energy modules to be controlled both by the microcontroller and externally by a human operator (e.g. to power up the system from a primary battery when it is first installed). In this situation it is important that the microcontroller is able to both read and set the status of the module, and justifies the control lines being bidirectional. The quiescent power consumption of this block can be minimised by choosing a micropower comparator and using high-value resistors.

With an LMC7215 micropower comparator configured as shown in Figure 4.1, the quiescent current draw of this circuit was found to be 1.8μA at 3V. This compares favourably with the data sheet current draw, 0.7μA, of the comparator alone. The circuit was verified as operating without oscillation and starts up in the 'off' position. This circuit configuration is used for many of the modules described later in this chapter. As an aside, it must be ensured that the that the state retention capacitor is suitably large to overcome other capacitances in the control circuit (which includes the multiplexer module and microcontroller), otherwise the act of interrogating the module by the microcontroller may cause the output state to be toggled. The correct operation of this block with an MSP430 and CC2430EM was verified.

4.3.5 Over/Undervoltage protection and regulation

As discussed in Section 3.5.4, it is essential to provide undervoltage protection to the microcontroller to ensure that it starts up correctly, and overvoltage protection to limit the supply voltage to prevent damage. Two types of circuit can be used to maintain the correct operation of the system. Firstly, the undervoltage protection circuit shown in Figure 4.2 acts to disconnect the power supply to the microcontroller if the 'raw' voltage is too low. The device features a micropower CMOS voltage detector which has built-in hysteresis, meaning that with a 2.0V variant of the voltage detector, the circuit will turn on at around 2.1V and off at approximately 2.0V. Secondly, overvoltage protection can be achieved through the circuits in Figure 4.3. The circuit in Figure 4.3a again exploits a voltage detector and is used to disconnect an energy harvester from the rest of the circuit, thus preventing further charging. The circuit shown in Figure 4.3b simply exploits a voltage regulator IC, which will typically be a linear device.

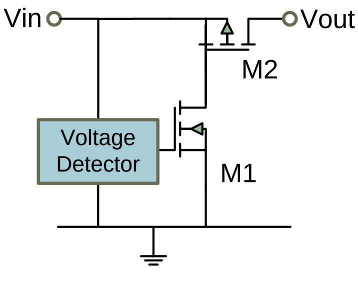

Figure 4.2: Undervoltage protection circuit.

Alternatively, the undervoltage and overvoltage protection circuits can be combined if a linear regulator with an enable input is used. As shown in Figure 4.4, the output from the voltage detector is fed directly into the enable input of the voltage regulator. The circuit therefore cuts off its output when its input voltage is below the sensed voltage of

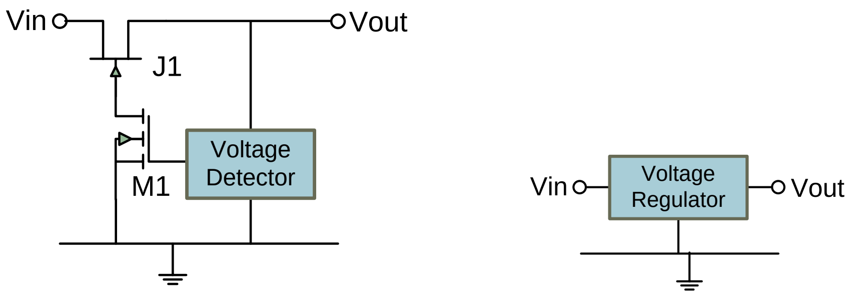

(A) Circuit 1 (B) Circuit 2

FIGURE 4.3: Options for overvoltage protection circuits: (a) uses a MOSFET to disconnect the energy harvester and thus limit the voltage, while (b) simply uses a linear regulator.

the voltage detector, and limits its maximum output voltage to the rating of the voltage regulator. This circuit is recommended for use on the multiplexer module, but the other circuit configurations are used on energy modules.

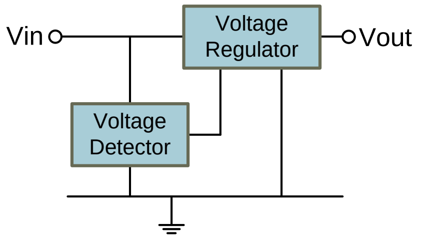

FIGURE 4.4: Combined undervoltage and overvoltage protection circuit.

The suggested circuit has been used in the prototype multiplexer module in this case study. Figure 4.5 shows the results of testing of this functionality. It can be observed that when the supply voltage rises above 2V it is tracked by the output voltage, until it is regulated to 3V. The output voltage then falls to zero when the supply voltage drops below 2V. This operation is achieved using a Torex XC61C 2.0V CMOS-output voltage detector and a Torex XC6215 LDO 3.0V linear regulator. The quiescent power consumption of the voltage detector has been verified at below 1μA, with the voltage regulator consuming a similar amount of quiescent current. The figure shows that the voltage drop through the regulator is also negligible.

4.3.6 Power and energy estimation

Some methods for power monitoring were introduced in Section 3.6.6. In the prototype modules produced in this case study, 'closed circuit' current measurement and 'open-circuit' voltage measurement have been used to estimate the amount of power being produced. While in-line current measurement ('current shunt') would be desirable, unfortunately due to practical reasons it is very difficult to use in this system. For in-line

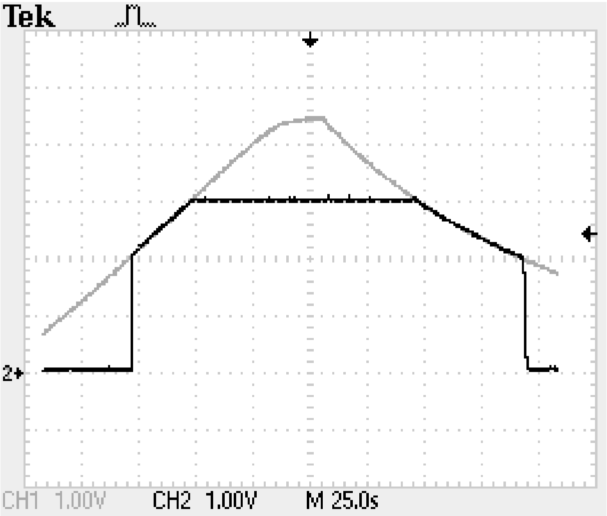

FIGURE 4.5: Test of combined undervoltage and overvoltage protection circuit. Grey line denotes 'raw' voltage on energy multiplexer, black line shows 'regulated' voltage provided to microcontroller.

current measurement, a resistor must be connected so as to interrupt the positive supply line; the differential voltage across that resistor must then be measured. This is problematic as the resistor voltage must be small (of around 1Ω to avoid affecting the efficiency of the system) so the measured voltage will be small; the real performance of micropower rail-to-rail operational amplifiers is also imperfect. It would also be non-trivial to decide which supply rail to drive the operational amplifier from: if using the raw voltage on the module, the output may be outside the acceptable input range for the microcontroller; alternatively, if driven from the regulated voltage, it would be impossible to achieve operation with inputs up to the raw supply rail voltage on the module.

For this reason, the alternative schemes of measuring the open-circuit voltage, or current through a fixed load, are used by this system. The voltage measurement is normally divided by means of a voltage divider in order to bring it into the acceptable range for the microcontroller. The resistor values on the voltage divider are set to provide an appropriate level of impedance to the measured device (e.g. for open-circuit measurements, the impedance will be very high to simulate open-circuit; for closed-circuit, they will be smaller and appropriate for the load the device has been modelled at). The parameters stored on the electronic data sheet on the module enable conversion between the measured voltage and the estimate of power output or energy stored.

An example of a voltage test circuit is shown in Figure 4.6. For purposes of clarity, pull-up resistors are not shown in this schematic. It may be observed that the operational amplifier is in a unity gain buffer arrangement, and its power supply is the regulated (microcontroller) supply. Its power supply will normally be controlled by V_{ctrl} in order to reduce the quiescent power consumption of the system, but this is not shown in the diagram. The voltage divider circuit is switched by the V_{ctrl} line, but the effective impedance of the MOSFET M1 is negligible compared to those of R_1 and R_2. The output

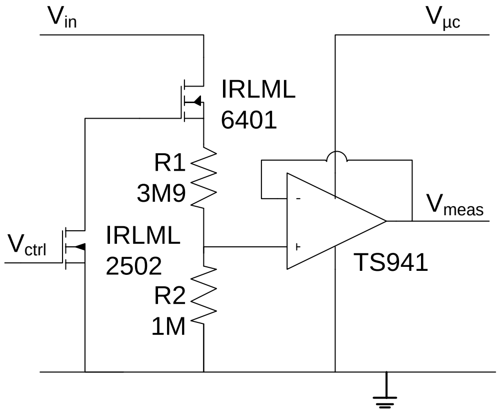

Figure 4.6: Example of voltage measurement circuit, with resistor values permitting measurement of the open-circuit voltage.

from the operational amplifier can be considered to be a low-impedance buffered replica of the divided voltage. The measured voltage from the voltage divider is dependent on the standard voltage divider equation:

$$\frac{V_{meas}}{V_{in}} = \frac{R_2}{R_1 + R_2} \tag{4.1}$$

The total impedance presented to the device in question can simply be expressed as:

$$R_{tot} = R_1 + R_2 \tag{4.2}$$

Therefore, with knowledge of these equations, the impedance of R_1 and R_2 can be set at appropriate values to ensure that the divided voltage is within the acceptable range for all possible values of the measurand. For this purpose, υ will represent the maximum raw input voltage and ω will be the maximum voltage detectable by the microcontroller ADC input. Therefore, for this application:

$$\upsilon \cdot \left(\frac{R_2}{R_1 + R_2} \right) \leq \omega \tag{4.3}$$

Methods for determining the state-of-charge, or energy stored, in a supercapacitor (Section 3.6.4) and battery (Section 3.6.5) have been introduced. The above scheme is applicable to these applications. For supercapacitors, open-circuit voltage is normally used to estimate the amount of energy stored; for batteries, the voltage across a known load is normally tested. The necessary parameters to convert this into an estimate of stored energy are held on the electronic data sheet on each module.

4.4 Multiplexer module

4.4.1 Functional overview

The purpose of the multiplexer module is to deliver a reconfigurable energy subsystem by allowing the microcontroller to interface with the energy modules, and facilitating the flow of electrical energy between the modules. The basic hardware requirements of this module were listed in Section 3.5.1. The prototype multiplexer module is shown in Figure 4.7 and its schematic can be found in Appendix A, Figure A.1.

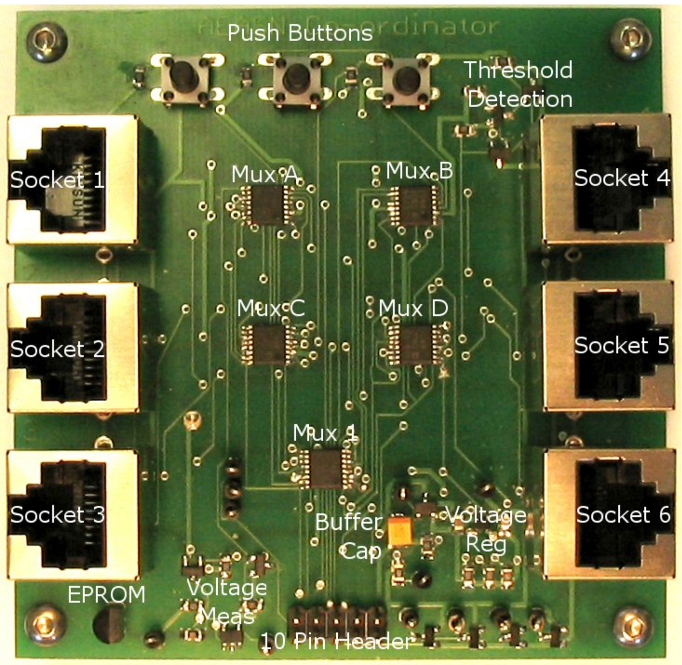

FIGURE 4.7: Prototype energy multiplexer module.

The connections between the multiplexer module and the other energy modules are through RJ45 sockets, compliant with the scheme defined in Table 3.6. The interface between the multiplexer module and the microcontroller is through a 2-row 10-way header, compliant with the scheme outlined in Table 3.5. The multiplexer module appears as two separate addresses: address ‘0’ is the low-power, passive monitoring circuit without a 1-wire EPROM, and address ‘7’ is the device that allows the raw voltage on the multiplexer module to be measured and the device to be interrogated. The effective connections from each of these addresses are shown in tables 4.1 and 4.2 respectively. A simplified schematic, which shows the data connections on the multiplexer module, is shown in Figure 4.8, and a simplified schematic showing the power connections between the modules is shown in Figure 4.9.

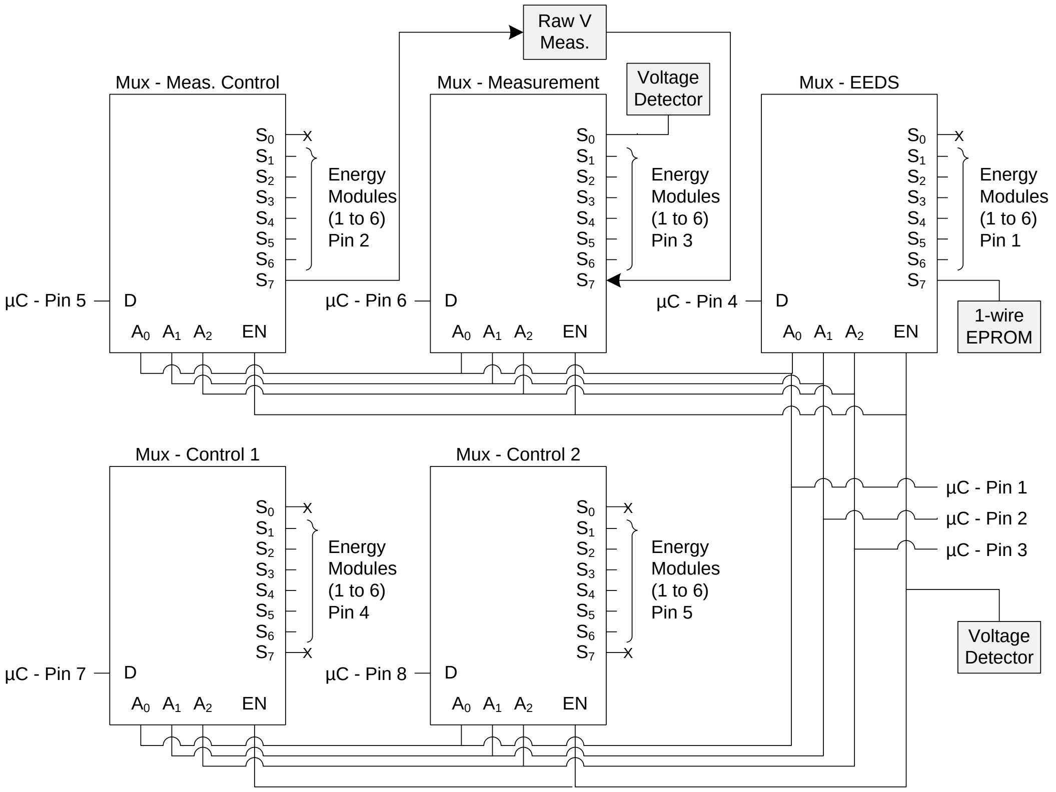

FIGURE 4.8: Simplified schematic of multiplexer module, showing data connections. Pin numbers refer to Common Hardware Interface pin numbers.

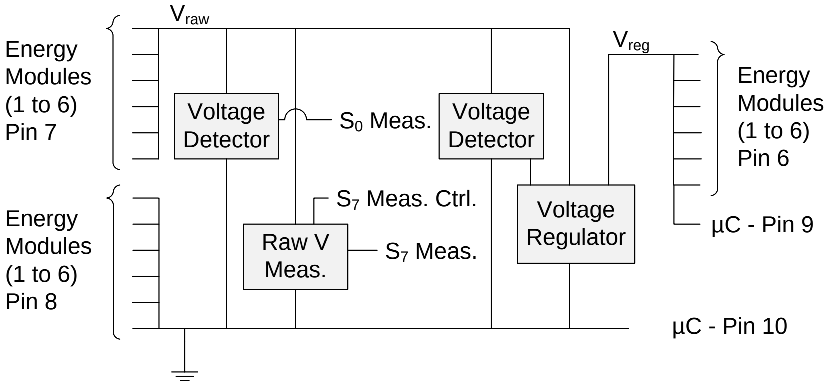

FIGURE 4.9: Simplified schematic of multiplexer module, showing power connections. Pin numbers refer to Common Hardware Interface pin numbers.

Pin	Type	Function
2	Meas. Control	None
3	Measurement	Digital: threshold crossing detection
4	Control	None
5	Control	None

Table 4.1: Interface pins from multiplexer module (address '0').

Pin	Type	Function
2	Meas. Control	Perform raw voltage measurement
3	Measurement	Analogue: raw voltage measurement
4	Control	None
5	Control	None

Table 4.2: Interface pins from multiplexer module (address '7').

4.4.2 Energy-awareness circuitry

In order that the microcontroller can monitor the 'unregulated' (up to 4.5V) voltage on the multiplexer module, a resistor divider and operational amplifier-based unity gain buffer arrangement is provided. This brings the potential 0-4.5V unregulated voltage range into the 0-1V range supported by most microcontroller ADCs. This facility is managed and monitored through address '7', and allows the microcontroller to monitor the unregulated voltage on demand. There is also a resistor providing the pull-up functionality for the 1-wire bus. The EEDS on the multiplexer module is also accessed through address '7'; the provision of the multiplexer module EEDS facility on address '7', rather than address '0', means that the one-wire bus does not consume power while the system rests in its default (address '0') state.

4.4.3 Additional features

Additional circuitry includes pull-down resistors for the address lines, and a pull-up resistor for the 1-wire bus. Diode clamping is provided by an array of NXP BAT754 Schottky diodes, which prevent the outputs from the multiplexer module from exceeding the limits of the supply lines of the microcontroller. As shown in the photograph, three push switches are located on the top edge of the board; these are an artefact of an earlier version of the scheme where all four management lines were of mixed purpose and the push buttons were used to trigger interrupts on the microcontroller (they were connected to the low-power monitoring lines of the system on address '0'). The direction and type of each of the four management lines is now mandated (measurement control, measurement, and 2x control) to remove the potential for dangerous conflict when energy modules are exchanged during node operation. The facility is currently provided to trigger an interrupt when the unregulated voltage passes 2.7V by the use of an additional voltage detector and MOSFET arrangement. This is an arbitrary selection but is used to show the ability of the system to indicate when a voltage threshold has been passed.

4.4.4 Start-up and voltage regulation

The maximum unregulated voltage supported by the multiplexer module is 4.5V, and this is regulated down to a maximum of 3.0V by a LDO linear regulator. A linear regulator was chosen for this design due to its simplicity and low quiescent power consumption. It supports currents of up to 150mA. Undervoltage protection is provided by a 2.0V Maxim XC61C voltage detector, having a CMOS output stage, which feeds into the enable input of the linear regulator. A tantalum 100μF capacitor provides a small low-ESR buffer which compensates for the current spike when the module output is turned on and the microcontroller starts up. The voltage regulation functionality of this module was shown earlier, in Figure 4.5. The start-up performance of the system has been verified with both the TI eZ430-RF2500 and TI CC2430 microcontroller modules.

4.4.5 Data multiplexing

The prototype multiplexer module supports the connection of up to six energy modules through its RJ45 sockets. It includes five Analog Devices ADG708 8-to-1 analogue switches (four are used for the module management lines, and one is used for 1-wire communications to the EEDS on each module). The analogue switches are used for data rather than power, so their on-resistance is actually of little importance. They have an enable pin which is simply connected to the regulated supply voltage of the module, meaning that they are effectively shut down when the voltage on the system is too low to sustain operation.

4.4.6 Overall efficiency

As shown in the schematics, there are no diodes or other passive components in the electrical path between the energy modules and the microcontroller. Therefore the main impact from the multiplexer module on the overall efficiency of the system is the quiescent power consumption of its components, and the efficiency loss through the linear regulator. Having five analogue switches with a quiescent current draw of 1μA and two voltage detectors each with a current draw of 0.7μA, plus the 0.8μA quiescent current draw of the linear regulator, this equates to an overall quiescent current draw of approximately 7.2μA. The efficiency loss through the linear regulator will impact most significantly when the raw voltage is above 3V. The other measurement circuitry draws no current except when measurement operations are in progress.

4.5 Energy modules

4.5.1 Photovoltaic module

Functional description

The photovoltaic (PV) cell and this PCB (from the schematic in Appendix A, Figure A.2 and shown in Figure 4.10) should be taken together to represent the photovoltaic 'module'. An EPROM holds the EEDS data with the operating parameters of the circuitry and PV cell in combination, so it should be noted that in this scheme the actual harvesting device and its power conditioning circuit are considered as one module.

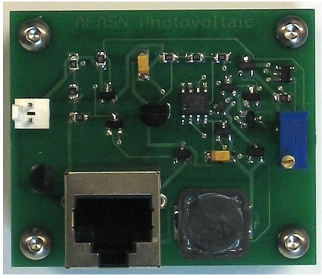

Figure 4.10: Circuit board for the photovoltaic module.

The circuit interfaces with indoor amorphous silicon PV cells, with an operating voltage of between 2.5V and 5.0V. In the demonstrator system it is connected to a Schott OEM 1116929. This cell is capable of producing >1mW of power under bright indoor lighting. The circuit works to hold the cell at its optimal voltage, regardless of the unregulated voltage on the multiplexer module. This improves the efficiency of the system and delivers faster charging times when cold-starting the system.

It should be noted that the operating voltage of the PV cell is set using a variable resistor on the PCB. Overvoltage protection is delivered using a XC61C voltage detector and FET combination, which disconnects the photovoltaic cell when the maximum system voltage is reached. The same FET combination (feeding into an op-amp buffer arrangement) is used to permit the microcontroller to analyse the open-circuit voltage of the cell and hence estimate the nominal power being harvested.

Pin	Type	Function
2	Meas. Control	Disconnect cell to perform measurement
3	Measurement	Analogue: open-circuit voltage of cell
4	Control	None
5	Control	None

Table 4.3: Interface pins from photovoltaic module.

Maximum power point circuit

A circuit for indoor PV energy harvesting has been developed (Figure 4.11), which consists of a modified buck-boost converter circuit with additional isolation and metrology circuitry. During normal operation, this circuit acts to maintain a constant voltage across its input terminals in order to keep the PV cell at a voltage set by R4. The PV cell is kept at this fixed voltage (in the range of maximum power point voltages of the cell at expected light levels) in order to keep its operation near its indoor MPP voltage. This simplification is acceptable as the normal range of indoor light levels is 100-1,000 lux and in this range the power loss due to voltage clamping at a fixed voltage has been determined to be less than 3%.

The combination of JFET J1 and MOSFET M1 act to disconnect the load from the photovoltaic module when a ‘high’ signal is raised on the V_{ctrl} line. This permits the open-circuit voltage (V_{oc}) of the cell to be measured. However, a complication of this circuit is that, as it is based on a buck-boost converter, the input and output stages do not share a common ground (effectively the ground of the input is the V_{cc} of the output). For this reason, a high-impedance resistor divider comprised R1 and R2 is used to bring the V_{oc} signal into a range which can be interpreted by the microcontroller. The output from this divider is fed through a unity gain buffer around IC1 to provide the required low-impedance input to the ADC of the microcontroller. Resistors R3 and R4 act to ensure that the circuit operates normally on start-up, when supercapacitor C2 has built up insufficient voltage for the microcontroller to become active, and the switching converter is required to operate normally.

The V_{oc} of the module can be calculated by means of Equation 4.4, where α is the ratio of R1 to R2, and V_C is the voltage at which the microcontroller is operating (i.e. the voltage across supercapacitor C2).

$$V_{oc} = (V_{meas} \times (\alpha + 1)) - V_{\mu c} \tag{4.4}$$

Here, R6 and D1 provide a reference voltage input to the micropower comparator IC2. R7 and R8 provide hysteresis to the system. In normal operation (when V_{ctrl} is low), C1 acts as a small buffer capacitor. When the voltage across C1 exceeds the threshold set by R5, comparator IC2 gives a ‘low’ output which switches MOSFET M2 ‘on’ and permits current to flow through D2 and L1. After a very short period, the voltage across C1 will have dropped sufficiently to cause IC2 to turn M2 ‘off’, and for energy to be transferred from L1 through D3 to be stored in supercapacitor C2 (note the polarity of this component).

For SPICE simulation of the power conditioning circuit, a model was developed for the PV module used in this investigation. Typical models of solar cells, such as those pro-

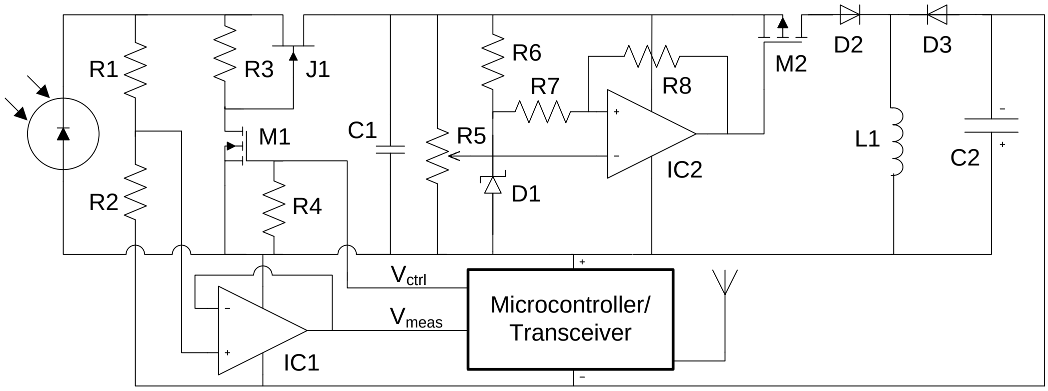

FIGURE 4.11: The developed PV energy harvesting circuit, which can be interrogated by a microcontroller.

posed by Dondi *et al.* [120], are unsuitable for use with small cells in low-light conditions due to their reliance on the I_s parameter, which must be extremely small and hence falls outside the range of parameters that can be simulated by SPICE. The actual model used in this investigation was adapted from that proposed by Hageman [125], and is shown in Figure 4.12.

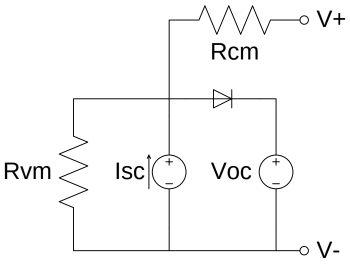

FIGURE 4.12: SPICE model for small PV cells.

Power estimation technique

The data sheet parameters for this PV cell [28] have been plotted and a logarithmic trend line has been added, as shown in Figure 4.13. In this instance, the open-circuit voltage is approximated to the light level by Equation 4.5.

$$V_{oc} = 0.2571 \ln(E_V) + 2.9128 \tag{4.5}$$

Where E_V is the illuminance level in lux, and can be generalised as Equation 4.6, where A and B are parameters to be found for the individual PV module.

$$V_{oc} = A \ln(E_V) + B \tag{4.6}$$

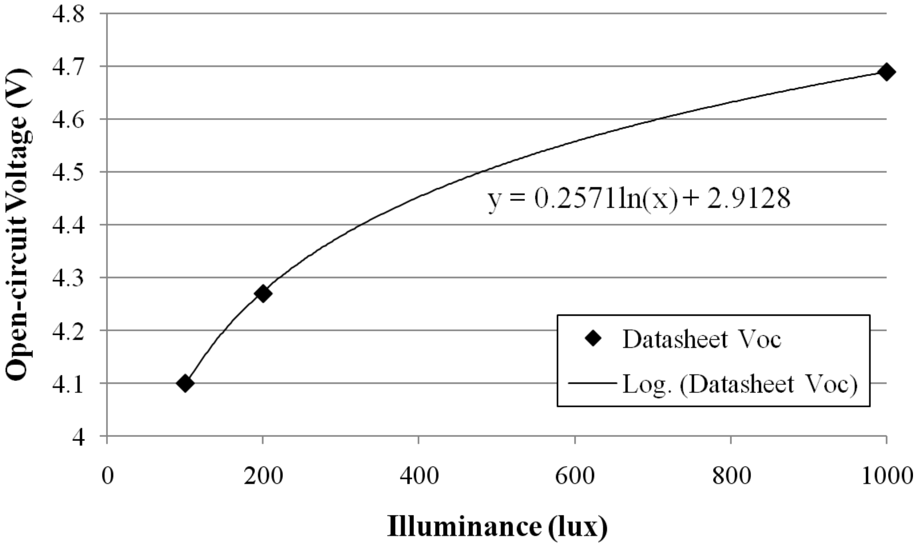

FIGURE 4.13: Logarithmic fit of V_{oc} against illuminance, for Schott Solar OEM 1116929 Indoor PV module.

This equation can be rearranged, as shown in Equation 4.7 to determine the level of illuminance from V_{oc}.

$$E_V = e^{\frac{V_{oc}-B}{A}} \tag{4.7}$$

A useful property of silicon PV cells is that their MPP voltage (V_{mpp}) is related to their V_{oc} by parameter k. This parameter is typically between 0.70 and 0.80 (Equation 4.8), and can be determined for individual modules [126]. This property can be used by simpler maximum power point tracking circuits. Furthermore, the current obtained from the PV module at its MPP (I_{mpp}) is related to its illuminance by parameter m, as shown in Equation 4.9.

$$V_{mpp} = kV_{oc} \tag{4.8}$$

$$I_{mpp} = mE_V \tag{4.9}$$

Parameter	Description	Value
k	Ratio between V_{oc} and V_{mpp}	0.71
m	Ratio between E_V and I_{mpp}	5.4×10^{-7}
A	Natural log fit of $V_{oc} - E_V$	0.2571
B	Natural log fit of $V_{oc} - E_V$	2.9128

TABLE 4.4: Parameters found for Schott Solar OEM 1116929 Indoor PV Module.

There are certain limitations to this model, in that the parameter k only holds if the module is under uniform illumination (i.e. no shadowing). Secondly, parameter m holds only for relatively low levels of current. While it varies by less than 1% in the range 100-1,000 lux, it can be expected to vary more widely in brighter deployment environments.

However, the situation of interest to this investigation (indoor, artificially-lit environments) means that this simplification is acceptable. Lastly, the equation for nominal power assumes that the cell is operated at its maximum power point and the conversion circuitry is 100% efficient. The following section gives an idea of the efficiency of the circuit and other complications, but the result given for nominal power is sufficient to give an idea of the energy harvesting status of the node, for use by energy-aware algorithms.

Performance evaluation

SPICE simulations indicate that this circuit runs at over 70% efficiency with the PV module described, under normal indoor lighting. Although the absolute efficiency of the circuit could not be tested (due to the difficulties in ascertaining the maximum power from incident light), practical tests comparing the circuit shown in Figure 4.11 against a conventional diode-only system show a 30% improvement in node start-up times under normal office lighting. The results of a 'race' between a conventional circuit (with the supercapacitor connected through a diode) and the new switching-based circuit (similar to that shown in Figure 4.11) is shown in Figure 4.14. Here, it may be observed that the switching circuit delivers significantly better performance than the diode-based circuit at lower store voltages. The difference in gradient at higher voltages is small, meaning that the efficiency of both circuits is similar in this situation. Therefore, it may be inferred that there is no significant performance penalty at higher voltages for utilising this MPP switching converter circuit. The system has been tested and evaluated in an office environment with a mix of natural and fluorescent lighting. From cold-starting, the system steadily charged the supercapacitor energy store C2 until the system voltage reached approximately 2.1V, at which point the microcontroller became active and started transmitting with a 30s sleep period. At its absolute peak level of harvesting, placed in close proximity to a fluorescent lamp, the system reported a nominal power level of 3.5mW but a more typical level was around 1mW.

4.5.2 Vibration energy harvesting module

Functional description

The vibration module PCB (from the schematic in Appendix A, Figure A.3 and shown in Figure 4.15) is designed to interface with a Perpetuum PMG17 vibration energy harvester. The manufacturers have found, in real deployments, that this device can generate 500μW on 80% of machines, and 1.0mW on 60% of machines [14]. It provides a half-wave rectified output limited to 8V. The circuitry on this PCB uses a high-efficiency step-down converter to limit this voltage to 4.5V. To increase the efficiency of the system, the device waits (by means of a voltage detector IC) until the output

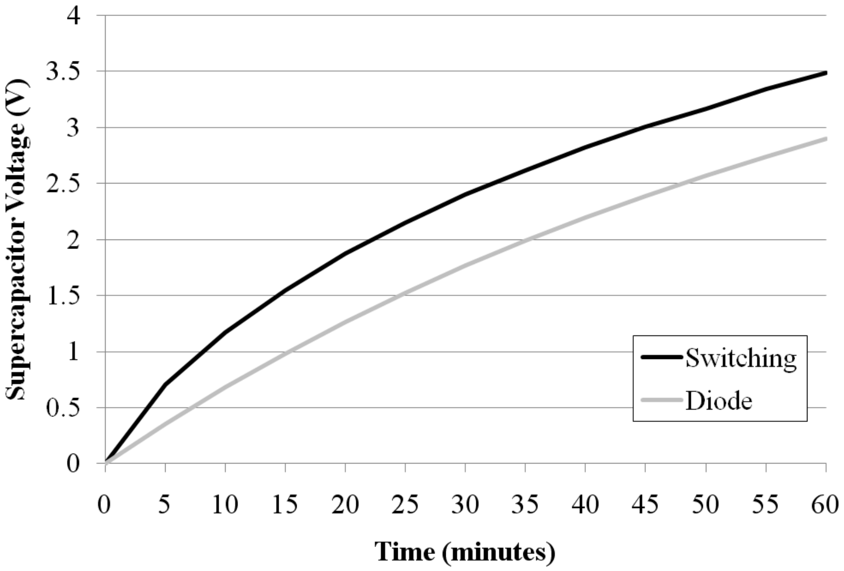

Figure 4.14: Comparison of MPP switching converter circuit against conventional diode-only circuit. Test carried out with 0.5F supercapacitors from the same batch and identical 1116929 PV cells under office lighting at 1pm on an October afternoon, approximate brightness 1,100 lux.

capacitor is charged up before allowing energy to be output to the multiplexer module. The connections between this module and the multiplexer module are shown in Table 4.5.

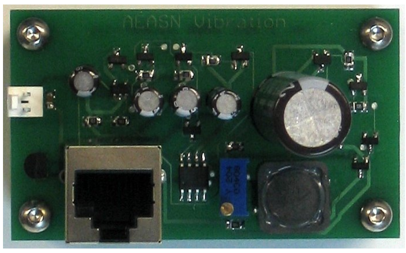

Figure 4.15: Circuit board for the vibration module.

The nominal output power from the vibration energy harvester is estimated by the microcontroller by shutting down the step-down converter and isolating its associated input capacitance. A known load is then switched in across the output of the vibration generator and the voltage across this load is measured to determine the instantaneous power level. The EEDS stores the characteristics of the energy harvester and the details of the known load. In this case, the 'known load' is in fact a 66kΩ voltage divider which feeds into the input of a unity gain buffer. The voltage divider and unity gain buffer supply are both switched by the digital measurement input line, meaning that they only draw current when measurements are in progress. In addition, the operational amplifier is powered from the regulated digital line provided by the multiplexer module, while the voltage divider takes the rectified output from the generator; this works to limit the output from the module to within the bounds of the regulated digital supply of the microcontroller in case of malfunction.

Pin	Type	Function
2	Meas. Control	Connect generator to fixed load
3	Measurement	Analogue: measured voltage across fixed load
4	Control	None
5	Control	None

Table 4.5: Interface pins from vibration module.

Impact of energy-awareness circuitry

Unlike the example of the photovoltaic module, in order to deliver energy-awareness there is no requirement for additional 'in-line' circuitry between the generator and the output from the circuit. The enable input to the switching converter is used to disconnect the generator from its normal load in order that measurements can be carried out. Therefore, the only impact of energy-awareness circuitry on this circuit is apparent when measurement activities are in progress (and these are only likely to take place every few seconds or minutes and take a few milliseconds to complete).

4.5.3 Other energy-harvesting modules

The *wind energy harvesting* module full-wave rectifies the turbine output, which is then buffered in a capacitor before being fed through a step-up switching converter. The step-up converter used in this circuit consumes a relatively high 50μA, with a 3μA shutdown current. Similar to the vibration energy harvesting circuit, the power generated is estimated by driving the rectified output from the generator through a known load and monitoring the output. The circuit has an overvoltage protection mechanism as shown in Figure 4.3a, except that the JFET transistor in that circuit is exchanged for a MOSFET and additional Schottky barrier diode. Once again, due to the use of a shutdown pin on the converter IC, there is no need to interrupt the power path for energy-awareness circuitry, so the only efficiency cost of the energy-awareness circuit is that when measurements in progress. The pin connections for the wind module are shown in Table 4.6.

Pin	Type	Function
2	Meas. Control	Connect rectified generator output to fixed load
3	Measurement	Analogue: voltage across fixed load
4	Control	None
5	Control	None

Table 4.6: Interface pins from wind module.

The *thermoelectric generator* gives a DC output so does not require rectification. The voltage produced by the generator is stepped-up using a dedicated IC (the quiescent current consumption of the step-up converter is 16μA) with a shutdown input. The power produced by the generator is measured by connecting it through a fixed load, before rectification. Once again, in common with the wind module, there are no additional components in the power path to affect the efficiency of the circuit during normal operation. The interface for the thermoelectric module is shown in Table 4.7.

Pin	Type	Function
2	Meas. Control	Connect generator to fixed load
3	Measurement	Analogue: voltage across fixed load
4	Control	None
5	Control	None

Table 4.7: Interface pins from thermoelectric module.

4.5.4 Mains module

The mains module permits the system to operate from mains power. The PCB (from the schematic in Appendix A, Figure A.4 and shown in Figure 4.16) has a standard 2.1mm jack socket and hence is compatible with a range of mains power adapters. The PCB will regulate a 5.0 to 11.5V DC input down to 4.5V, using a Maxim MAX639 switching regulator. The EEDS identifies the type of module. Additional circuitry permits the microcontroller to ascertain whether the mains adapter is supplying power to the system (through a simple digital flag). The microcontroller cannot act to turn off this supply as it is assumed to be a zero-cost resource which should be taken advantage of whenever it is available; in this case, the overall efficiency of this module is immaterial.

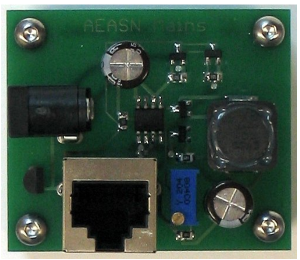

Figure 4.16: Circuit board for the mains module.

Pin	Type	Function
2	Meas. Control	None
3	Measurement	Digital: supply connected
4	Control	None
5	Control	None

Table 4.8: Interface pins from mains module.

4.5.5 Primary battery module

Design overview

As stated in Section 4.2.3, this module supports a range of battery types including a lithium thionyl chloride 1/2AA cell, a CR2430 coin cell, and a pair of alkaline AAA cells. The module, from the schematic in Appendix A, Figure A.6 and shown in Figure 4.17, uses the same PCB as the secondary battery module (except that a number of the components are not fitted in this case). The module has a bistable multivibrator circuit, as described in Section 4.3.4, which controls the discharge state of the battery. It may be observed that the PCB is also fitted with two push-buttons. These interact with the discharge state retention circuit and allow the discharge state of the module to be controlled manually. This is useful when installing the system for the first time as it allows the system installer to ensure that the system can start up instantly from the battery, without having to wait for other energy buffers to be filled from harvested energy. As the microcontroller outputs are tri-stated when not actively setting the state of the energy module, there is rarely a conflict between the push-buttons and the microcontroller state. In the rare case of a conflict, the microcontroller state will take precedence as the push-buttons are connected through 10kΩ resistors to the state retention capacitor. The current consumption, in the case that the microcontroller and push-button are in conflict, would be below 500μA. If the user erroneously pushes both buttons simultaneously, the resulting current would be below 200μA, and the status control would revert to either the 'on' or 'off' state after the buttons are released.

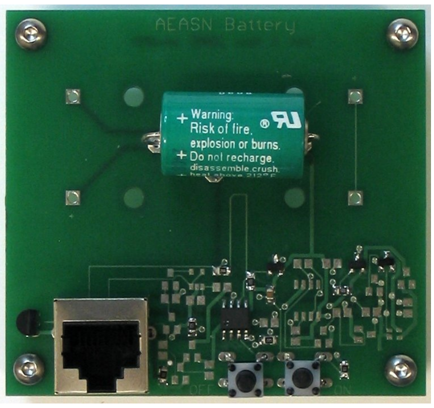

FIGURE 4.17: Circuit board for the primary battery module.

The circuit facilitates two types of state-of-charge determination: its open-circuit voltage, or its closed-circuit voltage across a known load. The measured parameter is buffered by an operational amplifier in a unity gain buffer arrangement. The type of test is controlled by the value of resistors in the voltage divider: large (MΩ-scale) resistors will approximate to open-circuit, while smaller resistors (kΩ-scale) will apply a fixed known load across the cell. At the time of the test it is important that the discharge output is 'off' to ensure that readings are accurate. Table 4.9 shows the management connections from this module.

Pin	Type	Function
2	Meas. Control	Connect battery to voltage divider
3	Measurement	Analogue: battery voltage through fixed load
4	Control	Enable discharge from battery
5	Control	None

Table 4.9: Interface pins from primary battery module.

Performance evaluation

The provision of a control facility for this module imposes a 1.8μA quiescent current draw to maintain the state of the bistable multivibrator. Additionally, the interruption of the power path by one MOSFET and a Schottky barrier diode means that there will be an associated voltage drop. At 1mA and 3V, the voltage drop is around 260mV; the presence of the diode causes an approximate 9% efficiency loss, but is unavoidable due to the risk of unwanted recharging of the primary cell. For simplicity, there is currently no voltage step-up capability. This means that the module cannot supply a higher voltage than that of the cell(s). This is of little impact to the overall operation of the circuit, as it simply means that the batteries will not charge a supercapacitor energy buffer above their own voltage, which will typically be above 3V (the regulated voltage for the microcontroller).

4.5.6 Secondary battery module

Control and startup features

The secondary battery module is designed to accommodate a pair of AAA rechargeable low self-discharge NiMH batteries (in holders). It uses the same PCB as the primary battery module (shown in Figure 4.17), but with a number of additional components fitted to enable the recharging functionality. The additional circuitry permits the microcontroller to control the charging of rechargeable batteries fitted to the module. In common with the primary battery module, circuitry is provided to allow the microcontroller to assess the state-of-charge of the battery. This is either by analysing the open-circuit voltage, or the voltage after pulsed discharge through a small resistive load (set by resistors soldered onto the board).

This board has two bistable multivibrators, which maintain the ‘discharge enable’ and ‘charge enable’ status of the module. This means that these parameters can be asserted or negated by the microcontroller and that state will be maintained by the module. The two push-buttons on the bottom of the board are manual ‘on’ and ‘off’ switches, which permit the output to be manually enabled to allow the system to be cold-started. To deliver a near-instant start-up to the system, the 'on' button may be pressed , which will cause the system to receive power from the battery. The second bistable multivibrator, which controls recharging of the cells, is solely controlled by the microcontroller (there are no push buttons for this function).

The recharging mechanism is designed only for NiMH cells. NiMH cells have a nominal voltage of 1.2V but this rises on charging. For example, Sanyo Eneloop cells peak at over 1.6V when charging. Commonly, constant-current charging with charge termination techniques such as $-\Delta T$ or dT/dt are used for these cell types. However, in this application (particularly where energy is obtained directly from harvesting sources), a constant-current charge cannot be guaranteed and the cells will be charged in a piecemeal fashion whenever surplus energy is available. Indeed, a helpful aspect of this application is that the cells need not reach 100% charge. Therefore, the charge system uses a straightforward voltage threshold technique to manage the charge of the cells. Firstly, the raw voltage of the multiplexer module is tested to ensure it is above 3V. If so, a 3V linear regulator is enabled which causes current to flow from the multiplexer module towards the cell; should the voltage on the multiplexer module fall below 3V, the charge is terminated. In this way, the cell voltage is effectively regulated to 3V and the cell is continuously topped up to this voltage whenever energy is available and charging is enabled by the microcontroller. The cells never reach the 1.6V (3.2V in combination) 'full' voltage, so an over-charge condition will never be reached.

The EEDS stores information on the size of cells fitted. Table 4.10 shows the management connections for this module.

Pin	**Type**	**Function**
2	Meas. Control	Connect battery to voltage divider
3	Measurement	Analogue: battery voltage through fixed load
4	Control	Enable discharge from battery
5	Control	Enable recharge of battery

Table 4.10: Interface pins from secondary battery module.

Performance evaluation

Similar to the primary battery module, the secondary battery module has two bistable multivibrators that each consume 1.8μA. Additionally, when recharging of the cell is enabled, the voltage detector IC consumes an additional 0.7μA and the voltage regulator IC consumes 0.8μA of quiescent current. Futhermore, a diode is required in the recharge path to prevent the reverse flow of energy through the voltage regulator IC; again, this will result in an approximate 9% reduction in recharging efficiency when recharging at 1mA. The fact that a linear regulator is used means that efficiency will be limited when the raw voltage on the multiplexer module is significantly higher than 3V.

4.5.7 Supercapacitor module

The supercapacitor module (from the schematic in Appendix A, Figure A.5 and shown in Figure 4.18) is designed to accommodate both CAP-XX thin, flat supercapacitors such as the GS206F 0.55F model fitted in this prototype, and Panasonic Gold HW series supercapacitors. The DS2502+ EPROM stores information on the size and type of supercapacitor fitted. Additional circuitry can be added to allow the microcontroller to query the stored voltage on the supercapacitor, but this has not been fitted as, in the configuration used in the demonstration, the voltage on the supercapacitor is the same as the unregulated voltage on the multiplexer module. Provision has also been made for balancing resistors to be fitted to the module. This is arguably the simplest module developed for the case study, with no significant additional components. The management connections to the module are shown in Table 4.11.

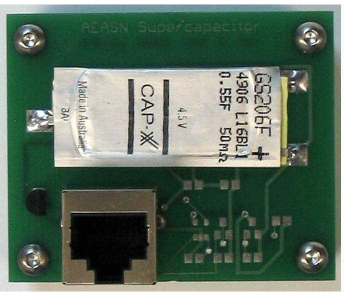

FIGURE 4.18: Circuit board for the supercapacitor module.

Pin	Type	Function
2	Meas. Control	Measure supercapacitor voltage
3	Measurement	Analogue: supercapacitor voltage measurement
4	Control	None
5	Control	None

TABLE 4.11: Interface pins from supercapacitor module.

4.6 System integration

4.6.1 Complete system

A demonstration system, including a multiplexer module and four energy modules (supercapacitor, battery, photovoltaic and mains), is shown in Figure 4.19. A further two energy module sockets on the multiplexer module are left unconnected. Energy modules can be connected to any RJ45 socket on the multiplexer module, and are connected here by standard 300mm RJ45 patch leads. The energy subsystem shown is connected to Port 0 of a TI CC2430 evaluation module (EM) via a 10-way IDC cable. The interface with the CC2430 EM is via its breakout board (without batteries attached).

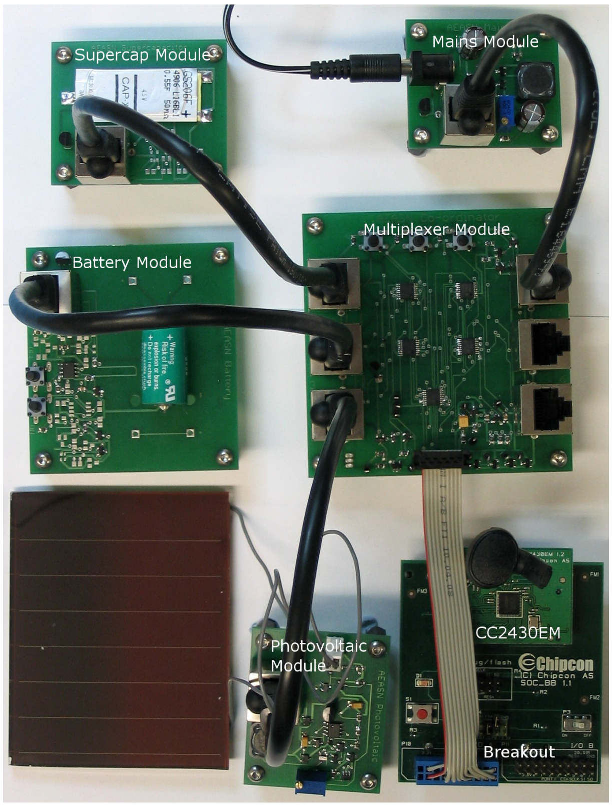

FIGURE 4.19: Complete system connection with battery, mains, supercap and photovoltaic modules. Connected to TI CC2430EM via its breakout board.

4.6.2 Default operation

The default behaviour of the system on first installation is to allow the energy harvesting device(s) to charge up the supercapacitor module. Once this store reaches approximately 2.1V, the system connects the power supply to the CC2430, which then starts up and tests its voltage. When this has reached a suitable level (nominally 2.7V) the microcontroller then performs the first energy-intensive tasks such as scanning its energy subsystem. To deliver a near-instant start-up to the system, the ‘on’ button may be pressed on the primary battery module, which will cause the system to receive power from the battery. Once the microcontroller has taken control of the energy subsystem, the microcontroller disconnects the primary battery in order to conserve the charge level on the cell.

Alternatively, the mains adapter may be turned on, which would also act to rapidly charge up the supercapacitor module. However, the microcontroller cannot act to turn off this supply as it is assumed to be a zero-cost resource which should be taken advantage of whenever it is available. The first scan of the energy subsystem is used to ascertain which sockets are occupied, what types of device are present, and their operating parameters. From this initial scan the microcontroller can reach an estimate of the amount of energy stored by the system. This data is stored in the microcontroller memory, so the EEDS of each module need only be scanned once (1-Wire activities are power-intensive so it is undesirable to carry out unnecessary communications).

Further detail about the software and system management operations, and implementation of electronic data sheet functionality, may be found in the description of the prototype system software in Chapter 5.

4.6.3 Overall evaluation

The quiescent current draw of the multiplexer module has been found to be in the region of 7.2μA. The quiescent power consumption of the primary battery module was 1.8μA and the secondary battery module was 5.1μA. Therefore, in standard operation the minimum quiescent current consumption of the energy subsystem with these components (energy harvesting modules tend to draw little quiescent power when not generating energy) is approximately 14.1μA. At 3V this equates to a quiescent power of around 42μW. This is significantly less than the 100μW-10mW that this system is designed to operate with, and thus can be considered to be a reasonable level of power consumption.

It has been shown that the presence of diodes in the path of the power supply lines have a major impact on the efficiency of the system, with low forward-voltage Schottky barrier diodes dropping 260mV (equating to a 9% efficiency loss at 3V and 1mA). For sources generating energy at lower voltages, the effective efficiency loss will clearly be much greater. In this project, diodes were considered a 'necessary evil' and were used sparingly where there was a risk of substantial amounts of energy being lost or of components being damaged.

The power consumption of taking measurements is also important; the operational amplifiers used in this project draw a quiescent current of around 1.2μA; however, it is likely that the effective energy cost of measurement operations will be many times this figure. For example, for the test of primary cells proposed earlier, closed-circuit current measurements with a small impedance actually discharge the cell at each test. In a similar way, for many energy harvesting devices, they must be disconnected from their load in order for the measurement to be taken; for a device generating 1mW, the system will miss out on 1mW of power for the duration of the test. Furthermore, when the microcontroller is engaged in taking measurements, it is likely to be in an active mode with its ADC enabled; once again, this is a substantial consumer of energy and must be optimised in order to avoid excessive usage of energy. The following chapter explores ways for the system to self-manage its energy resources while using as little energy as possible in achieving this objective.

The decision to use linear regulators was made in order to keep the complexity of the energy hardware low; it was also to keep the quiescent current draw of the circuit to a minimum. While this has indeed been the case, it limits the efficiency of the system when the raw voltage on the multiplexer is above 3V. For future revisions of the circuit, it would probably be worthwhile experimenting with step-down regulators which could kick in when this ceiling voltage level is exceeded. However, this would make little difference to the efficiency of the circuit when the raw voltage is below this level. It may also be worthwhile looking into the use of a Buck-Boost converter, in order that voltages below 2.0V could be also be boosted to be used by the microcontroller.

4.7 Summary

The case study described in this chapter described a realistic scenario, with a sensor node having a range of energy devices available (including energy harvesting devices, energy storage, and mains power). These represent a subset of the selection of energy resources that may be expected to be used in deployments of sensor nodes in a variety of scenarios, for example in a machinery monitoring application. The proposed architecture was evaluated by way of the case study. Basic circuitry was described and evaluated, which enables energy-awareness, voltage regulation, and other functionality for the system. The hardware designs of the multiplexer module, and the other relevant energy modules, were described in detail. The method for connecting the system together and its default operation were also explored. The efficiency of the overall system, and the impact of the additional circuitry required to deliver energy-awareness was evaluated. The design of the embedded software which interfaces with this hardware is documented in Chapter 5.

Chapter 5

Case Study: Deployment in a Prototype System – Software

5.1 Introduction

This chapter carries forward the case study outlined in Chapter 4 by describing and evaluating the software interface for the system, which is co-located with the communication stack on the microcontroller. This chapter also covers the EEDS content and mechanism for programming the content of data sheets. The microcontroller platforms used in this investigation, along with their important features of relevance to this work, are described in Section 5.2. The implementation of the EEDS for the deployed modules is outlined in Section 5.3, including examples for the data stored in the implemented modules and detail on the implementation and energy costs of the 1-Wire interface. The embedded software structure is described in Section 5.4, and detail on the energy stack is given in Section 5.5. High-level considerations for energy-aware operation and the overall evaluation of the system are considered in Section 5.6.

5.2 Microcontroller platform

5.2.1 Platform capabilities

The software developed under this project has been implemented on two separate microcontroller platforms: the eZ430-RF2500 and CC2430EM, both from Texas Instruments. The devices were shown in Section 2.7.1, and the capabilities of each device (of interest to this project) are described below.

The CC2430EM includes a CC2430 system-on-chip device which incorporates an enhanced 8051 microcontroller and 802.15.4 2.45-GHz transceiver. The CC2430 is an 8-bit device that has a maximum clock speed of 32MHz, and the particular device in use has 128kB of flash memory and 8kB of RAM. It operates from a supply voltage of 2.0-3.6V. The raw device has 21 general-purpose I/O pins, eight of which are connected to the internal ADC. It also has an internal 1.25V reference generator and an on-chip temperature sensor.

Conversely, the eZ430-RF2500 has an MSP430F2274 microcontroller and separate (non 802.15.4-compliant) 2.45GHz radio transceiver. The MSP430F2274 is a 16-bit device with a maximum clock speed of 16MHz, 32kB of flash memory and 1kB of RAM. Due to the restricted memory resources, the MSP430 was the more challenging platform for which this system was developed, and for which the most development effort was expended. It operates from a supply voltage of 1.8-3.6V. The raw device has 32 general-purpose I/O pins, 12 of which are connected to the internal ADC. The microcontroller also has a 1.5V internal reference generator and an on-chip temperature sensor.

5.2.2 Language, environment and debugger

Support for the CC2430 is provided by the IAR Embedded Workbench tool chain, whereas the MSP430 is supported by Code Composer Studio (from Texas Instruments). Both environments offer similar features in terms of code editing, project management, and debugging. Code is written in an extended version of C. The extensions differ for each microcontroller, which meant that it was necessary to implement a 'hardware abstraction layer' (documented later) to facilitate interactions with the physical aspects of each device. The fact that code written in C is supported by both devices meant that the remainder of the stack structure could be written in a generalised manner which was applicable to both devices (and is portable to many other microcontroller families).

Physical programming of devices, and debugging, was enabled by hardware supplied by the manufacturers as part of their evaluation kits. The eZ430-RF2500 was programmed via a simple USB dongle which also acted as a debugger and serial port (over the same USB interface). The eZ430-RF2500 was programmed via a SmartRF04EB, which is pictured in Figure 5.1. The SmartRF04EB provides a USB interface for programming/debugging and a separate serial connection for data via an RS232 port. The device shown in the figure is acting as a receiver for test transmissions from a node, and has a CC2430EM module mounted directly on the board.

Clearly, debugging devices while they were connected to energy harvesting systems, with a fluctuating energy supply, was very challenging. It was necessary to remove resistor R1 from the eZ430-RF2500 board in order to allow it to function on a different supply voltage from the USB interface (by default the USB interface provides a regulated 3.6V supply to the device). In many cases it was also necessary to connect the mains module to the energy subsystem in order to guarantee a certain power supply to the device for debugging purposes (halting a device in its active state for debugging uses a relatively high level of power, especially when the transceiver is active, which quickly depletes the energy stored in a supercapacitor). However, both systems have also been tested in a stand-alone mode, operating from harvested energy.

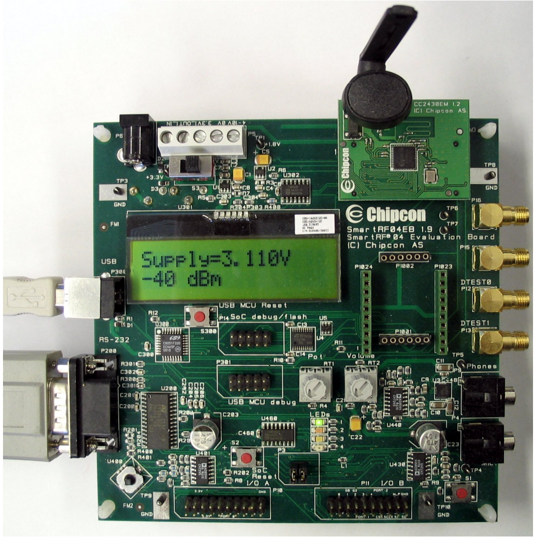

Figure 5.1: SmartRF04EB programming/debugging platform, used to interface with the CC2430EM.

5.2.3 Low-power modes and energy characteristics

The TI MSP430 has five low-power states in addition to its active mode. In the deepest low power mode, the CPU and all clocks and peripherals are disabled, meaning that the system can only be woken by an external interrupt. In shallower sleep modes, certain peripherals such as clocks and DC-DC converters are disabled. The depth of sleep has implications for the length of time in transitioning to the active mode, and so the overall power consumption and responsiveness of the processor. A comparison of the current draw of the various power modes is shown in Figure 5.2. The MSP430 module used in this project has a separate transceiver, and the power consumption of the radio in receive mode is often equal to or higher than its consumption in transmit mode. For this reason, in order to conserve valuable energy, it is essential to ‘sleep’ the radio, rather than leaving it in receive mode when idle. In this project, the MSP430 switches between active mode and LPM3, and is generally configured to be woken by its sleep timer (which is controlled by its very low power 32kHz oscillator). The CC2430 has a comparable current draw to the MSP430 in its active and sleep modes. The system developed under this project leaves the CC2430 device in power mode 2, which (similar to the MSP430 LPM3) leaves the 32kHz oscillator active and draws less than 1μA, allowing the device to be woken by its sleep timer. The CC2430 has an integrated radio transceiver, and this is also stopped whenever the device is not actively transmitting.

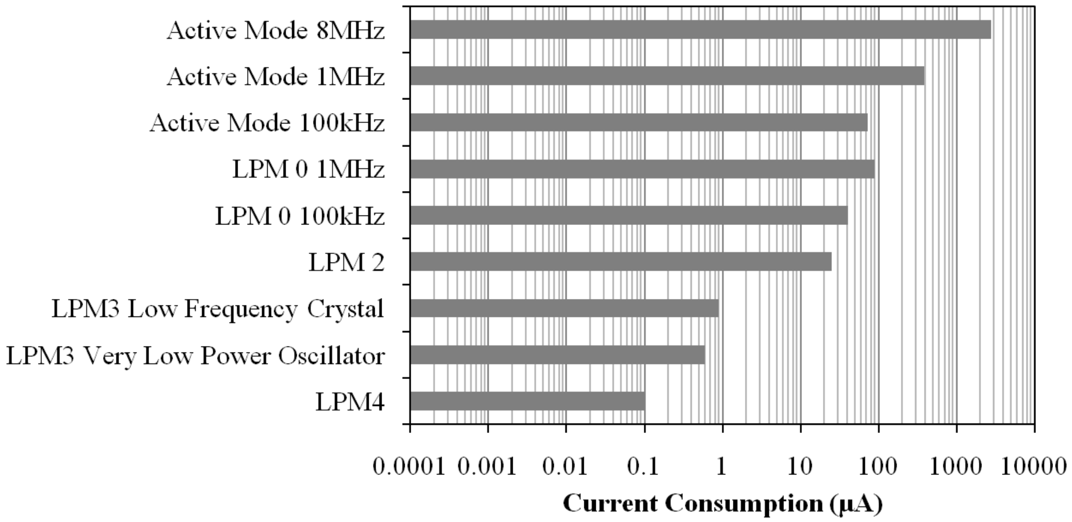

FIGURE 5.2: Current draw of the Texas Instruments MSP430F2274 in its various power modes. Data obtained from [127].

5.2.4 Hardware abstraction layer functions

As part of the embedded software structure implemented under this project, it was necessary to include a hardware abstraction layer which is unique for each microcontroller. It provides the ultimate interface between the embedded software stack and the physical hardware on the device. It is unfortunately the case that the actual method of interfacing with peripherals (including ADCs and general-purpose I/O pins) is unique to each microcontroller family, and even devices within the same family, depending on their feature set. A number of functions and macros have been implemented under this project, including:

- `halSampleADC`, which accepts the port and pin numbers as inputs, configures the ADC, and returns the result of the ADC conversion as a scaled `int`, e.g. with a value of `1500` corresponding to a voltage of 1.5V.

- `halSampleTemperature`, which directs the on-chip temperature sensor output through the ADC and returns the result as a scaled `unsigned int` (in degrees Celsius, so `200` corresponds to 20°C).

- `halSampleSupplyVoltage`, which uses the on-chip facility to monitor the supply voltage being provided to the microcontroller, utilising the ADC and returning the result as a scaled 8-bit result (nominally an `unsigned char`), with `230` corresponding to 2.30V.

- `halDirPortPin`, which sets the direction (i.e. output or high-impedance input) of individual pins on the microcontroller. The port, pin, and direction are all passed to the function as `unsigned char` variables.

- `halSetPortPinOutput`, which sets the actual output (i.e. high or low) of the general-purpose I/O pin specified. The port, pin, and output state are sent to the function as `unsigned char` variables.

- `halReadPortPin`, which reads the digital input to the general-purpose I/O pin specified; the port and pin are specified as `unsigned char` variables and the result is also returned as an `unsigned char`.

- `halEraseFlash`, which is used to erase the blocks of flash memory that are used to store the microcontroller's copy of the energy module EEDS.

- `halInitialiseEEDSPointers`, which is used to initialise pointers to the memory locations for the energy electronic data sheet of each energy module (ordered by multiplexer address number).

The following macros are also provided, which configure the sleep timer of the microcontroller and allow it to be put into a low-power mode:

- `halInitSleepTimer`, which sets up the sleep timer facility, setting up the clock divider and oscillator input appropriately.

- `halShortSleep`, which sleeps the microcontroller for a short time, generally used to allow the ADC reading to settle.

- `halLongSleep`, which sleeps the microcontroller for a longer period, generally of the order of a few seconds.

- `halSleep`, which takes an `unsigned char` as an input; this is used for duty-cycling the node, and controls the duration of the sleep. The specified value controls the interval of the sleep timer (in seconds), and the microcontroller enters its low-power sleep state.

A number of other definitions are also provided, which define simple properties such as custom data types and macros for efficiently bit-masking and processing data. The hardware abstraction layer also hosts one-wire interface functions, which are described separately in Section 5.3. Effectively, this layer permits the energy stack to be coded in a device-agnostic fashion by removing the detail of interfacing with the physical device. It allows the rest of the modules to be written in plain C, which means that it can be compiled for any microcontroller type without the need for modification.

5.3 Energy electronic data sheets

5.3.1 Overview

As discussed in Section 4.3.3, the EEDS hardware selected for this system is the DS2502+ 1kB add-only EPROM. The device must be programmed before deployment in the system, as it requires programming voltages of around +12.0V; however, the facility is provided for the 1-Wire memory to be programmed with the 1-Wire device soldered in-situ into the energy module. A cable was fabricated to interface between the EEDS pin of the RJ45 socket of energy modules through to the RJ11 jack required by the programming device. The memories were programmed using a DS9097E COM port adapter from Maxim-Dallas via their iButton Viewer PC application; the programming device has an external 12V input which provides the required programming voltages. The programming set-up is shown in Figure 5.3. In-situ programming, however, was not possible for the EEDS device on the multiplexer module: this is due to the fact that the 1-Wire EPROM on this module is connected through a multiplexer IC which cannot be controlled easily when the device is not under the command of the microcontroller. An in-system programming facility may be desirable for future iterations of the system.

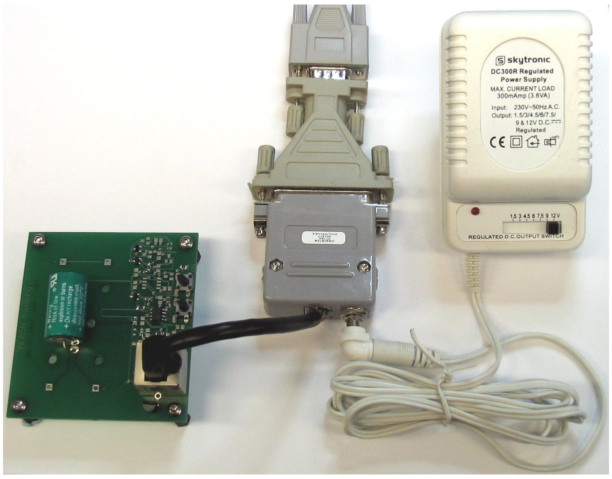
skytronic
DC300R Regulated Power Supply
MAX. CURRENT LOAD 300mAmp (3.6VA)
Input: 230V~50Hz A.C.
Output: 1.5/3/4.5/6/7.5/ 9 & 12V D.C.
Regulated
1.5 3 4.5 6 7.5 9 12V
REGULATED D.C.OUTPUT SWITCH

Figure 5.3: Set-up for EEDS on an energy module to be programmed over a 1-Wire interface, via a DS9097E COM port adapter connected to a PC serial port.

5.3.2 Functions for 1-Wire communications

The functions implemented for the 1-Wire interface are shown in the list below. The 1-Wire interface functions are incorporated into the hardware abstraction layer of the energy stack, as there is the possibility that alternative types of memory may be used to implement the EEDS functionality. However, much of the plug-and-play functionality of the system is dependent on features provided by the 1-Wire IC. One of the most important functions is the `onewireReset` function, which resets the 1-Wire bus and listens for a presence pulse from a 1-Wire device on the bus. This is used by the functions in the energy stack to detect whether an energy module is connected to a port (and can therefore prompt further interrogation). Functions have also been written to permit bits, bytes, and blocks of data to be read from the 1-Wire memory, and for command bytes to be written to the bus. These can prompt responses from the 1-Wire device including its device ID, or allow specific memory addresses to be read. Due to the presence of a pull-up resistor to enable the 1-Wire bus, the microcontroller normally leaves the pin used for 1-Wire communications in its high-impedance (input) state. Communications from the microcontroller are actuated by the microcontroller changing the status of the pin to a low output (as opposed to a high-impedance input), which pulls the line low. Responses from the 1-Wire device will also pull the line low.

- `onewireDelay2us` is a delay function that implements a multiple-of-2μs delay, which is necessary due to the time-sensitive nature of 1-Wire communications. This function is trimmed for specific microcontrollers and clock speeds.
- `onewireReset` sends a reset signal over the 1-Wire bus. If a presence pulse is detected (i.e. if a 1-Wire device responds to the reset signal), the function returns a non-zero result.
- `onewireWriteByte` writes a byte of data to the 1-Wire bus (which will typically be a command, as data cannot actually be written to the EPROM memory in this system due to the high voltages required for this operation).
- `onewireWriteBit` writes a single bit to the 1-Wire bus. It is generally called by the `onewireWriteByte` function.
- `onewireReadBlock` reads a block of data (of a specified length) from the 1-Wire EPROM memory.
- `onewireReadByte` reads a single byte of data from the 1-Wire EPROM memory.
- `onewireReadBit` reads one bit from the 1-Wire bus. It is generally called by the `onewireReadByte` function.
- `onewireUpdateCRCByte` permits a CRC to be generated from the data read from the 1-Wire device. This can the be compared to the CRC generated by the device itself in order to check for communication errors.

5.3.3 Performance costs of 1-Wire communications

As discussed in Section 4.3.3, 1-Wire ICs are two-terminal devices which have one pin connected to ground, with the remaining pin being used for both data and power. The DS2502+ device used in this project requires a ≈5kΩ pull-up resistor on the bus line.

As covered earlier, the design of the system means that the 1-Wire devices draw no quiescent current when the system is not actively communicating with energy devices (i.e. when it is sitting in address `'0'`). At other times, when the device is not actively engaged in communications, the input load current is typically 5μA. At times when the microcontroller needs to pull the bus 'low', there is clearly an amount of current dissipated through the $\approx$5kΩ resistor, which is proportional to the regulated voltage; for example with a 3V regulated voltage, approximately 600μA will be dissipated. This is clearly a substantial level of power, but given that the line is pulled low for relatively short periods, the overall energy requirement is minimised.

In order to further minimise the energy demand from the system, the entire data sheet is read from each device and stored in memory on the microcontroller. This means that the parameters can be accessed by the energy stack at any time without delay or further energy cost. The timings of the 1-Wire operations used by the system are (with recommended timings shown in brackets) [128]:

- **Reset:** Hold bus low for 480-640μs (480μs), sample bus after 63-78μs (70μs), wait for at least 410μs (410μs).
- **Read Bit:** Hold bus low for 5-15μs (6μs), sample bus after 5-12μs (9μs), wait for at least 50μs (55μs).
- **Write 1:** Hold bus low for 5-15μs (6μs), wait for at least 59μs (64μs).
- **Write 0:** Hold bus low for 60-120μs (60μs), wait for at least 8μs (10μs).

For the system implemented here, the following process is followed to read the device ID and EEDS data, which are then stored in memory on the microcontroller:

1. **Reset** bus and check for response. If a response is received, proceed.
2. **Write Byte** [33h] – 'read ROM' command.
3. **Read Byte** – family code of 1-Wire EPROM, discard.
4. 6 x **Read Byte** – save as six-byte device ID and store in microcontroller memory.
5. **Write Byte** [CCh] – 'skip ROM' command.
6. **Write Byte** [F0h] – 'read memory' command to bus.
7. 2 x **Write Byte** – [00h] to bus (start read from address zero).
8. **Read Byte** – CRC of command.
9. Multiple **Read Byte** commands – dependent on type of device, read and store EEDS parameters in microcontroller memory.

The typical execution times for these operations mean that the time taken up until the start of item 9 is approximately 8.24ms. Each further byte read takes a further 560μs. For the system developed here, there are up to 13 additional bytes to be read from the data sheet. The read time for this would be 7.28ms, which means an overall read time of 15.5ms. The shortest data sheet implemented in this case study has four additional bytes, which equates to an additional read time of 2.24ms, or an overall read time of 10.5ms. The minimum amount of time taken per address is 960μs, in the case that a device is not connected and therefore no further actions need to be taken beyond the 'reset' operation. This operation must be carried out for each socket on the multiplexer module. In the extreme case where all sockets are occupied and devices have the maximum length of data sheet, the read operation for the six devices takes approximately 93ms.

The multiplexer module data sheet must also be interrogated, but has only five bytes of data after the CRC is returned. The total read time, in this case, is approximately 11ms. For a combined read of the multiplexer module, and all other module, data sheets, the operations will take up to 104ms. Assuming that the 1-Wire bus is being pulled low by either device for 50% of this time, the energy disippated through the pull-up resistor can be calculated as 94μJ over this time. As an example, the waveform of the system reading the electronic data sheet on the supercapacitor module is shown in Figure 5.4.

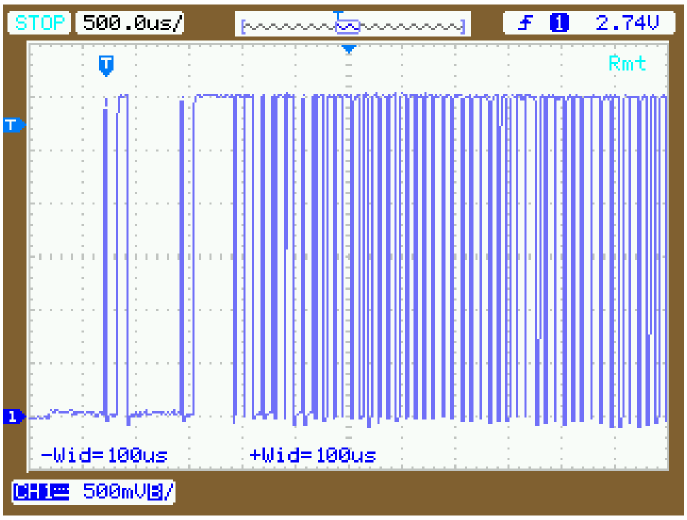

FIGURE 5.4: Oscilloscope trace of the microcontroller reading the 1-Wire EEDS on the supercapacitor module.

5.3.4 Data sheet format

The content of each module data sheet is dependent on the module's functionality. Structs that define the data stored for each type of device are defined in the `etypes.h` header file, which is accessible by all layers of the energy stack. Parameters for energy modules (other than the multiplexer module) are stored, as shown in Listing 5.1, in the

```
typedef struct _TModule {
  TDeviceID DeviceID;
  unsigned char DeviceType;
  unsigned char Measurement;
  unsigned char Multiplier;
  unsigned char MaxOutput;
  TParams Parameters;
} TModule;
```

Listing 5.1: Struct for energy module EEDS parameters

```
#define MEAS_UNMEASURABLE 0x00
#define MEAS_ONOFFMAXIMUM 0x01
#define MEAS_ENDOFLIFE 0x02
#define MEAS_LINEAR 0x03
#define MEAS_SQUARE 0x04
#define MEAS_CUBIC 0x05
#define MEAS_CURVE 0x06
#define MEAS_COMPLEX 0x07
```

Listing 5.2: Measurement types for devices

TModule struct which follows the format defined in Table 3.1. In the system implemented under this project, a number of device types were defined in order to enable an energy-aware node to be delivered in as efficient a manner as possible. The parameters of the devices are stored in the Parameters field (the structs that are defined under the TParams field of the TModule struct are shown in Listing 5.5). The TDeviceID field is simply the six-byte serial number of the 1-Wire memory and the DeviceType field refers to the device type as defined in Table 3.3. The Measurement field refers to the measurement scheme for the device (i.e. how the microcontroller can translate the sensed value into an estimate of power or energy), which is defined in Listing 5.2. The Multiplier field indicates how to scale the measured value before entering this conversion (scaled up by 10 to be stored as an unsigned char), and the MaxOutput field defines the maximum output voltage (also multiplied by 10).

The multiplexer module EEDS stores information specific to the role of the multiplexer module. The TMuxData struct that defines the format of this data is shown in Listing 5.3. The TDeviceID field stores the six-byte serial number of the 1-Wire memory and the Multiplier field indicates how to scale the measured value of the raw voltage (multiplied by 10 to be stored as an unsigned char). The NumPorts field states how many modules the multiplexer module can support (up to six), which enables the scheme to be used for smaller multiplexer modules which support fewer energy modules. The MaxVoltage and MinVoltage fields state the maximum and minimum raw voltage that the multiplexer module can support while remaining functional, and the RegulatedVoltage field represents that the multiplexer will regulate to. These voltage values are scaled up by a factor of ten, as with the other energy modules, so that the values can be stored as an unsigned char. This minimises the amount of memory re-

```
typedef struct _TMuxData {
  TDeviceID DeviceID;
  unsigned char Multiplier;
  unsigned char NumPorts;
  unsigned char MaxVoltage;
  unsigned char MinVoltage;
  unsigned char RegulatedVoltage;
} TMuxData;
```

Listing 5.3: Struct for multiplexer EEDS parameters

```
typedef union _TParams {
  TParamCurve ParamCurve;
  TParamComplex ParamComplex;
  TUInt IntMultiplier;
  TPrimaryParams PrimaryParams;
} TParams;
```

Listing 5.4: TParams union for storing module parameters

quired to stored these parameters, and the amount of energy required to read this data from the 1-Wire EPROM memory.

The parameters stored for the energy module are represented in the `Parameters` field of the `TModule` struct. The parameter fields are shown in Listing 5.5. The `TParamCurve` field stores complex parameters used in this case study by the photovoltaic module. The `PrimaryParams` field stores operational data for primary batteries for which state-of-charge cannot be calculated; it simply stores the maximum capacity as an `unsigned int`, and an end-of-life threshold value that indicates when the store is approaching empty. Curves are represented by the `TParamCurve` struct, which defines a set of individual points that are interpolated between in order to determine the state-of-charge of an energy store. The total amount of energy is stored alongside this curve, and each point on the interpolated curve is represented by a `TParamCurveSingle` data point, which stores the voltage and the percentage of 'full' energy with which it corresponds. In order to minimise the amount of memory used by these fields, the voltage values are stored in `HalfVolts` field, which in fact correspond to the measured voltage multiplied by 50 and stored as an `unsigned char`. This enables a voltage range of 0. . . 5.10V to be stored effectively, with a 20mV resolution, in an 8-bit data field.

5.3.5 Example data sheet contents

The contents of two data sheets are shown here for illustration purposes. The mechanisms for reading the electronic data sheet values, interrogating the energy modules, and calculating the overall energy status of the node is documented later. Table 5.1 shows the datasheet for the NiMH battery module. In this case, the device type field identifies it as a secondary battery module which can be controlled by the microcontroller to enable

```
typedef struct _TParamComplex {
  TFloat a;
  TFloat b;
  TFloat c;
  unsigned char d;
} TParamComplex;

typedef struct _TPrimaryParams {
  unsigned char EndOfLife;
  TUInt MaxCapacity;
} TPrimaryParams;

typedef struct _TParamCurve {
  TParamCurveSingle Point [4];
  TUInt TotalEnergy;
} TParamCurve;

typedef struct _TParamCurveSingle {
  unsigned char HalfVolts;
  unsigned char Percent;
} TParamCurveSingle;
```

Listing 5.5: Parameters to enable energy-awareness for energy modules

both charging and discharging. It states that the measurement of the state-of-charge of the device is via a curve, whose points are given (e.g. 100% charge corresponds to a voltage of 2.88V – double 1.44V). It also shows that its maximum voltage is 2.9V and that the measured values from the ADC (in the range 0..1V) must be multiplied by 4.9 to arrive at the actual battery voltage.

NiMH Battery Module		
Device Type	01 0010 11	0x47
Measurement	Curve	0x06
Multiplier	4.9 (49)	0x31
Max Output	2.9 (29)	0x1D
Total Energy	6912	0x00 00 1B 00
Curve Points	144/100 132/88 122/13 100/0	0x90/0x64 0x84/0x58 0x7A/0x0D 0x64/0x00

Table 5.1: Electronic Data Sheet for NiMH battery module.

Similarly, an example of a data sheet for the photovoltaic module is shown in Table 5.2. The device type identifies the module as a photovoltaic module. The measurement scheme is defined as complex, and the method for interpretation of the values is shown in Section 5.5.2. Again, the multiplier indicates that the measured value must be scaled by 4.9 to arrive at the actual voltage across the photovoltaic module. The maximum output of the module is stated as 6.0V, which is the open-circuit voltage of the cell under peak illumination conditions. Four additional parameters are given (A, B, C, and D), three of which are floats. The parameters are related to those shown earlier, in Table 4.4.

Data sheet parameters A and B are simply the values from Table 4.4 scaled up by 100, parameter C is the product of $(k \times m)$, and parameter D is the $\alpha + 1$ (scaled up by 10) as given in Section 4.5.1. The parameters were adjusted in this way to maintain the precision and efficiency of the calculation, while minimising the storage size of the electronic data sheet parameters for this module.

Photovoltaic Module		
Device Type	10 0010 00	0x46
Measurement	Complex	0x07
Multiplier	4.9 (49)	0x31
Max Output	6.0 (60)	0x36
A	25.71	0x41 CD AE 14
B	291.28	0x43 91 A3 D7
C	0.003813	0x3B 79 E3 86
D	7.8 (78)	0x4E

Table 5.2: Electronic Data Sheet for photovoltaic module.

A selection of data sheets for other modules produced by the author can be found in Appendix B.

5.4 Embedded software structure

5.4.1 Overall structure

The overall structure of the software on the sensor node was introduced in Section 3.7 and is shown in Figure 5.5. The focus of the work undertaken and described in this thesis is concerned with the energy subsystem; the communication and sensing stacks have only received cursory attention. It is left for future investigations to decide the optimal way of interfacing with, and processing the data from, transducers in the intelligent sensing stack. Only a basic implementation of the sensing stack was produced, and a pre-existing communication stack was used under this project. This section describes the overall features of the system, and how the system is co-ordinated. Detailed information on the content and operation of the energy stack is given in Section 5.5.

5.4.2 Communication stack

The communication stacks used in the prototype systems are inherited from example code provided by Texas Instruments. The CC2430EM uses the Simple Packet Protocol (which is no longer supported), and the eZ430-RF2500 uses the SimpliciTI protocol (which is being actively developed for a range of platforms). Both protocols are cut-down, efficient radio stacks which interface with the 2.45GHz radio transceivers on these platforms.

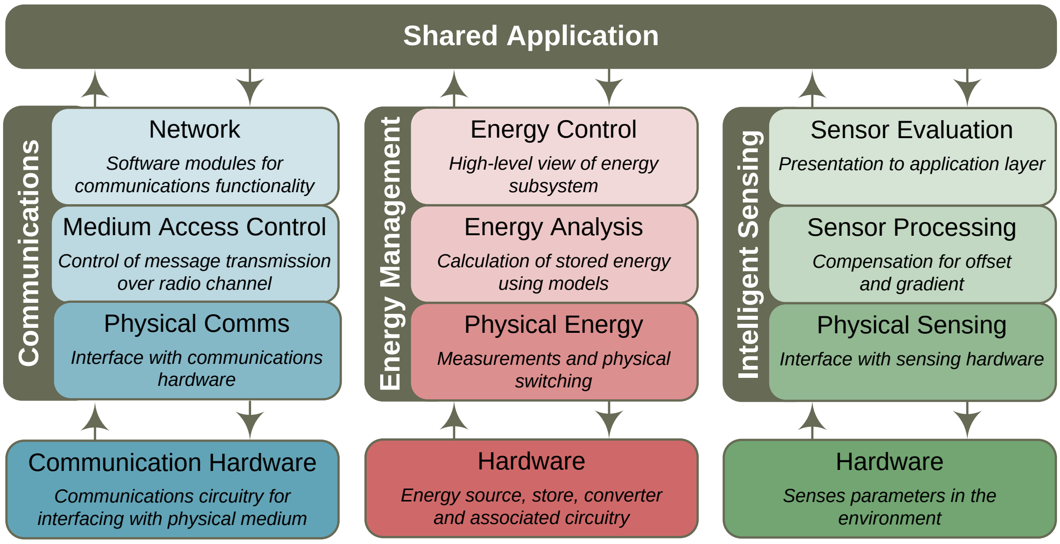
Shared Application
Communications
Network
Software modules for communications functionality
Medium Access Control
Control of message transmission over radio channel
Physical Comms
Interface with communications hardware
Communication Hardware
Communications circuitry for interfacing with physical medium
Energy Management
Energy Control
High-level view of energy subsystem
Energy Analysis
Calculation of stored energy using models
Physical Energy
Measurements and physical switching
Hardware
Energy source, store, converter and associated circuitry
Intelligent Sensing
Sensor Evaluation
Presentation to application layer
Sensor Processing
Compensation for offset and gradient
Physical Sensing
Interface with sensing hardware
Hardware
Senses parameters in the environment

FIGURE 5.5: A combined stack, comprising stacks for communications, energy management, and sensing.

```
// initialise radio
radioInit(frequency, myAddr);

// send data
radioSend(sendBuffer, sizeof(sendBuffer), remoteAddr, DO_NOT_ACK);
STOP_RADIO();
```

LISTING 5.6: Code to interface with Simple Packet Protocol communication stack

CC2430EM: Simple Packet Protocol

The communication stack implemented in the system is based on the Texas Instruments Simple Packet Protocol (SPP). The protocol permits data payloads of up to 125 bytes and supports source/destination addressing and broadcasting, along with sequence bits and acknowledgements. Data frames received through the SPP stack have a received signal strength indicator (RSSI) byte. The communication system is set up through the `radioInit` command shown in Listing 5.6.

In the demonstrator, transmissions are made on a fixed channel and are unacknowledged. This minimises the amount of time that the transceiver must be active for and thus reduces the overall power requirement of the device. Data is transmitted through the `radioSend` command, which is also shown in Listing 5.6.

eZ430-RF2500: SimpliciTI

Communications for this device are provided by the SimpliciTI stack, which was developed by Texas Instruments. The protocol is more capable than the SPP, but has a code size of approximately 4k. It supports a number of network-related tasks and has three

```
// Initialise radio with new address
SMPL_Ioctl(IOCTL_OBJ_ADDR,IOCTL_ACT_SET,&sourceAddress);
SMPL_Init(0);
//Sleep Radio
SMPL_Ioctl(IOCTL_OBJ_RADIO, IOCTL_ACT_RADIO_SLEEP, 0);

// Wake up radio
SMPL_Ioctl( IOCTL_OBJ_RADIO, IOCTL_ACT_RADIO_AWAKE, 0);
// Send packet
SMPL_Send(SMPL_LINKID_USER_UUD, msg, sizeof(msg));
// Sleep radio
SMPL_Ioctl(IOCTL_OBJ_RADIO, IOCTL_ACT_RADIO_SLEEP, 0);
```

Listing 5.7: Code to interface with SimpliciTI communication stack

layers as shown in Figure 5.6, although it is debatable whether the Lite HAL layer is truly a layer. It is this sort of capable but resource-efficient communication protocol which is ideally suited to resource-constrained wireless sensor nodes. The method of sending data, and managing the transceiver, is shown in Listing 5.7.

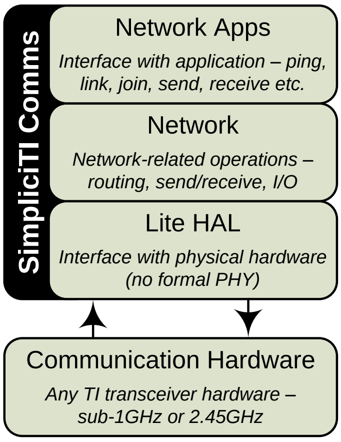
SimpliciTI Comms
Network Apps
Interface with application – ping, link, join, send, receive etc.
Network
Network-related operations – routing, send/receive, I/O
Lite HAL
Interface with physical hardware (no formal PHY)
Communication Hardware
Any TI transceiver hardware – sub-1GHz or 2.45GHz

Figure 5.6: The SimpliciTI communication stack, adapted from [72].

5.4.3 Sensing stack

The structure of the sensing stack was introduced in Section 3.7.3. A basic sensing stack has been developed to interface with the on-chip temperature sensor. The workings of this system are similar to the energy stack. The PYS layer interfaces with the ADC to obtain an analogue reading from the temperature sensor. This is translated by the SPR layer which accounts for offset and gradient (through pre-determined values that must be derived for each individual device). The final temperature reading is presented by the SEV layer to the shared application layer. As no electronic data sheet format has been developed for the sensing hardware, it was necessary to hard-code the device models into the stack software. Clearly, in future iterations of the system, it will be desirable to be able to connect a range of sensors to the system and for them to self-identify their interface and calibration coefficients in a similar way to the energy hardware.

5.4.4 Energy stack

An energy stack, compliant with the structure introduced in Section 3.7.2, has been developed and is described in full in Section 5.5. The energy stack has been designed to interface with a range of energy hardware via a multiplexer module as specified in Section 3.5, making use of the data stored on the EEDS of each energy module. The energy stack enables the energy-aware operation of the system, by allowing the incoming power and stored energy to be measured and the energy priority of the system to be computed. It also allows the system to make decisions about whether to enable charging or discharging of energy stores. The three distinct layers allow the physical interfacing with the components to be effectively separated from the higher-level computation, thus meaning that higher levels can be written in a device-agnostic way. There are certain limitations, inherent in the necessity of using fixed-point variable types, which are described later; however, the system has been developed to be as flexible as possible and where relevant these limitations are defined and tailored for use in sub-milliwatt sensor nodes.

5.4.5 Application layer and control scheme

The shared application layer interfaces with the three individual stacks. In the implementation developed under this project, the application layer takes information from the energy stack in order to control its duty cycle (effectively sleeping for longer in the case that the energy status is lower). Data is taken from the sensing stack and used to format messages to be sent through the communication stack. The system developed acts as an autonomous temperature sensor, sensing, formatting messages, and transmitting them through the communication stack at a duty cycle appropriate for the energy status.

5.5 Energy stack

5.5.1 Physical Energy (PYE) layer

Datasheet functions

The layer implements two separate functions for reading in data from the EEDS on energy modules and the multiplexer module. The reason that two functions are needed is that the structure of the multiplexer EEDS is significantly different to that of the other energy modules, and the data from them may be stored in different locations on the microcontroller. In the case of the MSP430 implementation of the system, data on the energy modules is stored in flash while data on the multiplexer system is stored in RAM. This is due to the limited amount of RAM available on the MSP430 node, compared with the amount of flash.

- `pyeGetMuxData` sets the address as `'7'` and interrogates the 1-Wire device on the multiplexer module. Data about the multiplexer module are stored in a struct, as defined in Listing 5.3.
- `pyeGetModuleData` erases the stored EEDS for all energy modules and sequentially interrogates each energy module from address 1 to the last address (maximum 6). The data are read into structs as defined in Listing 5.5.

These functions utilise the procedures outlined in Section 5.3 to interrogate the 1-Wire memory EPROMs, and store data in locations indicated by pointers.

Initialisation and change detection

Essential to the energy-aware operation of the node, these functions initialise the pins on the device to be initialised, and enable changes to the devices connected to the multiplexer module to be detected by the microcontroller.

- `pyeInit` initialises the inputs and outputs from the microcontroller, along with the pointers to the data sheet locations. In the case of the MSP430, the EEDS data for energy modules are stored in flash; pointers direct to the appropriate flash location, or other memory location for alternative microcontrollers. Address pins are set as outputs and initialised to zero, and the EEDS interface pin is configured as an input pin (but with a zero output, so that when its direction is changed it will pull the line low). The measurement control line is set as an output and initialised to zero, and the measurement line is set as an input. The device control pins are both set as inputs (but again with zero outputs). The `halInitialiseEEDSPointers` function is called to initialise the EEDS pointers appropriately.
- `pyeRescan` sequentially queries each port on the multiplexer module and issues a 1-Wire 'reset', checking for a presence pulse in reply. If a presence pulse is detected, and there is no record in memory of a device being connected to that address, the function returns a `'1'`. Similarly, if there is no device detected when the system has a record of one being connected, the function also returns a `'1'`. The function returns `'0'` if no changes are detected.
- `pyeRefresh` is similar to the `pyeRescan` function, but instead of simply issuing a reset command and listening for a response, it also queries the device ID of each

energy module connected to the multiplexer. If a difference is detected from the ID recorded in the microcontroller memory, the function returns a '1', otherwise it returns a '0'.

The pyeRefresh or pyeRescan functions are expected to be called periodically in order to check for changes in the energy subsystem. They both allow newly connected devices to be recognised, and similarly allow the disconnection of devices to be detected. A change triggers a full re-scan of the energy hardware of the system in order to update the EEDS table held in the memory of the microcontroller. An important distinction between the functions is that pyeRescan just checks for the presence of modules at addresses on the multiplexer module, while pyeRefresh actually checks that the modules have the same ID code as those recorded in memory. Hence, pyeRefreah is a more robust function as it will detect if modules have been 'swapped' on a port since the previous update; however, it consumes more energy as it invokes a read of the 1-Wire memory on each port (as opposed to a straightforward reset) and invariably is more time-consuming. The choice of which method to use is left to the system designer, and will depend on the likelihood of devices being swapped between re-scans of the energy subsystem (and the impact of the EEDS on the microcontroller being out-of-date). It may be the case that a hybrid (perhaps with one re-scan per day) method of change detection may be effective whilst remaining energy-efficient.

Device interfacing

The device interfacing functions deal with the physical interface to the energy modules. They deal with setting address pins and obtaining measurements.

- pyeSetAddress takes an unsigned char input (the address that is desired) and sets the address pins appropriately.
- pyeTestSupplyVoltage simply calls the halSampleSupplyVoltage to sample the supply voltage of the microcontroller, and returns the supply voltage as an unsigned char (multiplied by 10, so that 2.2V would be reported as 22).
- pyeGetMeasurement configures the on-board ADC to take a measurement. The function takes an unsigned char input (the address of the device of interest) in case the address has not already been set. It initiates a measurement and returns it as an unsigned int. The module scales the value appropriately, dependent on the value of the multiplier field in the device EEDS. The value returned is the voltage (multiplied, and scaled up by 100).
- pyeGetChargeStatus reads the charge status of the module; if charging is enabled, it returns a '1', otherwise it returns a '0'. This function is useful to verify the

state of the bistable multivibrator on energy storage modules, which may or may not be overridable using buttons on the module.

- `pyeSetChargeStatus` sets the charge status of the module, which will be retained by the bistable multivibrator on the energy module.
- `pyeGetDischargeStatus` reads the discharge status of the module; if discharging is enabled, it returns a `'1'`, otherwise it returns a `'0'`. This function is useful to verify the state of the bistable multivibrator on energy storage modules, which may or may not be overridable using buttons on the module.
- `pyeSetDischargeStatus` sets the discharge status of the module, which will be retained by the bistable multivibrator on the energy module.

Together, they enable the physical interface with the energy devices, permitting the charge and discharge of energy storage devices to be enabled and disabled, and measurements to be carried out in order to assess the energy status of the node.

Flash write requirements

An intricacy of interfacing with the flash memory on microcontroller devices is that the supply voltage must be above a certain voltage-frequency threshold (as shown for the MSP430 in Figure 5.7) for flash write operations to be carried out reliably. This imposes an important constraint on the system: as the flash memory cannot be written to below a certain voltage, this means that data cannot be written to the MSP430's memory space allocated for EEDS data. Effectively this means that the system must start-up into the 'unknown' state and delay reading the module electronic data sheets until the microcontroller supply voltage has risen above this threshold. It also means that, should the voltage again drop below this threshold, the electronic data sheet values cannot be overwritten or manipulated. This fact conflicts with the conventional need to keep the supply voltage to the microcontroller as low as possible in order to minimise its power consumption.

5.5.2 Energy Analysis (EAN) layer

Energy and power estimation functions

These are key functions for this layer of the stack, that are used to calculate the overall energy status of the node. Three functions are provided: `eanGetPower` allows the system to estimate the amount of incoming energy at a given instant; `eanGetEnergy` estimates the energy stored on the system, and `eanGetVoltEnergy` estimates the amount of energy that would be stored by the system, given a certain system voltage.

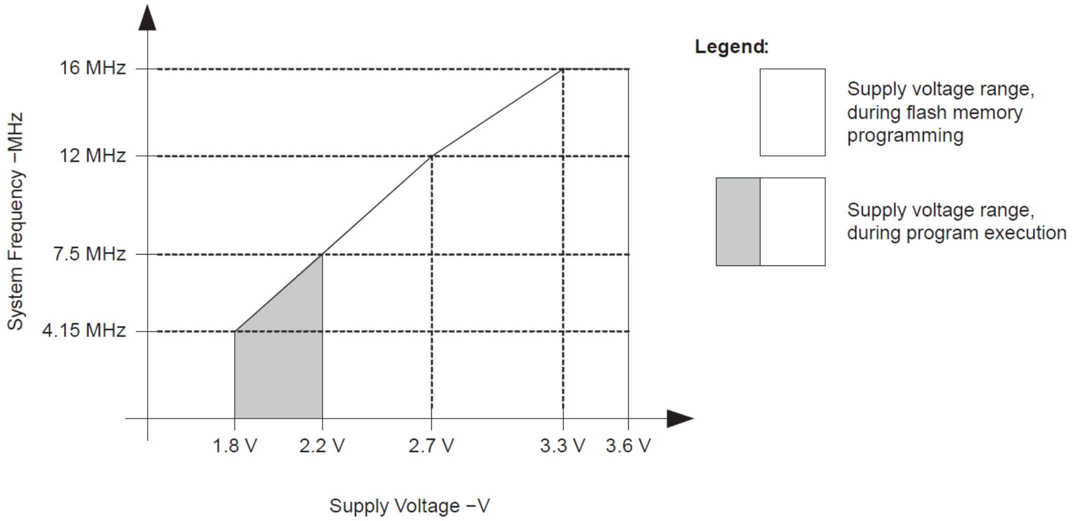

FIGURE 5.7: Voltage and system frequency frequency requirements for writing to the MSP430 flash (reproduced from [127]).

- `eanGetPower` is used to estimate the amount of power being generated by the system at a given moment. It sequentially analyses each device connected to the multiplexer module and, if the device is an energy source (as opposed to an energy store), it carries out a measurement on the device. The measurement is then converted to an estimate of power using the mathematical functions listed below and the parameters from its electronic data sheet. The function returns an estimate of power as an `unsigned int`, and is measured in microwatts. Given the limits of the `unsigned int` variable, this allows the system to represent incoming power between zero and 65.5mW.

- `eanGetEnergy` is used to estimate the amount of energy stored in energy storage devices. It sequentially analyses each device connected to the multiplexer module and, if the device is an energy store (as opposed to an energy source), it carries out a measurement on the device. The measurement is then converted into an estimate of energy stored, using the mathematical functions below. The function returns an estimate of energy as an `unsigned int`, and is measured in J/100 (i.e. tens of millijoules). The units used in this estimation are necessary to be able to represent the large range of energy that may be stored in batteries (up to tens of kilojoules) down to supercapacitors (typically a few joules) with an `unsigned int` (which has range `0..65,535`).

- `eanGetVoltEnergy` is used to estimate the amount of energy that could be stored in the energy storage devices, with the raw voltage on the multiplexer module at a given voltage. It sequentially analyses each device connected to the multiplexer module and, if the device is an energy store (as opposed to an energy source), it uses data on the maximum voltage from the device EEDS and the voltage on the multiplexer module (given as an input) and takes the lower of the two. It then estimates the amount of energy that would be stored by the device connected to the system at the given voltage. The function returns an estimate of energy as an `unsigned int`, and is measured in J/100 (i.e. tens of millijoules), in a similar way to the `eanGetEnergy` function.

In combination, the data from the `eanGetVoltEnergy` and `eanGetEnergy` functions allow the useable proportion of energy stored on the system to be calculated. This information is used by the EAN layer to calculate the EP value for the node.

Mathematical functions

The calculations of power and energy carried out in this layer rely on a number of mathematical functions:

- `eanCalculateCurve` estimates the energy stored, given the input voltage, along a piecewise-linear approximated discharge curve (as shown in Figure 3.7 and represented for the primary battery in the electronic data sheet in Table 5.1). The function accepts the measured voltage as an `unsigned char` input and returns the energy stored as an `unsigned int`, in tens of microwatts.
- `eanMathExponential` takes two inputs: an exponent as a `float`, and the number of terms to compute it to as an `unsigned char`. The functions returns the Taylor expansion of e^x, computed to the specified number of terms (increasing number of terms improves its precision, but impacts on performance and can result in overflow if taken to extremes). The result is returned as a `float`.
- `eanMathFactorial` takes an `unsigned int` as an input, calculates its factorial, and returns it as an `unsigned long`. It is required by the other mathematical functions that carry out Taylor expansions.
- `eanMathPower` takes two inputs: a number as a `float` and a power as an `unsigned char`. It returns the number raised to the power, as a `float`.
- `eanMultiplyRaise` takes three inputs: a number (x) as an `unsigned int`, a multiplier (A) as an `unsigned char`, and a power (y) as an `unsigned char`. The function returns the result of Ax^y as an `unsigned int`.
- `eanCalculateComplex` is a custom function used for calculating the power from a photovoltaic module. It takes two inputs: the measured voltage and the raw voltage on the multiplexer module, both as `unsigned char` variables, in order to estimate the nominal power from the photovoltaic module. It makes use of the exponential function described above, and implements the calculations described in Section 4.5.1. The result is returned as an `unsigned int`.

There are a number of intricacies associated with using these functions, that are considered at the end of this subsection.

Device management functions

These functions are provided for system initialisation and to enable the periodic refresh of data in the microcontroller's copy of the EEDS of the energy modules.

- `eanInit` is called on system start-up to initialise relevant EAN variables to zero, and calls the `pyeInit` function.
- `eanStartUp` tests the supply voltage of the microcontroller; if it is below the threshold value it returns a '`0`'; otherwise, it reads the EEDS data from all modules into the microcontroller memory and returns a '`1`'.
- `eanRefresh` checks the microcontroller supply voltage; if above the threshold value it checks for changes using the `pyeRefresh` function. If no change is detected, the function returns a '`1`'; if it was unable to complete due to low supply voltage it returns a '`0`', otherwise (if changes were found), it returns a '`2`'.
- `eanRescan` checks the microcontroller supply voltage; if above the threshold value it checks for changes using the `pyeRescan` function. If no change is detected, the function returns a '`1`'; if it was unable to complete due to low supply voltage it returns a '`0`', otherwise (if changes were found), it returns a '`2`'.

Together these functions enable the energy status to be updated periodically, and for the addition or removal of energy modules to be detected and appropriate action taken.

Detail of capabilities

The limitations of a resource-constrained microcontroller mean that some mathematical functions need to be performed with care in order to maintain the precision of results. For example, the calculations carried out for estimating the power obtained from the photovoltaic module involves the use of a Taylor expansion to implement Equation 4.7 mathematically. The Taylor expansion of the exponential function, e^x, is shown in Equation 5.1. The calculation involves a substantial amount of floating-point arithmetic, which is challenging for these resource-constrained microcontrollers. Indeed, the limitations of the fixed-point numbers also mean that the precision of the Taylor expansion approximation is limited. As an example, Figure 5.8 shows the computation of e^8, using the expansion shown in Equation 5.1, to a varied amount of terms. Due to the limits of the `long` variable which is used to hold the result of the factorial function, the thirteenth term ($13! = 6,227,020,800$) is the highest term that can be computed; as e^x

is raised to higher powers, the precision becomes more limited, therefore $x = 8$ is the highest power that can be computed with reasonable precision (with approximately 5% error) to 13 terms. In realising the calculations to estimate the power being generated by the photovoltaic module (as shown in equations 5.2 and 5.3, which relate to the parameters given in Table 5.2), care must be taken to ensure that (in normal operation) e^x is not raised to a power beyond 8; in some cases it may be necessary to optimise the parameters held in the EEDS for photovoltaic modules in order to ensure this.

$$e^x = \sum_{n=0}^{\infty} \frac{x^n}{n!} = 1 + x + \frac{x^2}{2!} + \frac{x^3}{3!} + \frac{x^4}{4!} + \cdots \tag{5.1}$$

$$V_{oc} = \left(V_{meas} \times \frac{d}{10}\right) - V_{raw} \tag{5.2}$$

$$P = V_{oc} \times c \times e^{\frac{V_{oc}-b}{a}} \tag{5.3}$$

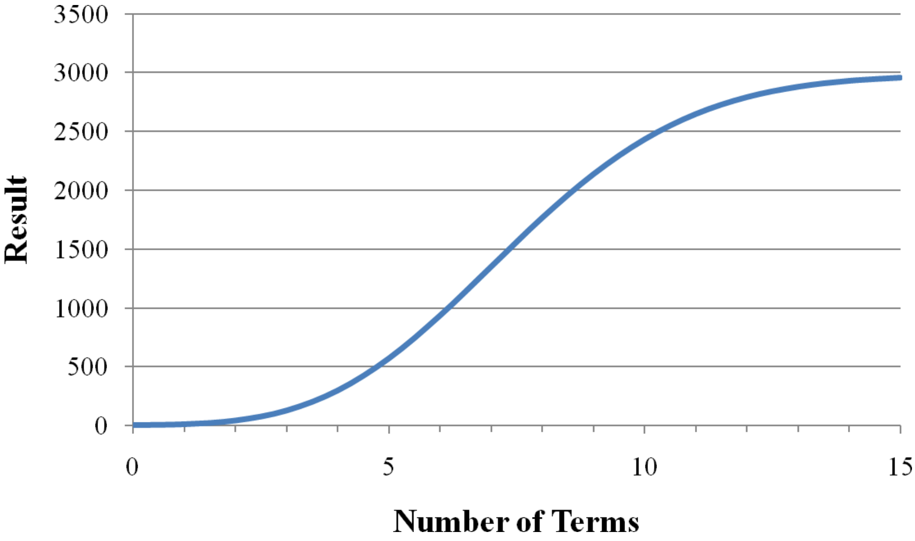

FIGURE 5.8: Calculation of e^8 using Taylor expansion, showing how the number of terms affects the precision of the result.

Another detail is that sentinel values are used by some of the functions to indicate that the system is connected to the mains: the `eanGetPower` function returns the maximum value for the `unsigned int` variable (`65,535`) in order to signal that it is a device supplying a large amount of power. This is interpreted by the other functions as a signal that the device is under mains power and allows the EP value to be set accordingly.

5.5.3 Energy Control (ECO) layer

The ECO layer makes a number of functions available which enable the microcontroller to configure the energy stack, and prompt it to update. The functions include:

```
typedef enum _ENERGY_PRIORITY{
  PP_MAINS,
  EP_5,
  EP_4,
  EP_3,
  EP_2,
  EP_1,
  EP_EMPTY,
  EP_UNKNOWN
}ENERGY_PRIORITY;

typedef struct _ENERGY_THRESHOLDS{
  unsigned char ET_4;
  unsigned char ET_3;
  unsigned char ET_2;
  unsigned char ET_1;
  unsigned char ET_0;
}ENERGY_THRESHOLDS;
```

Listing 5.8: Energy priority enumeration and threshold struct from ECO layer

- `ecoSetThresholds` enables the energy priority thresholds to be manipulated; they are initialised to the states shown in Table 3.7.

- `ecoSetupEnergy` is called to initialise the energy stack variables; it is called on first device start-up.

- `ecoUpdateEnergy` is called regularly and updates the energy status values.

- `ecoQuerySupplyVoltage` enables the application to query the supply voltage of the microcontroller; this is occasionally useful for other node functions.

Further functions can be implemented to allow the application running on the sensor node to obtain more detailed information on the energy hardware; for example, this may be useful to allow the node to transmit information on the function of each of its energy modules (perhaps for fault-finding purposes to identify a malfunctioning device). Listing 5.8 shows the structs for the energy priority and threshold values held by the node. In this implementation, the thresholds are percentage values (representing the amount of useable energy on the node, compared with the capacity of the node). However, in alternative implementations, the node may use ‘absolute’ energy values; this would be especially useful in heterogeneous networks where nodes have widely varying energy subsystems, and would be enabled by simply exchanging the modules in the ECO layer of the stack. This is a key benefit of the stacked node architecture.

```
while(1)
{
  ecoUpdateEnergy();
  if (ecoPowerStatus != (EP_EMPTY | EP_UNKNOWN))
  {
    appGetData(msg);
    SMPL_Ioctl( IOCTL_OBJ_RADIO, IOCTL_ACT_RADIO_AWAKE, 0);
    SMPL_Send(SMPL_LINKID_USER_UUD, msg, sizeof(msg));
    SMPL_Ioctl(IOCTL_OBJ_RADIO, IOCTL_ACT_RADIO_SLEEP, 0);
  }
  switch (ecoEnergyStatus) {
    case EP_5: SleepDuration = 1;
      break;
    case EP_4: SleepDuration = 2;
      break;
    case EP_3: SleepDuration = 4;
      break;
    case EP_2: SleepDuration = 8;
      break;
    case EP_1: SleepDuration = 16;
      break;
    case EP_MAINS: SleepDuration = 1;
      break;
    default: SleepDuration = 60;
      break;
  }
  halSleep(SleepDuration);
}
```

Listing 5.9: Main task loop in shared application layer

5.6 Evaluation

5.6.1 Implementing energy-adaptive behaviour

The process of delivering energy-adaptive behaviour is straightforward, as shown by the code shown in Listing 5.9 which shows the operational loop that has been implemented on the eZ430-RF2500. In this application, the `ecoUpdateEnergy` function is called to check the energy status of the node and update the EP value. Dependent on the EP value (if it is different from `EP_EMPTY` or `EP_UNKNOWN`), the system will sense the temperature and transmit it. Another application-layer function (`appGetData`) is called which obtains the data from the sensing stack and formats it into a message to be transmitted through the SimpliciTI protocol stack. The EP value then dictates the period that the node will sleep for. In this implementation, the maximum sleep period is 60s, and the minimum is 1s. Provided that a minimum 16s reporting interval can be supported by the power source on the node, the system will continually operate and will generally 'settle' into one of the modes (or oscillate between two of them), given a constant power input; alternatively, if no power is harvested by the system, the device's reporting frequency will decline gracefully as the stored energy is depleted.

5.6.2 Energy-related performance

As stated above, a number of mathematical functions have been implemented which allow the energy status of the node to be computed. The most resource-intensive calculation is that for the photovoltaic module, which involves a substantial amount of floating-point arithmetic. This was taken as a 'worst-case' example to evaluate the time taken to estimate the power being generated by the device. This calculation was timed as taking 7.16ms to complete. Being the most demanding calculation, it can be inferred that the energy or power calculations for the remaining modules will take place more quickly. However, as a worst case, one can state that the ADC measurement and associated calculation for each module will complete within a 10ms period. Given that there are potentially six modules connected to the system, it follows that the update of the energy status of the node will be completed within 60ms. Given that this refresh will be carried out periodically, this imposes a minimal resource requirement on the sensor node. The update rate can be tailored to take account of the last known EP value of the node, in order that the system update frequency can adapt to the available energy, and deliver an increased update rate when energy is plentiful (which is desirable as, in this state, it will normally be used more rapidly).

5.6.3 Embedded software features

The embedded software stack has been implemented to be applicable to a range of microcontrollers. The basic hardware requirements have already been stated; however, the full system has been implemented on an MSP430 microcontroller with a minimal amount of RAM and flash. The system incorporates a full communication stack and energy stack. The interface with the pins on the microcontroller, and with its internal ADC, is enabled through a hardware abstraction layer. The hardware abstraction layer will be different for each type of microcontroller; however, this enables the rest of the energy stack to remain hardware-agnostic. The mechanism for reading the electronic data sheets on energy modules and storing them in memory means that the microcontroller can rapidly access information on the modules for use in computation. The energy stack provides the shared application layer with a standardised interface of energy priority values, and a number of other interfaces that allow the energy status of the node to be calculated, monitored, and manipulated.

5.6.4 Comparison against state-of-the-art systems

The software architecture described and evaluated in this thesis offers a number of key benefits over existing systems. In particular, the software implemented on the limited number of state-of-the-art systems which incorporate multiple energy resources is highly tailored to specific types of energy device. While the existing solutions deliver a limited amount of energy-awareness, the act of altering the energy hardware which is connected to these devices also necessitates adaptation of the embedded software. This entails the parameters of the new energy hardware being obtained and the embedded software being altered accordingly. Depending on the characteristics of the device, this may need new routines to be coded to enable the calculation of the energy status. After this, the software would need to be re-compiled, and the microcontroller reprogrammed. In the case of systems which are deployed in the field, this would be a time-consuming and unreliable process. Indeed, where a number of energy devices may be 'trialled' in a situation in order to find the best way of powering a sensor node, when they are changed frequently, the act of reconfiguring the energy hardware would be arduous and impractical. The software solution reported in this thesis greatly simplifies the process of reconfiguring the energy hardware of the device, ensuring that the embedded software remains aware of its energy status without the need for code alteration, compilation, or device reprogramming. This is believed to be a compelling argument and is arguably an essential feature to enable the energy hardware of sensor nodes to be selected as appropriate to the deployment environment and activity of the sensor node.

5.7 System testing and results

The system has been tested with the configuration shown in Figure 4.19. The first test performed involved starting with an empty supercapacitor and allowing it to charge from the mains module. The result of this test is shown in Figure 4.5. In this test, Channel 1 is the raw voltage on the multiplexer module and Channel 2 is the regulated voltage which the microcontroller is connected to. It may be observed that the node reaches the 2.0V turn-on voltage after approximately 50s, and that the regulated voltage continues to rise until it is regulated to 3.0V. The raw voltage reached a maximum of 4.5V, before the mains supply was manually turned off and the system was discharged through a 180Ω resistor. The regulated voltage follows the decay of the raw voltage until it falls below 2.0V, after which time the microcontroller is disconnected from the supply and the output falls to approximately 0.0V.

The test system is able to operate autonomously as a sensor node. In the second test, with the Hyperterminal output shown in Figure 5.9 being taken from the PC connected to the receiver node, the system was charged up from cold, using the photovoltaic module (which took less than one hour under an indoor light intensity of 900 Lux) in the configuration shown earlier. The system was then reset, and the initial sweep of the energy subsystem resulted in the first group of transmissions (of the serial number of each of the energy module EPROMs). As the voltage on the supercapacitor is 2.8V the system is in PP_3 and wakes up every two seconds to perform a re-scan of its energy hardware. Approximately 20s after start-up, the vibration module was connected to socket 5 of the multiplexer module. This resulted in an additional transmission showing that a device had been added to socket 5. Approximately 10s after this, the photovoltaic module was disconnected from socket 3 and connected to socket 6, which resulted in two transmissions: firstly to shown that socket 3 was now empty; secondly to show that a device had now been connected to socket 6.

The third test presented here involved the monitoring of the photovoltaic energy module. The microcontroller was instructed to query the device, and to report the measured value. From this, the open-circuit voltage (and hence nominal power) can be found from the equations given in Section 4.5.1. With a light intensity measured at 900 Lux, the measurement output from the photovoltaic module was 1.09V. The unregulated voltage on the multiplexer module was 3.89V which led to an estimated open-circuit voltage estimate of 4.54V. The expected open-circuit voltage at this light intensity was 4.65V. Therefore the error in the estimated open-circuit voltage is approximately 2%. Given that standard tolerance resistors were used in this module, it is expected that the accuracy of this estimate can be improved.

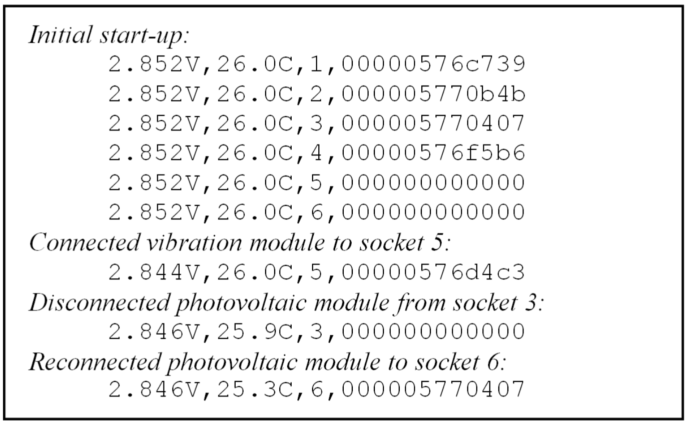

```
Initial start-up:
      2.852V,26.0C,1,00000576c739
      2.852V,26.0C,2,000005770b4b
      2.852V,26.0C,3,000005770407
      2.852V,26.0C,4,00000576f5b6
      2.852V,26.0C,5,000000000000
      2.852V,26.0C,6,000000000000
Connected vibration module to socket 5:
      2.844V,26.0C,5,00000576d4c3
Disconnected photovoltaic module from socket 3:
      2.846V,25.9C,3,000000000000
Reconnected photovoltaic module to socket 6:
      2.846V,25.3C,6,000005770407
```

Figure 5.9: Annotated Hyperterminal output from second test..

Further experimentation has been carried out with the complete energy stack and multiple connections to energy modules. While this system-level testing has not evaluated the accuracy of energy estimates of each module per se, it allowed measurements of the processing time to be carried out as presented earlier in this chapter, and for the operation of the overall system to be observed. Sanity checks were carried out, with the energy and power estimates being checked to ensure that they were within reasonable ranges; further, the system was used to power the microcontrollers, starting up from cold and operating from a range of energy modules. Modules were exchanged during the system's operation and estimates of energy and power were automatically revised to take account of the hardware changes.

5.8 Summary

This chapter carried forward the case study outlined in Chapter 4 by describing and evaluating the software interface for the system, which is co-located with the communication stack on the system's microcontroller. The microcontroller platforms used in this investigation, along with their important features of relevance to this work, were described. The implementation of the EEDS for the deployed modules has been outlined, including examples for the data stored in the modules and detail on the implementation and energy costs of the 1-Wire interface. The embedded software structure was also described. Detail was given on the implementation of the functions in the energy stack, including detailed consideration of the implications of certain mathematical functions. High-level considerations for energy-aware operation were also discussed, and the overall evaluation of the system was also considered. The embedded software structure that has been implemented for this device provides a robust and flexible system for monitoring and managing the energy hardware on the sensor node. While some of the mathematical functions carried out are demanding for a resource-constrained microcontroller, the complete energy assessment process on the MSP430F2274 platform (which lacks a hardware multiplier) has been demonstrated to complete within a few tens of milliseconds. Given that updates of the energy status on the node in the prototype application happen, at most, once per second (falling to once per minute when energy is low), and the update frequency can easily be manipulated in software, this represents a relatively small power cost, in view of the substantial additional features it brings.

Chapter 6

Conclusions and Future Work

6.1 Summary of work

Wireless sensor nodes offer the facility to remotely monitor parameters such as temperature, pressure, and vibration, in machines, buildings, or the environment. Wireless sensor nodes must be capable of operating autonomously, and for many this means they must operate without the constraint of a wired power supply. Conventionally, these devices have been powered by non-rechargeable batteries which are replaced when depleted. Energy harvesting (also known as energy scavenging) now offers the potential to sustain the operation of sensor nodes indefinitely. In this process, environmental energy is converted into electrical energy, which is then used to power the sensor node. The sporadic nature of energy harvesting means that energy must be used carefully and buffered in rechargeable batteries or supercapacitors. Ideally, nodes should be energy-aware and adapt their operation to the available energy; however, this is non-trivial in systems that feature complex energy subsystems that may potentially include a number of energy harvesters and energy storage devices. The current state-of-the-art in wireless sensor nodes and their energy supplies was discussed in detail in Chapter 2.

The work carried out under this project started with a new concept: to take the integration of wireless sensor nodes a step further by enabling the energy hardware on sensor nodes to be configured at the time of deployment in a plug-and-play manner. The work carried out spans across several areas and has addressed a number of academic challenges. This thesis detailed the development of a novel and comprehensive scheme for reconfigurable energy-aware sensor nodes: the described system allows sensor nodes to support up to six simultaneously-connected energy devices (energy sources or stores). It allows each device to be individually monitored by the microcontroller in order to ascertain the amount of energy stored or power generated and, where appropriate, permits the device to be managed. Energy modules can be attached to and removed from the system in a plug-and-play manner and incorporate electronic data sheets that store operational data for each module. The embedded software on the sensor node is structured to allow the system to interface flexibly with a range of energy devices and to present a single interface to the application running on the sensor node.

The contributions of this research are threefold: firstly, the system is enabled by a new hardware interface between the energy devices and microcontroller; secondly, an embedded software structure was implemented to interface with the energy hardware; and thirdly, energy-aware modules compliant with the scheme have been produced. The scheme has been evaluated by way of a prototype which accommodates a range of energy devices. The end result is an energy subsystem for micropower wireless sensor nodes that supports a range of energy devices and enables energy-aware operation. The proposed scheme was described in detail in Chapter 3, which outlined the features of the energy electronic data sheet, common hardware interface, and the associated software and algorithms.

The proposed scheme has been evaluated with a case study system. Chapter 4 described the development of the system hardware, including a range of energy modules (supporting batteries, supercapacitors, mains power and a number of energy harvesting sources) and an energy multiplexer module. The design of each module was explained, and its energy-management features and the impacts of the energy-awareness and management circuitry were described. The software for the prototype system was described and evaluated in Chapter 5. This included the contents and structure of the implemented electronic data sheets, the actual energy stack developed in the project, and the interface between the energy stack and the application layer.

6.2 Interpretation of the results

The scheme described in this thesis delivers a flexible architecture for wireless sensor nodes through the implementation of a reconfigurable energy subsystem. The system incorporates an energy ‘stack’ with a simplified interface to the application running on the microcontroller. The developed scheme extends the state-of-the-art of energy-aware sensor nodes by addressing the challenge of allowing a variety of energy hardware to be connected to a sensor node in a plug-and-play manner, and the software interface allows the microcontroller to interface with this hardware in order that it can be aware of its energy resources, and act to manage them where appropriate. This is an important development, as it means that sensor nodes no longer need to be developed for specific energy hardware, and appropriate energy devices can be attached to the sensor node at the time of system deployment. The scheme also permits the energy devices to be changed after deployment and allows the microcontroller to detect these changes and adapt the node’s operation accordingly.

The energy demands of the implemented system are conservative, provided that the update frequency of the energy status is kept low. The quiescent power draw of each module has been measured as of the order of a few microwatts, and the multiplexer module (which enables the scheme) also draws similar levels of power. Therefore, in a milliwatt-scale sensor node (which was the intended application of this technology) the quiescent power consumed by the hardware enabling this scheme is (dependent on the actual hardware connected) typically a few tens of microwatts. Notably, it has been observed that a single Schottky diode in a 1mA current path causes an approximate 9% efficiency loss; transistors were used wherever possible, but in some applications it was necessary to use diodes for the purposes of device protection. Many of the diodes would be required in any energy-harvesting system, so this should not be considered to be a drawback that is specific to this scheme; rather it is a reminder that careful design is necessary to ensure that the efficiency of these systems remains high.

An important note is that, while the demonstrated architecture facilitates the connection of up to six energy modules, the scheme would allow for 'cut-down' systems to be developed which could accommodate as few as one or two energy modules; for systems with a single energy module, the multiplexer would simply act as a through-connector with a voltage regulation capability (the only data sheet that would be needed on this system would be that of the energy module, so the microcontroller could interface with that directly). For simplified devices with two or more energy modules, a simplified energy multiplexer module, with fewer ports, would be used. This would deliver savings in terms of cost and, most probably, reduce the physical size of the device.

The fact that the bulk of the code developed for the prototype system has been written in C means that it is transferable to a range of platforms commonly used in wireless sensor nodes. Two separate platforms have been used in the development of this scheme: the CC2430 (based on an 8-bit 8051 processor) and the MSP430 (based on a 16-bit RISC processor). The simplified interface with the application layer means that devices are able to self-manage their resources without the need to understand the intricacies of their energy subsystems. Of course, as the proposed scheme has been successfully demonstrated on low-power, highly resource-constrained sensor nodes, this means that it can easily be transferred to higher-power, more capable sensor nodes and deliver equivalent functionality.

Given the nature of technological advances, with a convergence between the power output of energy-harvesting devices and the power consumption of wireless sensor nodes, systems will need to operate close to the limits of energy availability. Energy-aware schemes such as that described in this thesis will become more important. This work is well-placed for future developments in energy harvesting and wireless sensor node technologies to enable energy-awareness for increasingly resource-constrained systems.

6.3 Recommendations for future work

6.3.1 Overview

This thesis has described the development of a scheme for reconfigurable energy-aware wireless sensor nodes. It has delivered a hardware interface and electronic data sheet format that enables plug-and-play configuration of the energy hardware of wireless sensor nodes. The system has been demonstrated by way of a case study, implemented on the MSP430 and CC2430 microcontroller platforms. The work so far has concentrated on the development of the energy stack and the energy hardware. The concept of reconfigurable sensor nodes, which are able to be connected and deployed in a plug-and-play manner, remains compelling. The future work anticipated includes reducing the form factor of the system and introducing a modular stacking architecture. Other proposed work includes the further development of the embedded software, to better define the sensing stack and improve the interconnection between the three separate stacks. It may also be interesting to look at the potential for taking this technology towards standardisation, most probably through an industry organisation.

6.3.2 Hardware development

As mentioned in Section 4.3.2, it is anticipated that future iterations of the device design will feature a stacking architecture. It is envisaged that a stacking 36-way (or greater) connector could be used, and that each stacking board will act as a pass-through for data signals to the board below. In order for this to be realised, the physical size (particularly the height) of each module's PCB must be reduced. The reduced form factor and improved integration would be essential for deployment in an end-product.

The physical packaging of the device would also have to be explored. At the moment, each energy device requires its own power-conditioning and interface circuitry (the interface circuitry acts as a go-between from the energy device to the rest of the system). This may be viewed as a strength of the developed architecture, in that the system designer is free to select an appropriate power conditioning device to interface between the energy device and the rest of the system; however, in the developed system (particularly for the energy harvesting devices) it is quite an inelegant solution (each energy device has to have a go-between PCB which then connects to the multiplexer module). Instead, it may be desirable for each energy harvesting device to have its power conditioning circuitry integrated into its package, so that a simple connector could go from the energy module (meaning the energy harvester and its interface circuitry as one block) to the multiplexer module, without the need for a go-between. This could interface directly with the stacking system proposed above.

6.3.3 Software development

The work carried out thus far has focussed on the development of the energy stack; while the sensor stack was proposed, development work carried out has been minimal (indeed, the sensing application targeted by the case study was straightforward). In future work, it may be useful to look at how the sensing stack can be developed to deliver a similar plug-and-play capability for the sensing hardware of wireless sensor nodes. Indeed, the sensing stack could provide standard functions for data processing and event detection and could conceivably be controlled through a simplified interface by the application layer (with the application layer only having minimal involvement in the collection and processing of data). The application layer could then act as a simple go-between and scheduler, acting to collect data from the sensing stack and move it across to the communication stack, dependent on the amount of energy available (indicated by the energy stack). This would deliver a true plug-and-play solution for sensor nodes.

It may also be interesting to look at the network-level interactions between sensor nodes with the complete plug-and-play system. Mechanisms could be put in place for them to co-ordinate their sensing tasking and scheduling in order that they can make best use of their individual sensing hardware and energy resources. This would require the development of network interaction capabilities, which could conceivably be devolved to their own 'stack', along similar lines to the energy and sensing stacks that have been proposed under this work.

6.3.4 Towards standardisation

At the time of writing this thesis, a proposal was out for ballot with the International Society of Automation (ISA) to form a "Power Sources Working Group" under the ISA100 family of standards [129]. The aim of the provisional working group is to "develop standards to enable users to compare, specify and interface power/energy sources for 'non line powered, low power, wireless sensor nodes' ". The ultimate aim is to promote the interchangeability of energy devices for sensor nodes. In short, this will standardise the quoted power capabilities of energy sources (including energy harvesting devices and batteries) and the quoted power requirements of sensor nodes. The standard will also look at mains and transmitted power supply options. A deliverable may also be a common connector standard, although the number of pins required is currently open to debate and is related to the expected capabilities of connected system (with regard to the energy-awareness and device management capabilities).

The aims of the proposed standard have a number of parallels with the work described in this thesis. The fact that industry has recently realised that interchangeability and interfacing between wireless sensor nodes and their energy resources is important is, in effect, a validation of the original motivation for this work. Indeed, the system described in this thesis goes beyond what is being proposed in that it introduces an electronic data sheet concept and provides a method for multiple energy resources to be connected to a single sensor node in a plug-and-play manner. It is hoped that, as this standard develops, the work carried out under this thesis can feed into discussions to enable the capabilities realised under this prototype system to be transferred to commercial applications.

6.4 A look to the future...

In the last few years, there has been a rapid pace of development in energy harvesting and storage (leading to an increase in the amount of power than can be generated, and the efficiency with which it can be stored) along with a continued march of integrated circuit development (leading to microcontrollers and transceivers which are cheaper, faster, and more energy-efficient). This means that there is now an increasing overlap between the amount of energy that can be generated through energy harvesting and the amount of energy required for wireless sensing. Photovoltaic technology (including families for indoor use) is now mature, and vibration and thermoelectric energy harvesters are finding widespread commercial applications, although these are typically in the 'test deployment' or evaluation stage at present. Low self-discharge batteries are now readily available and improvements in supercapacitor technologies have decreased their internal resistance and reduced the problems of leakage.

There is no reason to believe that the pace of development will slow substantially in the coming years. Solid-state rechargeable lithium batteries are now being launched onto the market, and promise thousands of recharge cycles and 20-year lifetimes. It is expected that developments in vibration, thermoelectric, and wind energy harvesting will continue, spurred by the success of deployments in the field. Furthermore, developments in microcontroller technology will further reduce the power consumption of sensor nodes while increasing their capabilities. However, perhaps the most fluid area is in wireless communication standards development: with many standards families being developed (including Bluetooth Low Energy, ZigBee Green Power, and the EnOcean Alliance) there is currently some confusion over which standard will dominate. In the coming years, I expect to see one standard emerge as dominant (or for each to find their own niche) which will, in turn, increase confidence and encourage investment in wireless sensing systems for industrial applications.

Appendix A

Module schematics

This chapter shows schematics for the:

1. Multiplexer Module (Figure A.1).
2. Photovoltaic Module (Figure A.2).
3. Vibration Module (Figure A.3).
4. Mains Module (Figure A.4).
5. Supercapacitor Module (Figure A.5).
6. Battery Module (Figure A.6).

These modules were described in full in Chapter 4.

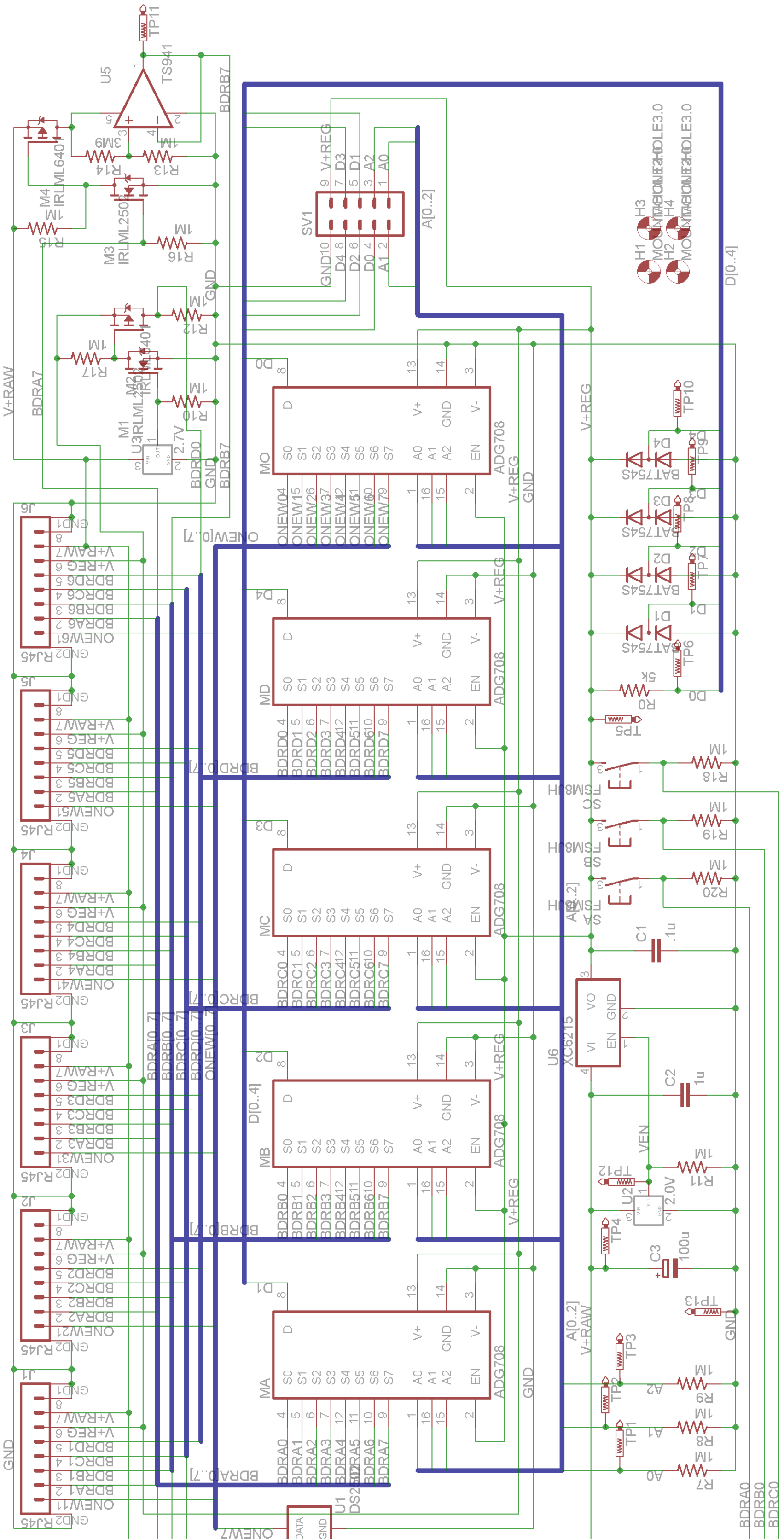

Figure A.1: Multiplexer module schematic

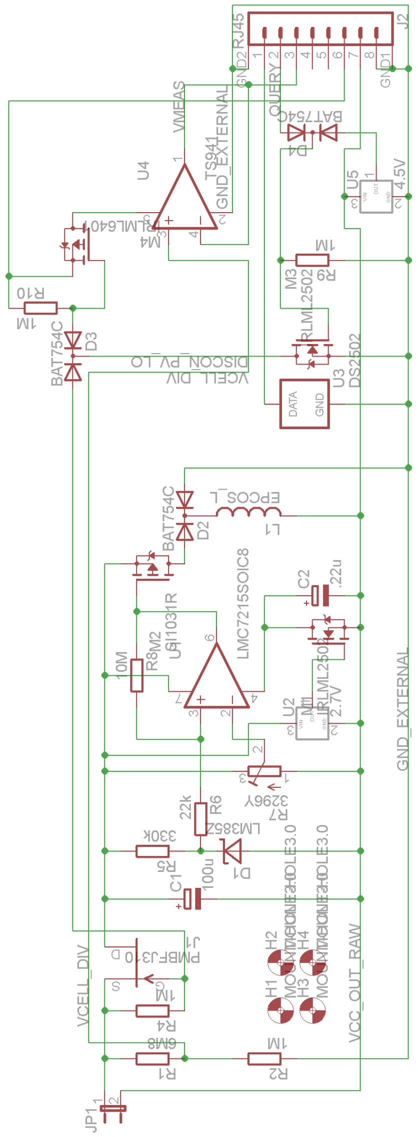

FIGURE A.2: Photovoltaic module schematic

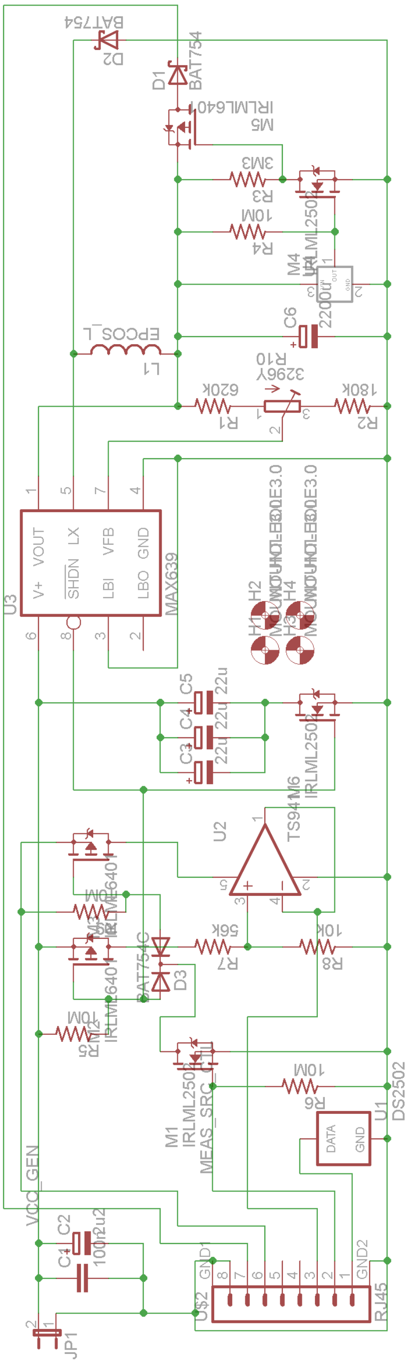

FIGURE A.3: Vibration module schematic

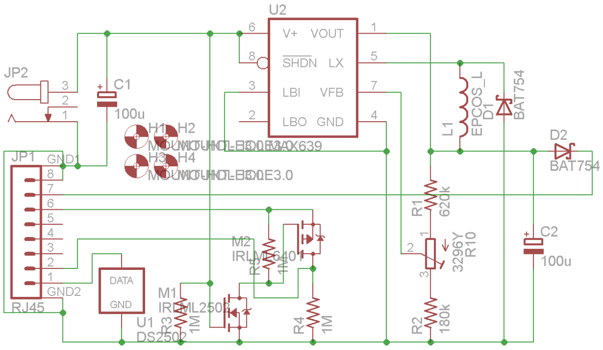

Figure A.4: Mains module schematic

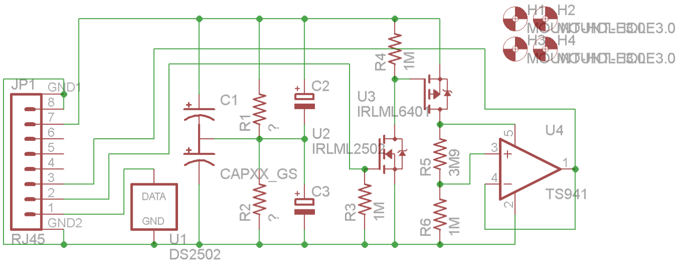

Figure A.5: Supercapacitor module schematic

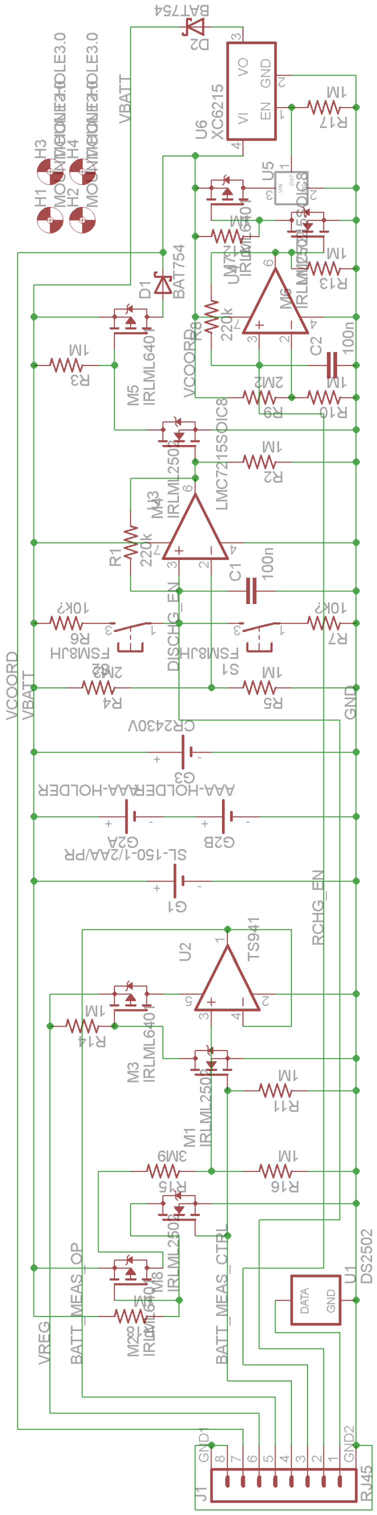

FIGURE A.6: Battery module schematic

Appendix B

Energy Electronic Data Sheet Contents

Mains Module		
Device Type	10 0001 00	0x84
Measurement	OnOffMaximum	0x01
Multiplier	10	0x0A
Max Output	4.5 (45)	0x25

Table B.1: Electronic Data Sheet for mains module.

Vibration Energy Harvester Module		
Device Type	10 0011 00	0x8C
Measurement	Square	0x03
Multiplier	6.6 (66)	0x42
Max Output	9.0 (90)	0x5A
PMultiplier	15	0x 00 00 00 0F

Table B.2: Electronic Data Sheet for vibration energy harvester module.

Primary Battery Module		
Device Type	10 0001 10	0x46
Measurement	EndOfLife	0x02
Multiplier	4.9 (49)	0x31
Max Output	3.6 (36)	0x24
PEndOfLife	20	0x14
PMaxCapacity	10260	0x00 00 28 14

Table B.3: Electronic Data Sheet for primary battery module.

Supercapacitor Module		
Device Type	01 0011 00	0x4C
Measurement	EndOfLife	0x02
Multiplier	4.9 (49)	0x31
Max Output	4.5 (45)	0x2D
PMultiplier	0.275 (28)	0x1C

Table B.4: Electronic Data Sheet for supercapacitor module.

Appendix C

Selected Publications

The following publications are included here:

1. Weddell, A. S., Grabham, N. J., Harris, N. R. and White, N. M. (2009) Modular Plug-and-Play Power Resources for Energy-Aware Wireless Sensor Nodes. *Sixth Annual IEEE Communications Society Conference on Sensor, Mesh and Ad Hoc Communications and Networks - SECON 2009*, 22-26 June 2009, Rome, Italy.

2. Weddell, A. S., Merrett, G. V., Harris, N. R. and Al-Hashimi, B. M. (2008) Energy Harvesting and Management for Wireless Autonomous Sensors. *Measurement + Control*, 41 (4).

3. Weddell, A. S., Harris, N. R. and White, N. M. (2008) Alternative Energy Sources for Sensor Nodes: Rationalized Design for Long-Term Deployment. *International Instrumentation and Measurement Technology Conference*, May 12-15, 2008, Victoria, British Columbia, Canada.

Weddell, A. S., Grabham, N. J., Harris, N. R. and White, N. M. (2009) Modular Plug-and-Play Power Resources for Energy-Aware Wireless Sensor Nodes. In: Sixth Annual IEEE Communications Society Conference on Sensor, Mesh and Ad Hoc Communications and Networks - SECON 2009, 22-26 June 2009, Rome, Italy.

This publication is not available in the online version of this thesis, but may be downloaded from `http://eprints.ecs.soton.ac.uk/17325/`

Weddell, A. S., Grabham, N. J., Harris, N. R. and White, N. M. (2009) Modular Plug-and-Play Power Resources for Energy-Aware Wireless Sensor Nodes. In: Sixth Annual IEEE Communications Society Conference on Sensor, Mesh and Ad Hoc Communications and Networks - SECON 2009, 22-26 June 2009, Rome, Italy.

This publication is not available in the online version of this thesis, but may be downloaded from `http://eprints.ecs.soton.ac.uk/17325/`

Weddell, A. S., Grabham, N. J., Harris, N. R. and White, N. M. (2009) Modular Plug-and-Play Power Resources for Energy-Aware Wireless Sensor Nodes. In: Sixth Annual IEEE Communications Society Conference on Sensor, Mesh and Ad Hoc Communications and Networks - SECON 2009, 22-26 June 2009, Rome, Italy.

This publication is not available in the online version of this thesis, but may be downloaded from `http://eprints.ecs.soton.ac.uk/17325/`

Weddell, A. S., Grabham, N. J., Harris, N. R. and White, N. M. (2009) Modular Plug-and-Play Power Resources for Energy-Aware Wireless Sensor Nodes. In: Sixth Annual IEEE Communications Society Conference on Sensor, Mesh and Ad Hoc Communications and Networks - SECON 2009, 22-26 June 2009, Rome, Italy.

This publication is not available in the online version of this thesis, but may be downloaded from `http://eprints.ecs.soton.ac.uk/17325/`

Weddell, A. S., Grabham, N. J., Harris, N. R. and White, N. M. (2009) Modular Plug-and-Play Power Resources for Energy-Aware Wireless Sensor Nodes. In: Sixth Annual IEEE Communications Society Conference on Sensor, Mesh and Ad Hoc Communications and Networks - SECON 2009, 22-26 June 2009, Rome, Italy.

This publication is not available in the online version of this thesis, but may be downloaded from `http://eprints.ecs.soton.ac.uk/17325/`

Weddell, A. S., Grabham, N. J., Harris, N. R. and White, N. M. (2009) Modular Plug-and-Play Power Resources for Energy-Aware Wireless Sensor Nodes. In: Sixth Annual IEEE Communications Society Conference on Sensor, Mesh and Ad Hoc Communications and Networks - SECON 2009, 22-26 June 2009, Rome, Italy.

This publication is not available in the online version of this thesis, but may be downloaded from `http://eprints.ecs.soton.ac.uk/17325/`

Weddell, A. S., Grabham, N. J., Harris, N. R. and White, N. M. (2009) Modular Plug-and-Play Power Resources for Energy-Aware Wireless Sensor Nodes. In: Sixth Annual IEEE Communications Society Conference on Sensor, Mesh and Ad Hoc Communications and Networks - SECON 2009, 22-26 June 2009, Rome, Italy.

This publication is not available in the online version of this thesis, but may be downloaded from `http://eprints.ecs.soton.ac.uk/17325/`

Weddell, A. S., Grabham, N. J., Harris, N. R. and White, N. M. (2009) Modular Plug-and-Play Power Resources for Energy-Aware Wireless Sensor Nodes. In: Sixth Annual IEEE Communications Society Conference on Sensor, Mesh and Ad Hoc Communications and Networks - SECON 2009, 22-26 June 2009, Rome, Italy.

This publication is not available in the online version of this thesis, but may be downloaded from `http://eprints.ecs.soton.ac.uk/17325/`

Weddell, A. S., Grabham, N. J., Harris, N. R. and White, N. M. (2009) Modular Plug-and-Play Power Resources for Energy-Aware Wireless Sensor Nodes. In: Sixth Annual IEEE Communications Society Conference on Sensor, Mesh and Ad Hoc Communications and Networks - SECON 2009, 22-26 June 2009, Rome, Italy.

This publication is not available in the online version of this thesis, but may be downloaded from `http://eprints.ecs.soton.ac.uk/17325/`

Weddell, A. S., Merrett, G. V., Harris, N. R. and Al-Hashimi, B. M. (2008) Energy Harvesting and Management for Wireless Autonomous Sensors. *Measurement + Control*, 41 (4).

This publication is not available in the online version of this thesis, but may be downloaded from `http://eprints.ecs.soton.ac.uk/15342/`

Weddell, A. S., Merrett, G. V., Harris, N. R. and Al-Hashimi, B. M. (2008) Energy Harvesting and Management for Wireless Autonomous Sensors. *Measurement + Control*, 41 (4).

This publication is not available in the online version of this thesis, but may be downloaded from `http://eprints.ecs.soton.ac.uk/15342/`

Weddell, A. S., Merrett, G. V., Harris, N. R. and Al-Hashimi, B. M. (2008) Energy Harvesting and Management for Wireless Autonomous Sensors. *Measurement + Control*, 41 (4).

This publication is not available in the online version of this thesis, but may be downloaded from `http://eprints.ecs.soton.ac.uk/15342/`

Weddell, A. S., Merrett, G. V., Harris, N. R. and Al-Hashimi, B. M. (2008) Energy Harvesting and Management for Wireless Autonomous Sensors. *Measurement + Control*, 41 (4).

This publication is not available in the online version of this thesis, but may be downloaded from `http://eprints.ecs.soton.ac.uk/15342/`

Weddell, A. S., Merrett, G. V., Harris, N. R. and Al-Hashimi, B. M. (2008) Energy Harvesting and Management for Wireless Autonomous Sensors. *Measurement + Control*, 41 (4).

This publication is not available in the online version of this thesis, but may be downloaded from `http://eprints.ecs.soton.ac.uk/15342/`

Weddell, A. S., Merrett, G. V., Harris, N. R. and Al-Hashimi, B. M. (2008) Energy Harvesting and Management for Wireless Autonomous Sensors. *Measurement + Control*, 41 (4).

This publication is not available in the online version of this thesis, but may be downloaded from `http://eprints.ecs.soton.ac.uk/15342/`

Weddell, A. S., Merrett, G. V., Harris, N. R. and Al-Hashimi, B. M. (2008) Energy Harvesting and Management for Wireless Autonomous Sensors. *Measurement + Control*, 41 (4).

This publication is not available in the online version of this thesis, but may be downloaded from `http://eprints.ecs.soton.ac.uk/15342/`

Weddell, A. S., Harris, N. R. and White, N. M. (2008) Alternative Energy Sources for Sensor Nodes: Rationalized Design for Long-Term Deployment. *International Instrumentation and Measurement Technology Conference*, May 12-15, 2008, Victoria, British Columbia, Canada.

This publication is not available in the online version of this thesis, but may be downloaded from `http://eprints.ecs.soton.ac.uk/15361/`

Weddell, A. S., Harris, N. R. and White, N. M. (2008) Alternative Energy Sources for Sensor Nodes: Rationalized Design for Long-Term Deployment. *International Instrumentation and Measurement Technology Conference*, May 12-15, 2008, Victoria, British Columbia, Canada.

This publication is not available in the online version of this thesis, but may be downloaded from `http://eprints.ecs.soton.ac.uk/15361/`

Weddell, A. S., Harris, N. R. and White, N. M. (2008) Alternative Energy Sources for Sensor Nodes: Rationalized Design for Long-Term Deployment. *International Instrumentation and Measurement Technology Conference*, May 12-15, 2008, Victoria, British Columbia, Canada.

This publication is not available in the online version of this thesis, but may be downloaded from `http://eprints.ecs.soton.ac.uk/15361/`

Weddell, A. S., Harris, N. R. and White, N. M. (2008) Alternative Energy Sources for Sensor Nodes: Rationalized Design for Long-Term Deployment. *International Instrumentation and Measurement Technology Conference*, May 12-15, 2008, Victoria, British Columbia, Canada.

This publication is not available in the online version of this thesis, but may be downloaded from `http://eprints.ecs.soton.ac.uk/15361/`

Weddell, A. S., Harris, N. R. and White, N. M. (2008) Alternative Energy Sources for Sensor Nodes: Rationalized Design for Long-Term Deployment. *International Instrumentation and Measurement Technology Conference*, May 12-15, 2008, Victoria, British Columbia, Canada.

This publication is not available in the online version of this thesis, but may be downloaded from `http://eprints.ecs.soton.ac.uk/15361/`

Weddell, A. S., Harris, N. R. and White, N. M. (2008) Alternative Energy Sources for Sensor Nodes: Rationalized Design for Long-Term Deployment. *International Instrumentation and Measurement Technology Conference*, May 12-15, 2008, Victoria, British Columbia, Canada.

This publication is not available in the online version of this thesis, but may be downloaded from `http://eprints.ecs.soton.ac.uk/15361/`

Bibliography

[1] C. Kompis and S. Aliwell, editors. *Energy Harvesting Technologies to Enable Wireless and Remote Sensing.* Sensors & Instrumentation KTN Action Group Report, June 2008. `http://server.quid5.net/~koumpis/pubs/pdf/energyharvesting08.pdf`. Last accessed May 2010.

[2] K. Martinez, P. Padhy, A. Elsaify, G. Zou, A. Riddoch, J. K. Hart, and H. L. R. Ong. Deploying a sensor network in an extreme environment. *Proceedings of Sensor Networks, Ubiquitous and Trustworthy Computing*, pages 186–93, 2006.

[3] G. Werner-Allen, K. Lorincz, M. Welsh, O. Marcillo, J. Johnson, M. Ruiz, and J. Lees. Deploying a wireless sensor network on an active volcano. *IEEE Internet Computing*, 10(2):18–25, 2006.

[4] F. M. Discenzo, D. Chung, and K. A. Loparo. Pump condition monitoring using self-powered wireless sensors. *Sound and Vibration*, pages 12–15, May 2006.

[5] J. Polastre, R. Szewczyk, and D. Culler. Telos: enabling ultra-low power wireless research. *2005 Fourth International Symposium on Information Processing in Sensor Networks*, pages 364–9, 2005.

[6] S. George. Development of a vibration-powered wireless temperature sensor and accelerometer for health monitoring. *Aerospace Conference, 2006 IEEE*, 2006:8 pp., 2006.

[7] P. Dutta, J. Hui, J. Jeong, S. Kim, C. Sharp, J. Taneja, G. Tolle, K. Whitehouse, and D. Culler. Trio: enabling sustainable and scalable outdoor wireless sensor network deployments. *The Fifth International Conference on Information Processing in Sensor Networks*, pages 407–15, 2006.

[8] D. Linden and T. B. Reddy, editors. *Handbook of Batteries.* McGraw-Hill, New York, 3rd edition, 2002.

[9] S. Jacobs. Utility meter operating 20 years on original lithium battery. *Metering International*, (3):1 pp., 2004.

[10] Tadiran Batteries GmbH. Lithium batteries technical brochure. `http://www.tadiranbatteries.de/eng/downloads/lbr06eng.pdf`, October 2008. Last accessed May 2010.

[11] D. Rakhmatov, S. Vrudhula, and D.A. Wallach. A model for battery lifetime analysis for organizing applications on a pocket computer. *IEEE Transactions on Very Large Scale Integration (VLSI) Systems*, 11(6):1019–30, 2003.

[12] Maxim/Dallas. *Rechargeable Batteries: Basics, Pitfalls, and Safe Recharging Practices*, 2005. Application Note AN3501.

[13] J.-M. Tarascon and M. Armand. Issues and challenges facing rechargeable lithium batteries. *Nature*, 414(6861):359–67, 2001.

[14] F. Simjee and P.H. Chou. Everlast: long-life, supercapacitor-operated wireless sensor node. *ISLPED'06 Proceedings of the 2006 International Symposium on Low Power Electronics and Design*, pages 197–202, 2006.

[15] X. Jiang, J. Polastre, and D. Culler. Perpetual environmentally powered sensor networks. *2005 Fourth International Symposium on Information Processing in Sensor Networks*, pages 463–8, 2005.

[16] Panasonic Industrial Company. Gold Capacitors Technical Guide. `http://www.panasonic.com/industrial/components/pdf/goldcap_tech-guide_052505.pdf`, May 2005. Last accessed May 2010.

[17] CAP-XX (Australia) Pty Ltd. Hs208 supercapacitor datasheet. `http://www.cap-xx.com/resources/datasheets/CAP-XX_HS208_Datasheet_v1.2.pdf`, February 2009. Last accessed May 2010.

[18] S. Roundy, D. Steingart, L. Frechette, P. Wright, and J. Rabaey. Power sources for wireless sensor networks. *Wireless Sensor Networks. First European Workshop, EWSN 2004. Proceedings.*, pages 1–17, 2004.

[19] J. D. Holladay, E. O. Jones, M. Phelps, and J. Hu. Microfuel processor for use in a miniature power supply. *Journal of Power Sources*, 108(1-2):21–27, 2002. Microfuel processors;.

[20] S. Whalen, A. Thompson, D. Bahr, C. Richards, and R. Richards. Design, fabrication and testing of the P_3 micro heat engine. *Sensors and Actuators A (Physical)*, A104(3):290–8, 2003.

[21] H. Li, A. Lal, J. Blanchard, and D. Henderson. Self-reciprocating radioisotope-powered cantilever. *Journal of Applied Physics*, 92(2):1122–7, 2002.

[22] J. P. Fleurial, G. J. Snyder, J. Patel, J. A. Herman, T. Caillat, B. Nesmith, and E. A. Kolawa. Miniaturized radioisotope solid state power sources. In *Space*

Technology and Applications International Forum Proceedings, Albuquerque, New Mexico, January 2000.

[23] L. Mateu and F. Moll. Review of energy harvesting techniques and applications for microelectronics. *Proceedings of SPIE - The International Society for Optical Engineering*, 5837 Part I:359–373, 2005.

[24] P. D. Mitcheson, E. M. Yeatman, G. K. Rao, A. S. Holmes, and T. C. Green. Energy harvesting from human and machine motion for wireless electronic devices. *Proceedings of the IEEE*, 96(9):1457–86, 2008.

[25] N. H. Reich, W. G. J. H. M. v. Sark, E. A. Alsema, S. Y. Kan, S. Silvester, A. S. H. v. d. Heide, R. W. Lof, and R. E. I. Schropp. Weak light performance and spectral response of different solar cell types. In *Twentieth European Photovoltaic Solar Energy Conference, Proceedings of*, Barcelona, Spain, 2005.

[26] J. F. Randall and J. Jacot. Is AM1.5 applicable in practice? Modelling eight photovoltaic materials with respect to light intensity and two spectra. *Renewable Energy*, 28(12):1851–64, 2003.

[27] SANYO Semiconductor Co., Ltd. Amorphous silicon solar cells / amorphous photosensors. `http://semicon.sanyo.com/en/pamph_pdf_e/EP120B.pdf`, November 2007. Last accessed May 2010.

[28] Schott Solar GmbH. ASI OEM Indoor Solar Modules. `http://www.schott.com/photovoltaic/english/products/oem_products/`, 2010. Last accessed May 2010.

[29] S. Roundy. Energy scavenging for wireless sensor nodes with a focus on vibration to electricity conversion. PhD Thesis, Mechanical Engineering, The University of California, Berkeley, 2003.

[30] S. Roundy, P. K. Wright, and J. M. Rabaey. *Energy Scavenging for Wireless Sensor Networks, with Special Focus on Vibrations.* Kluwer Academic, Boston, 2004.

[31] S. P. Beeby, M. J. Tudor, and N. M. White. Energy harvesting vibration sources for microsystems applications. *Measurement Science and Technology*, 17(12):R175–R195, 2006.

[32] S. Roundy and Y. Zhang. Toward self-tuning adaptive vibration-based microgenerators. volume 5649, pages 373–384. SPIE, 2005.

[33] R. Amirtharajah and A. P. Chandrakasan. Self-powered signal processing using vibration-based power generation. *IEEE Journal of Solid-State Circuits*, 33(5):687–95, 1998.

[34] Perpetuum Ltd. PMG17 Vibration Energy Harvesters. `http://www.perpetuum.com/pmg17.asp`, 2010. Last accessed May 2010.

[35] Ferro Solutions, Inc. VEH-460 Electromechanical Vibration Energy Harvester. `http://www.ferrosi.com/files/VEH460_May09.pdf`, May 2009. Last accessed May 2010.

[36] R. N. Torah, P. Glynne-Jones, M. J. Tudor, and S. P. Beeby. Energy aware wireless microsystem powered by vibration energy harvesting. *PowerMEMS 2007 - Submitted to the 7th Int. Workshop on Micro and Nanotechnology for Power Generation and Energy Conversion Applications*, 2007.

[37] S. Roundy and P. K. Wright. A piezoelectric vibration based generator for wireless electronics. *Smart Materials and Structures*, 13(5):1131–1142, 2004.

[38] AdaptivEnergy. Joule-Thief Modules. `http://www.adaptivenergy.com/application%20chart/index.html`, 2009. Last accessed May 2010.

[39] Midé Technology Corporation. Piezo energy harvester catalog. `http://www.mide.com/products/volture/volture_catalog.php`, 2010. Last accessed May 2010.

[40] S. Meninger, J. O. Mur-Miranda, R. Amirtharajah, A. Chandrakasan, and J.H. Lang. Vibration-to-electric energy conversion. *IEEE Transactions on Very Large Scale Integration (VLSI) Systems*, 9(1):64–76, 2001.

[41] J. P. Fleurial, G. J. Snyder, J. A. Herman, M. Smart, P. Shakkottai, P. H. Giauque, and M. A. Nicolet. Miniaturized thermoelectric power sources. In *34th Intersociety Energy Conversion Engineering Conference*, Vancouver, BC, Canada, 1999.

[42] H. Bottner, J. Nurnus, A. Gavrikov, G. Kuhner, M. Jagle, C. Kunzel, D. Eberhard, G. Plescher, A. Schubert, and K.-H. Schlereth. New thermoelectric components using microsystem technologies. *Journal of Microelectromechanical Systems*, 13(3):414–20, 2004.

[43] Micropelt GmbH. MPG D602 - D751 thin film thermogenerator sensing devices. `http://www.micropelt.com/down/datasheet_mpg_d602_d751.pdf`, March 2008. Last accessed May 2010.

[44] Tellurex Corporation. PG-1 Product Details. `http://www.tellurex.com/pdf/PG1_spec_sheet.pdf`, January 2009. Last accessed May 2010.

[45] R. Morais, S. G. Matos, M. A. Fernandes, A. L. G. Valente, S. F. S. P. Soares, P. J. S. G. Ferreira, and M. J. C. S. Reis. Sun, wind and water flow as energy supply for small stationary data acquisition platforms. *Computers and Electronics in Agriculture*, 64(2):120–132, 2008.

[46] C. Park and P. H. Chou. Ambimax: autonomous energy harvesting platform for multi-supply wireless sensor nodes. *2006 3rd Annual IEEE Communications Society Conference on Sensor and Ad Hoc Communications and Networks*, pages 168–77, 2006.

[47] J. Kymissis, C. Kendall, J. Paradiso, and N. Gershenfeld. Parasitic power harvesting in shoes. *Digest of Papers. Second International Symposium on Wearable Computers*, pages 132–9, 1998.

[48] T. Starner and J. A. Paradiso. *Low Power Electronics Design*, chapter 35, pages 1–30. CRC Press, 2004.

[49] B. Jiang, J. R. Smith, M. Philipose, S. Roy, K. Sundara-Rajan, and A. V. Mamishev. Energy scavenging for inductively coupled passive RFID systems. In *IMTC 2005 - Instrumentation and Measurement Technology Conference, Proceedings of*, Ottawa, Canada, May 2005.

[50] J. A. Paradiso and T. Starner. Energy scavenging for mobile and wireless electronics. *IEEE Pervasive Computing*, 4(1):18–27, 2005.

[51] Powercast Corporation. Powerharvester Receivers. `http://www.powercastco.com/products/powerharvester-receivers/`, 2010. Last accessed May 2010.

[52] A. Sample and J. R. Smith. Experimental results with two wireless power transfer systems. White paper, Intel Research Seattle, 2008.

[53] Midé Technology Corporation. SEH25w Piezoelectric Vibration & Solar Energy Harvester. `http://www.mide.com/products/volture/seh25w.php`, 2009. Last accessed May 2010.

[54] D. Kraemer, L. Hu, A. Muto, X. Chen, G. Chen, and M. Chiesa. Photovoltaic-thermoelectric hybrid systems: a general optimization methodology. *Applied Physics Letters*, 92(24):243503–1, June 2008.

[55] Watlow Ltd. Watlow sensors. `http://www.watlow.co.uk/products/sensors/`, 2004. Last accessed May 2010.

[56] IEEE Standards Association. IEEE standard for a smart transducer interface for sensors and actuators - mixed-mode communication protocols and transducer electronic data sheet (TEDS) formats. *IEEE Std 1451.4-2004*, 2004.

[57] National Instruments Corporation. An Overview of IEEE 1451.4 Transducer Electronic Data Sheets. Technical report, National Instruments, 2004.

[58] D. Potter. Smart plug and play sensors. *Instrumentation & Measurement Magazine, IEEE*, 5(1):28–30, Mar 2002.

[59] H. M. Willey. One cheap network topology [1-wire bus]. *Embedded Systems Programming*, 14(1):59–76, 2001.

[60] S. Bandari, C. Santiago, H. S. Mohammed, and J. Schmalzel. Component electronic datasheets in ISHM. pages 106 – 109, Houston, TX, United States, 2006.

[61] J. L. Schmalzel, F. Figueroa, J. A. Morris, and S. A. Mandayam. A road map for integrated systems health management. pages 522 – 524, Piscataway, NJ 08855-1331, United States, 2008.

[62] SBS Implementers Forum. System Management Bus (SMBus) Specification. `http://smbus.org/specs/smbus20.pdf`, August 2000. Last accessed March 2009.

[63] H. Taylor and L. W. Hruska. Standard smart batteries for consumer applications. page 183, New York, NY, USA, 1995.

[64] Power Management Bus Implementers Forum. PMBus Power Management Protocol Specification. `http://www.powersig.org/`, February 2007. Last accessed March 2009.

[65] IEEE Standards Association. IEEE standard for information technology - telecommunications and information exchange between systems - local and metropolitan area networks - specific requirements part 15.4: Wireless medium access control (MAC) and physical layer (PHY) specifications for low-rate wireless personal area networks (WPANs). *IEEE Std 802.15.4-2006 (Revision of IEEE Std 802.15.4-2003)*, 2006.

[66] ZigBee Standards Organization. ZigBee Specification Document 053474r17. `http://www.zigbee.org/Products/DownloadZigBeeTechnicalDocuments.aspx`, 2007. Last accessed April 2008.

[67] Microchip Technology Inc. MiWi Wireless Networking Protocol Stack. `http://ww1.microchip.com/downloads/en/AppNotes/01066a.pdf`, 2007. Last accessed April 2008.

[68] HART Communication Foundation. Wireless HART Technology. `http://www.hartcomm.org/protocol/wihart/wireless_technology.html`, 2009. Last accessed May 2010.

[69] IEEE Standards Association. IEEE standard for information technology - telecommunications and information exchange between systems - local and metropolitan area networks. *IEEE Std 802.11-2007 (Revision of IEEE Std 802.11-1999)*, June 12 2007.

[70] D. Vassis, G. Kormentzas, A. Rouskas, and I. Maglogiannis. The IEEE 802.11g standard for high data rate WLANs. *Network, IEEE*, 19(3):21–26, May-June 2005.

[71] Texas Instruments Inc. CC2430DK Development Kit User Manual. `http://www.ti.com/lit/pdf/swru133`, October 2007. Last accessed May 2010.

[72] Texas Instruments Inc. SimpliciTI Overview. `http://www.ti.com/litv/pdf/swru130`, July 2007. Last accessed April 2008.

[73] Infrared Data Association (IrDA). IrDA Data Specifications, year = 2006, howpublished = `http://www.irda.org/displaycommon.cfm?an=1&subarticlenbr=7`, note = Last accessed May 2008.

[74] Crossbow Technology Inc. MCS410 Cricket Wireless Location System Data Sheet. `http://www.xbow.com/Products/Product_pdf_files/Wireless_pdf/MCS410_Cricket_Datasheet.pdf`, January 2006. Last accessed May 2010.

[75] S. Pandya, J. Engel, J. Chen, Z. Fan, and C. Liu. CORAL: miniature acoustic communication subsystem architecture for underwater wireless sensor networks. *2005 IEEE Sensors*, page 4 pp., 2005.

[76] Tritech International Ltd. and Wireless Fibre Systems Ltd. Underwater Radio Modem S1510. `http://www.wirelessfibre.co.uk/index.php?page=downloads`, October 2006. Last accessed May 2010.

[77] J. K. Stevens and K. McCabe. IEEE begins wireless, long-wavelength standard for healthcare, retail and livestock visibility networks. `http://standards.ieee.org/announcements/pr_p19021Rubee.html`, June 2006. Last accessed May 2010.

[78] J. N. Al-Karaki and A. E. Kamal. Routing techniques in wireless sensor networks: a survey. *IEEE Wireless Communications*, 11(6):6–28, 2004.

[79] C. Ma, Y. Yang, and Z. Zhang. Constructing battery-aware virtual backbones in sensor networks. *Proceedings. 2005 International Conference on Parallel Processing*, pages 203–10, 2005.

[80] R.C. Shah and J.M. Rabaey. Energy aware routing for low energy ad hoc sensor networks. *2002 IEEE Wireless Communications and Networking Conference Record*, 1:350–5, 2002.

[81] Y. Liu and W. K. G. Seah. A priority-based multi-path routing protocol for sensor networks. *Personal, Indoor and Mobile Radio Communications, 2004. PIMRC 2004. 15th IEEE International Symposium on*, 1:216–220, Sept. 2004.

[82] T. Voigt, H. Ritter, and J. Schiller. Utilizing solar power in wireless sensor networks. *Proceedings 28th Annual IEEE International Conference on Local Computer Networks*, pages 416–22, 2003.

[83] A. Kansal and M. B. Srivastava. An environmental energy harvesting framework for sensor networks. *Proceedings of the 2003 International Symposium on Low Power Electronics and Design*, pages 481–6, 2003.

[84] K.A. Delin and S.P. Jackson. The sensor web: a new instrument concept. *Proceedings of the SPIE - The International Society for Optical Engineering*, 4284:1 – 9, 2001.

[85] C. M. Cianci, V. Trifa, and A. Martinoli. Threshold-based algorithms for power-aware load balancing in sensor networks. *Swarm Intelligence Symposium, 2005. SIS 2005. Proceedings 2005 IEEE*, pages 349–356, June 2005.

[86] V. Raghunathan, C. Schurgers, S. Park, and M. B. Srivastava. Energy-aware wireless microsensor networks. *IEEE Signal Processing Magazine*, 19(2):40–50, 2002.

[87] G. V. Merrett, N. R. Harris, B. M. Al-Hashimi, and N. M. White. Energy managed reporting for wireless sensor networks. *Sensors and Actuators A: Physical*, 142(1):379–389, March 2008.

[88] Energizer Battery Manufacturing Inc. Alkaline Manganese Dioxide Handbook and Application Manual. `http://data.energizer.com/PDFs/alkaline_appman.pdf`, 2006. Last accessed May 2010.

[89] T. Umemura, Y. Mizutani, T. Okamoto, T. Taguchi, K. Nakajima, and K. Tanaka. Life expectancy and degradation behavior of electric double layer capacitor Part I. volume 3, pages 944 – 948, Nagoya, Japan, 2003.

[90] P. Forstner. SLAA334A MSP430 Flash Memory Characteristics. `http://focus.ti.com.cn/cn/general/docs/lit/getliterature.tsp?literatureNumber=slaa334a&fileType=pdf`, April 2008. Last accessed May 2010.

[91] Texas Instruments, Inc. MSP430 16-bit Ultra-Low Power MCUs. `http://www.ti.com/msp430`, 2010. Last accessed May 2010.

[92] Microchip Technology Inc. eXtreme Low Power. `http://www.microchip.com/en_us/technology/xlp/`, 2010. Last accessed May 2010.

[93] Atmel Corporation. AVR Solutions. `http://www.atmel.com/products/avr/`, 2010. Last accessed May 2010.

[94] Crossbow Technology, Inc. Imote2 Data Sheet. `http://www.xbow.com/Products/Product_pdf_files/Wireless_pdf/Imote2_Datasheet.pdf`, April 2007. Last accessed May 2010.

[95] Texas Instruments, Inc. The all new CC430 combines leading MSP430 MCU and low-power RF technology. `http://www.ti.com/cc430`, 2010. Last accessed May 2010.

[96] J. Hill, M. Horton, R. Kling, and L. Krishnamurthy. The platforms enabling wireless sensor networks. *Communications of the ACM*, 47(6):41–6, 2004.

[97] Sun Microsystems, Inc. Sun SPOT World - Program the World! `http://www.sunspotworld.com/`, 2010. Last accessed May 2010.

[98] K. Martinez, R. Ong, and J. Hart. Glacsweb: a sensor network for hostile environments. *2004 First Annual IEEE Communications Society Conference on Sensor and Ad Hoc Communications and Networks*, pages 81–7, 2004.

[99] J. Schiller, A. Liers, H. Ritter, R. Winter, and T. Voigt. Scatterweb - low power sensor nodes and energy aware routing. *Proceedings of the Annual Hawaii International Conference on System Sciences*, pages 286–94, 2005.

[100] G. V. Merrett, A. S. Weddell, N. R. Harris, N. M. White, and B. M. Al-Hashimi. The unified framework for sensor networks: A systems approach. `http://eprints.ecs.soton.ac.uk/12955/`, September 2006. Last accessed May 2010.

[101] X. Jiang, J. Taneja, J. Ortiz, A. Tavakoli, P. Dutta, J. Jeong, D. Culler, P. Levis, and S. Shenker. An architecture for energy management in wireless sensor networks. *ACM SIGBED Review*, 4(3):31–36, 2007.

[102] D. Gay, M. Welsh, P. Levis, E. Brewer, R. v.=Behren, and D. Culler. The nesC language: A holistic approach to networked embedded systems. *Proceedings of the ACM SIGPLAN Conference on Programming Language Design and Implementation (PLDI)*, pages 1–11, 2003.

[103] D. K. Arvind, M. Adams, A. Burdett, T. Dillon, P. Garner, J. Gilby, G. Matich, and G. Peggs. Wireless sensor networks - a mission to the USA. Report of a DTI Global Watch Mission, DTI Global Watch, November 2005.

[104] V. Handziski, J. Polastre, J.-H. Hauer, C. Sharpt, A. Wolisz, and D. Culler. Flexible hardware abstraction for wireless sensor networks. *Proceedings of the Second European Workshop on Wireless Sensor Networks, EWSN 2005*, 2005:145–157, 2005.

[105] R. Szewczyk, A. Mainwaring, J. Polastre, J. Anderson, and D. Culler. An analysis of a large scale habitat monitoring application. *Proceedings of the Second International Conference on Embedded Networked Sensor Systems*, pages 214–26, 2004.

[106] Pei Zhang, Christopher M. Sadler, Stephen A. Lyon, and Margaret Martonosi. Hardware design experiences in ZebraNet. *SenSys'04 - Proceedings of the Second International Conference on Embedded Networked Sensor Systems*, pages 227–38, 2004.

[107] S. Bapat, V. Kulathumani, and A. Arora. Analyzing the yield of ExScal, a large-scale wireless sensor network experiment. *13th IEEE International Conference on Network Protocols*, page 10 pp., 2006.

[108] K. Langendoen, A. Baggio, and O. Visser. Murphy loves potatoes: experiences from a pilot sensor network deployment in precision agriculture. *Proceedings. 20th International Parallel and Distributed Processing Symposium*, page 8 pp., 2006.

[109] F. Chiti, A. De Cristofaro, R. Fantacci, D. Tarchi, G. Collodo, G. Giorgetti, and A. Manes. Energy efficient routing algorithms for application to agro-food wireless sensor networks. *2005 IEEE International Conference on Communications*, 5:3063–7, 2005.

[110] D. Estrin. Reflections on wireless sensing systems: from ecosystems to human systems. *2007 IEEE Radio and Wireless Symposium*, pages 1–4, 2007.

[111] V. Raghunathan, A. Kansal, J. Hsu, J. Friedman, and M. Srivastava. Design considerations for solar energy harvesting wireless embedded systems. *2005 Fourth International Symposium on Information Processing in Sensor Networks*, pages 457–62, 2005.

[112] P. Corke, P. Valencia, P. Sikka, T. Wark, and L. Overs. Long-duration solar-powered wireless sensor networks. *Proceedings of the 4th Workshop on Embedded Networked Sensors, EmNets 2007*, pages 33 – 37, 2007.

[113] J. Eliasson, P. Lindgren, J. Delsing, S. J. Thompson, and Y.-B. Cheng. A power management architecture for sensor nodes. *IEEE Wireless Communications and Networking Conference, WCNC*, pages 3010 – 3015, 2007.

[114] J. Taneja, J. Jeong, and D. Culler. Design, modeling, and capacity planning for micro-solar power sensor networks. In *IPSN '08: Proceedings of the 7th international conference on Information processing in sensor networks*, pages 407–418, Washington, DC, USA, 2008. IEEE Computer Society.

[115] GE Energy. Essential Insight.mesh Wireless Condition Monitoring. `http://www.gepower.com/prod_serv/products/oc/en/bently_nevada/essential_insight.htm`, 2010. Last accessed May 2010.

[116] M. H. Schneider, J. W. Evans, P. K. Wright, and D. Ziegler. Designing a thermoelectrically powered wireless sensor network for monitoring aluminium smelters. *Proceedings of the Institution of Mechanical Engineers, Part E: Journal of Process Mechanical Engineering*, 220(3):181–90, 2006.

[117] EnOcean GmbH. Thermal Energy Harvester ECT 100. `http://www.tdc.co.uk/index.php?key=ect100`, August 2007. Last accessed May 2010.

[118] A. Hande, T. Polk, W. Walker, and D. Bhatia. Indoor solar energy harvesting for sensor network router nodes. *Microprocessors and Microsystems*, 31(6):420–432, 2007.

[119] E. Leder, A. Sutor, and R. Lerch. Solar powered low-power sensor module with a radio communication and a user interface. *2005 IEEE Sensors*, page 4 pp., 2005.

[120] D. Dondi, D. Brunelli, L. Benini, P. Pavan, A. Bertacchini, and L. Larcher. Photovoltaic cell modeling for solar energy powered sensor networks. *Advances in Sensors and Interface, 2007, 2nd International Workshop on*, pages 1–6, June 2007.

[121] Texas Instruments, Inc. eZ430-RF2500-SEH Solar Energy Harvesting Development Tool User's Guide. `http://focus.ti.com/lit/ug/slau273/slau273.pdf`, January 2010. Last accessed May 2010.

[122] C. Park and P. H. Chou. Power utility maximization for multiple-supply systems by a load-matching switch. *Proceedings of the 2004 International Symposium on Low Power Electronics and Design*, pages 168 – 73, 2004.

[123] Duracell. Duracell alkaline-manganese dioxide technical bulletin. `http://www1.duracell.com/oem/Pdf/others/ATB-full.pdf`, 1997. Last accessed May 2010.

[124] G. V. Merrett, A. S. Weddell, N. R. Harris, B. M. Al-Hashimi, and N. M. White. A structured hardware/software architecture for embedded sensor nodes. In *17th International Conference on Computer Communications and Networks*, August 2008.

[125] S. G. Hageman. SPICE models a solar array. *Electronics Design News*, page 220, May 7 1992.

[126] T. Markvart and L. Castaner, editors. *Practical Handbook of Photovoltaics: Fundamentals and Applications.* Elsevier Science, Oxford, 2003.

[127] Texas Instruments, Inc. MSP430F2274 Mixed Signal Microcontroller. `http://focus.ti.com/lit/ds/symlink/msp430f2274-ep.pdf`, 2008. Last accessed May 2010.

[128] Maxim Integrated Products, Inc. Application Note 126: 1-Wire Communication Through Software. `http://www.maxim-ic.com/app-notes/index.mvp/id/126`, August 2009. Last accessed May 2010.

[129] R. Freeland. ISA100 Power Sources Working Group (TBC) - Encouraging a Single Power Source Standard. `http://www.hansonwade.com/events/energy-harvesting/presentations/Roy-Freeland-Encouraging-A-Single-Power-Source-Standard.pdf`, April 2010. Last accessed May 2010.